US 20110312755A1

(19) **United States**

(12) **Patent Application Publication**

SILVERBROOK et al.

(10) **Pub. No.: US 2011/0312755 A1**

(43) **Pub. Date: Dec. 22, 2011**

(54) **TEST MODULE WITH CHEMICAL LYSIS SECTION**

(75) Inventors: **KIA SILVERBROOK**, ROZELLE (AU); **MEHDI AZIMI**, ROZELLE (AU); **GEOFFREY RICHARD FACER**, ROZELLE (AU)

(73) Assignee: **GENEASYS PTY LTD**

(21) Appl. No.: **13/150,111**

(22) Filed: **Jun. 1, 2011**

Related U.S. Application Data

(60) Provisional application No. 61/356,018, filed on Jun. 17, 2010, provisional application No. 61/437,686, filed on Jan. 30, 2011.

Publication Classification

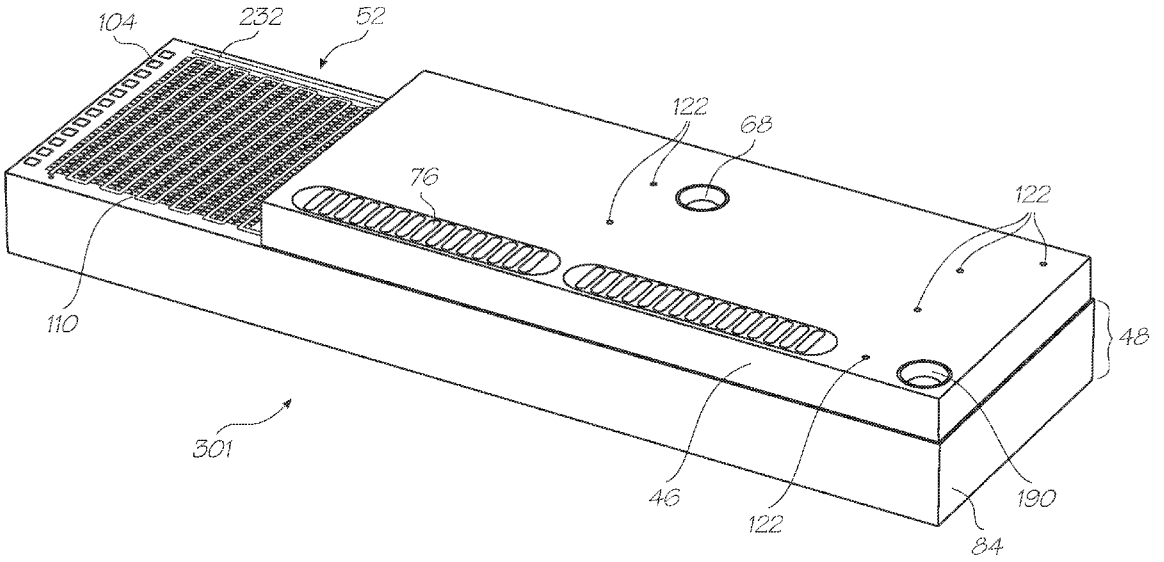
(51) **Int. Cl.**

C40B 60/12	(2006.01)
C12M 1/40	(2006.01)
C12M 1/33	(2006.01)

(52) **U.S. Cl.** **506/39**; 435/306.1; 435/303.1; 435/286.1

(57) **ABSTRACT**

A test module for lysing cells in a fluid, the test module having an outer casing with receptacle for receiving a fluid containing cells, a lysis reagent reservoir containing a lysis reagent and having an outlet valve, and, a lysis section in fluid communication with the receptacle for holding the fluid during lysis of the cells, wherein, the outlet valve is upstream of the lysis section and configured to open as the fluid flows into the lysis section thereby adding the lysis reagent to the fluid.



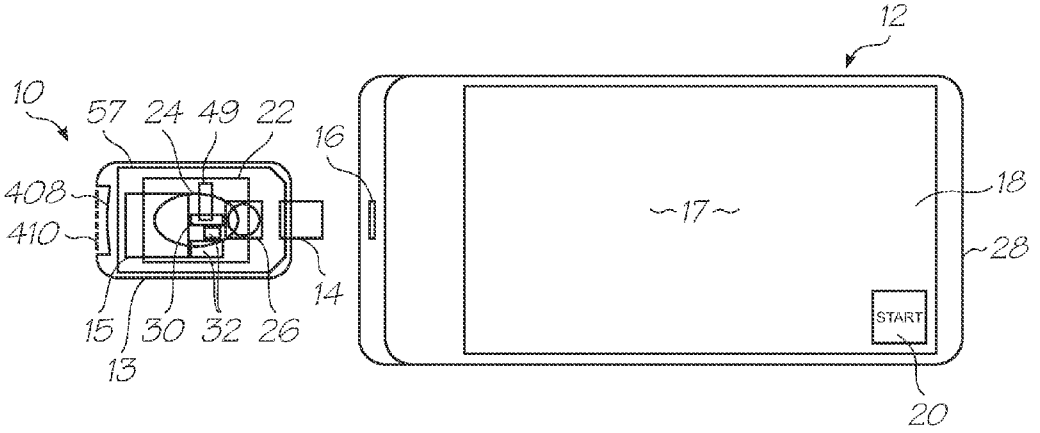

12
10
57
24
49
22
16
408
410
17
18
28
14
15
30
32
26
13
START
20

FIG. 1

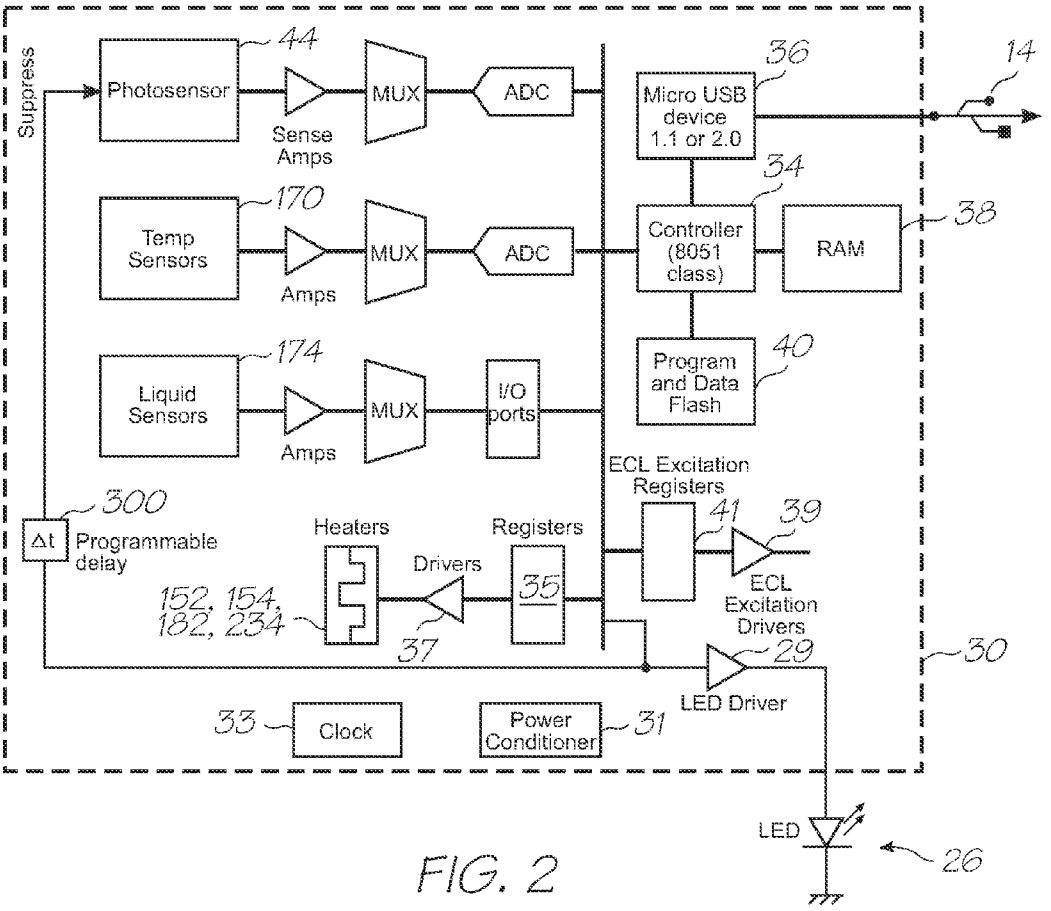

Suppress
Photosensor
44
Sense Amps
MUX
ADC
Micro USB device 1.1 or 2.0
36
14
Temp Sensors
170
Amps
34
Controller (8051 class)
RAM
38
Liquid Sensors
174
Program and Data Flash
40
I/O ports
ECL Excitation Registers
300
Δt
Programmable delay
Heaters
Registers
41
39
Drivers
152, 154, 182, 234
35
ECL Excitation Drivers
37
29
30
LED Driver
33
Clock
Power Conditioner
31
LED
26

FIG. 2

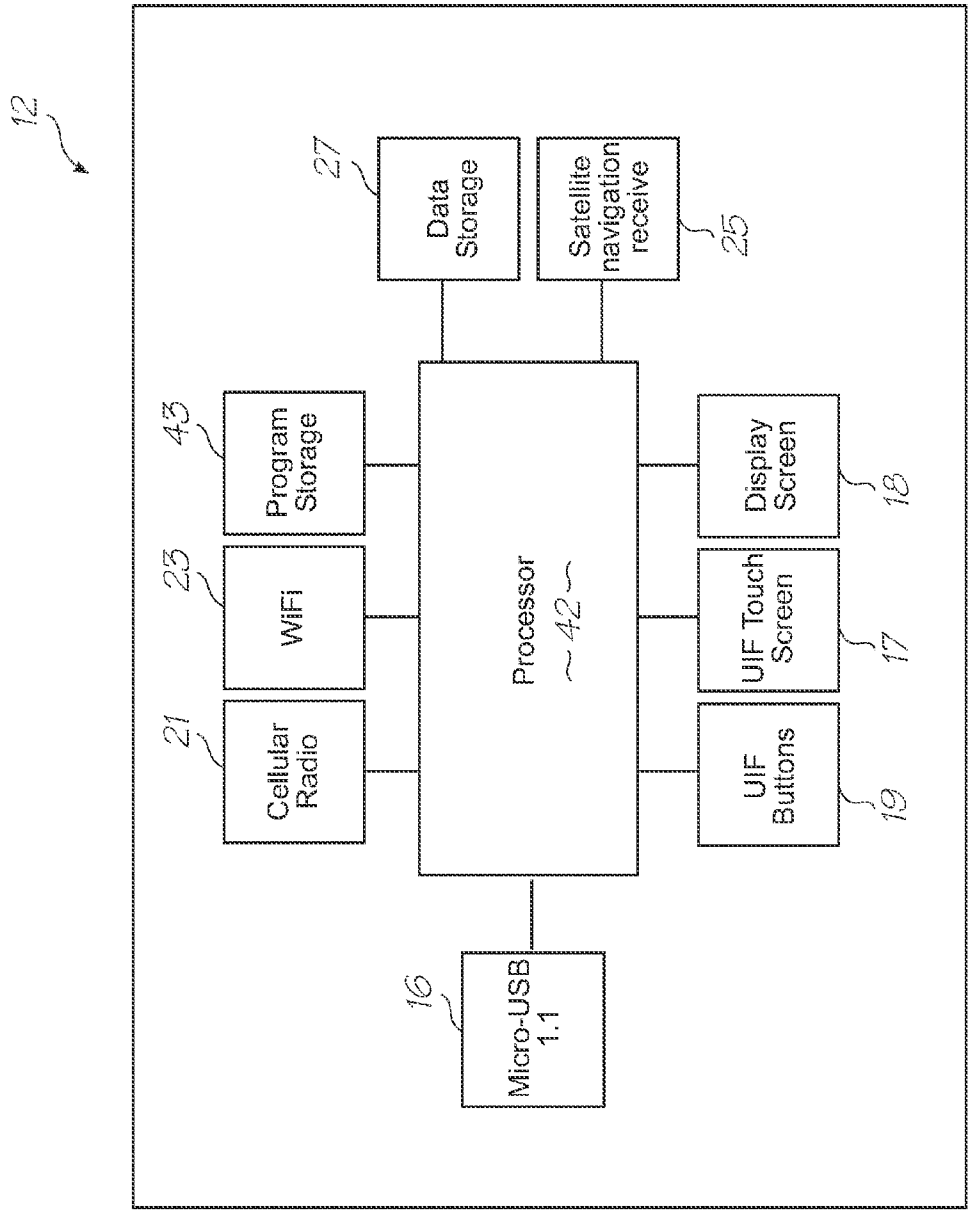

12
27
Data Storage
Satellite navigation receive
25
43
Program Storage
23
WiFi
21
Cellular Radio
Processor
42
Display Screen
18
UIF Touch Screen
17
UIF Buttons
19
16
Micro-USB 1.1

FIG. 3

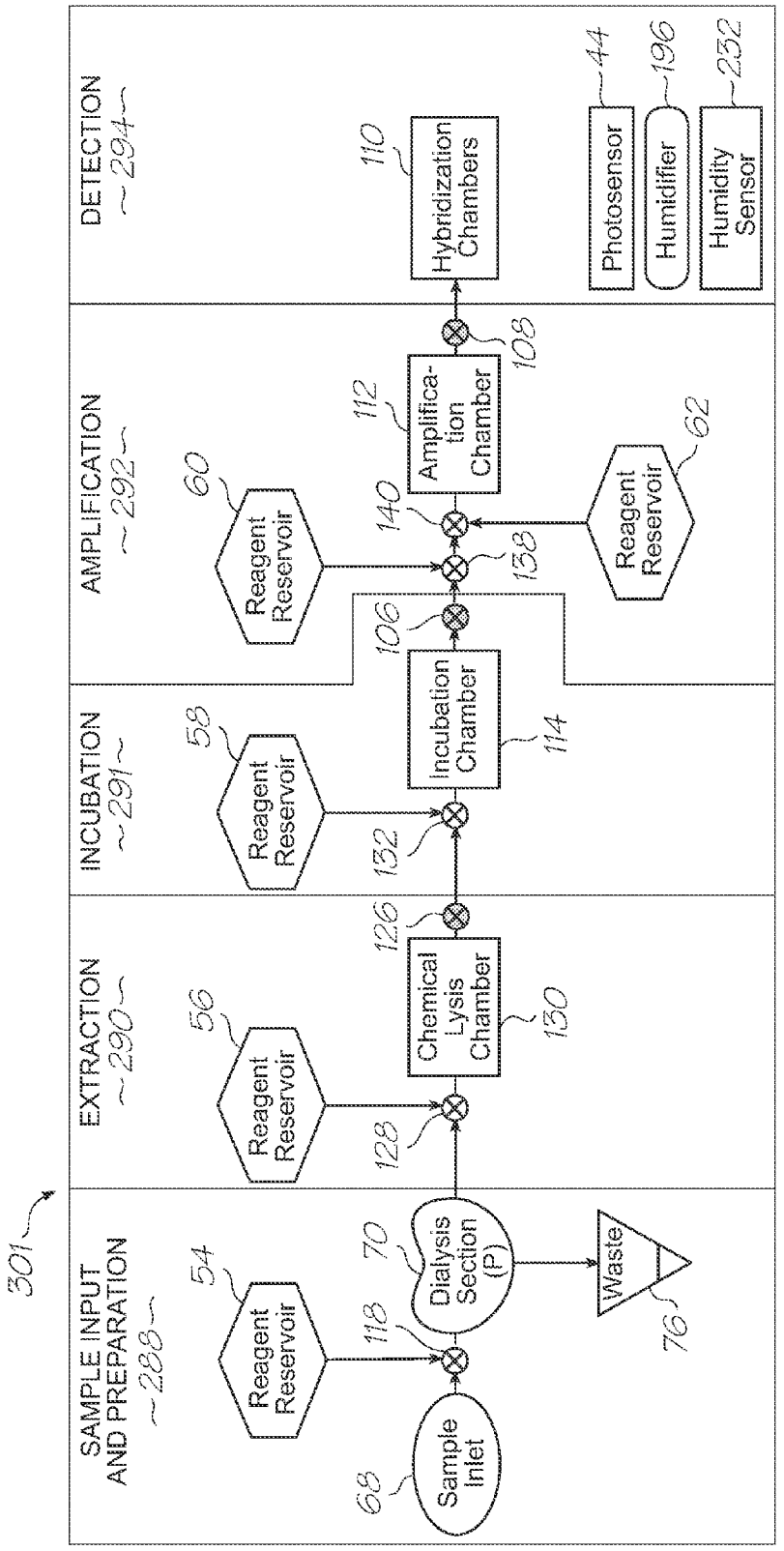

301
SAMPLE INPUT AND PREPARATION ~288~
EXTRACTION ~290~
INCUBATION ~291~
AMPLIFICATION ~292~
DETECTION ~294~
Sample Inlet
68
Reagent Reservoir
54
118
Dialysis Section (P)
70
Waste
76
Reagent Reservoir
56
128
Chemical Lysis Chamber
130
126
Reagent Reservoir
58
132
Incubation Chamber
114
106
Reagent Reservoir
60
140
Amplification Chamber
112
138
Reagent Reservoir
62
108
Hybridization Chambers
110
Photosensor
44
Humidifier
196
Humidity Sensor
232
KEY
⊗ Surface tension valve
⊗ Boiling - initiated valve
⊗ Thermal bend actuator valve
⊕ Fault tolerant valve array
P Pathogen target
L Leukocyte target

FIG. 4

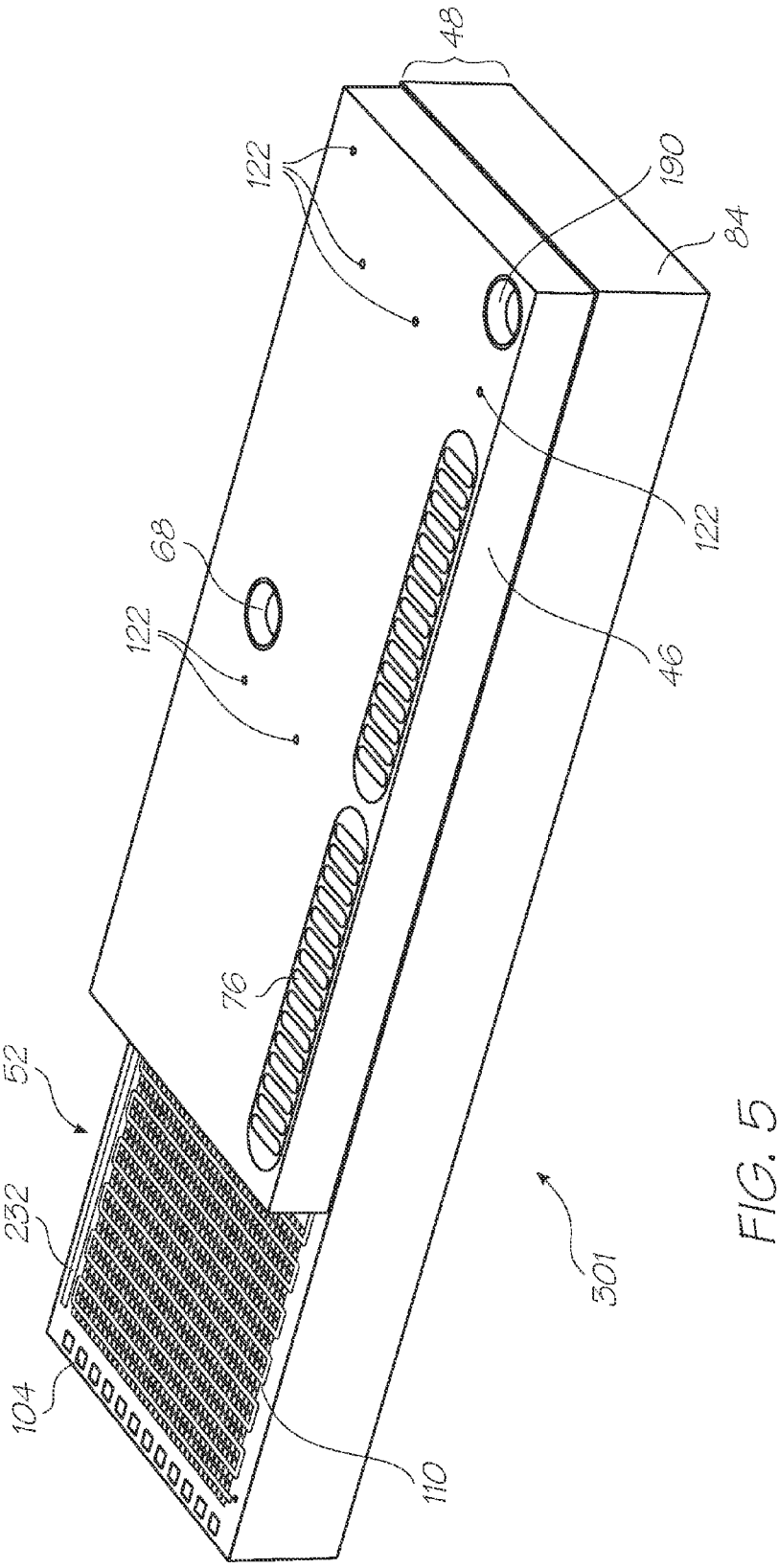


FIG. 5

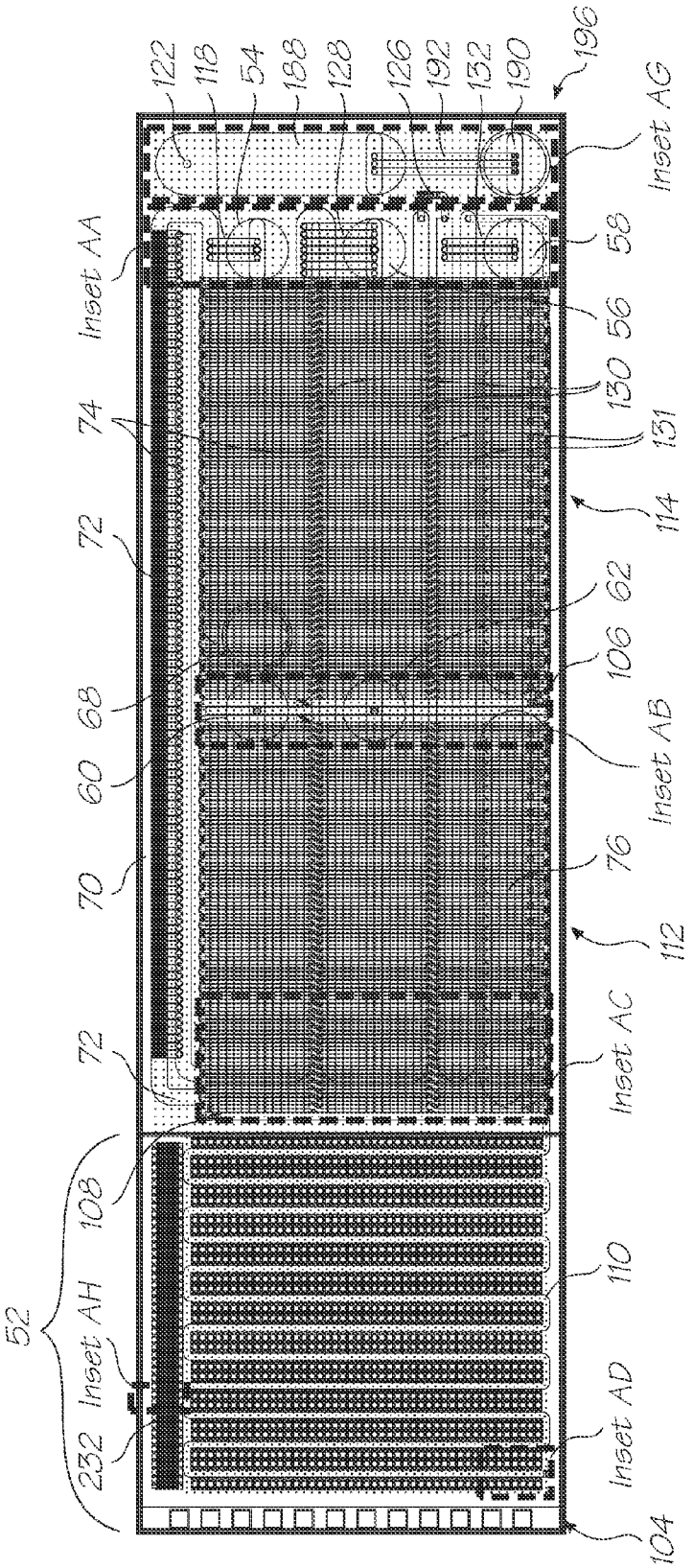

122
118
54
188
128
126
192
132
190
196
Inset AG
Inset AA
58
56
130
131
74
114
72
62
106
68
Inset AB
60
76
70
112
72
Inset AC
108
110
52
Inset AH
Inset AD
232
104

FIG. 6

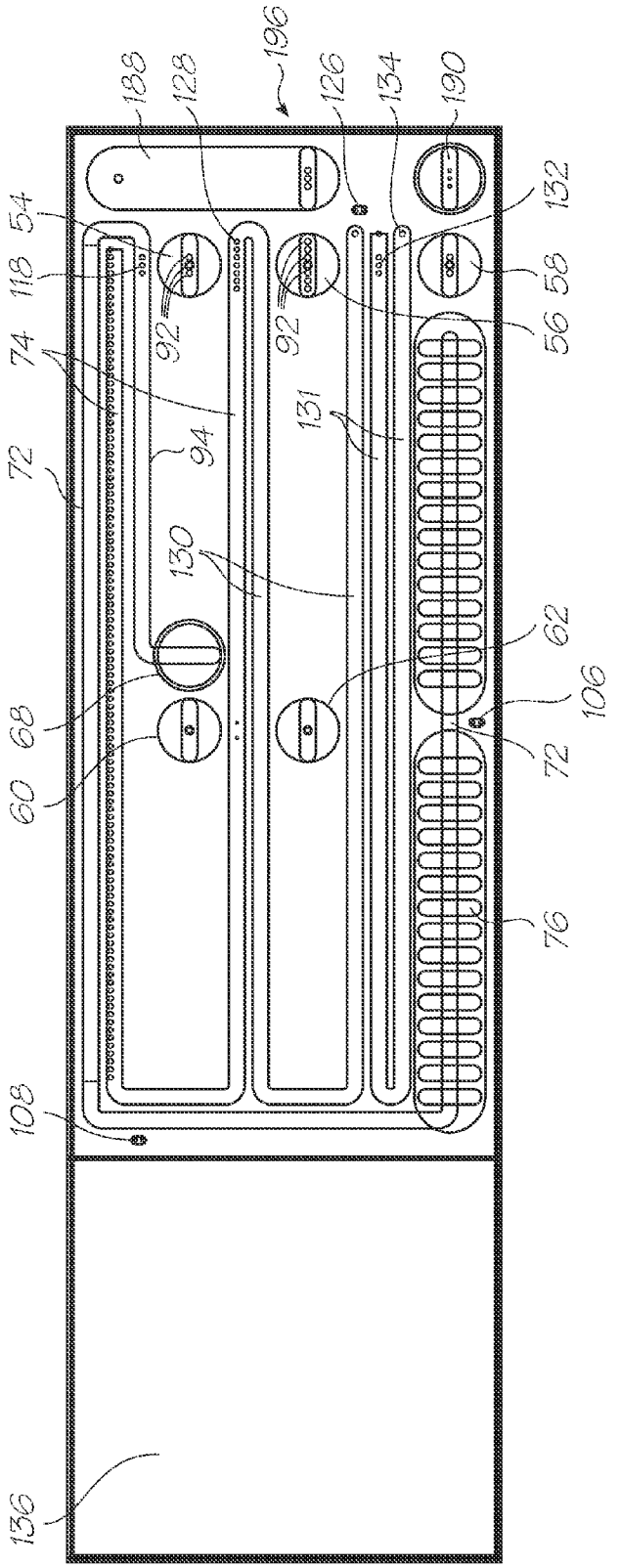

196
188
128
126
134
190
54
132
118
58
92
92
56
74
94
131
72
130
62
106
68
72
60
76
108
136

FIG. 7

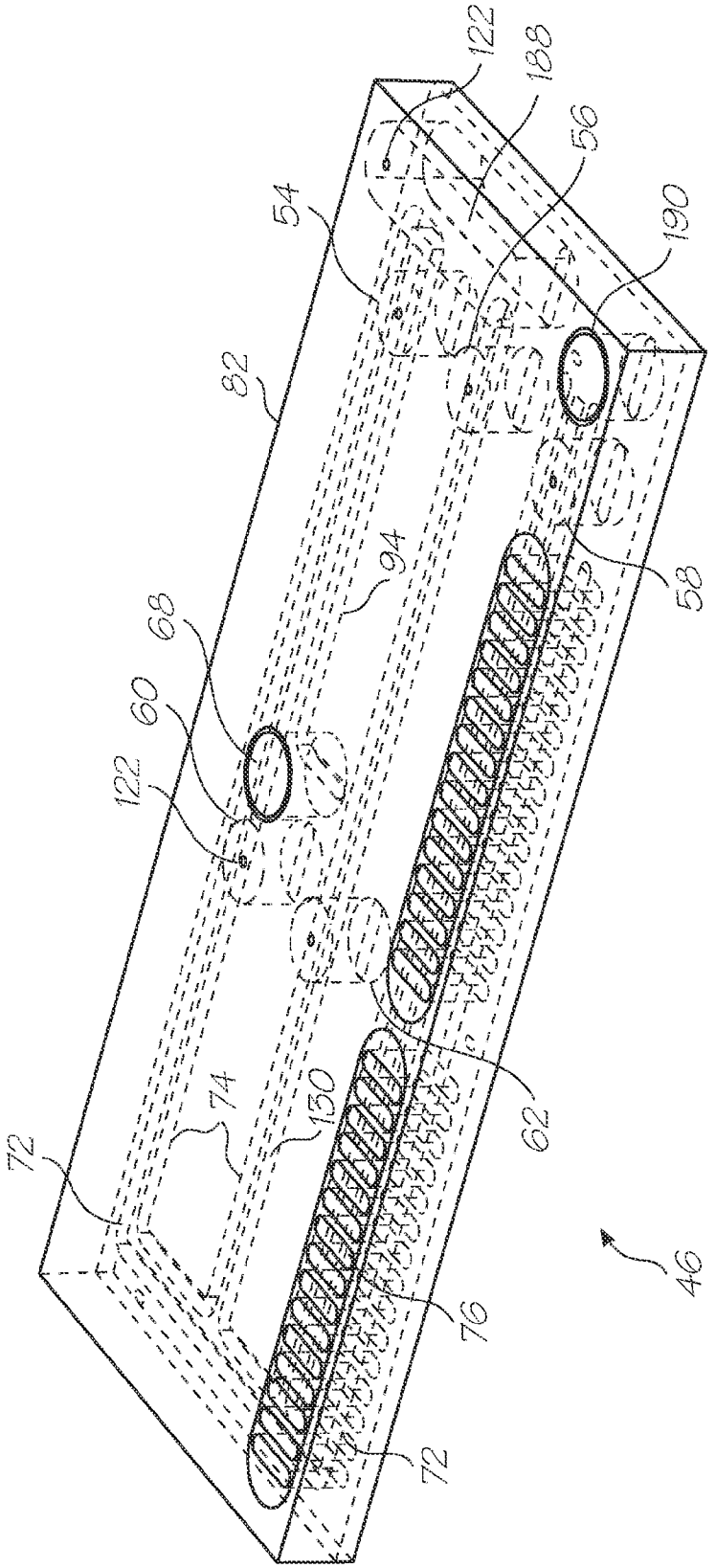


FIG. 8

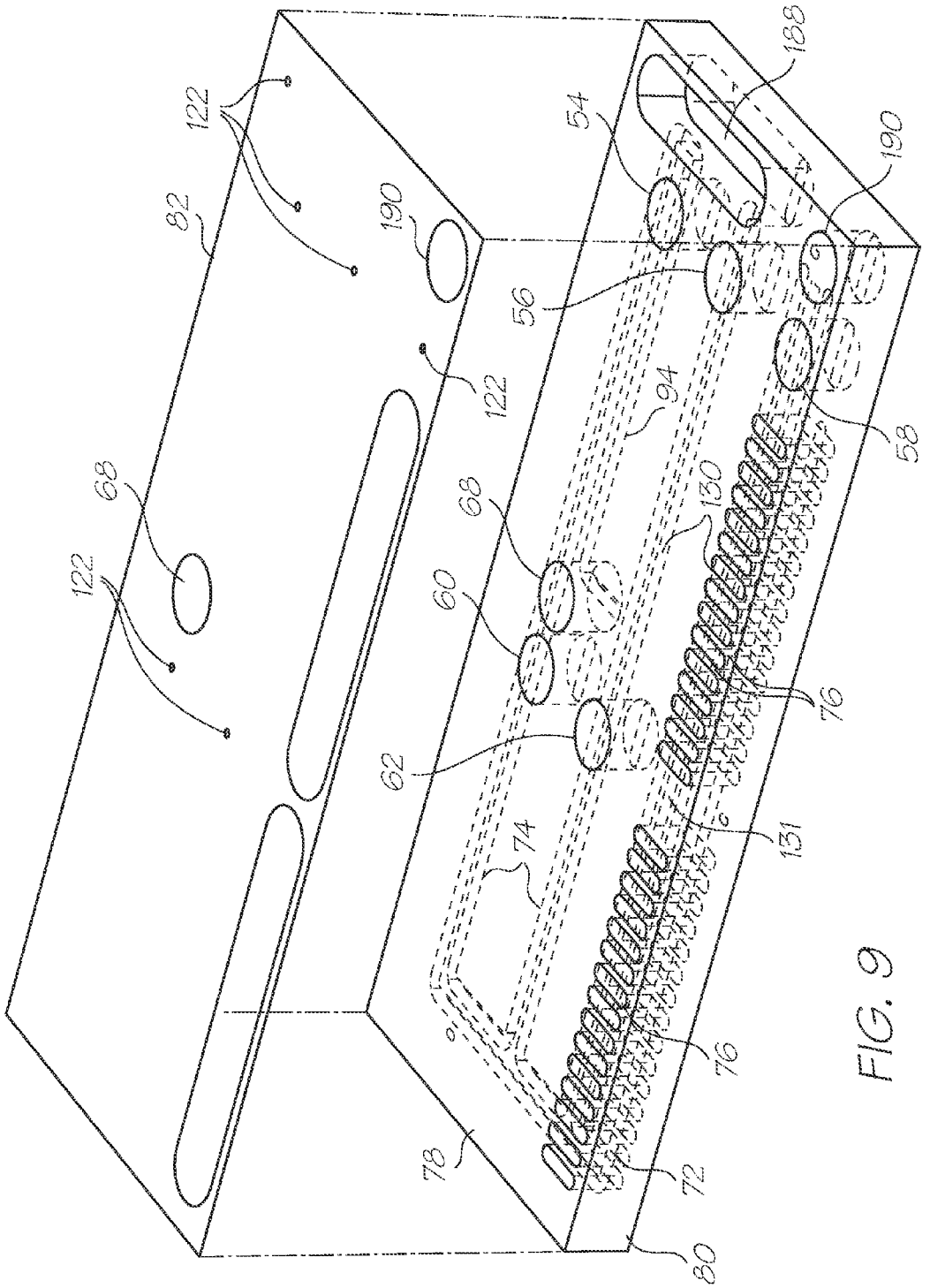

122
82
190
54
188
190
56
122
94
58
68
68
130
60
76
62
74
131
76
78
72
80

FIG. 9

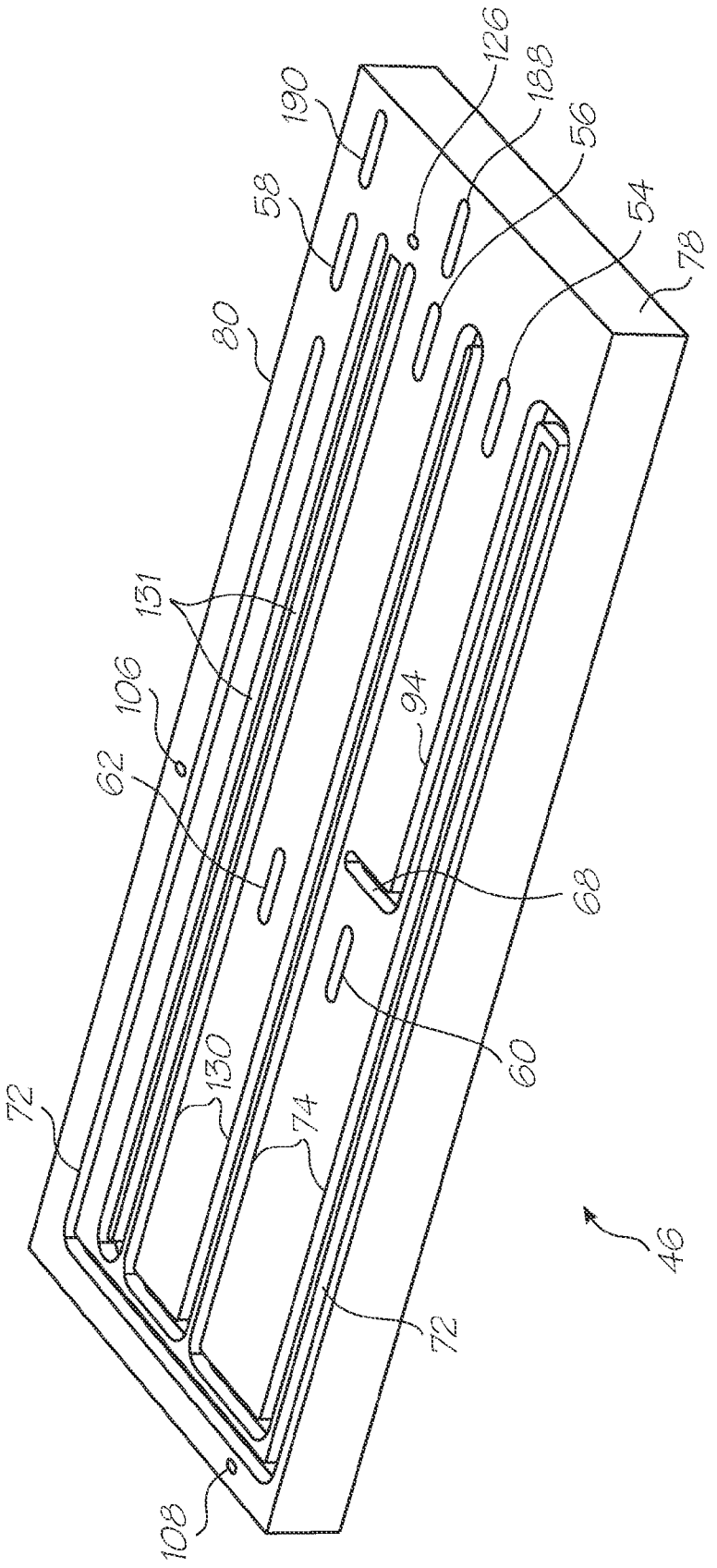


FIG. 10

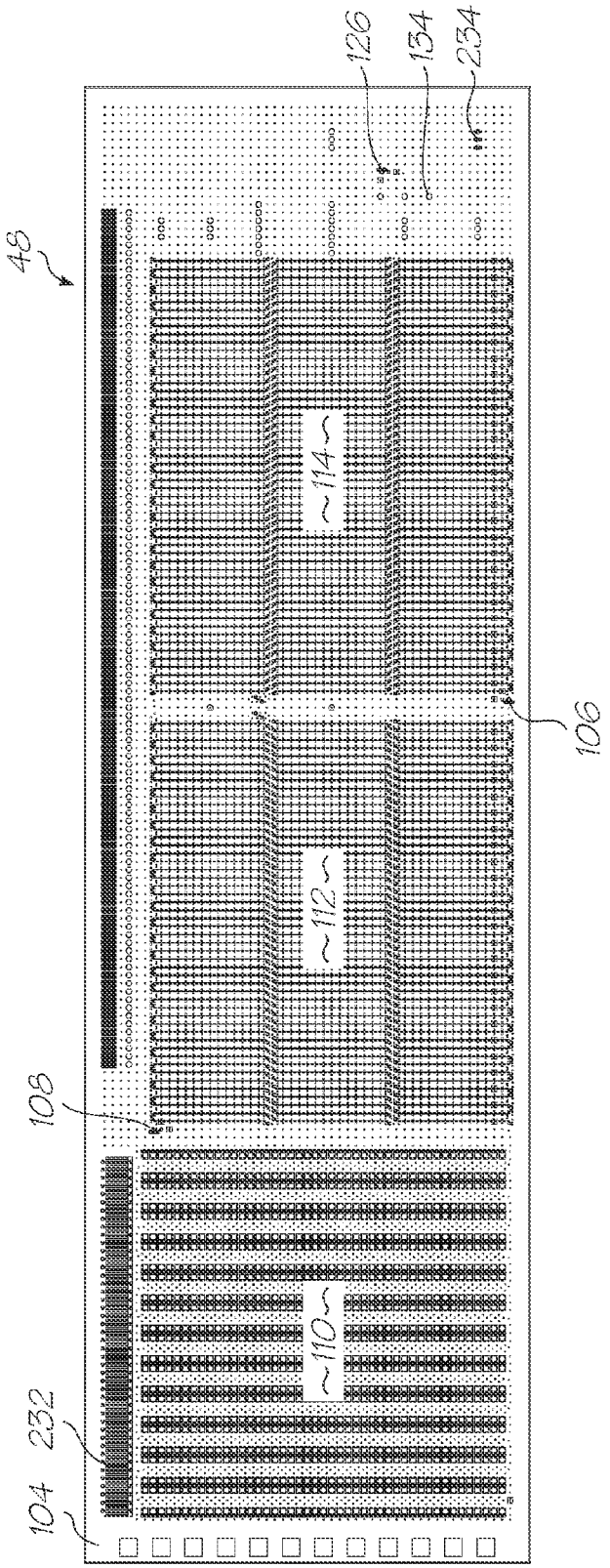


FIG. 11

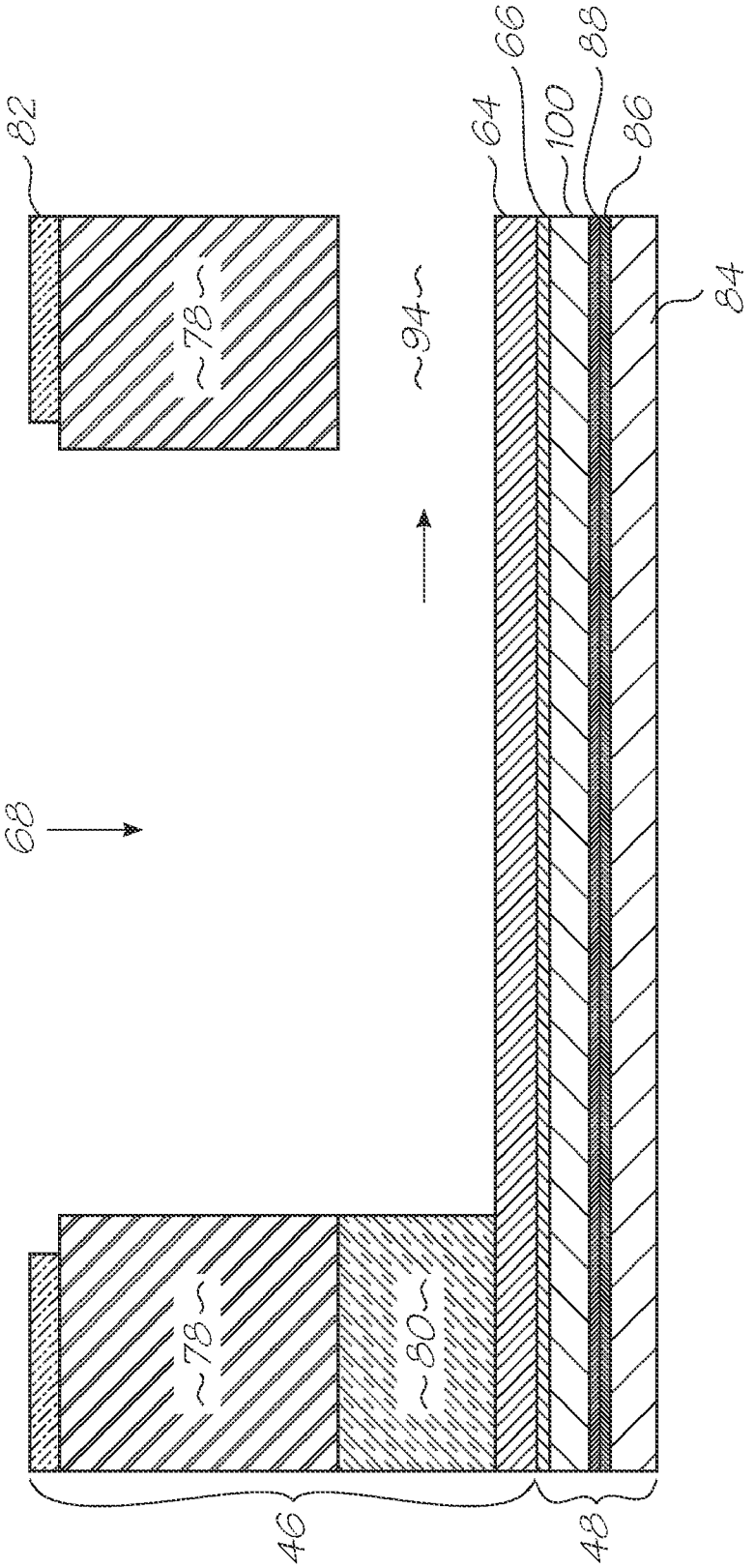


FIG. 12

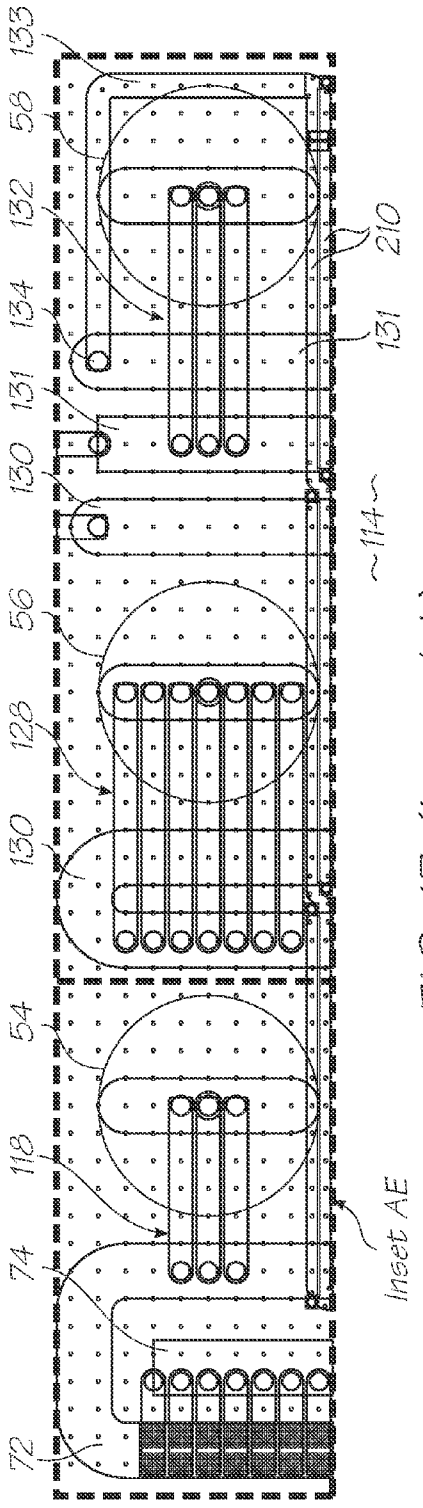


FIG. 13 (Inset AA)

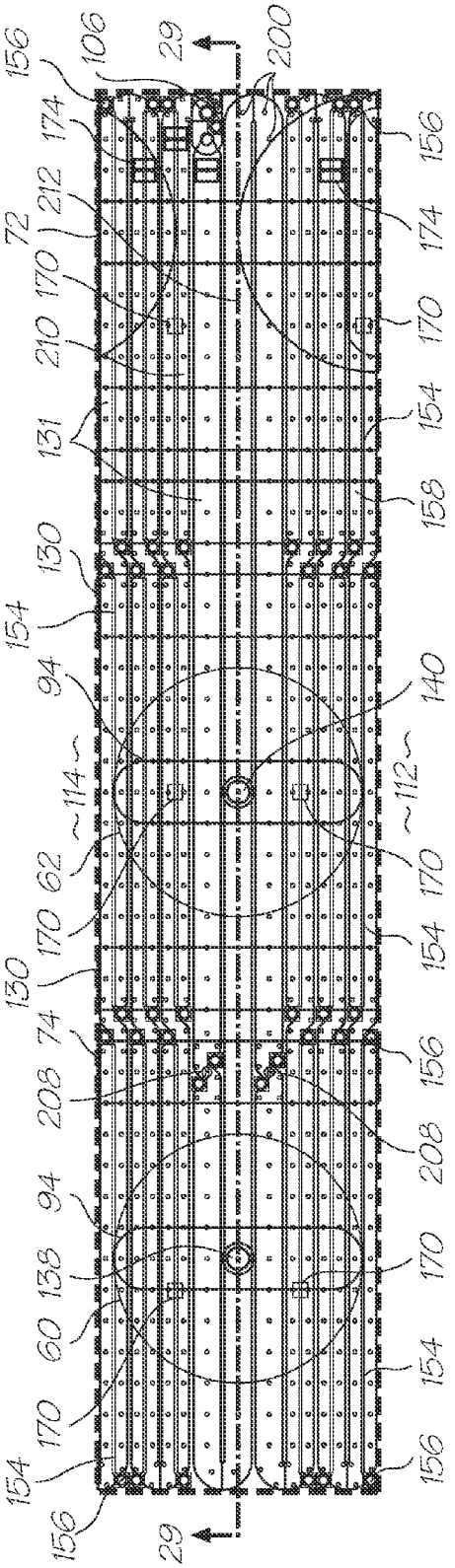


FIG. 14 (Inset AB)

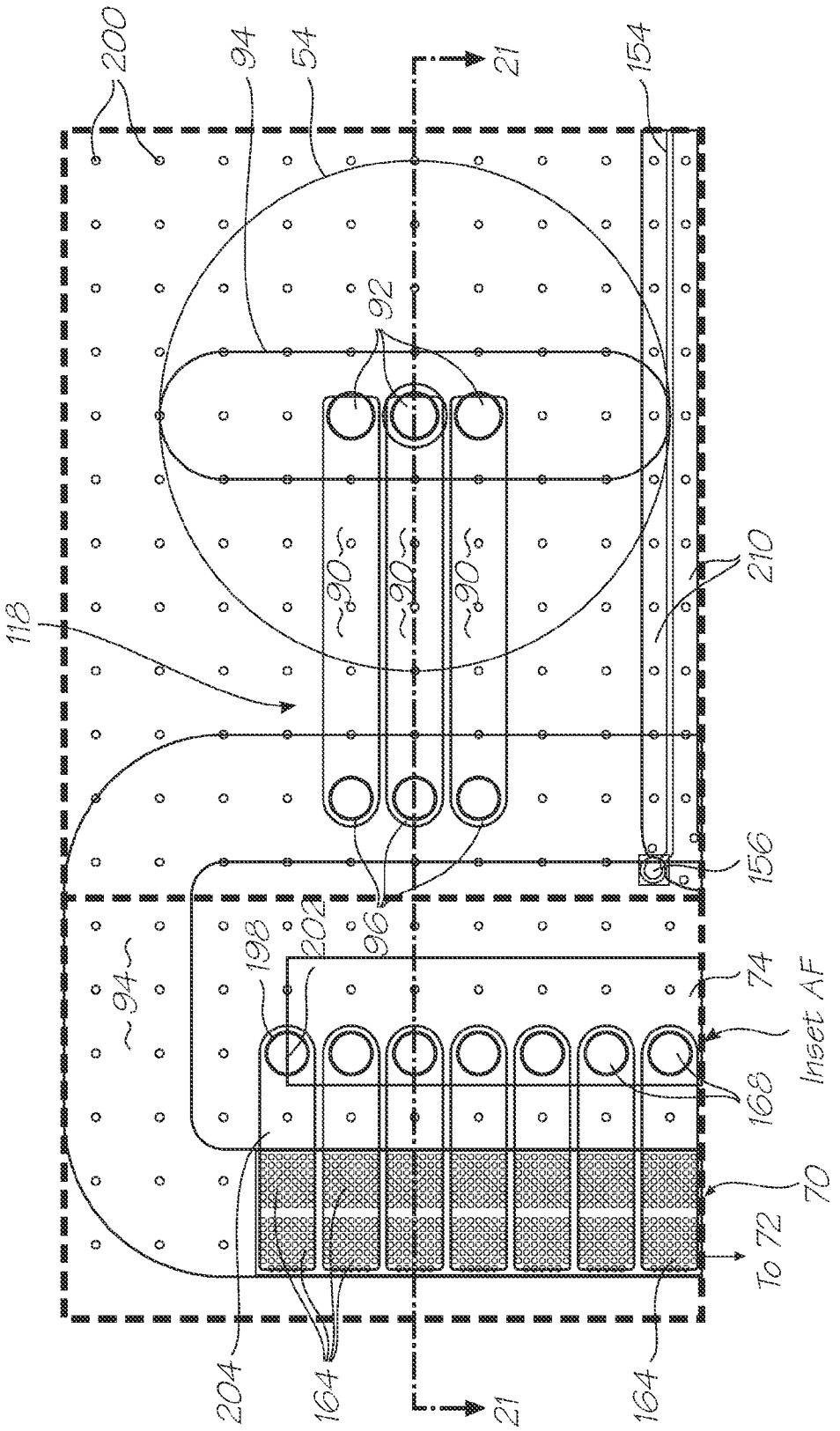


FIG. 15 (Inset AE)

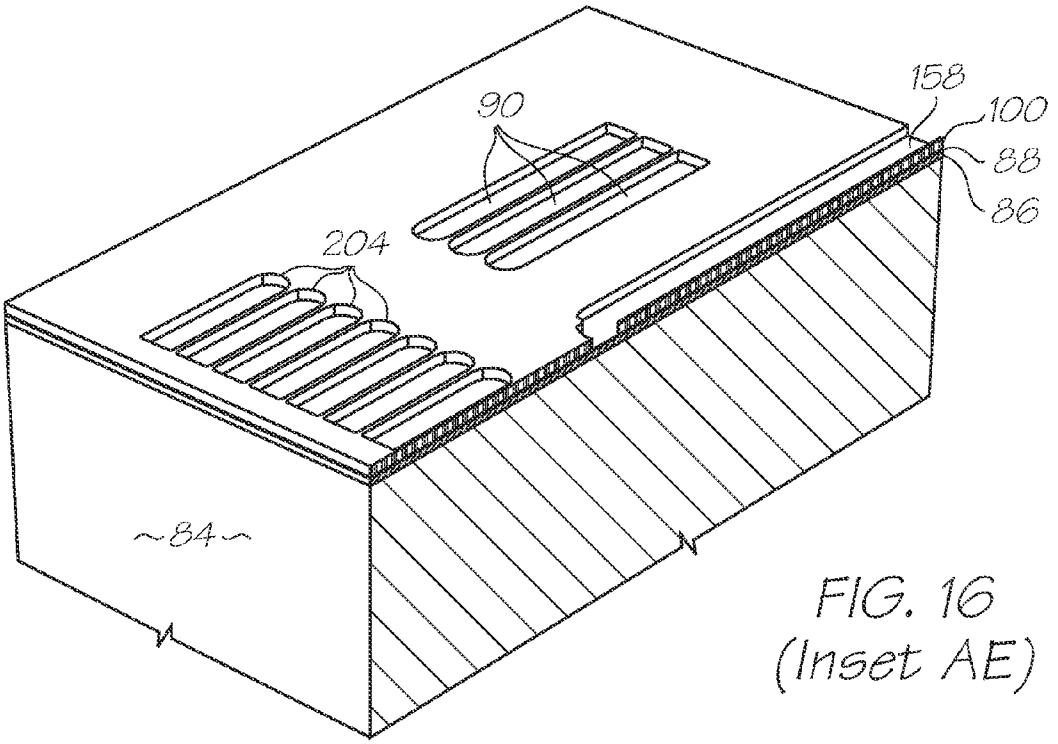


FIG. 16
(Inset AE)

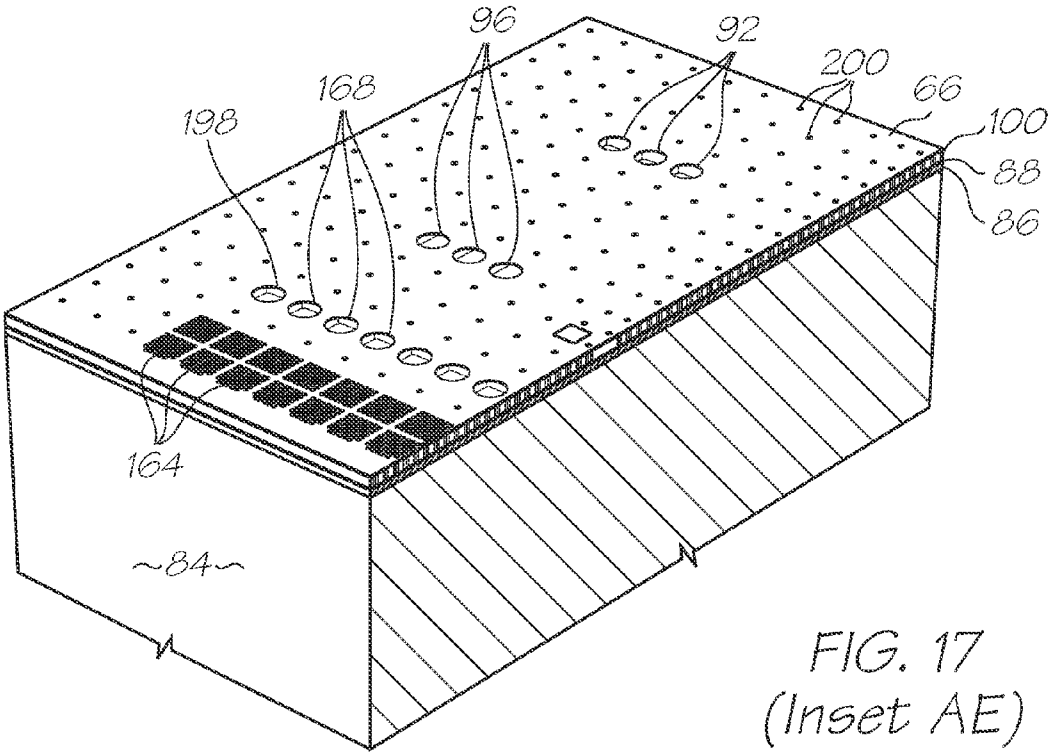


FIG. 17
(Inset AE)

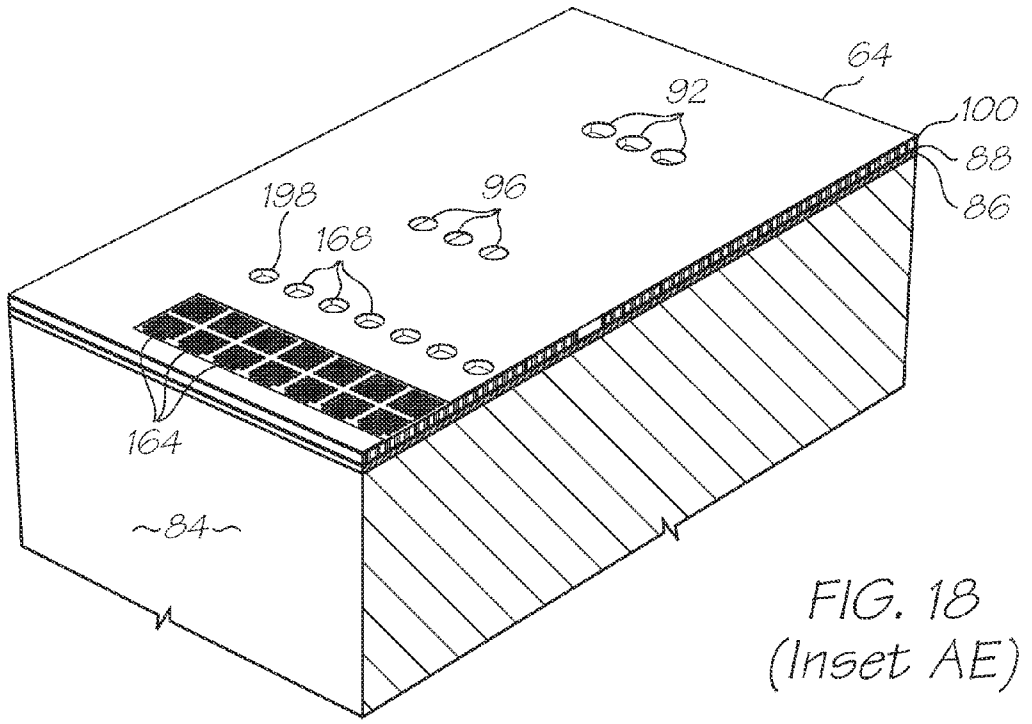


FIG. 18
(Inset AE)

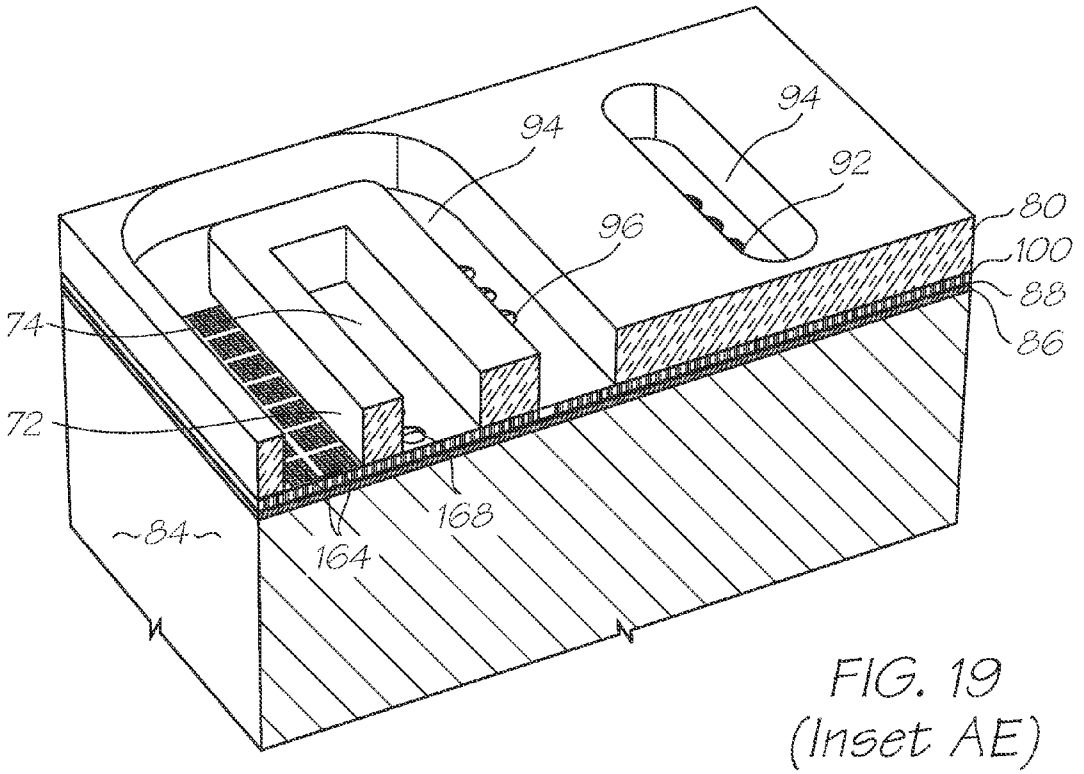


FIG. 19
(Inset AE)

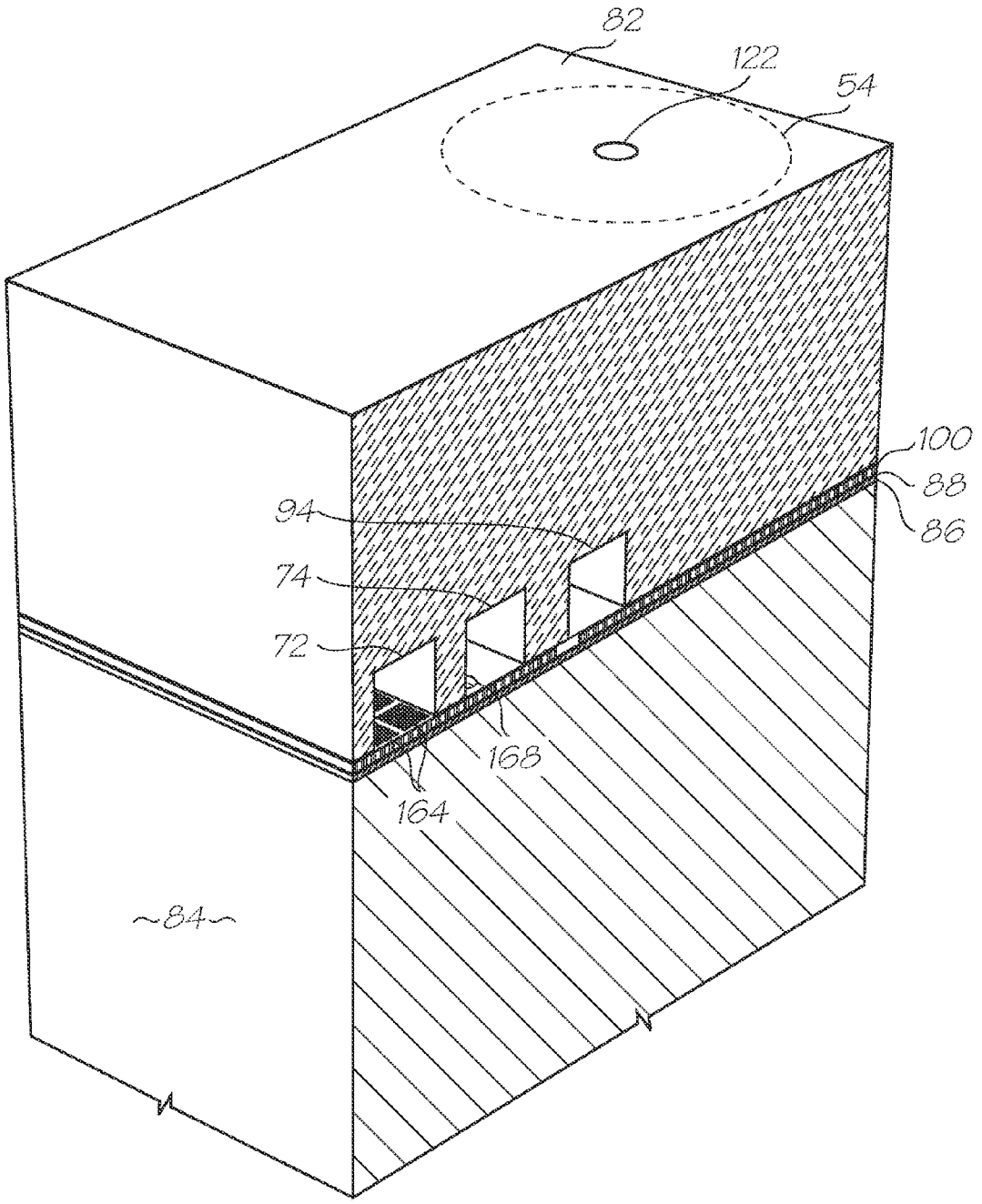


FIG. 20
(Inset AE)

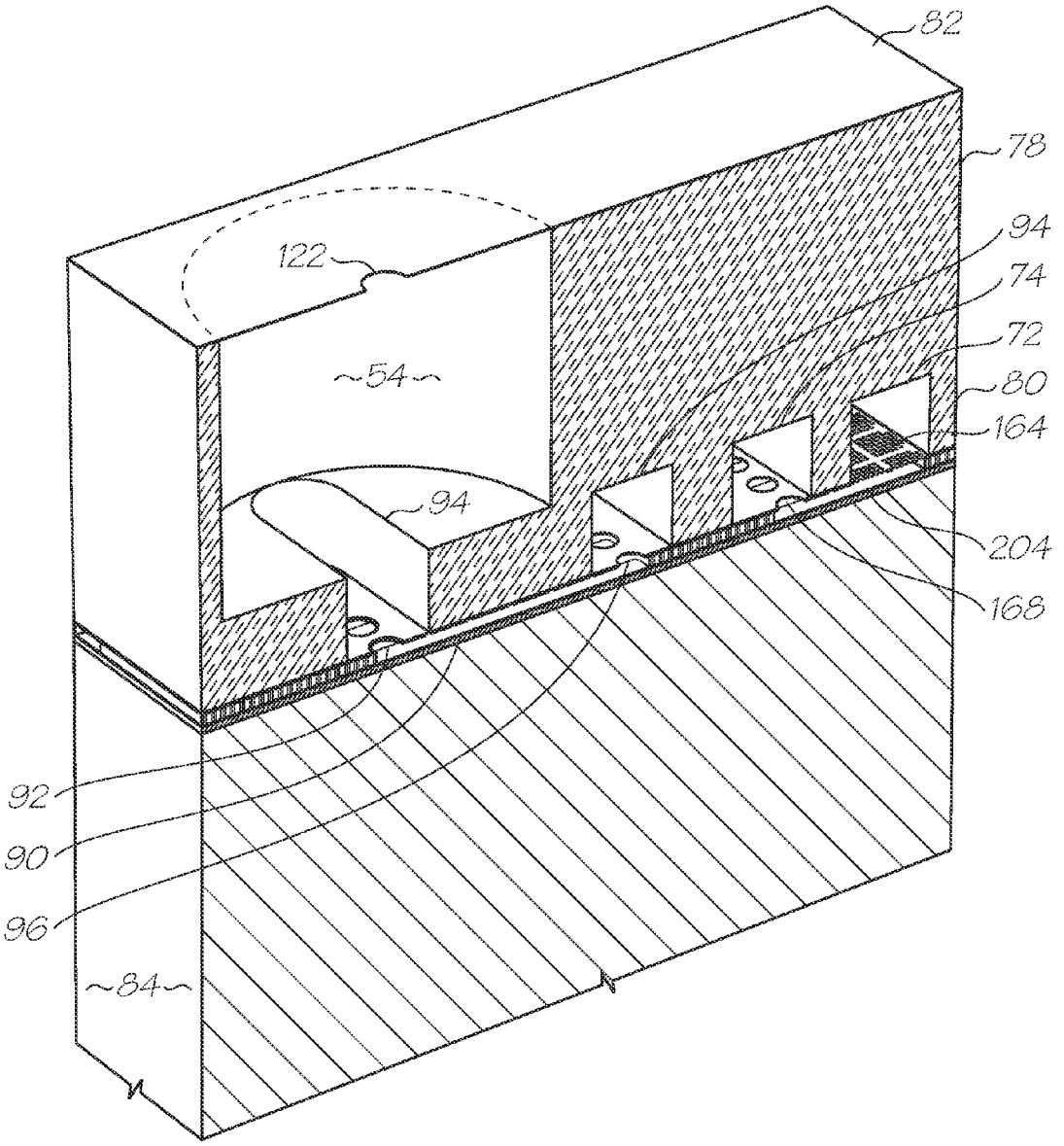


FIG. 21
(Inset AE)

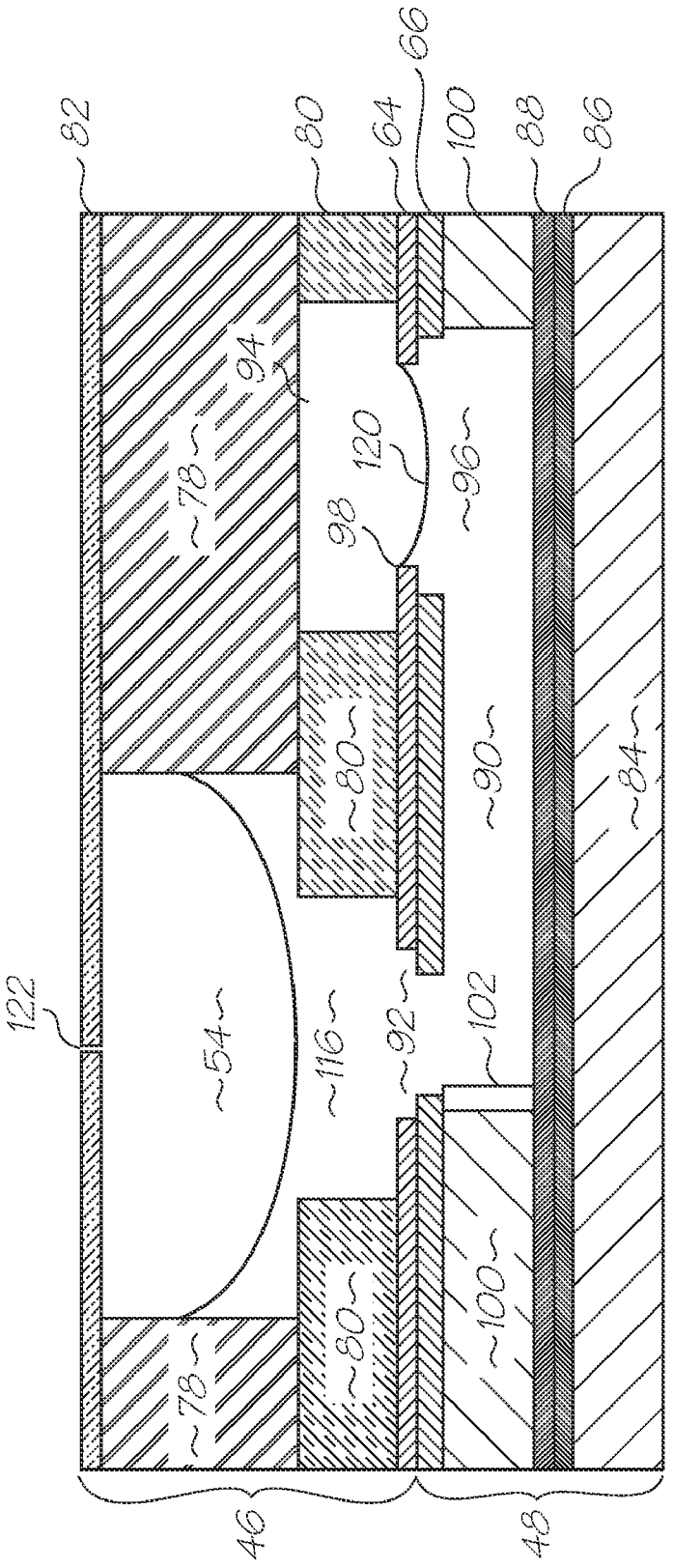

82
80
64
66
100
88
86
94
78
120
98
96
80
90
84
122
54
116
92
102
100
78
80
46
48

FIG. 22

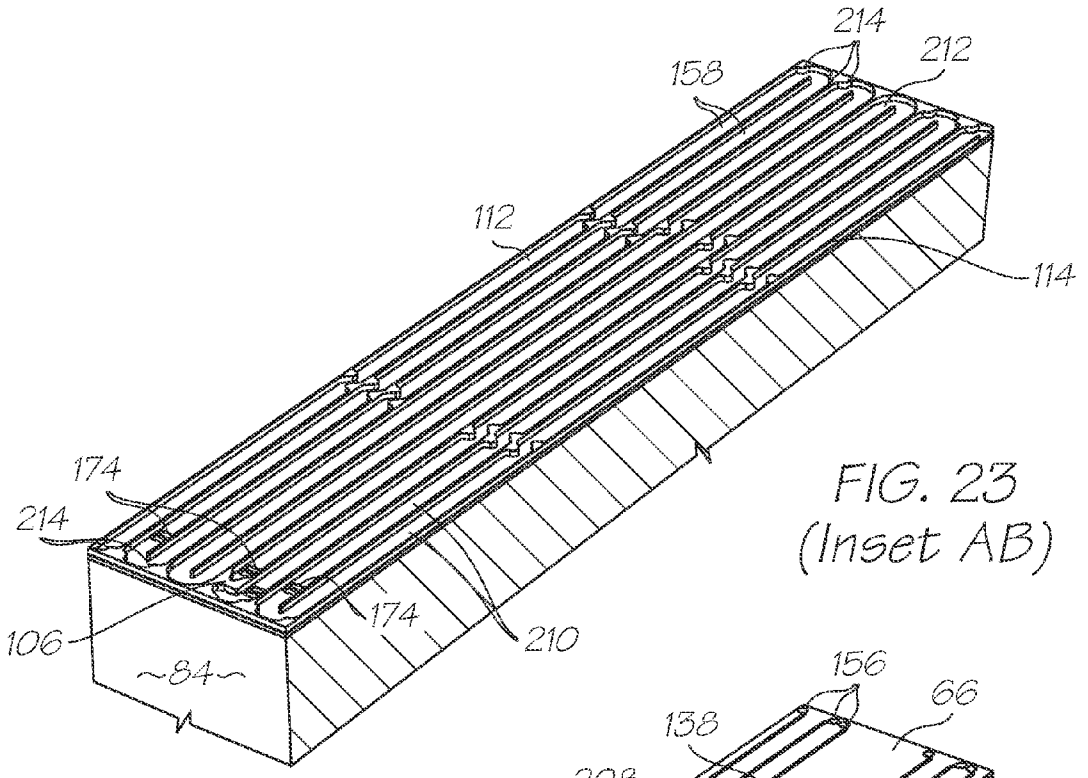


FIG. 23
(Inset AB)

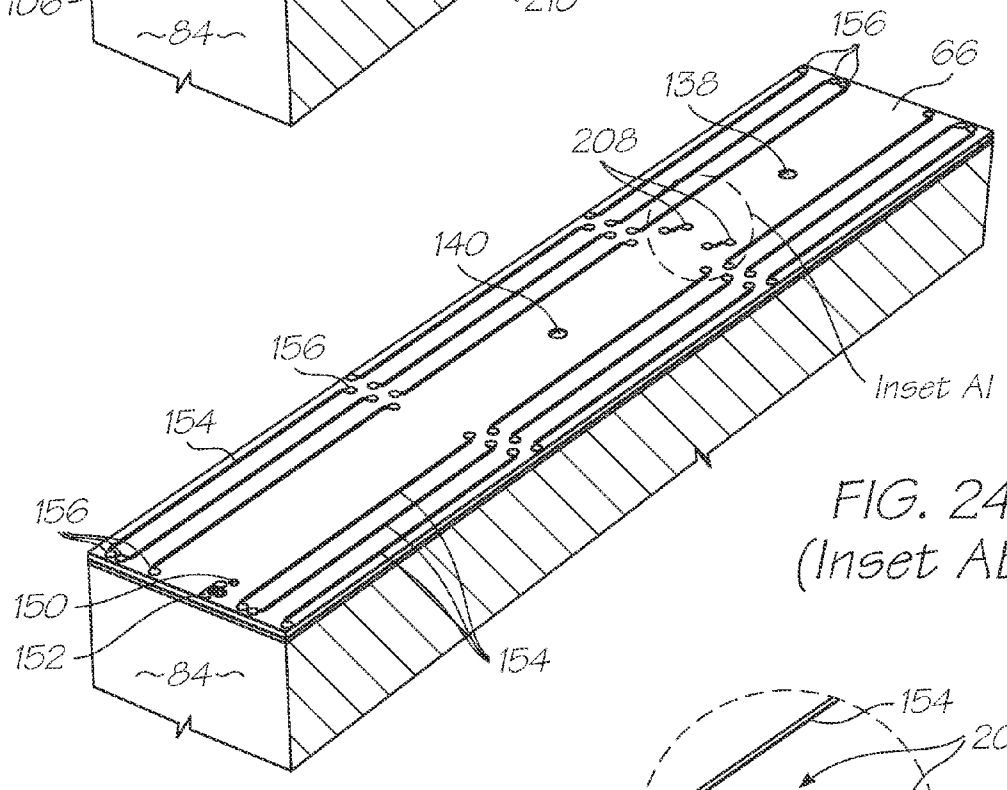


FIG. 24
(Inset AB)

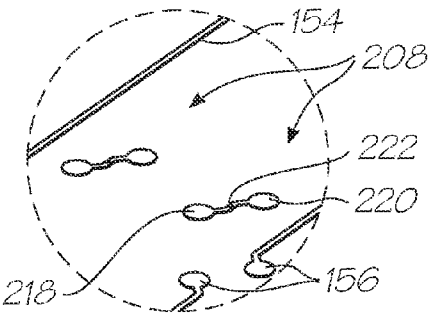


FIG. 25
(Inset AI)

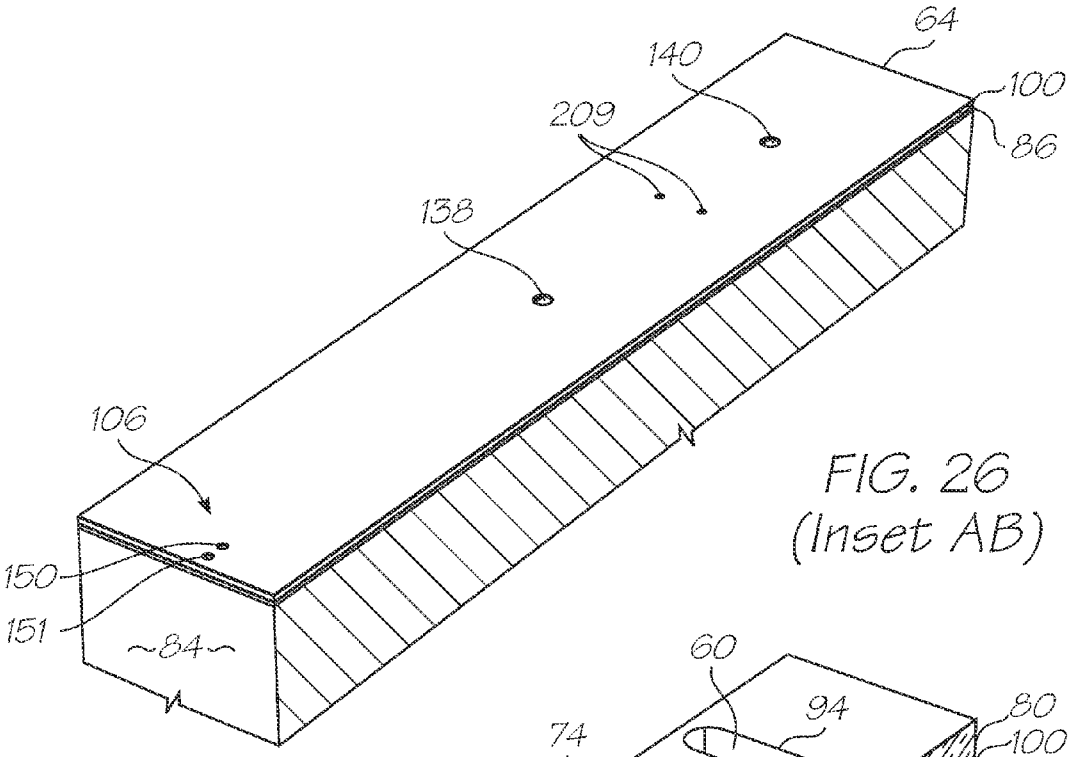


FIG. 26
(Inset AB)

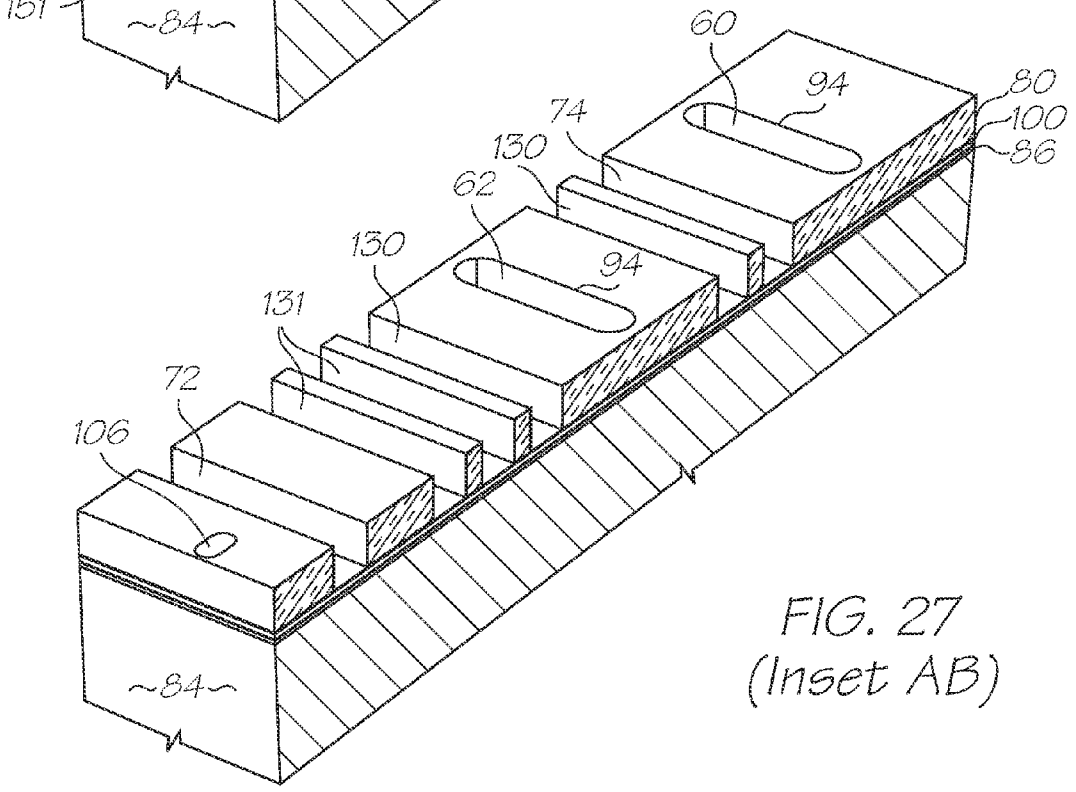


FIG. 27
(Inset AB)

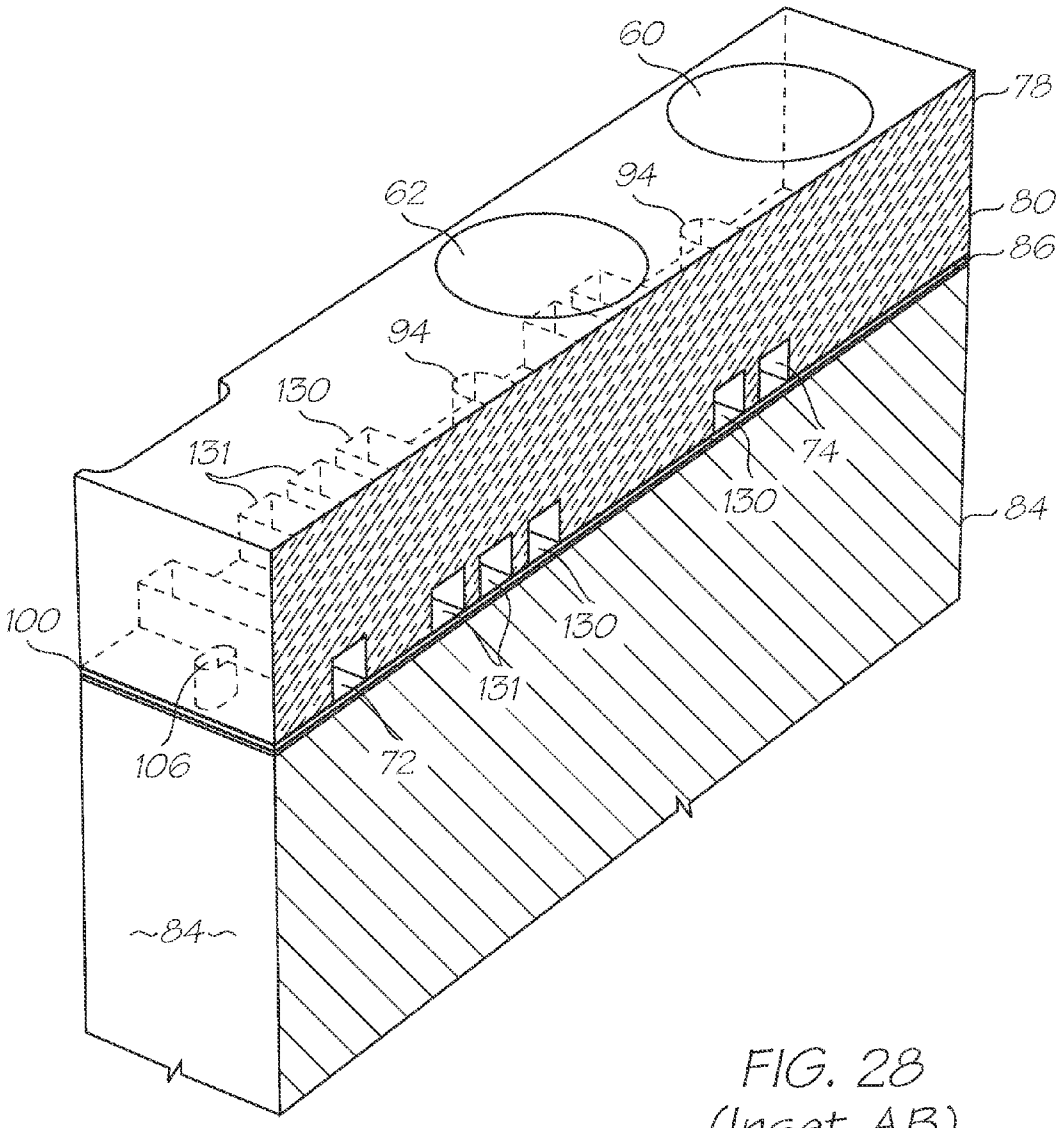


FIG. 28
(Inset AB)

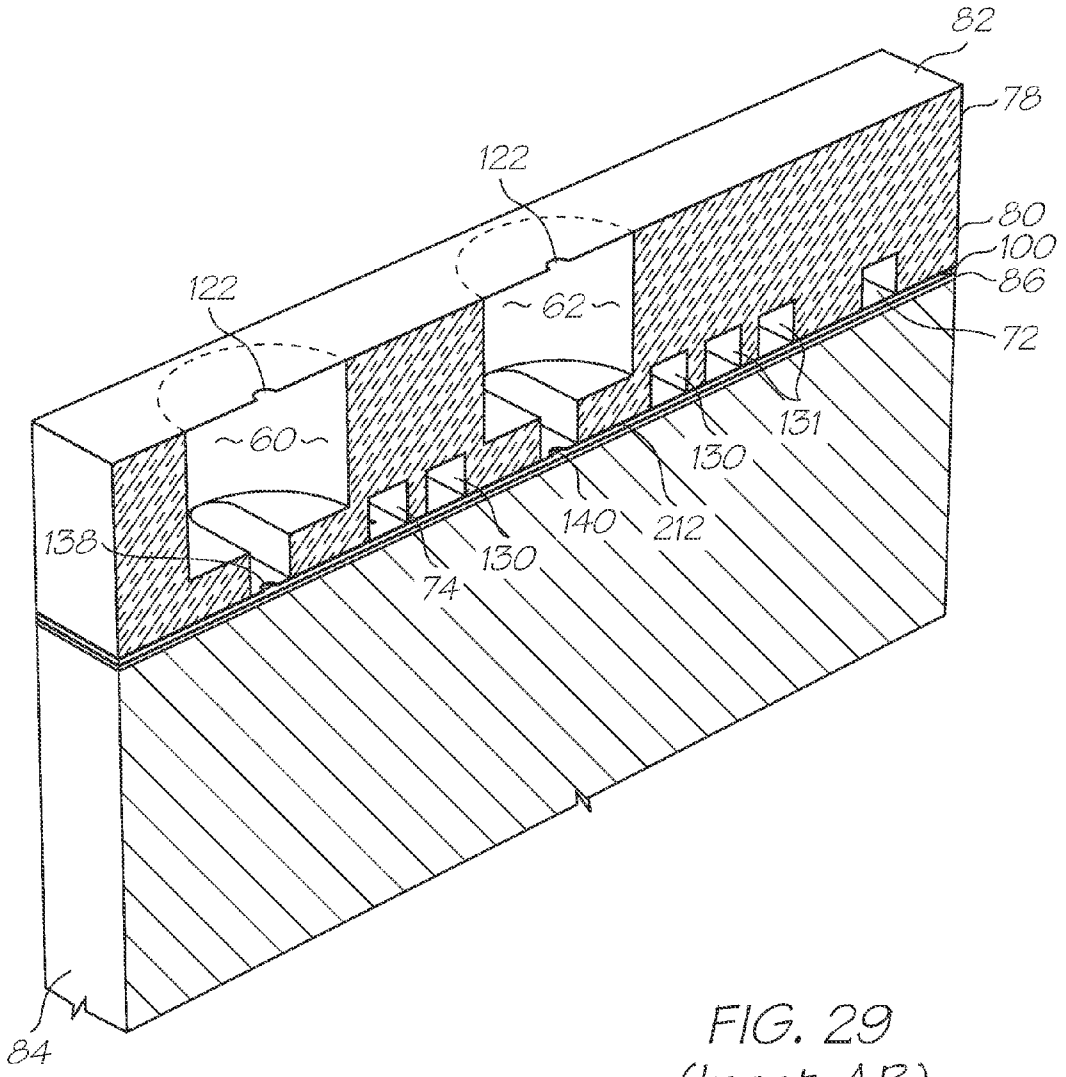


FIG. 29
(Inset AB)

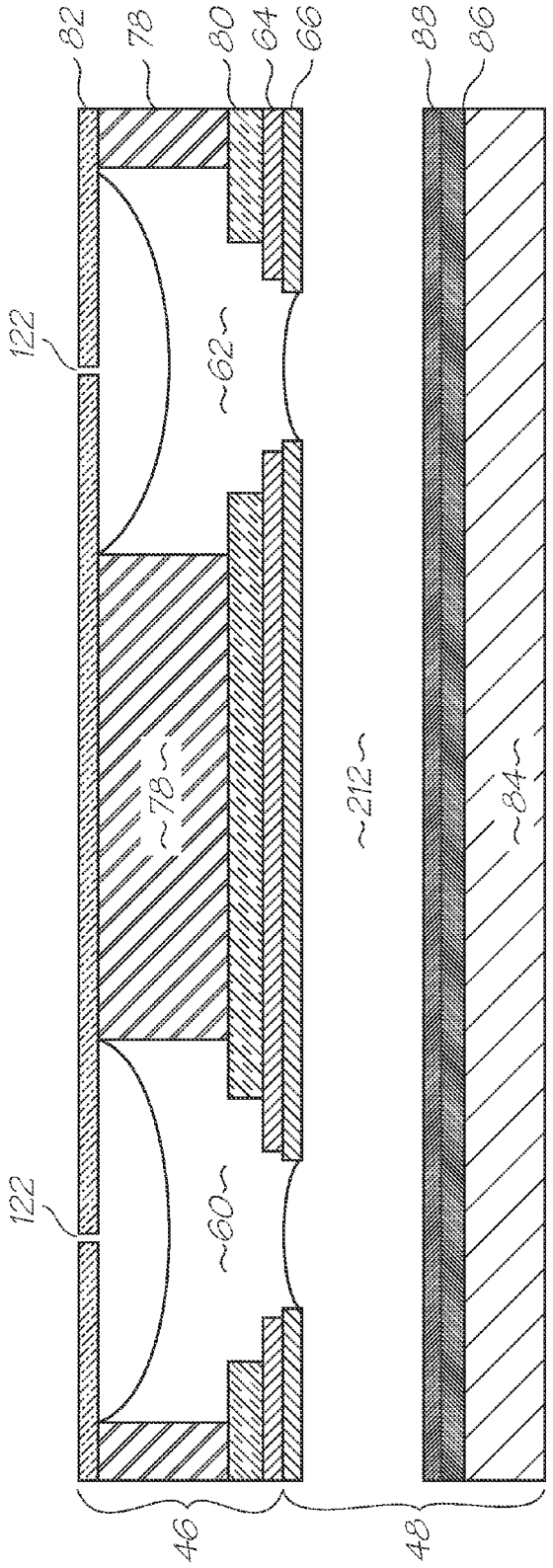

82
78
80
64
66
88
86
122
62
78
212
84
60
122
46
48

FIG. 30

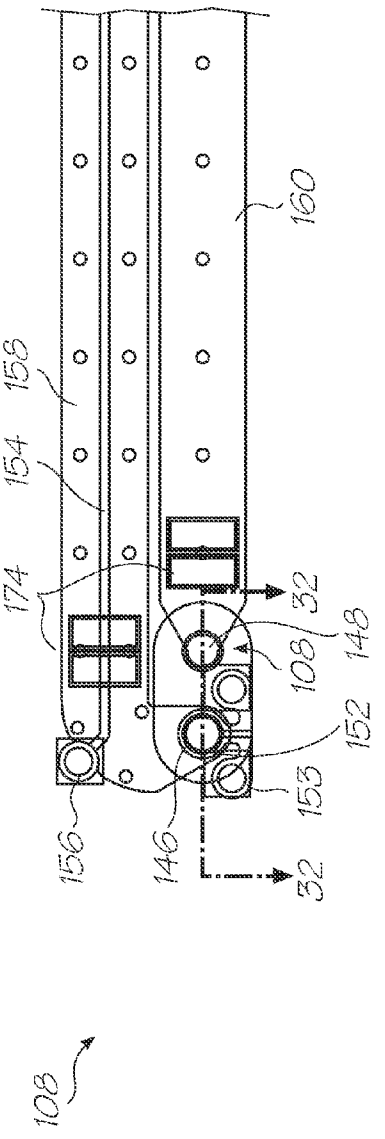

160
158
154
174
32
108
148
152
153
156
146
32
108

FIG. 31

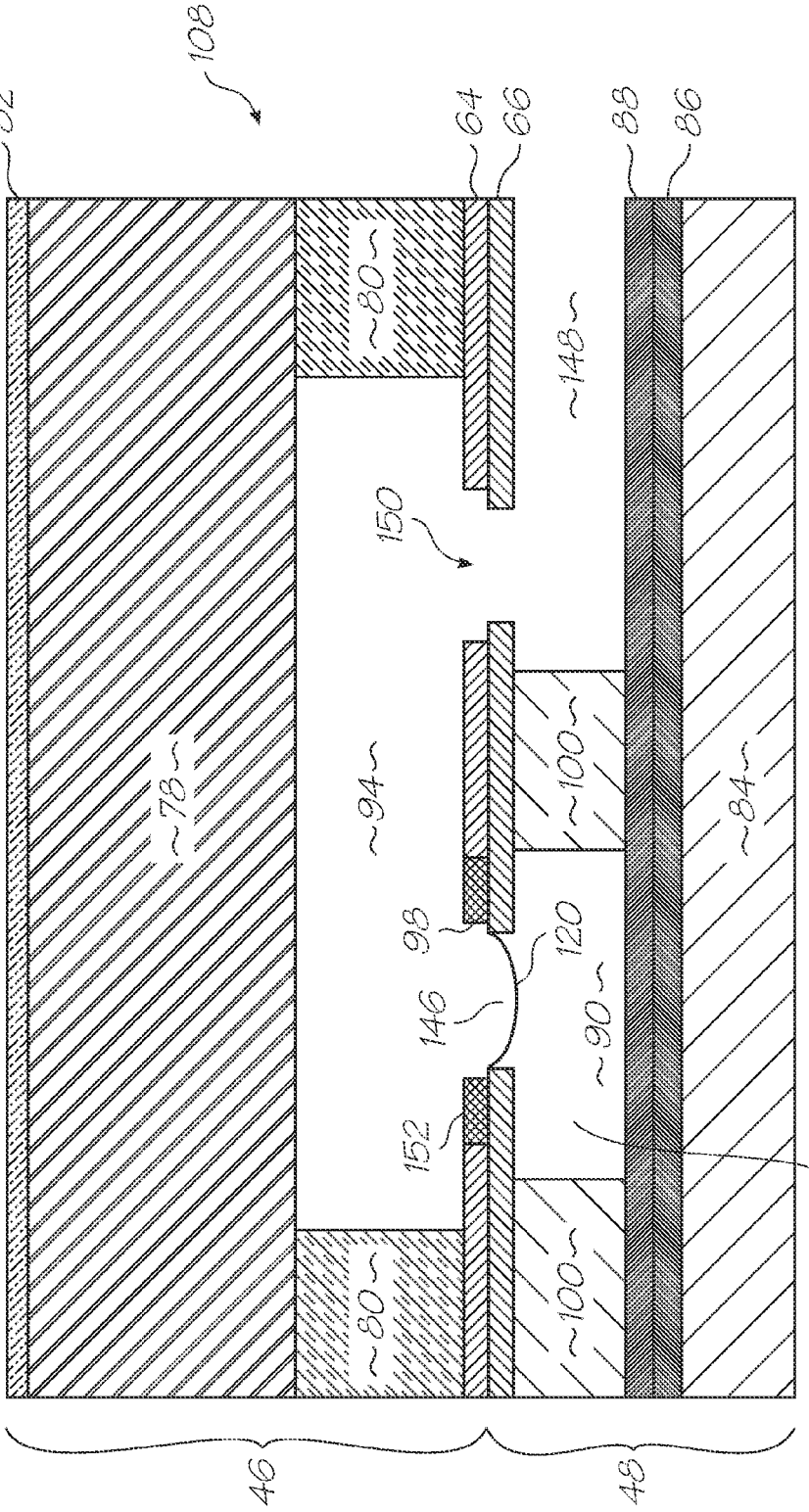

108
82
64
66
88
86
80
148
150
78
94
100
84
98
120
146
90
152
119
80
100
46
48

FIG. 32

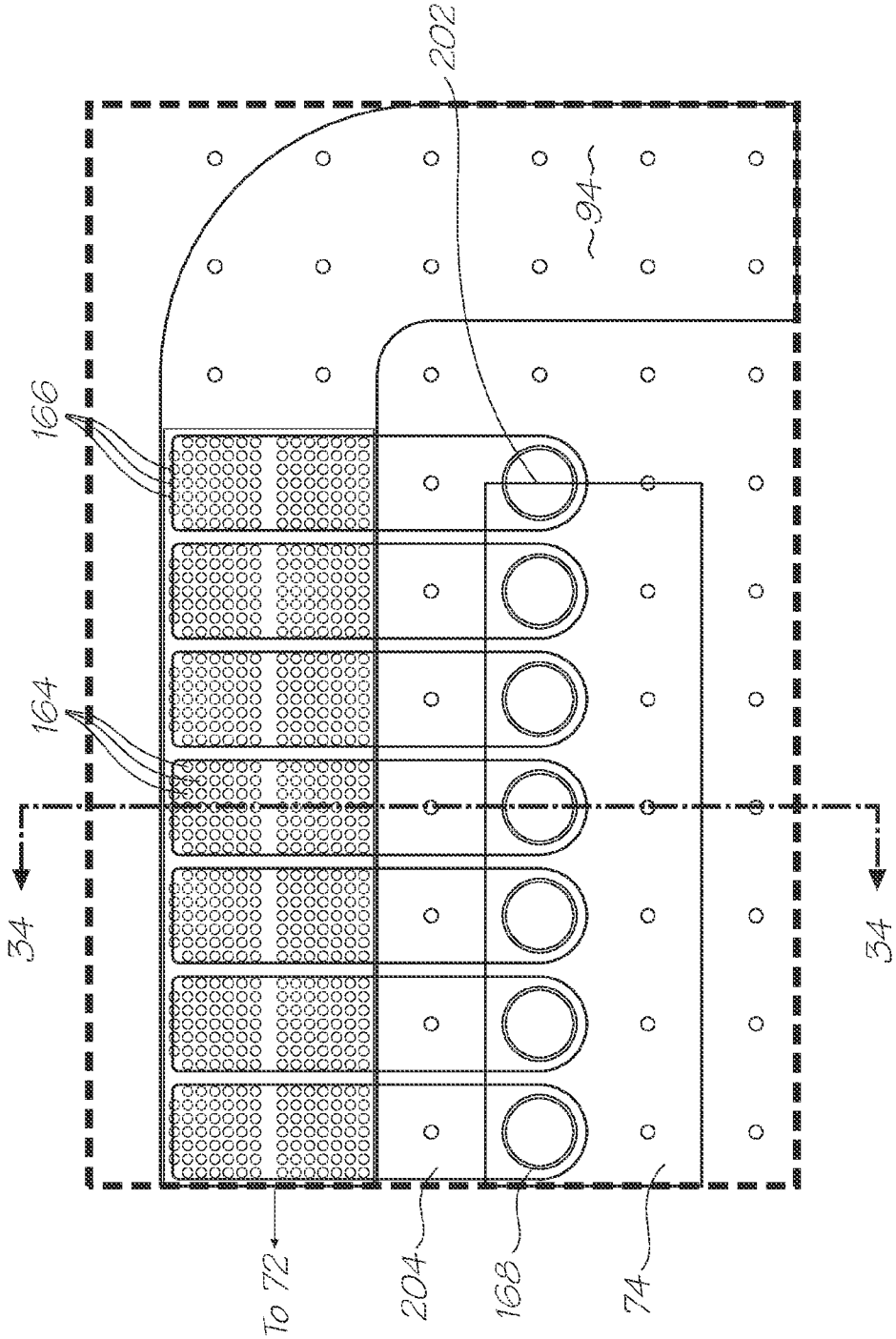


FIG. 33 (Inset AF)

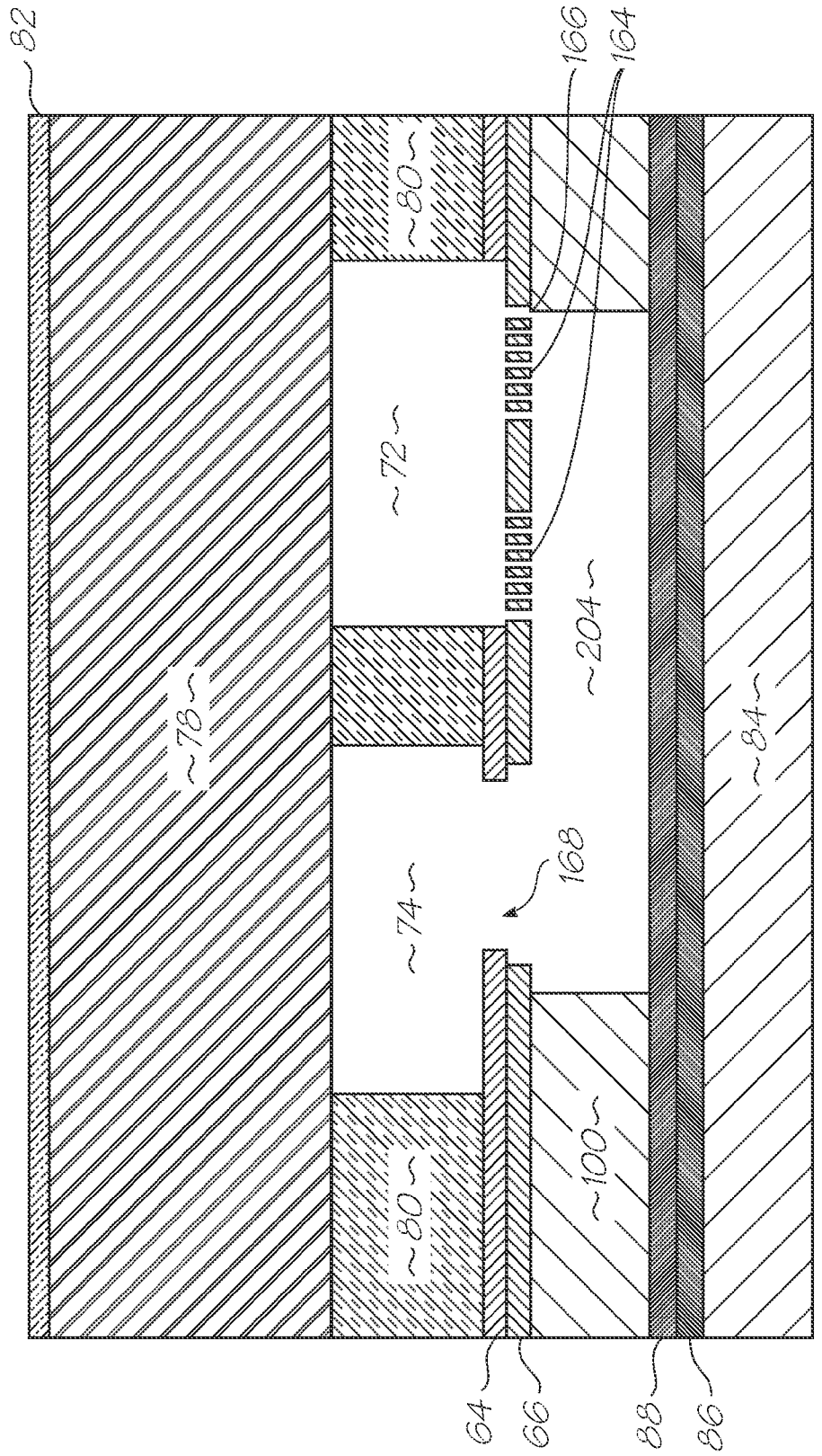


FIG. 34

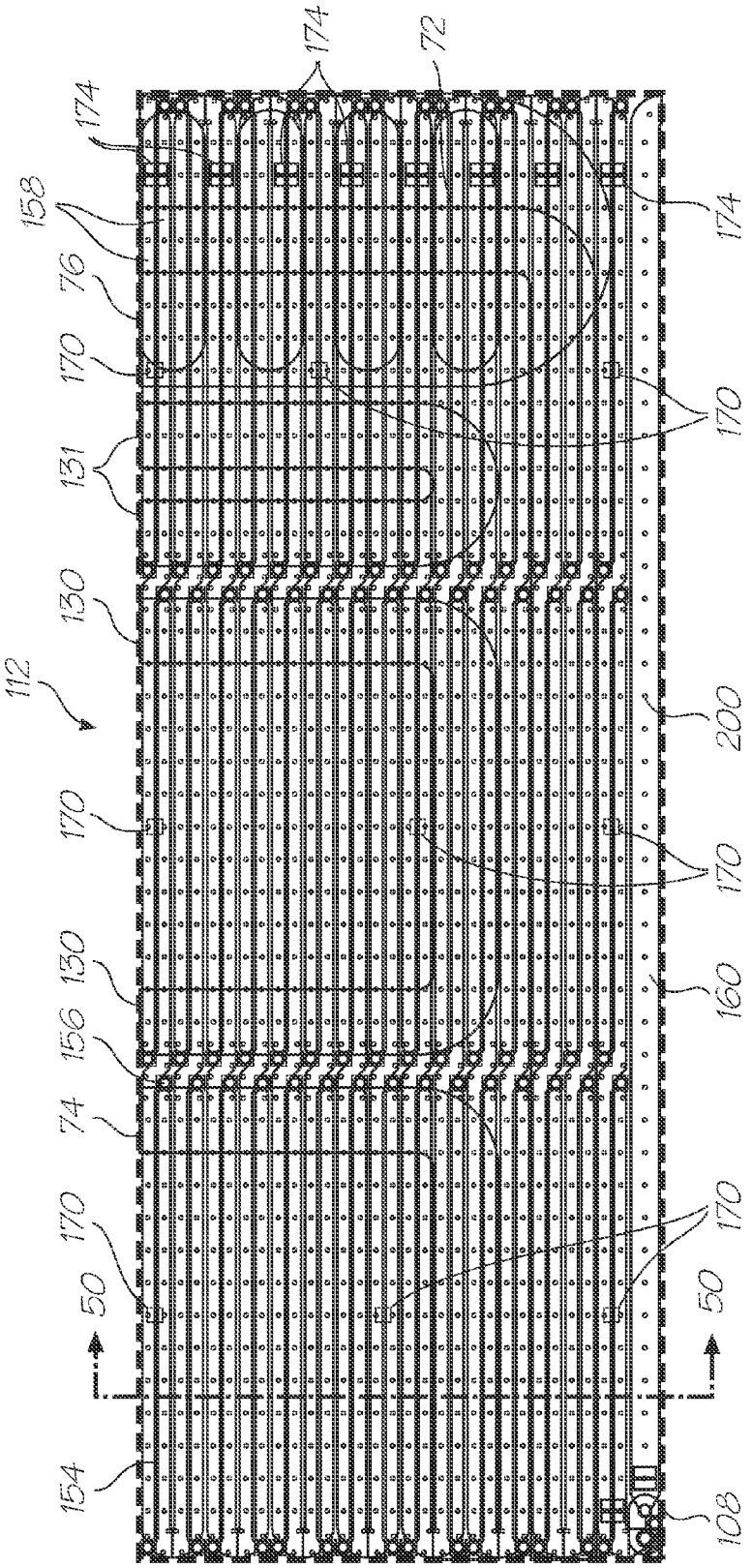


FIG. 35 (Inset AC)

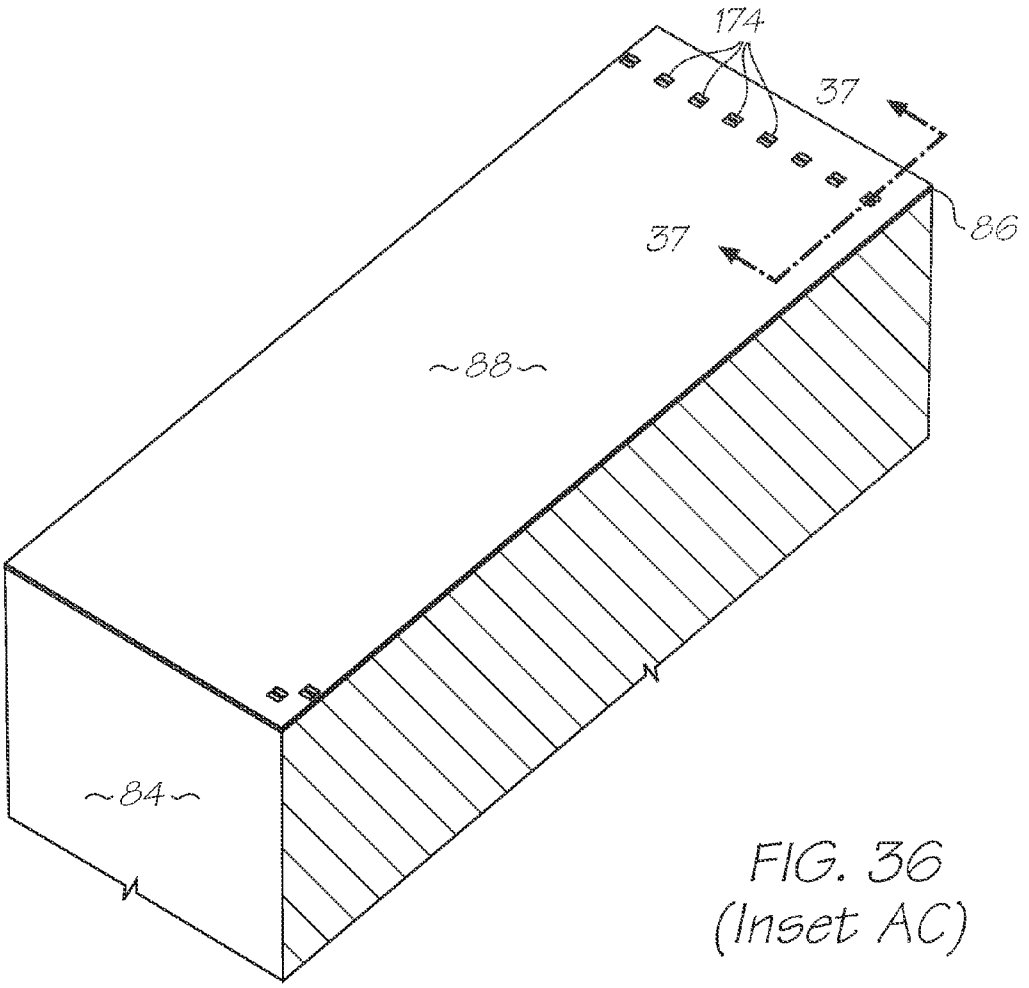


FIG. 36
(Inset AC)

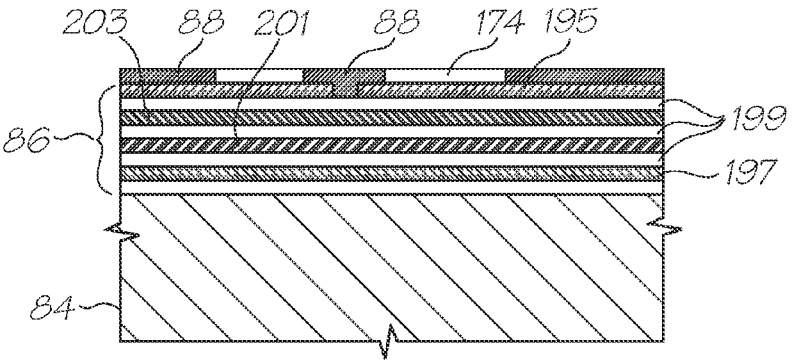


FIG. 37

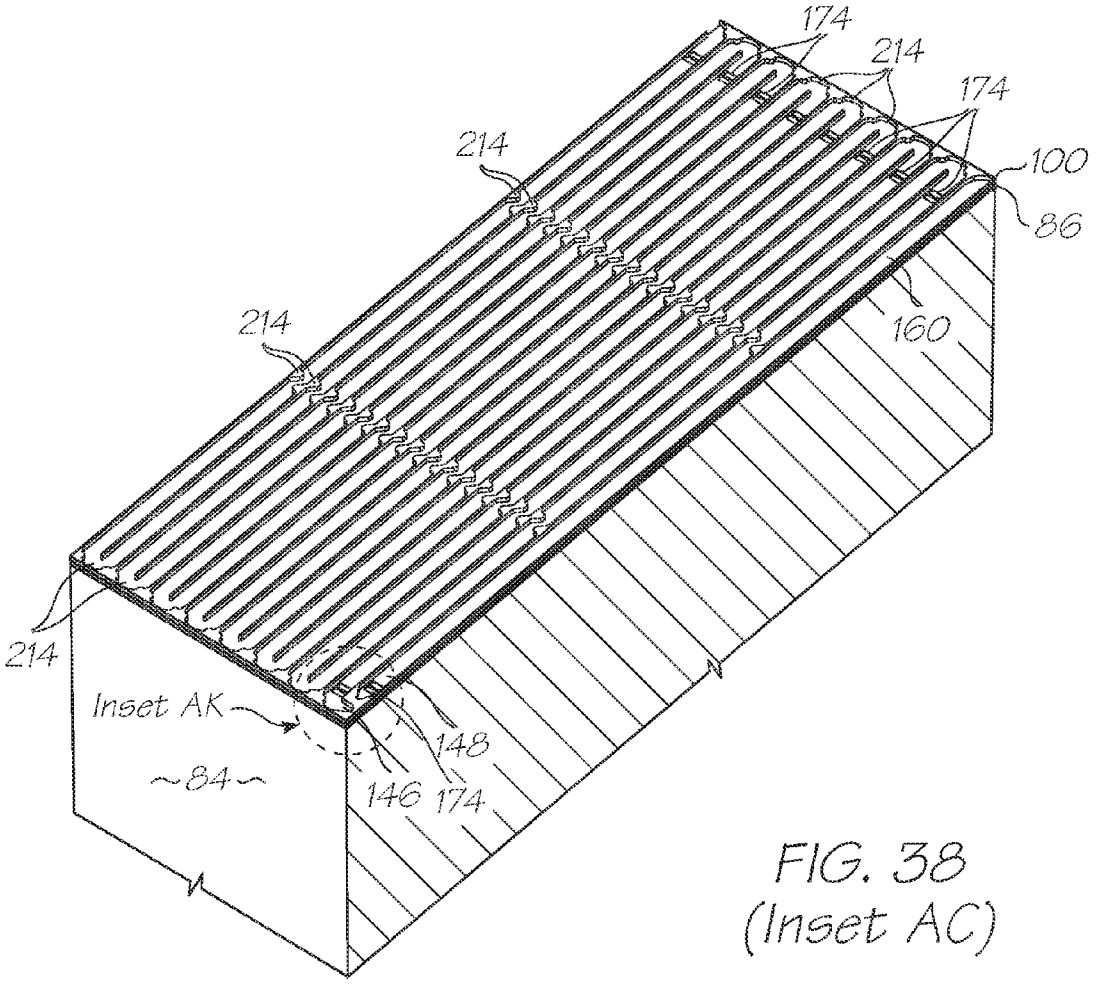


FIG. 38
(Inset AC)

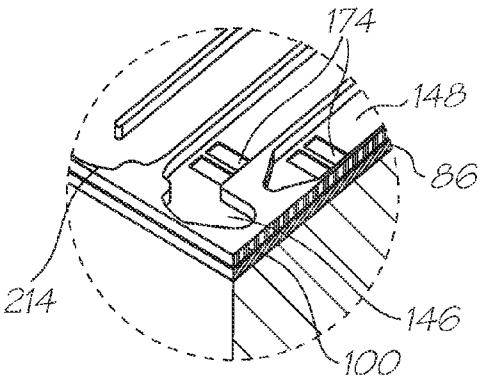


FIG. 39
(Inset AK)

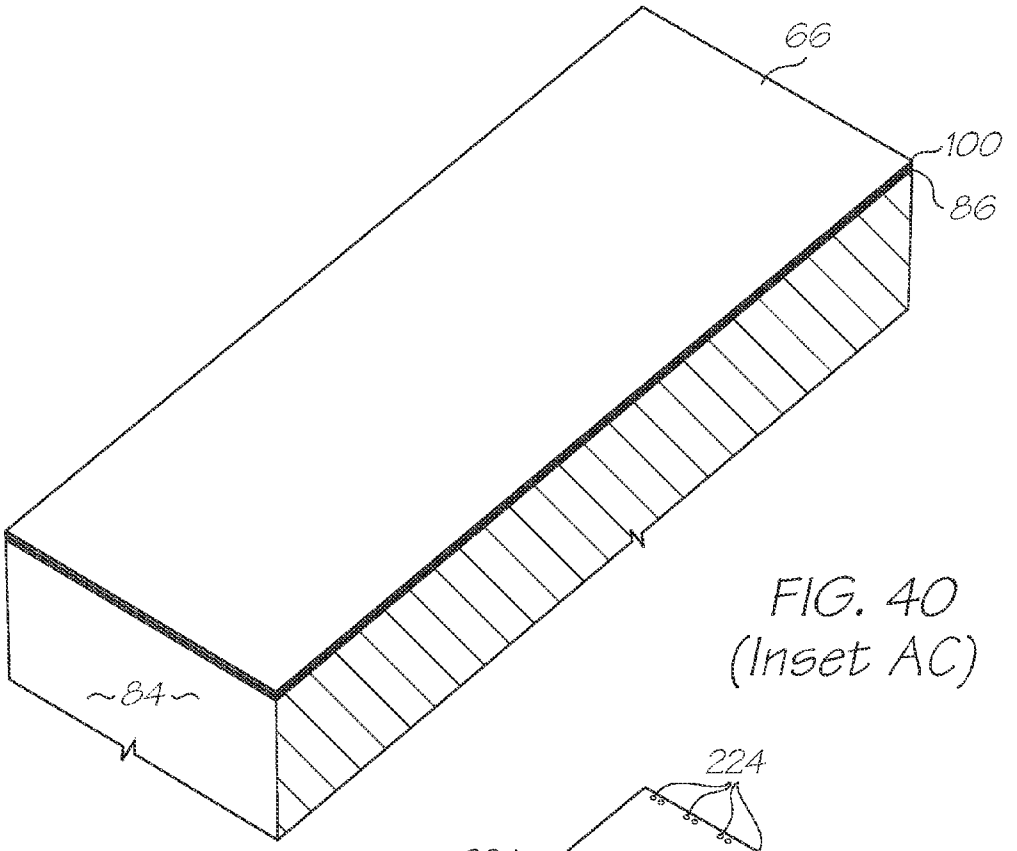


FIG. 40
(Inset AC)

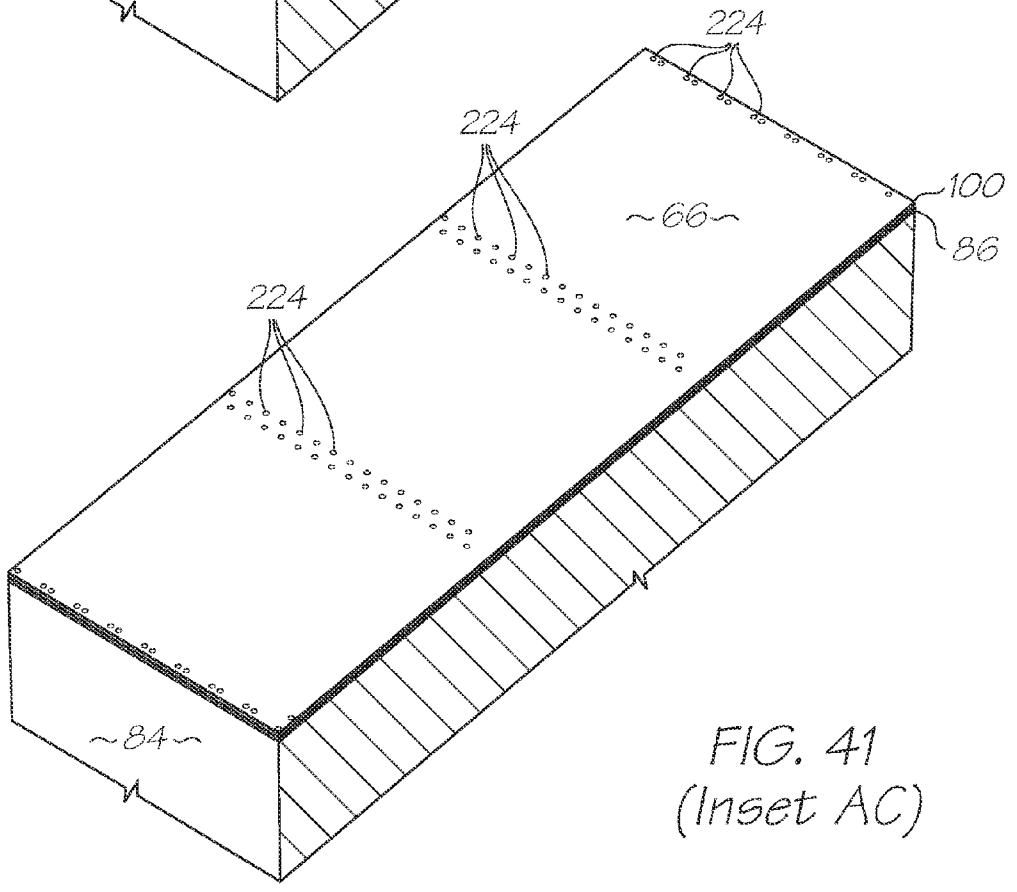


FIG. 41
(Inset AC)

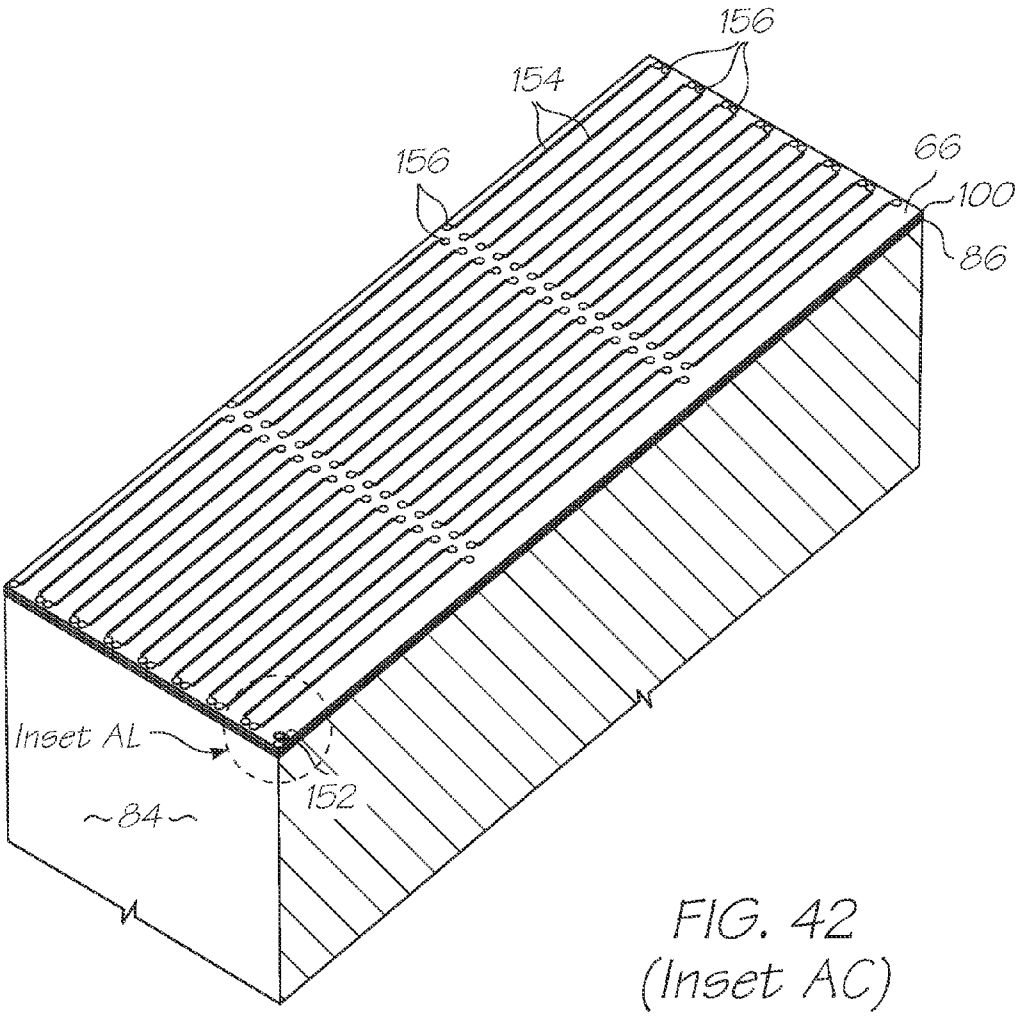


FIG. 42
(Inset AC)

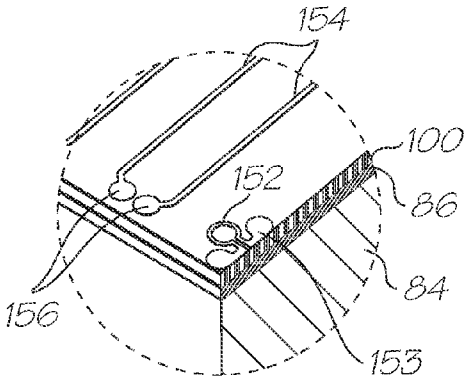


FIG. 43
(Inset AL)

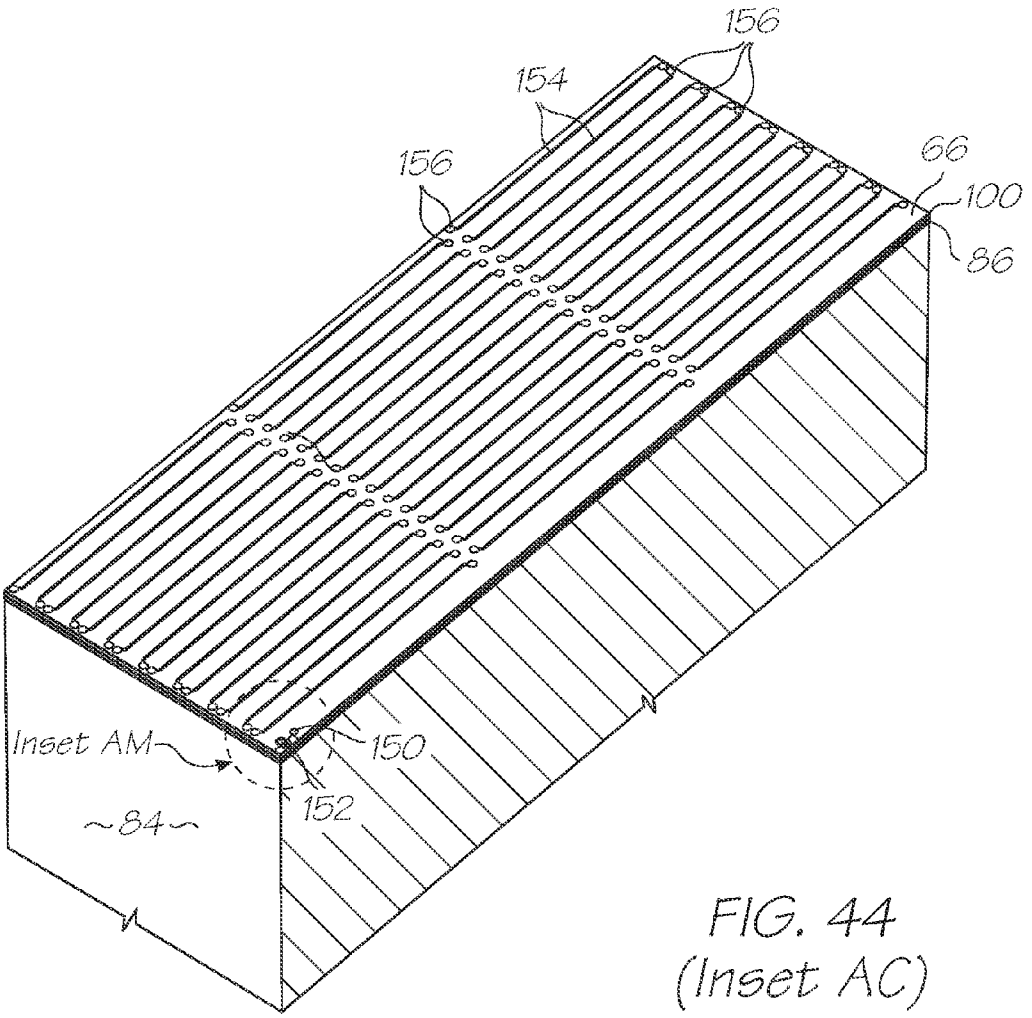


FIG. 44
(Inset AC)

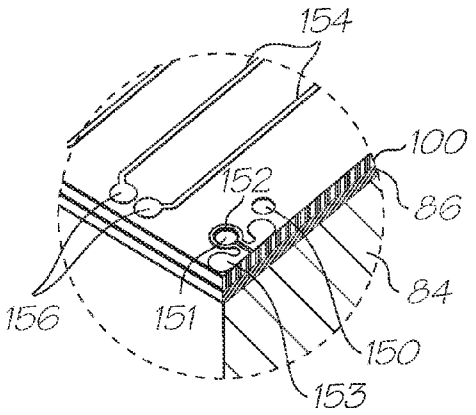


FIG. 45
(Inset AM)

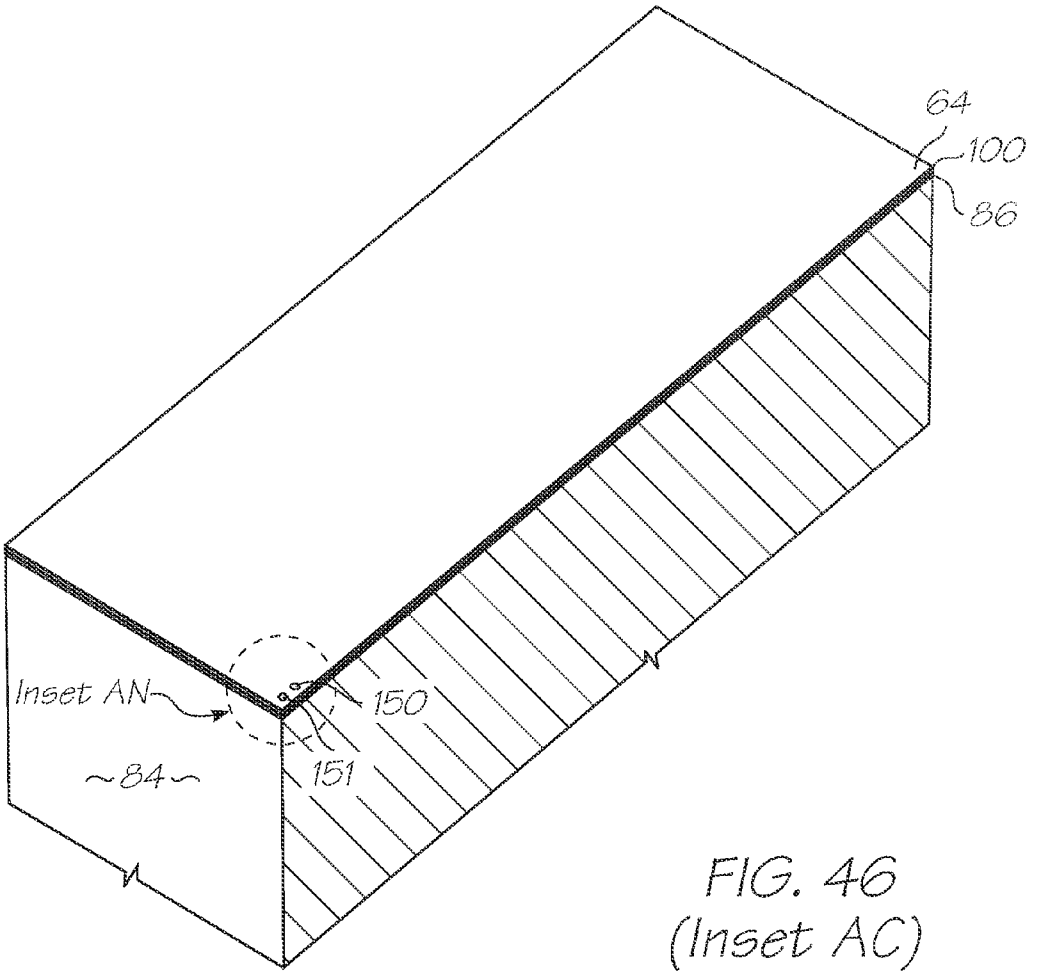


FIG. 46
(Inset AC)

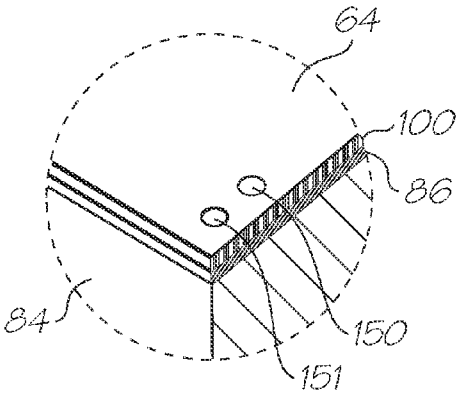


FIG. 47
(Inset AN)

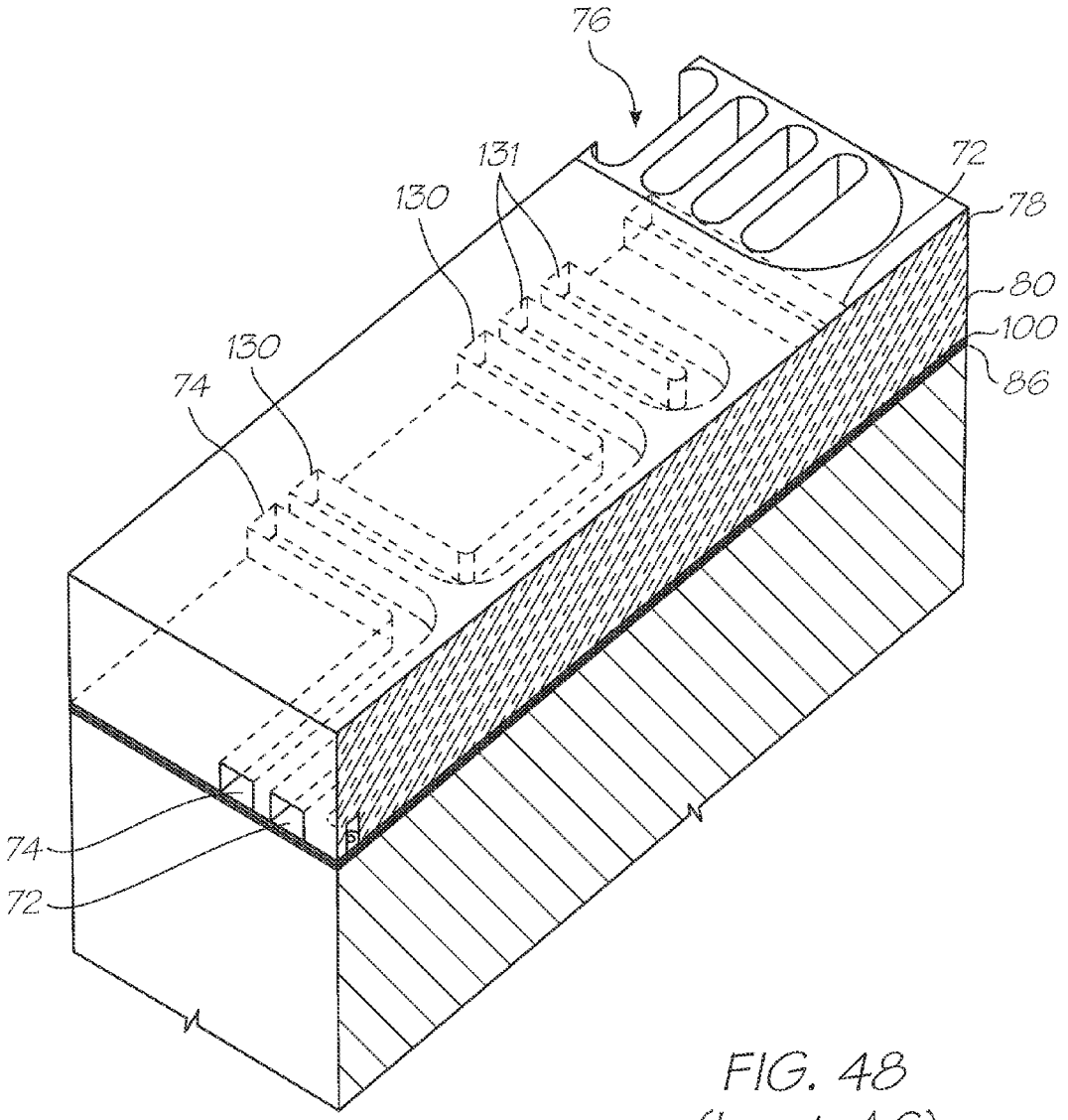


FIG. 48
(Inset AC)

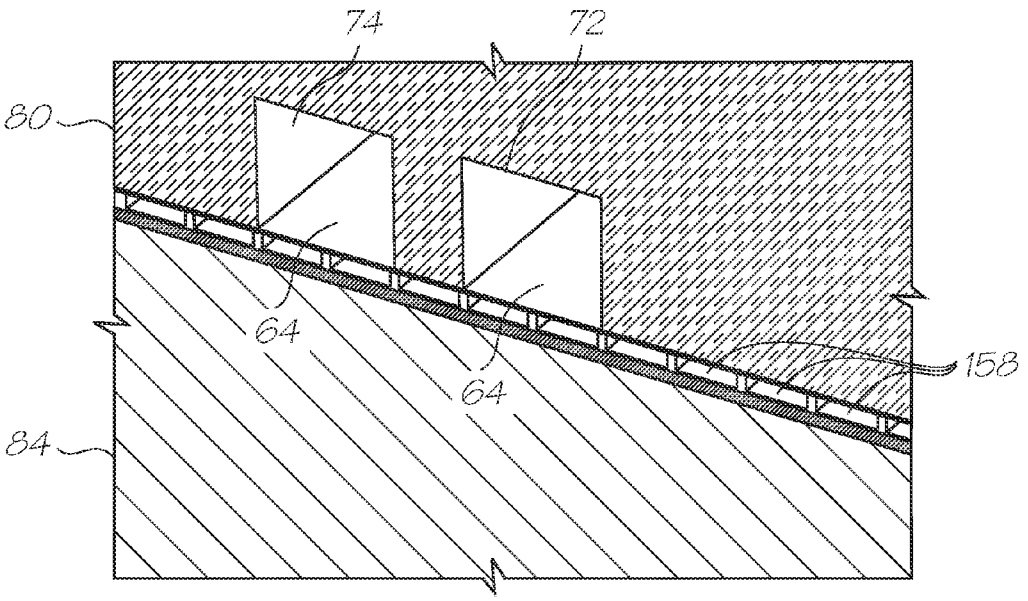


FIG. 49
(Inset AC)

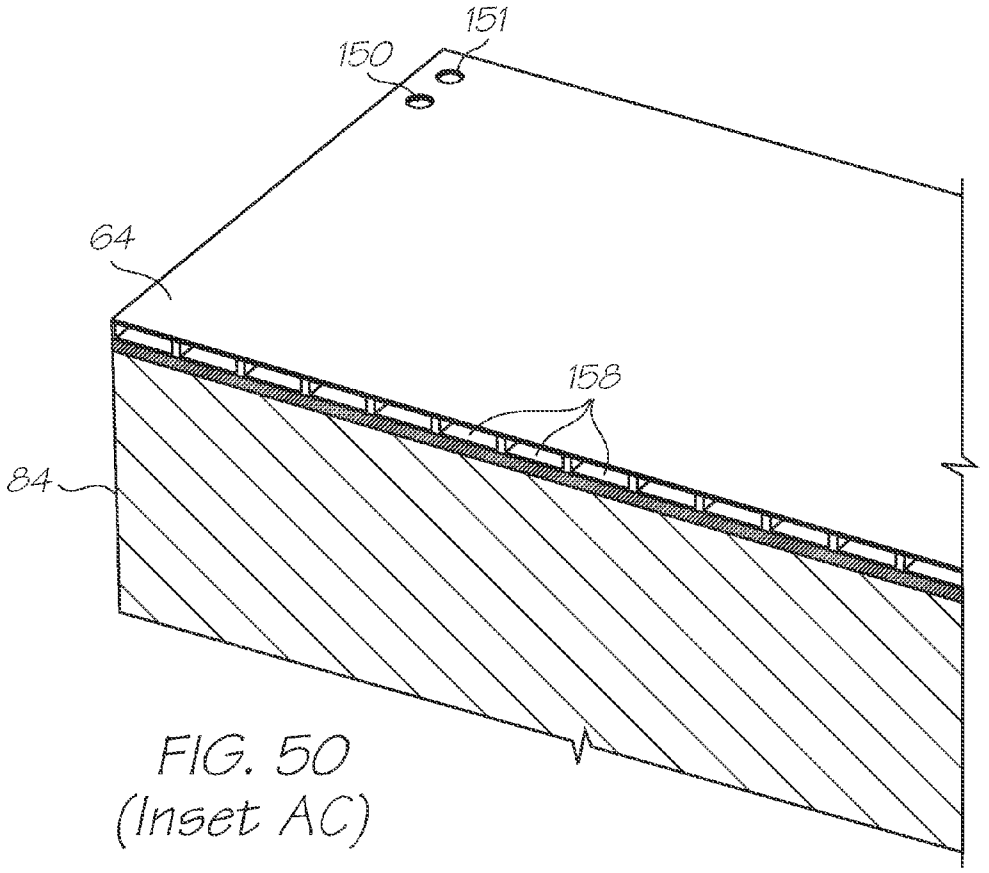


FIG. 50
(Inset AC)

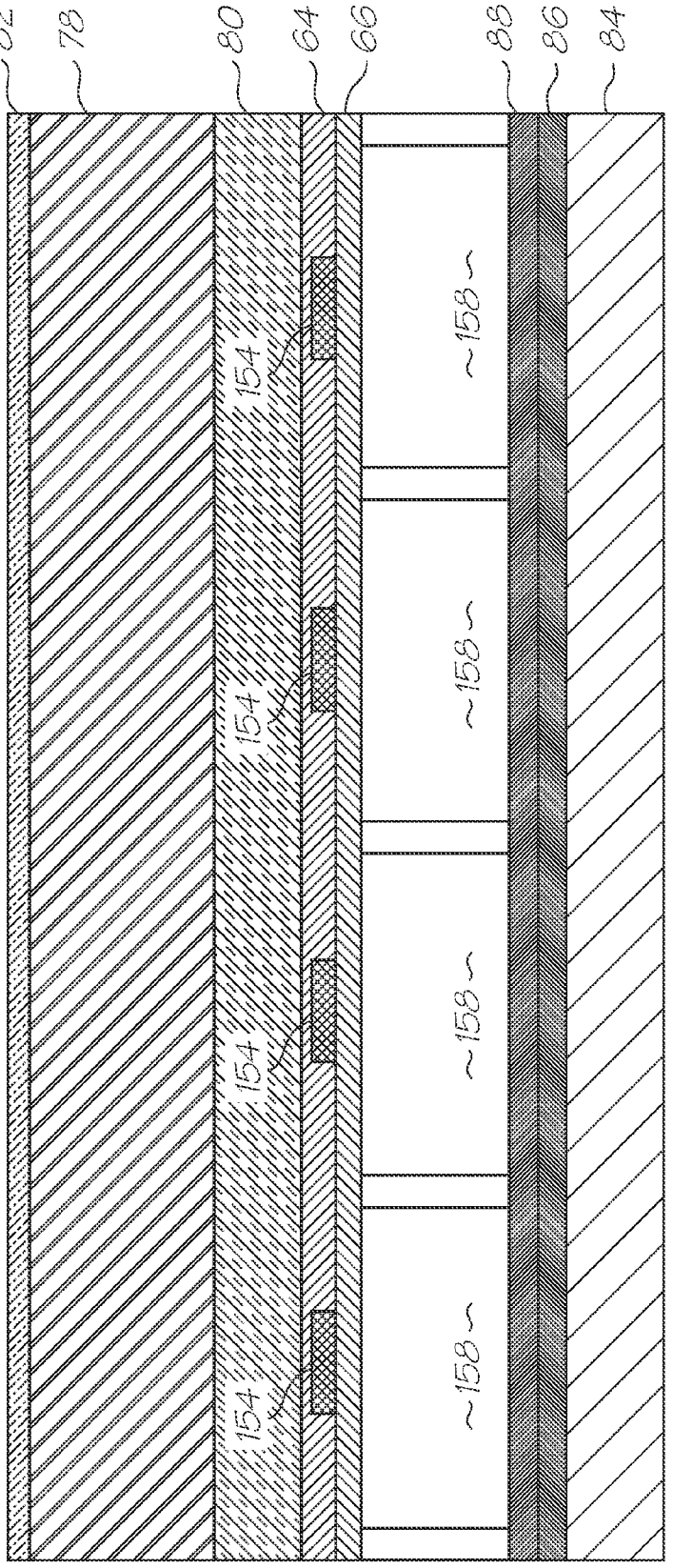


FIG. 51

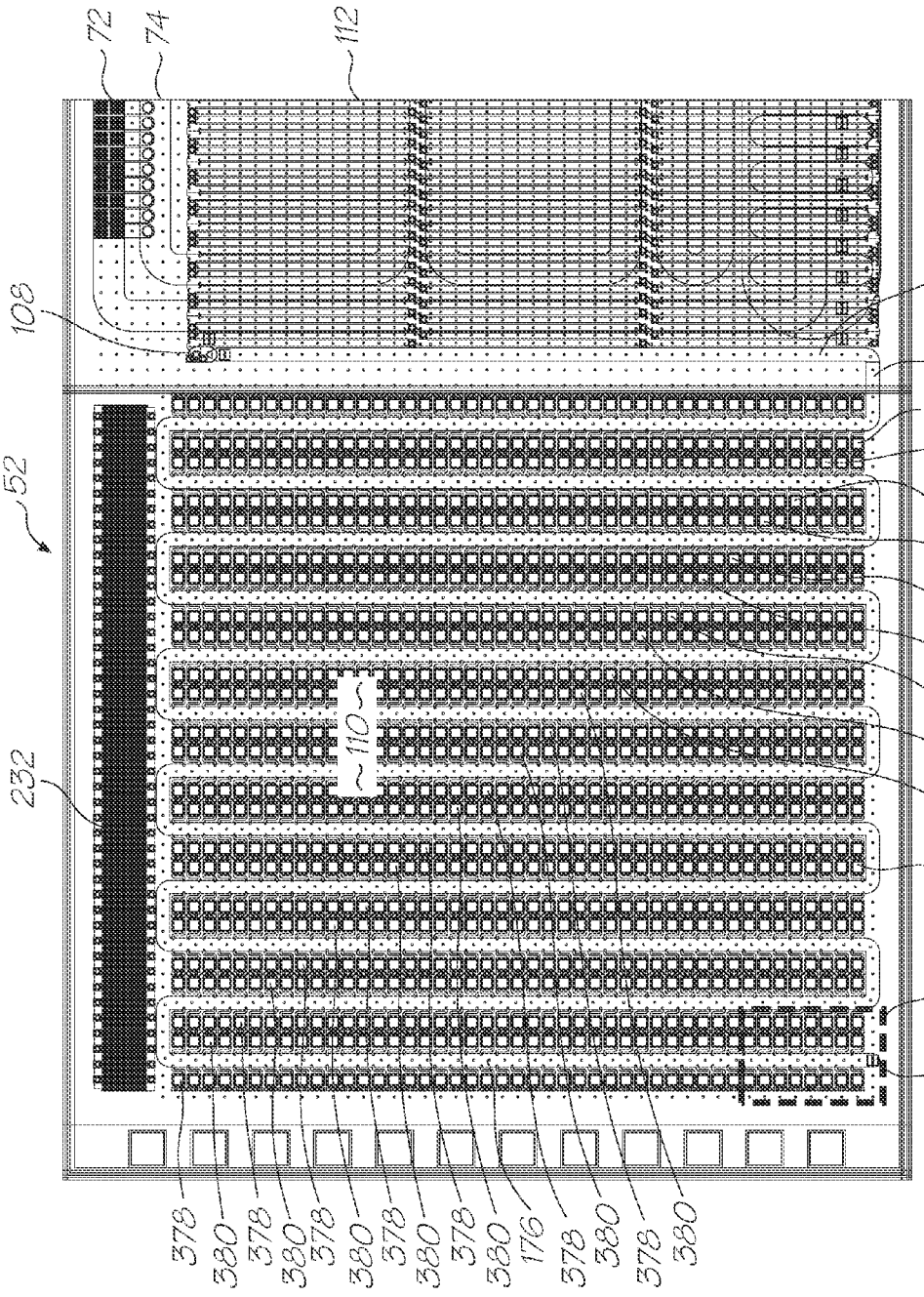


FIG. 52

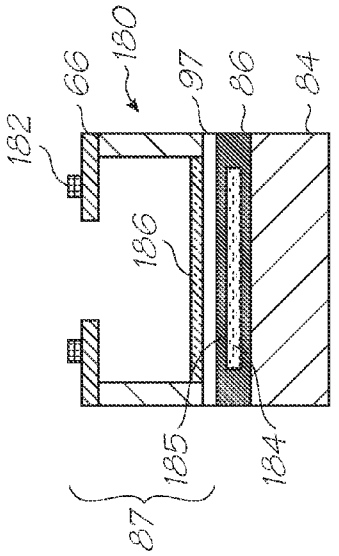


FIG. 54

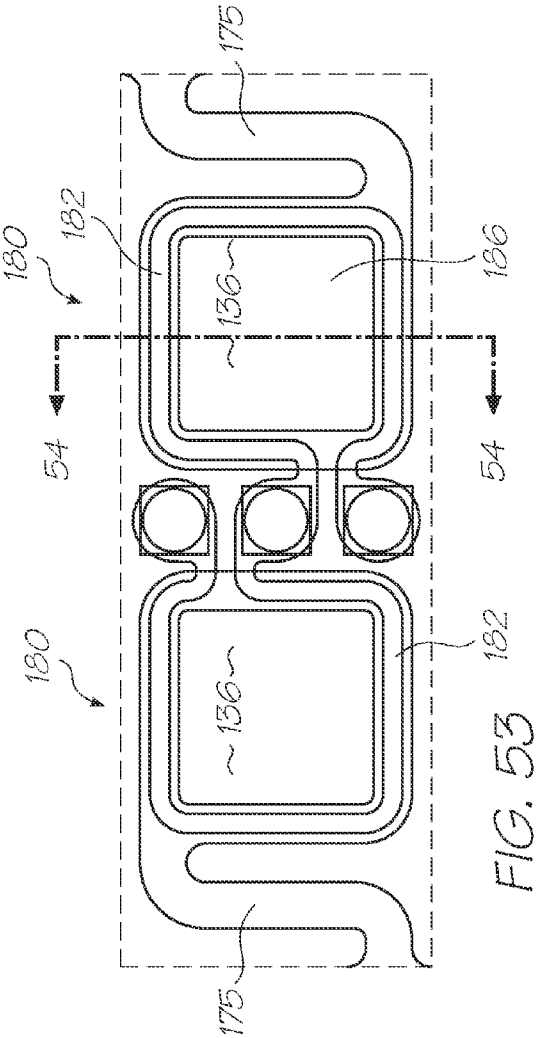


FIG. 53

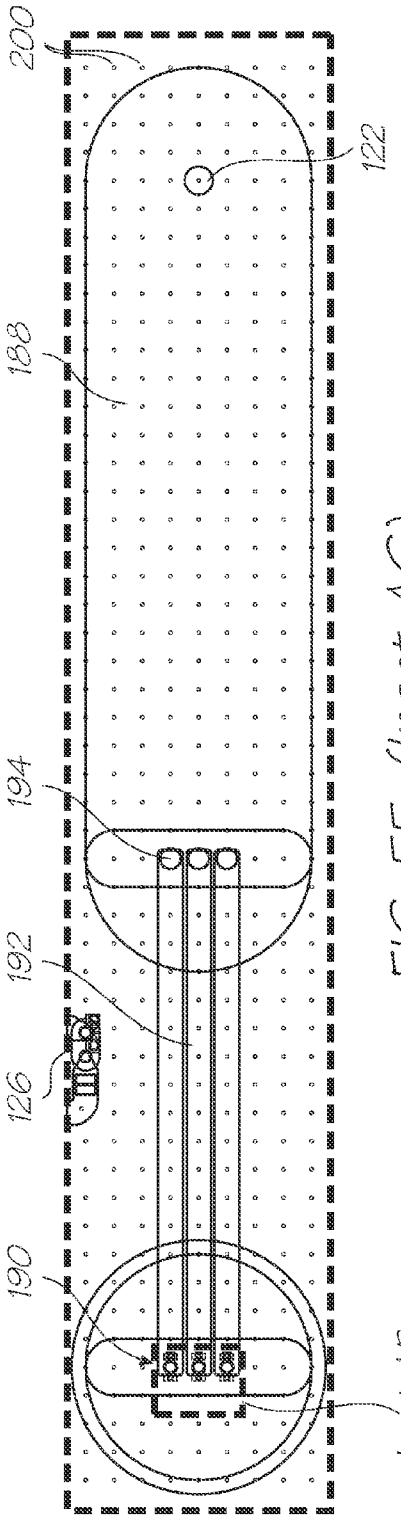


FIG. 55 (Inset AG)

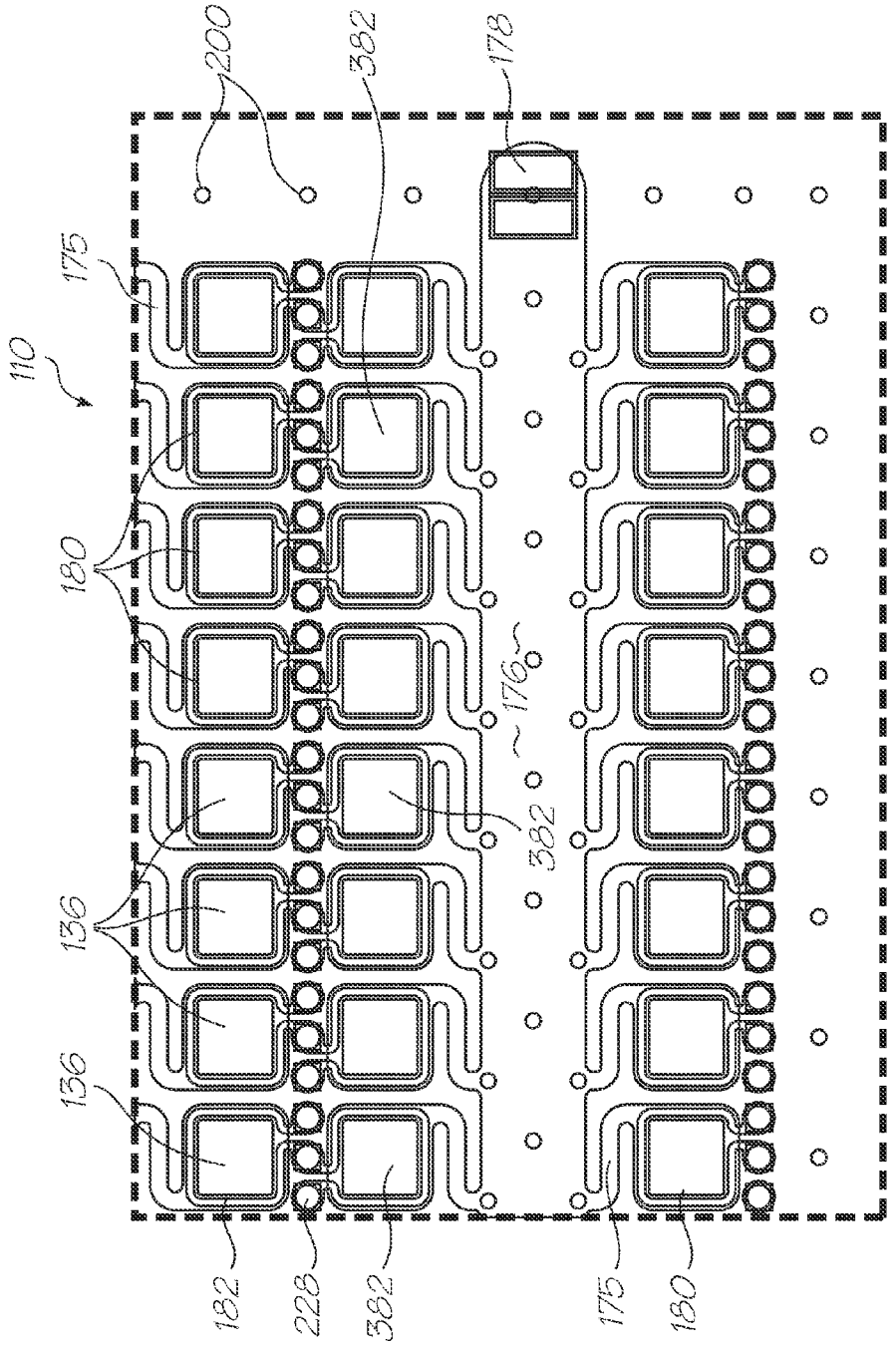


FIG. 56 (Inset AD)

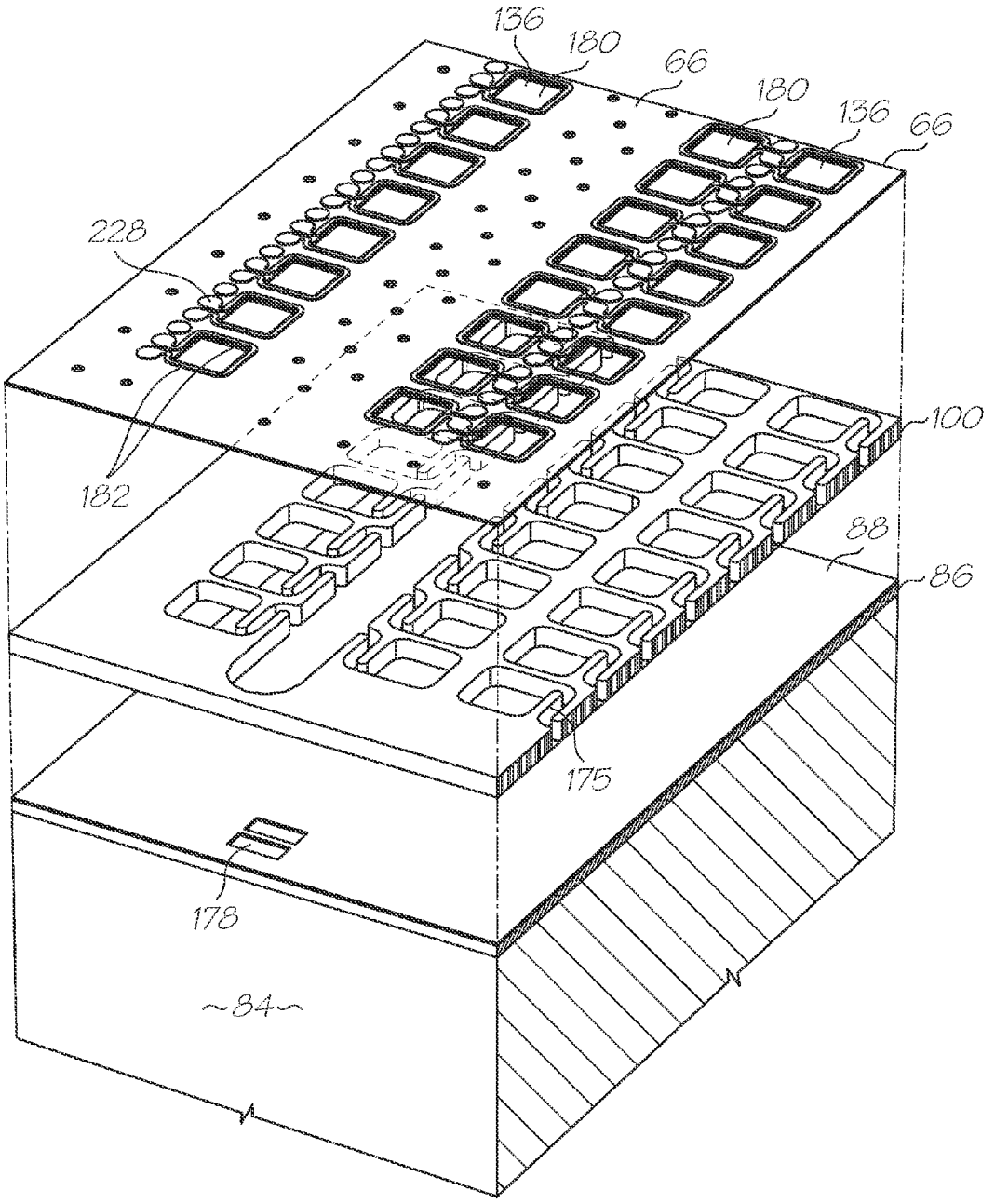


FIG. 57 (Inset AD)

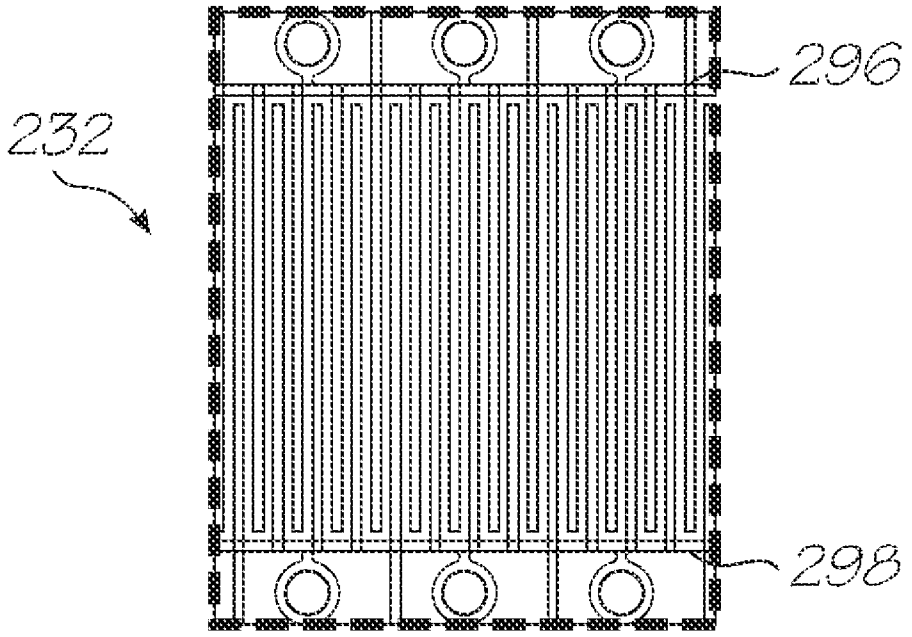


FIG. 58
(Inset AH)

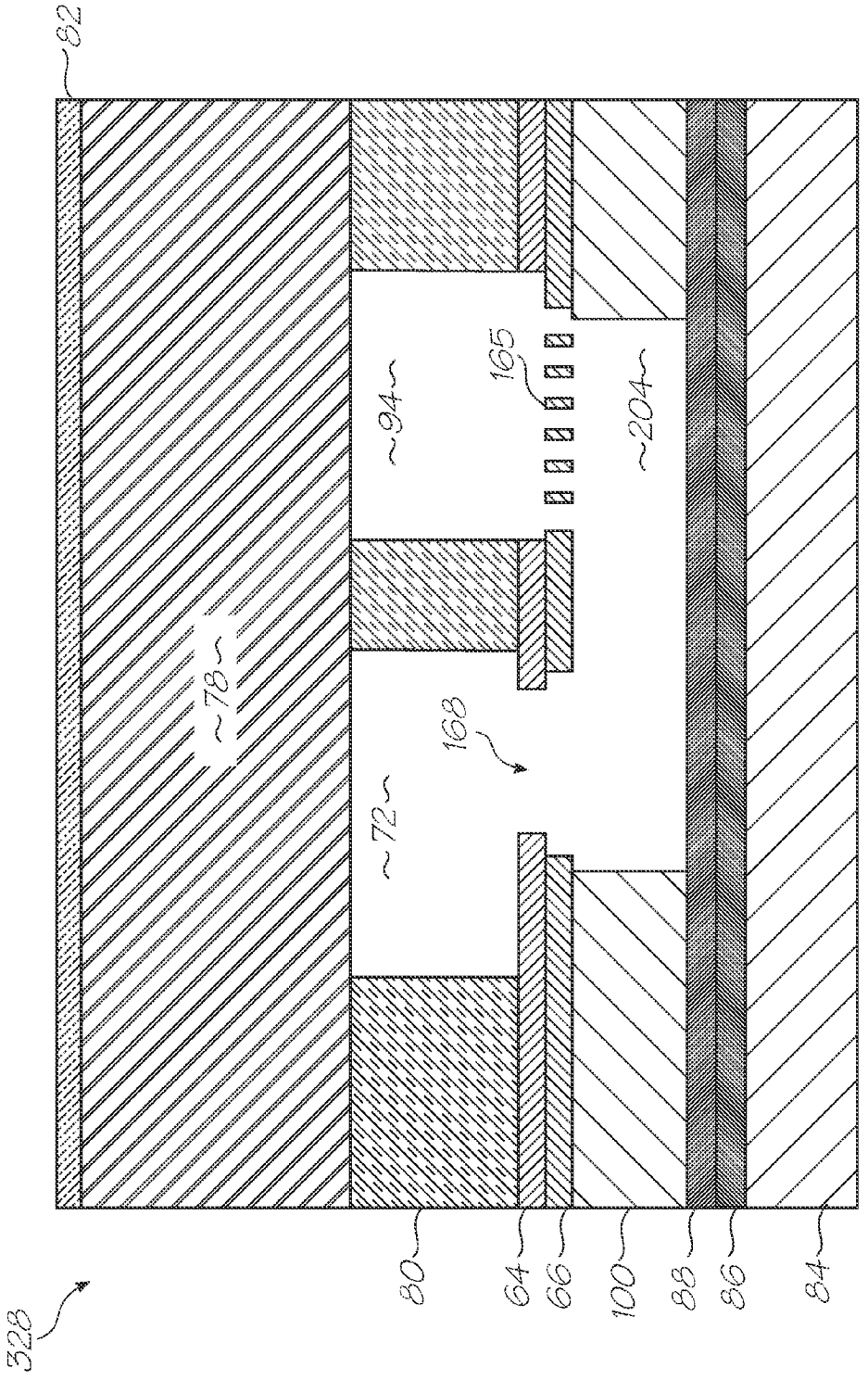


FIG. 59

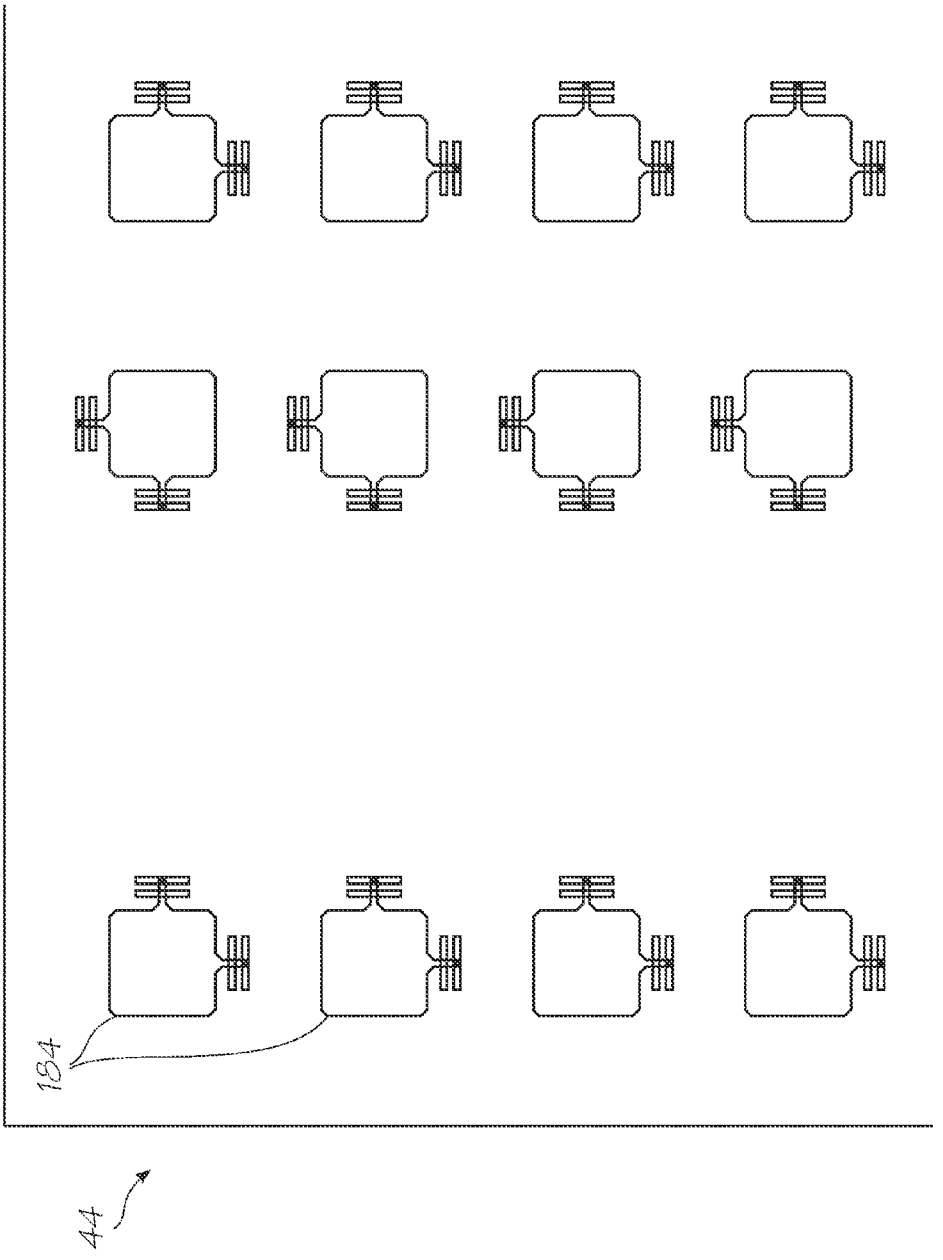


FIG. 60

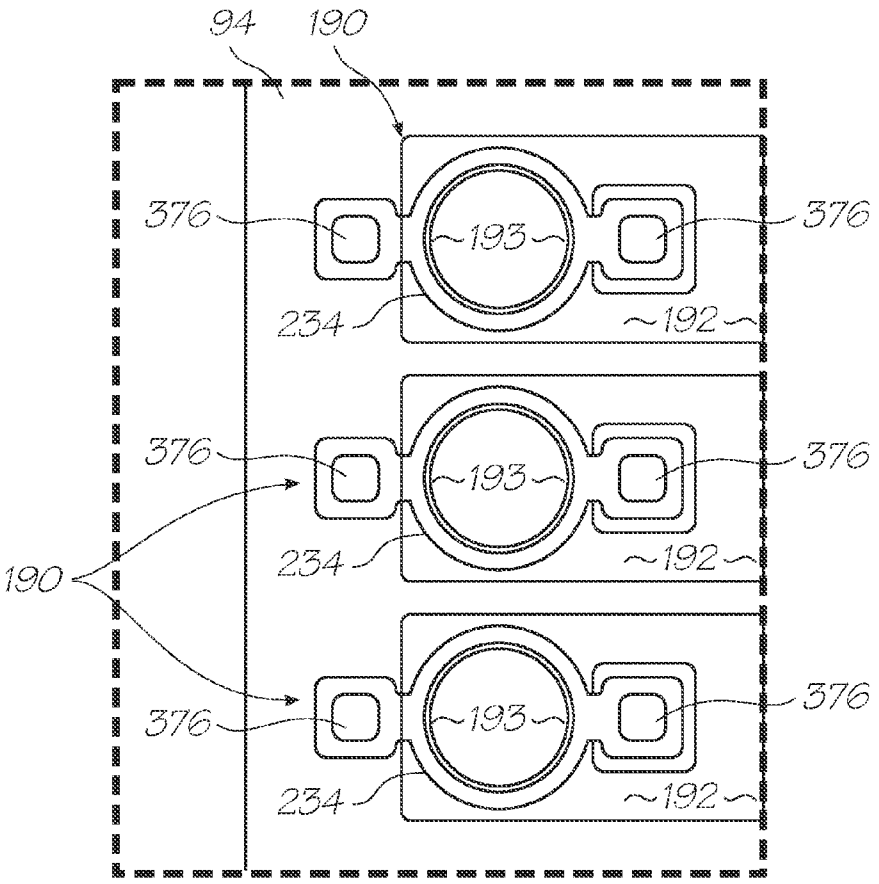


FIG. 61 (Inset AP)

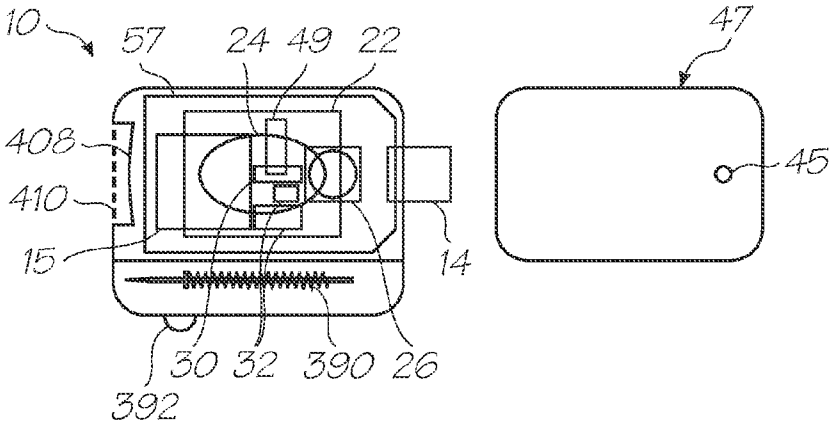


FIG. 63

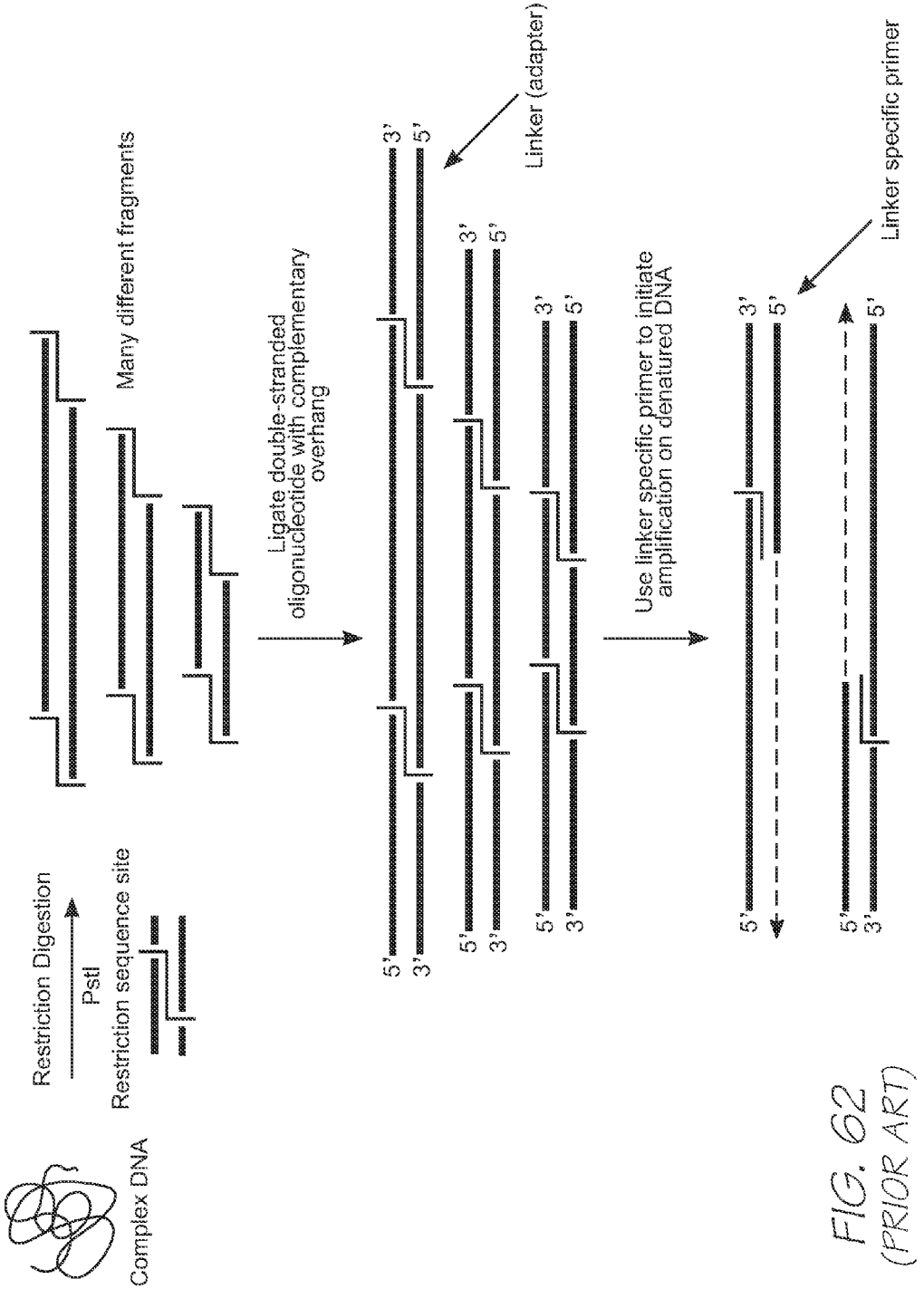


FIG. 62
(PRIOR ART)

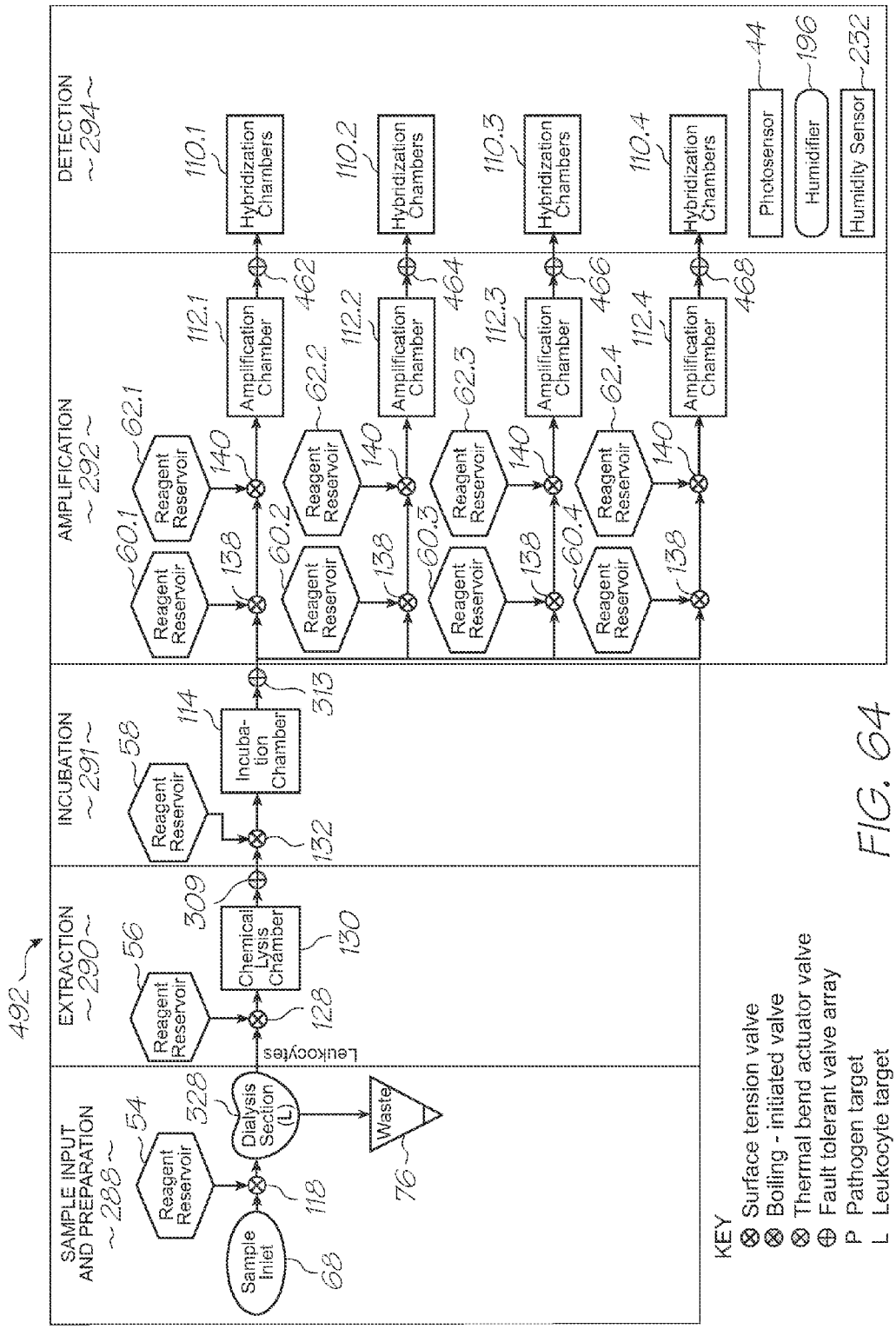

492
SAMPLE INPUT AND PREPARATION ~288~
EXTRACTION ~290~
INCUBATION ~291~
AMPLIFICATION ~292~
DETECTION ~294~
Sample Inlet
68
Reagent Reservoir
54
118
Dialysis Section (L)
328
Waste
76
Leukocytes
Reagent Reservoir
56
128
Chemical Lysis Chamber
130
309
Reagent Reservoir
58
132
Incubation Chamber
114
313
Reagent Reservoir
60.1
62.1
138
140
Amplification Chamber
112.1
462
Reagent Reservoir
60.2
62.2
138
140
Amplification Chamber
112.2
464
Reagent Reservoir
60.3
62.3
138
140
Amplification Chamber
112.3
466
Reagent Reservoir
60.4
62.4
138
140
Amplification Chamber
112.4
468
Hybridization Chambers
110.1
Hybridization Chambers
110.2
Hybridization Chambers
110.3
Hybridization Chambers
110.4
Photosensor
44
Humidifier
196
Humidity Sensor
232
KEY
⊗ Surface tension valve
⊗ Boiling - initiated valve
⊗ Thermal bend actuator valve
⊕ Fault tolerant valve array
P Pathogen target
L Leukocyte target

FIG. 64

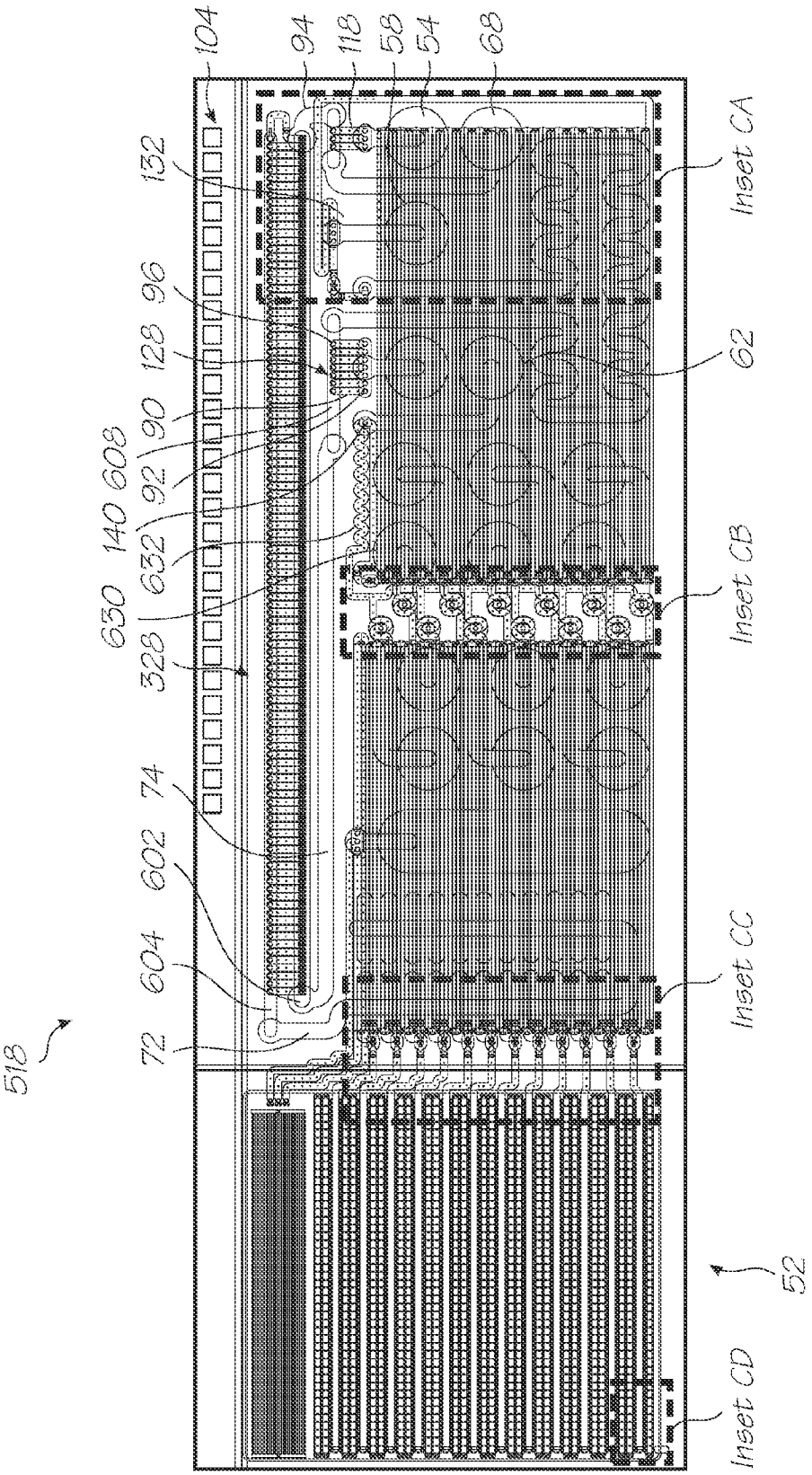

104
94
118
58
54
68
132
96
128
90
92
608
140
632
650
328
74
602
604
72
518
Inset CA
62
Inset CB
Inset CC
52
Inset CD

FIG. 65

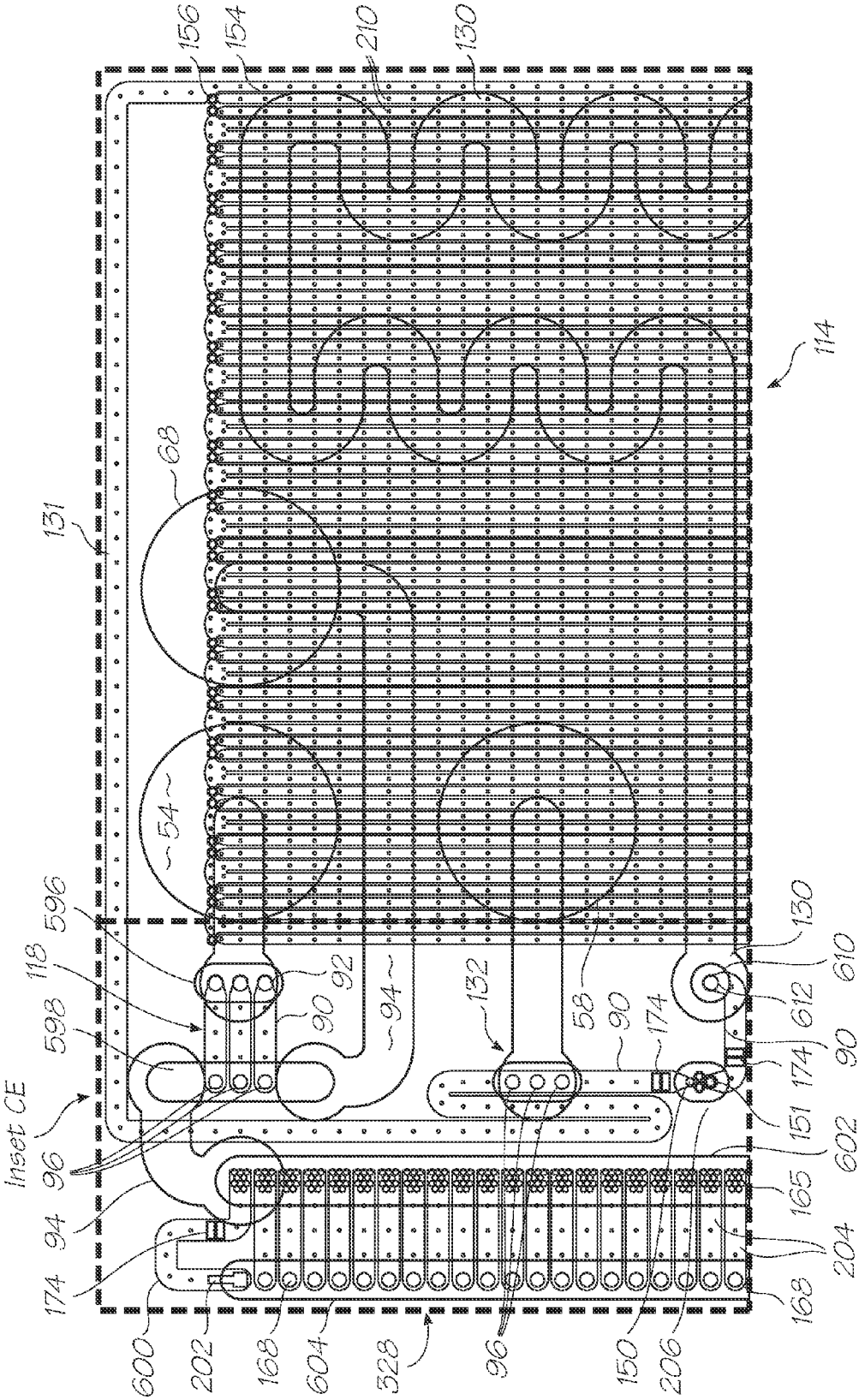


FIG. 66 (Inset CA)

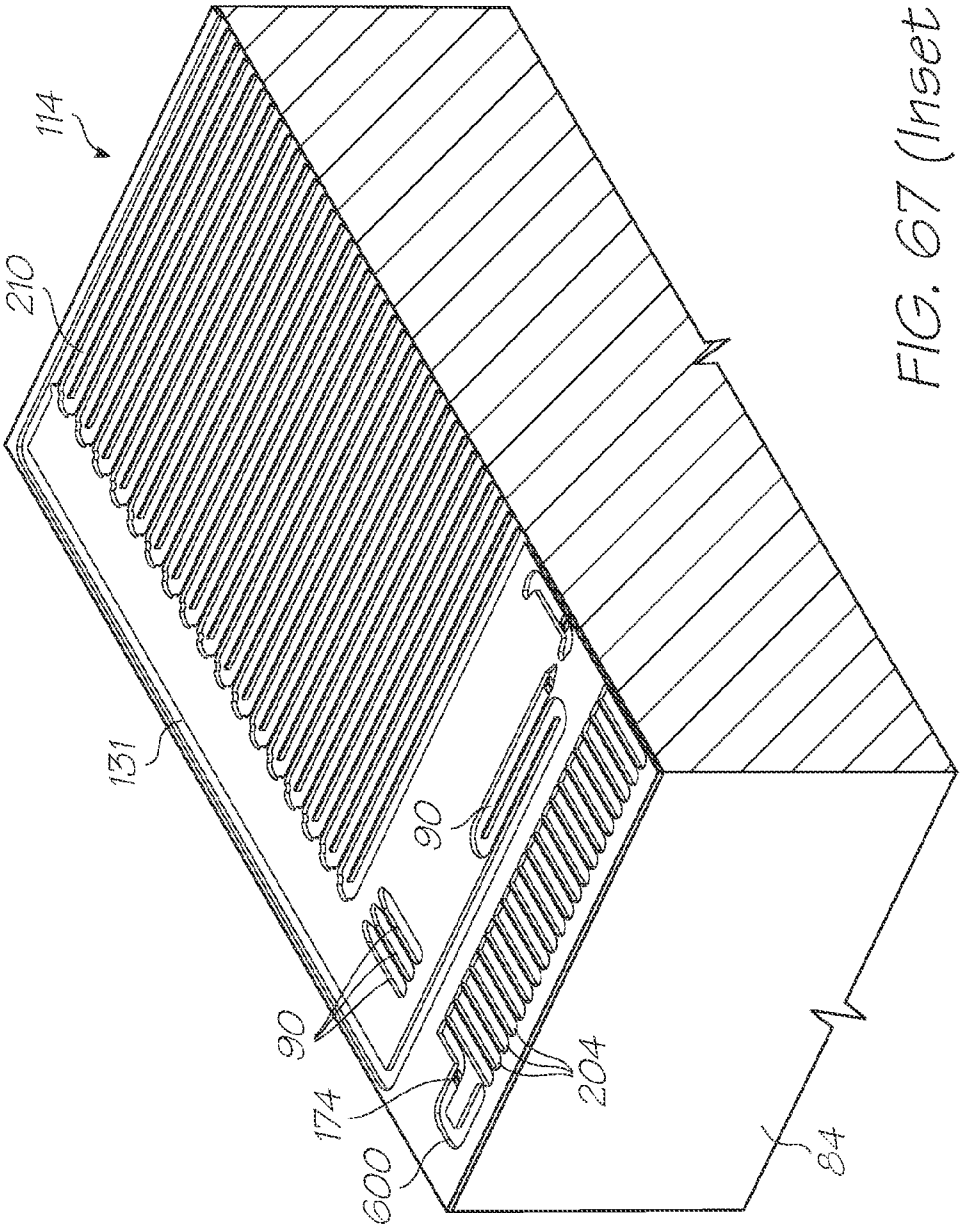


FIG. 67 (Inset CA)

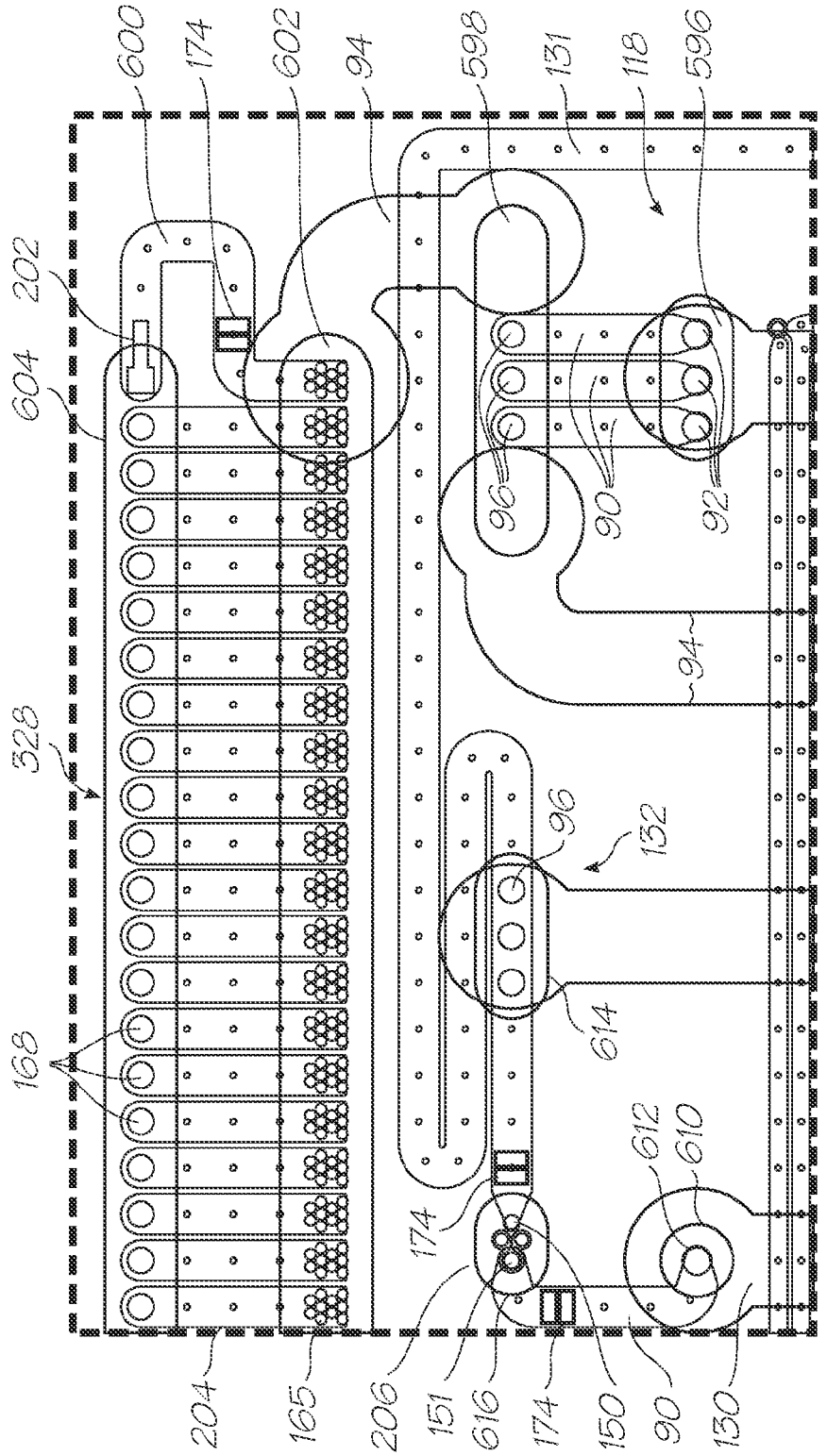


FIG. 68 (Inset CE)

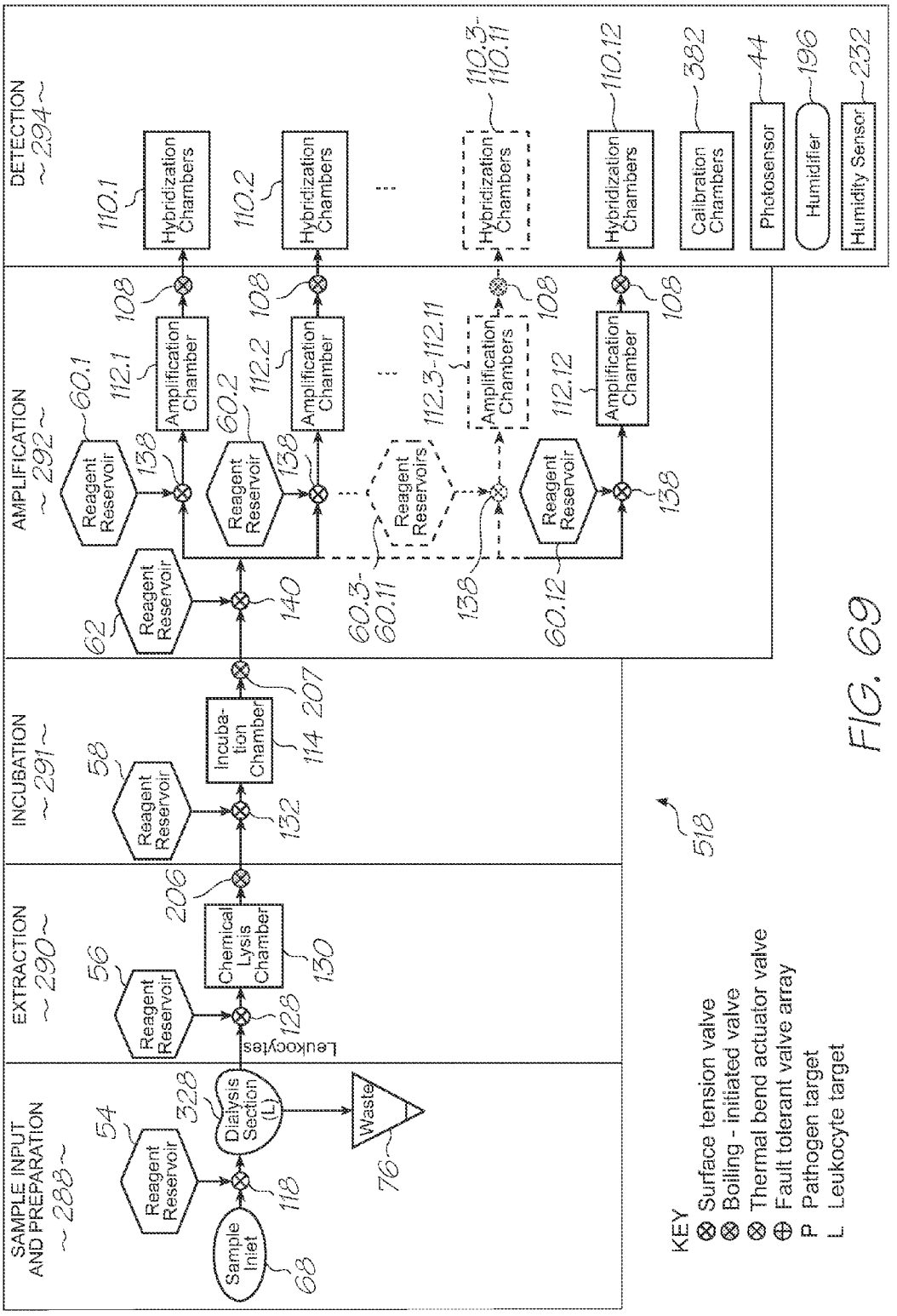

SAMPLE INPUT AND PREPARATION ~288~
EXTRACTION ~290~
INCUBATION ~291~
AMPLIFICATION ~292~
DETECTION ~294~
Reagent Reservoir
Sample Inlet
Dialysis Section (L)
Waste
Leukocytes
Chemical Lysis Chamber
Incubation Chamber
Amplification Chamber
Amplification Chambers
Reagent Reservoirs
Hybridization Chambers
Calibration Chambers
Photosensor
Humidifier
Humidity Sensor
KEY
Surface tension valve
Boiling - initiated valve
Thermal bend actuator valve
Fault tolerant valve array
P Pathogen target
L Leukocyte target

FIG. 69

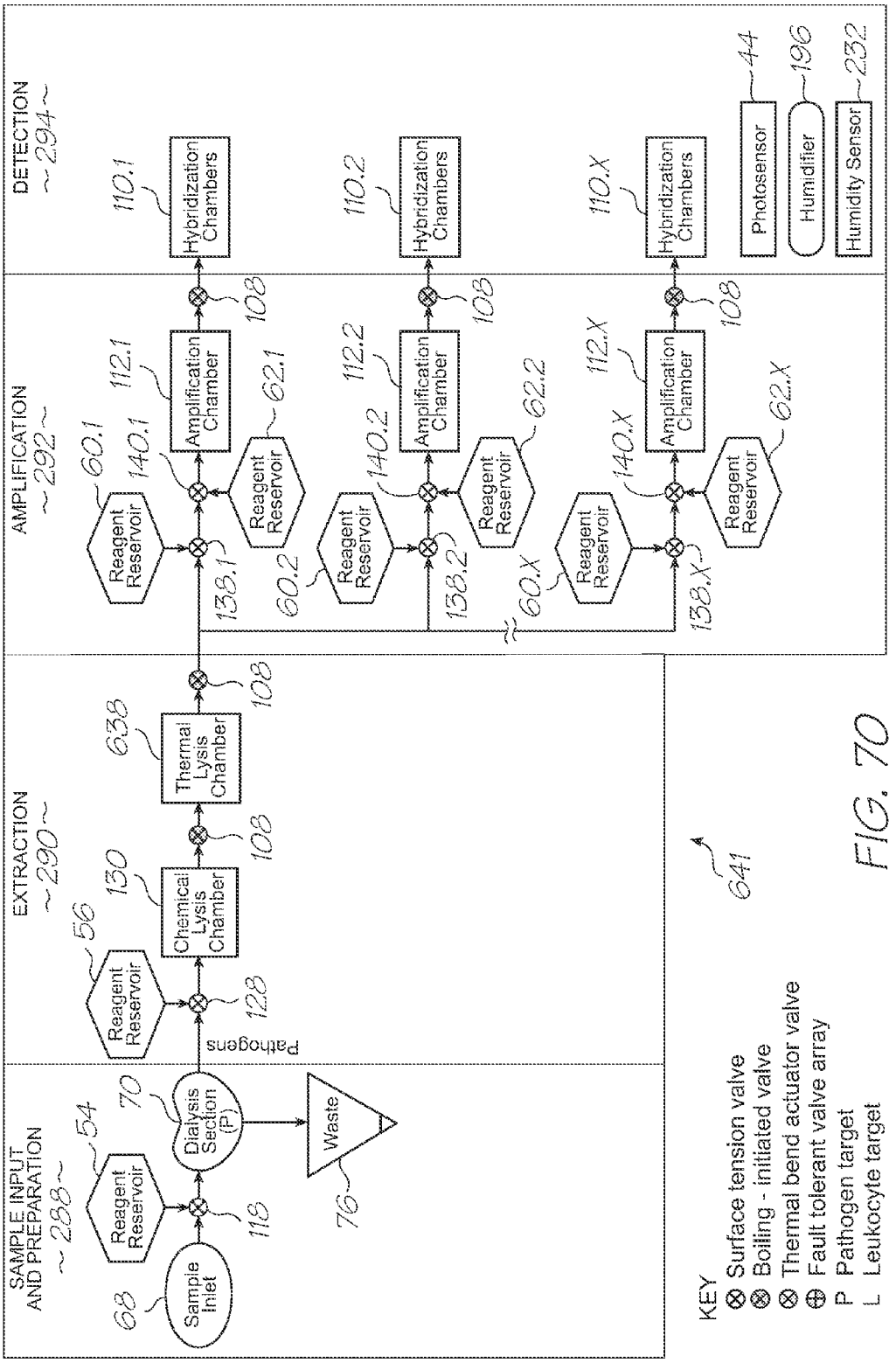

SAMPLE INPUT AND PREPARATION
~288~
EXTRACTION
~290~
AMPLIFICATION
~292~
DETECTION
~294~
Sample Inlet
68
Reagent Reservoir
54
118
Dialysis Section (P)
70
Waste
76
Pathogens
Reagent Reservoir
56
128
Chemical Lysis Chamber
130
Thermal Lysis Chamber
638
108
Reagent Reservoir
60.1
140.1
Amplification Chamber
112.1
Hybridization Chambers
110.1
62.1
138.1
Reagent Reservoir
60.2
140.2
Amplification Chamber
112.2
Hybridization Chambers
110.2
62.2
138.2
Reagent Reservoir
60.X
140.X
Amplification Chamber
112.X
Hybridization Chambers
110.X
62.X
138.X
Photosensor
44
Humidifier
196
Humidity Sensor
232
KEY
Surface tension valve
Boiling - initiated valve
Thermal bend actuator valve
Fault tolerant valve array
P Pathogen target
L Leukocyte target
641

FIG. 70

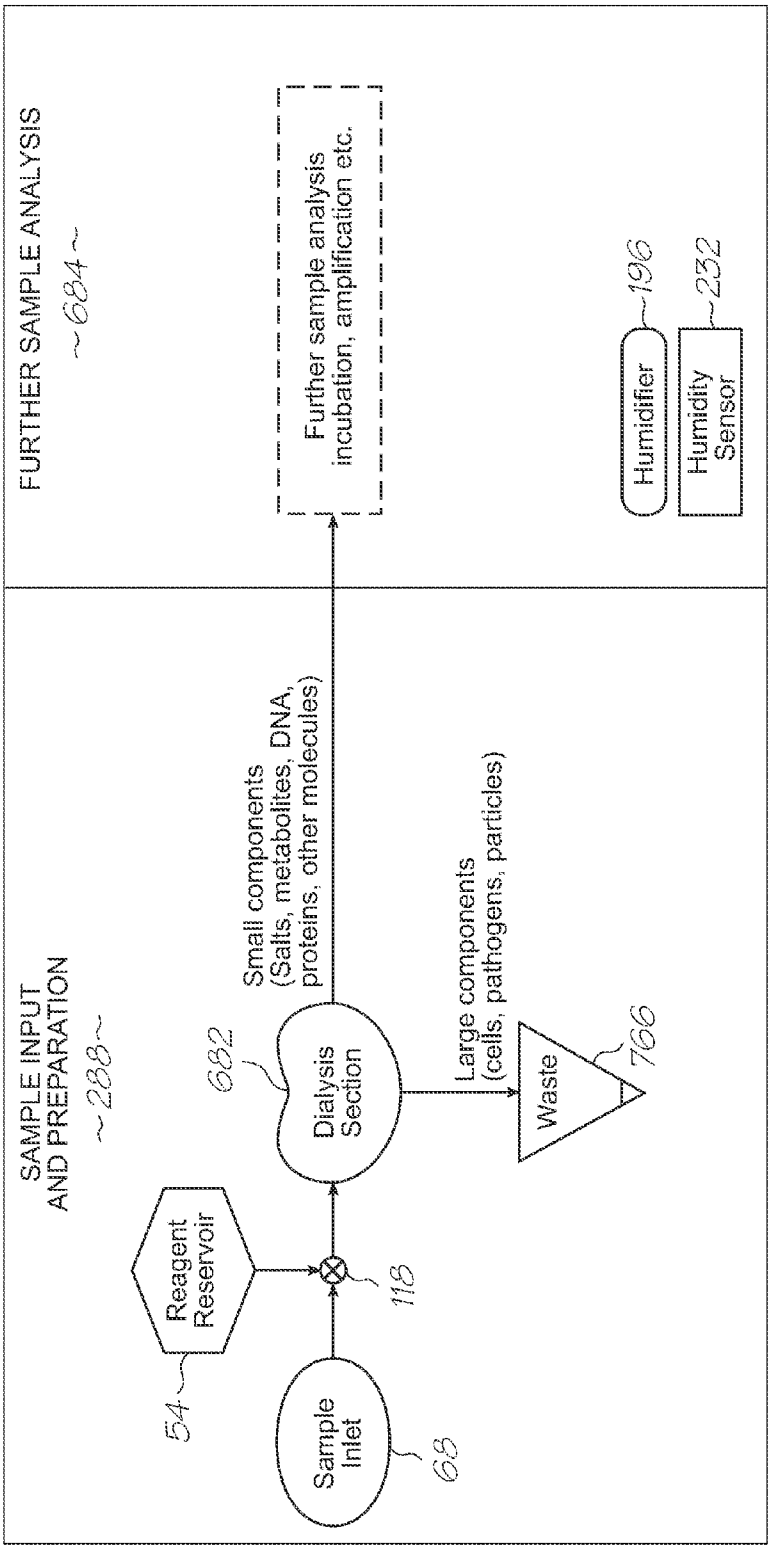

SAMPLE INPUT AND PREPARATION
~288~
FURTHER SAMPLE ANALYSIS
~684~
Sample Inlet
68
Reagent Reservoir
54
118
Dialysis Section
682
Small components (Salts, metabolites, DNA, proteins, other molecules)
Large components (cells, pathogens, particles)
Waste
766
Further sample analysis incubation, amplification etc.
Humidifier
196
Humidity Sensor
232
671
KEY
⊗ Surface tension valve
⊗ Boiling - initiated valve
⊗ Thermal bend actuator valve
⊕ Fault tolerant valve array
P Pathogen target
L Leukocyte target

FIG. 71

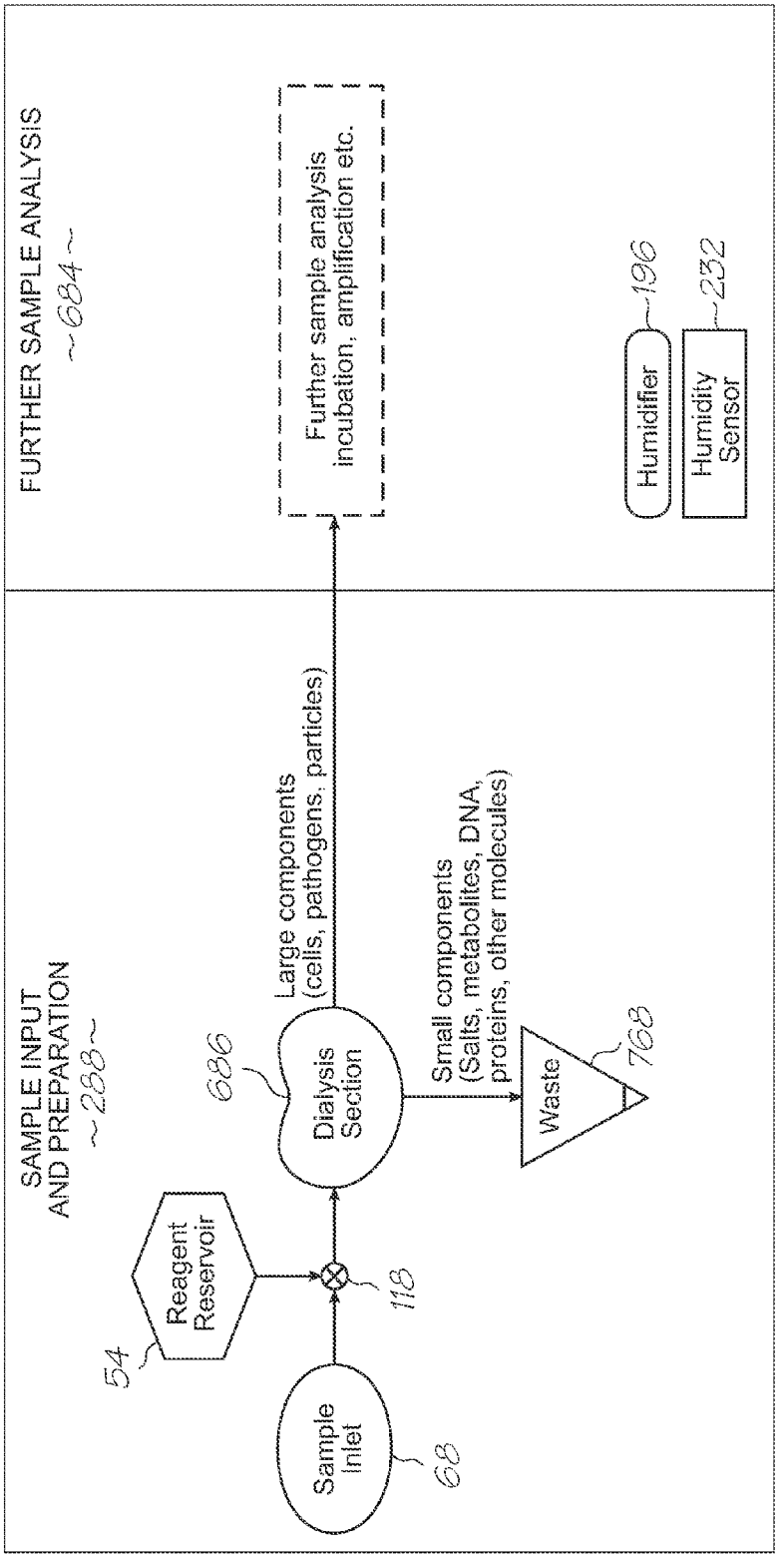

SAMPLE INPUT AND PREPARATION
~688~
FURTHER SAMPLE ANALYSIS
~684~
Sample Inlet
68
Reagent Reservoir
54
118
686
Dialysis Section
Large components (cells, pathogens, particles)
Small components (Salts, metabolites, DNA, proteins, other molecules)
Waste
768
Further sample analysis incubation, amplification etc.
Humidifier
196
Humidity Sensor
232
672
KEY
⊗ Surface tension valve
⊗ Boiling - initiated valve
⊗ Thermal bend actuator valve
⊕ Fault tolerant valve array
P Pathogen target
L Leukocyte target

FIG. 72

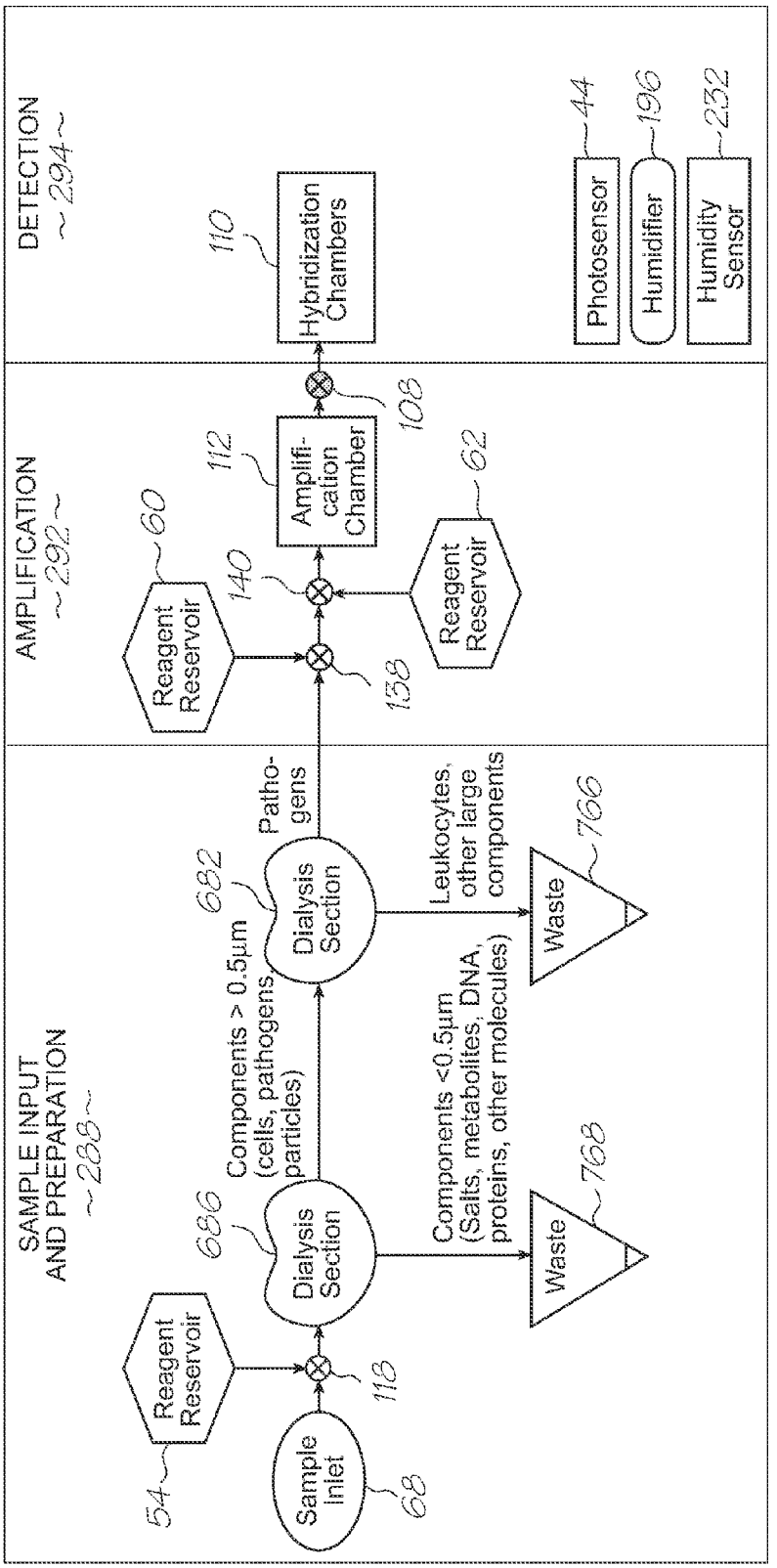

SAMPLE INPUT AND PREPARATION
~288~
AMPLIFICATION
~292~
DETECTION
~294~
Sample Inlet
68
Reagent Reservoir
54
118
Dialysis Section
686
Components > 0.5µm (cells, pathogens particles)
Components <0.5µm (Salts, metabolites, DNA, proteins, other molecules)
Waste
768
Dialysis Section
682
Patho-gens
Leukocytes, other large components
Waste
766
Reagent Reservoir
60
140
138
Reagent Reservoir
62
112
Amplifi-cation Chamber
108
110
Hybridization Chambers
Photosensor
44
Humidifier
196
Humidity Sensor
232
KEY
673
⊗ Surface tension valve
⊗ Boiling - initiated valve
⊗ Thermal bend actuator valve
⊕ Fault tolerant valve array
P Pathogen target
L Leukocyte target

FIG. 73

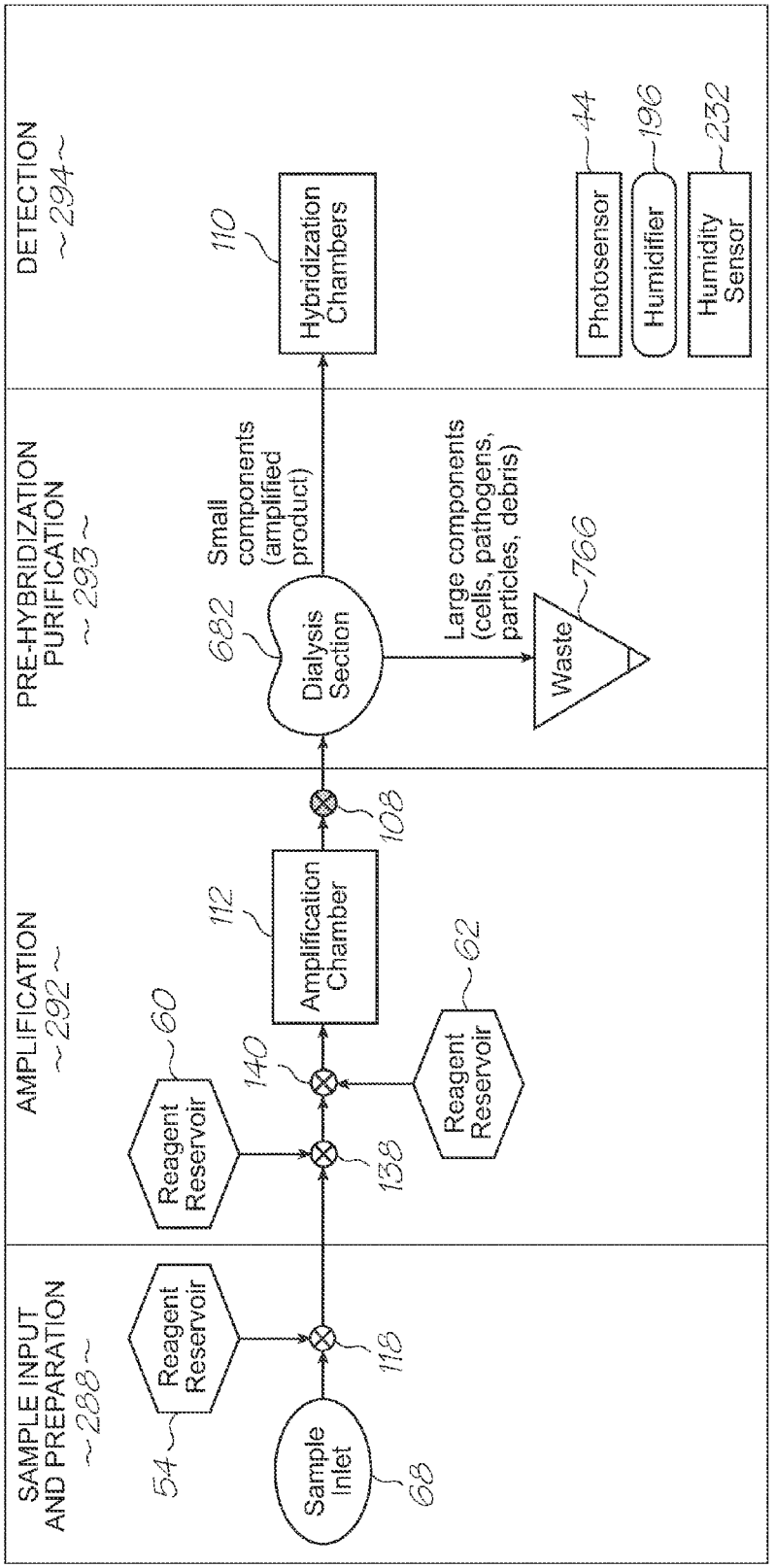

SAMPLE INPUT AND PREPARATION ~288~
AMPLIFICATION ~292~
PRE-HYBRIDIZATION PURIFICATION ~293~
DETECTION ~294~
Reagent Reservoir
54
Sample Inlet
68
116
Reagent Reservoir
60
140
138
112
Amplification Chamber
108
Reagent Reservoir
62
682
Dialysis Section
Small components (amplified product)
110
Hybridization Chambers
Large components (cells, pathogens, particles, debris)
Waste
766
Photosensor
44
Humidifier
196
Humidity Sensor
232
KEY
674
⊗ Surface tension valve
⊗ Boiling - initiated valve
⊗ Thermal bend actuator valve
⊕ Fault tolerant valve array
P Pathogen target
L Leukocyte target

FIG. 74

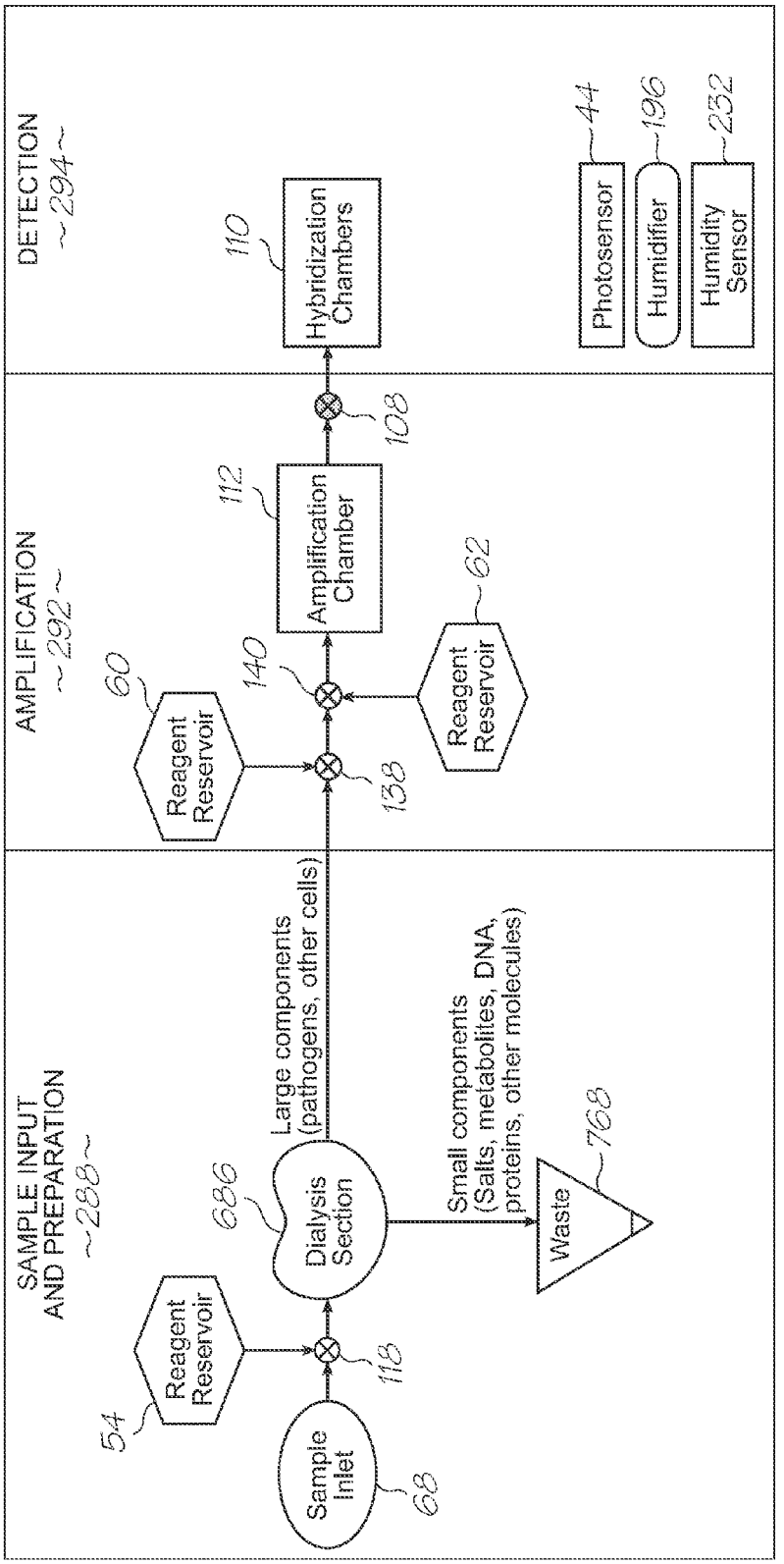

SAMPLE INPUT AND PREPARATION
~288~
AMPLIFICATION
~292~
DETECTION
~294~
Reagent Reservoir
54
Sample Inlet
68
118
686
Dialysis Section
Large components (pathogens, other cells)
Small components (Salts, metabolites, DNA, proteins, other molecules)
Waste
768
Reagent Reservoir
60
138
140
Amplification Chamber
112
108
Hybridization Chambers
110
Reagent Reservoir
62
Photosensor
44
Humidifier
196
Humidity Sensor
232
677
KEY
Surface tension valve
Boiling - initiated valve
Thermal bend actuator valve
Fault tolerant valve array
P Pathogen target
L Leukocyte target

FIG. 75

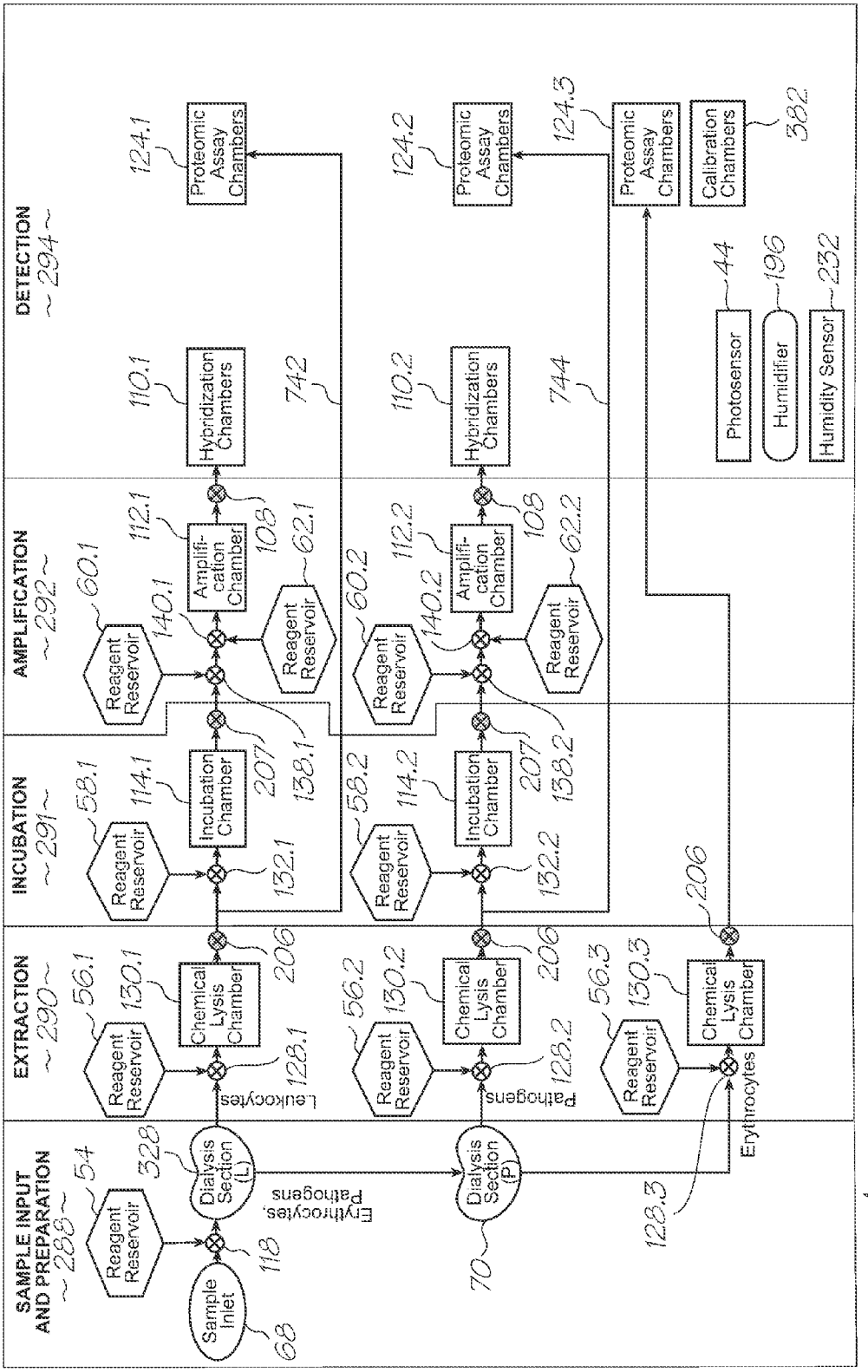

SAMPLE INPUT AND PREPARATION
~288~
EXTRACTION
~290~
INCUBATION
~291~
AMPLIFICATION
~292~
DETECTION
~294~
Reagent Reservoir
54
328
Dialysis Section (L)
Sample Inlet
68
118
Erythrocytes, Pathogens
70
Dialysis Section (P)
Reagent Reservoir
56.1
130.1
Chemical Lysis Chamber
206
128.1
Leukocytes
Reagent Reservoir
56.2
130.2
Chemical Lysis Chamber
206
128.2
Pathogens
Reagent Reservoir
56.3
130.3
Chemical Lysis Chamber
206
128.3
Erythrocytes
Reagent Reservoir
58.1
114.1
Incubation Chamber
207
138.1
132.1
Reagent Reservoir
58.2
114.2
Incubation Chamber
207
138.2
132.2
206
Reagent Reservoir
60.1
140.1
112.1
Amplification Chamber
108
Reagent Reservoir
62.1
Reagent Reservoir
60.2
140.2
112.2
Amplification Chamber
108
Reagent Reservoir
62.2
110.1
Hybridization Chambers
742
110.2
Hybridization Chambers
744
124.1
Proteomic Assay Chambers
124.2
Proteomic Assay Chambers
124.3
Proteomic Assay Chambers
Calibration Chambers
382
Photosensor
44
Humidifier
196
Humidity Sensor
232
728

FIG. 76

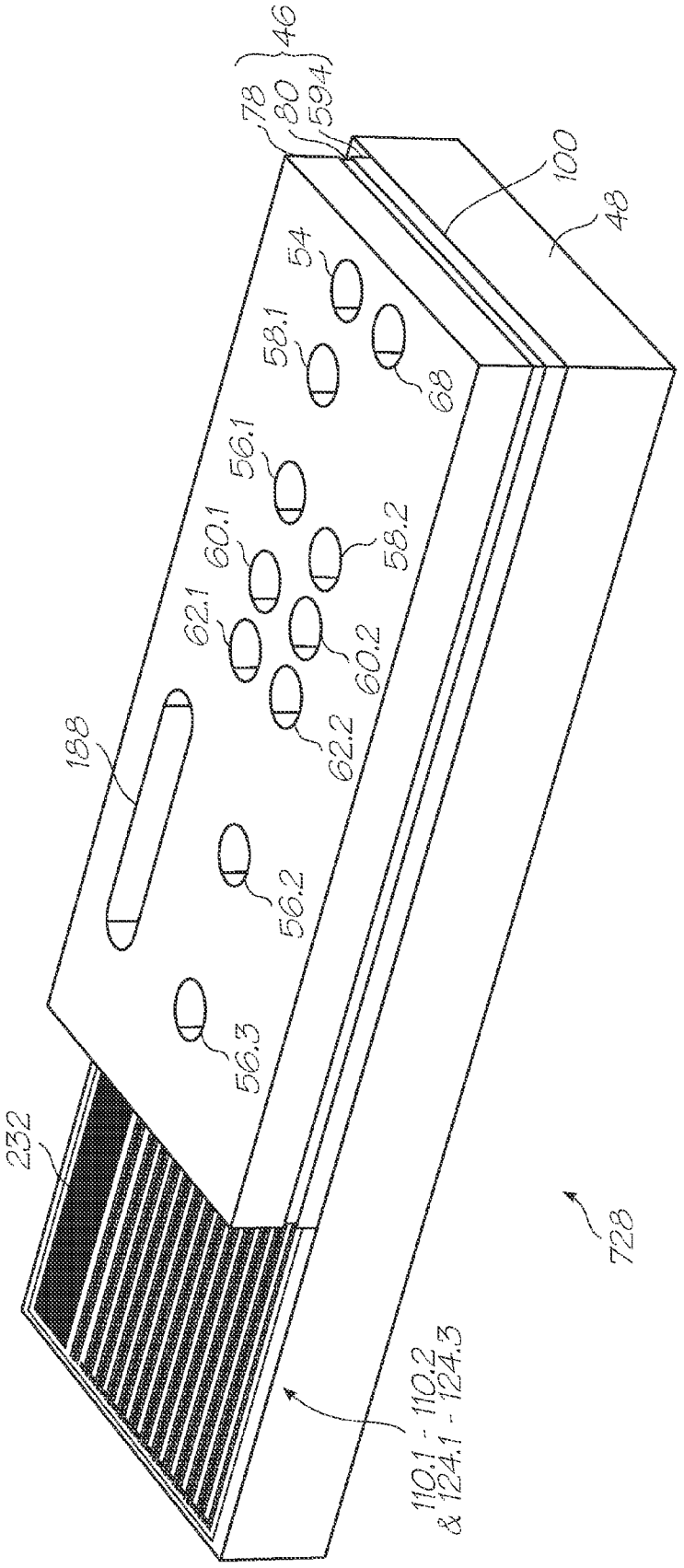

46
78
80
594
100
48
54
58.1
68
56.1
60.1
58.2
62.1
60.2
62.2
188
56.2
56.3
232
728
110.1 - 110.2
& 124.1 - 124.3

FIG. 77

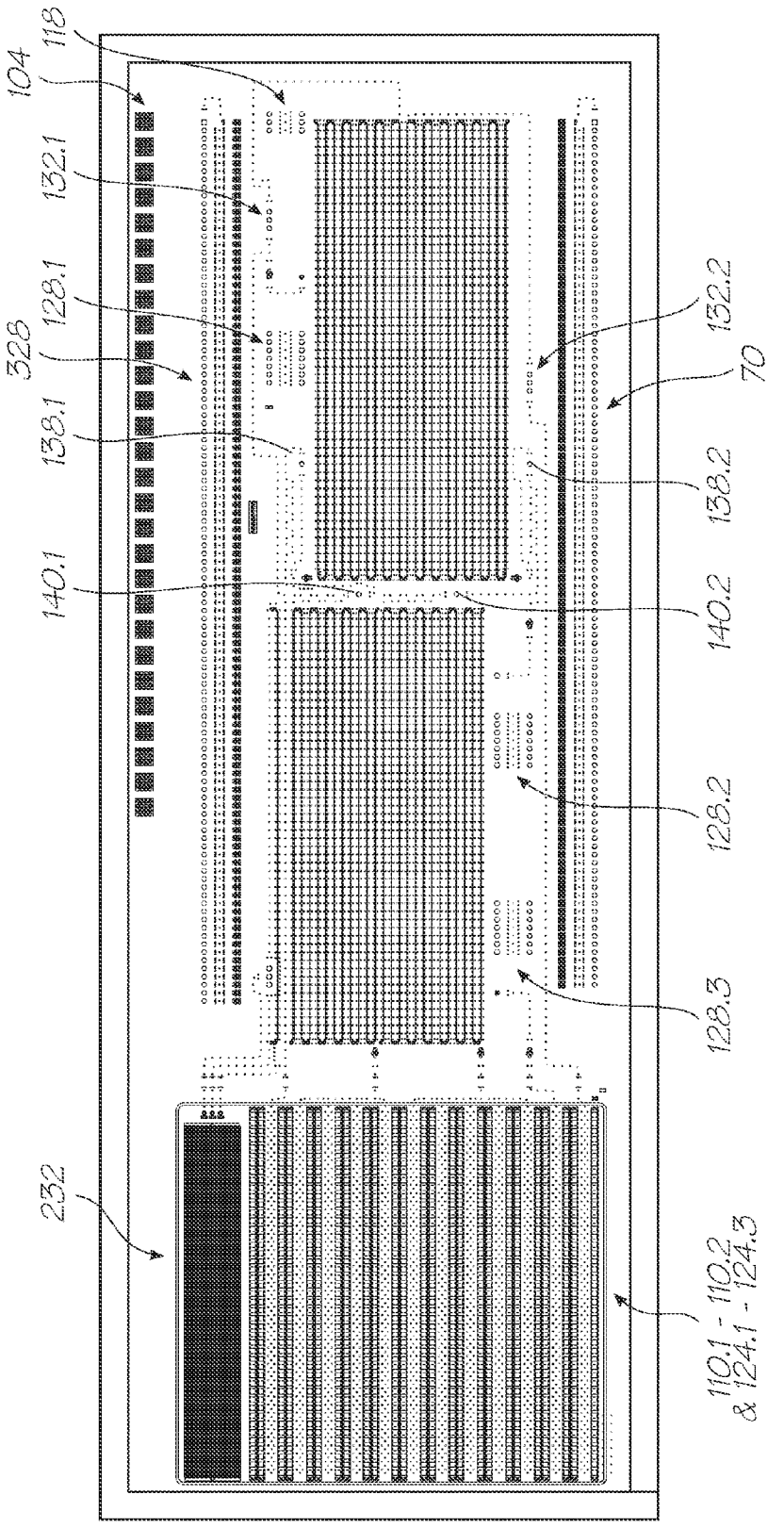

104
118
132.1
128.1
328
138.1
140.1
232
110.1 - 110.2
& 124.1 - 124.3
128.3
128.2
140.2
138.2
70
132.2

FIG. 78

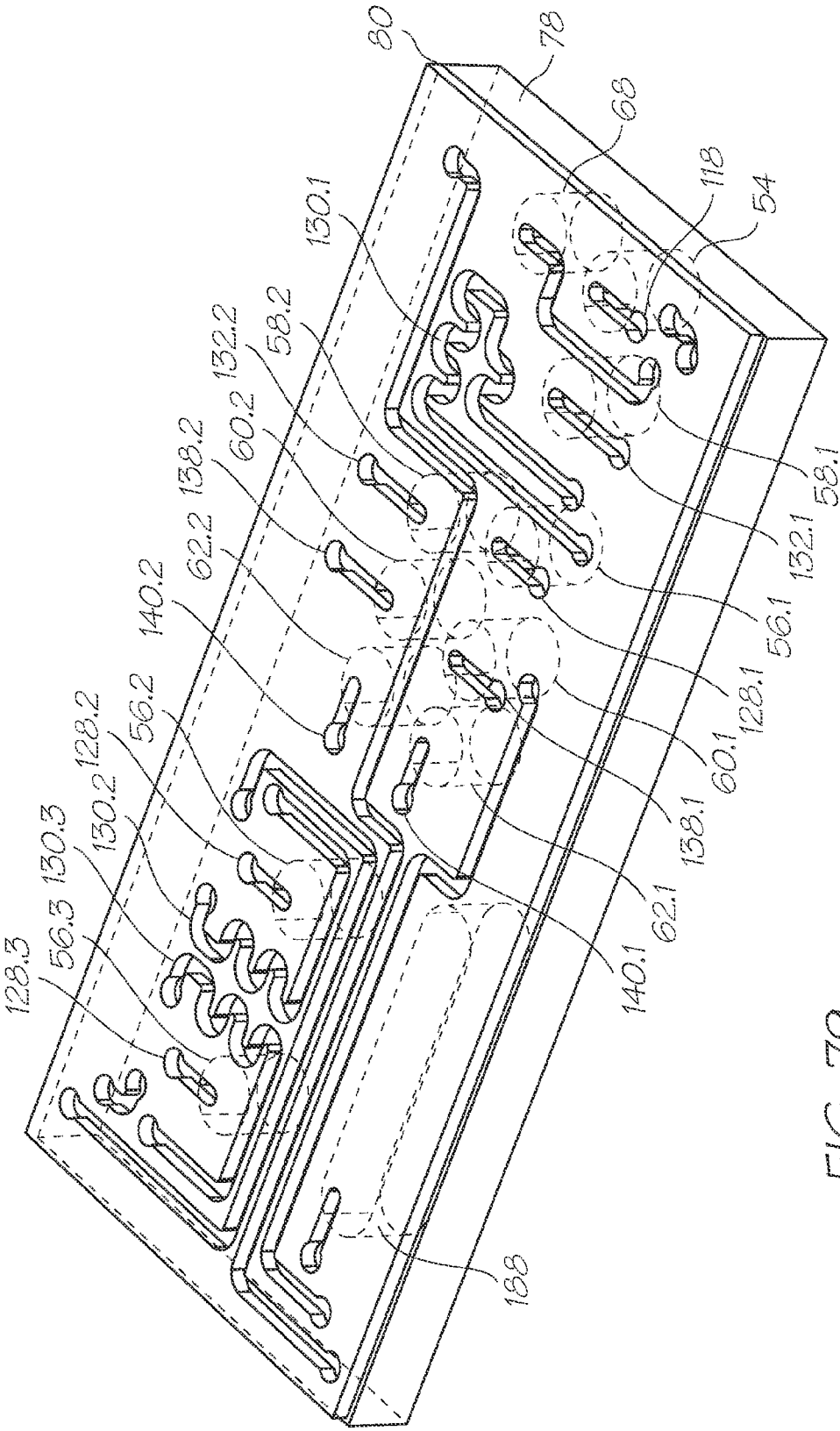

80
78
68
118
54
130.1
58.2
132.2
60.2
138.2
62.2
140.2
56.2
128.2
130.2
130.3
56.3
128.3
58.1
132.1
56.1
128.1
60.1
138.1
62.1
140.1
188

FIG. 79

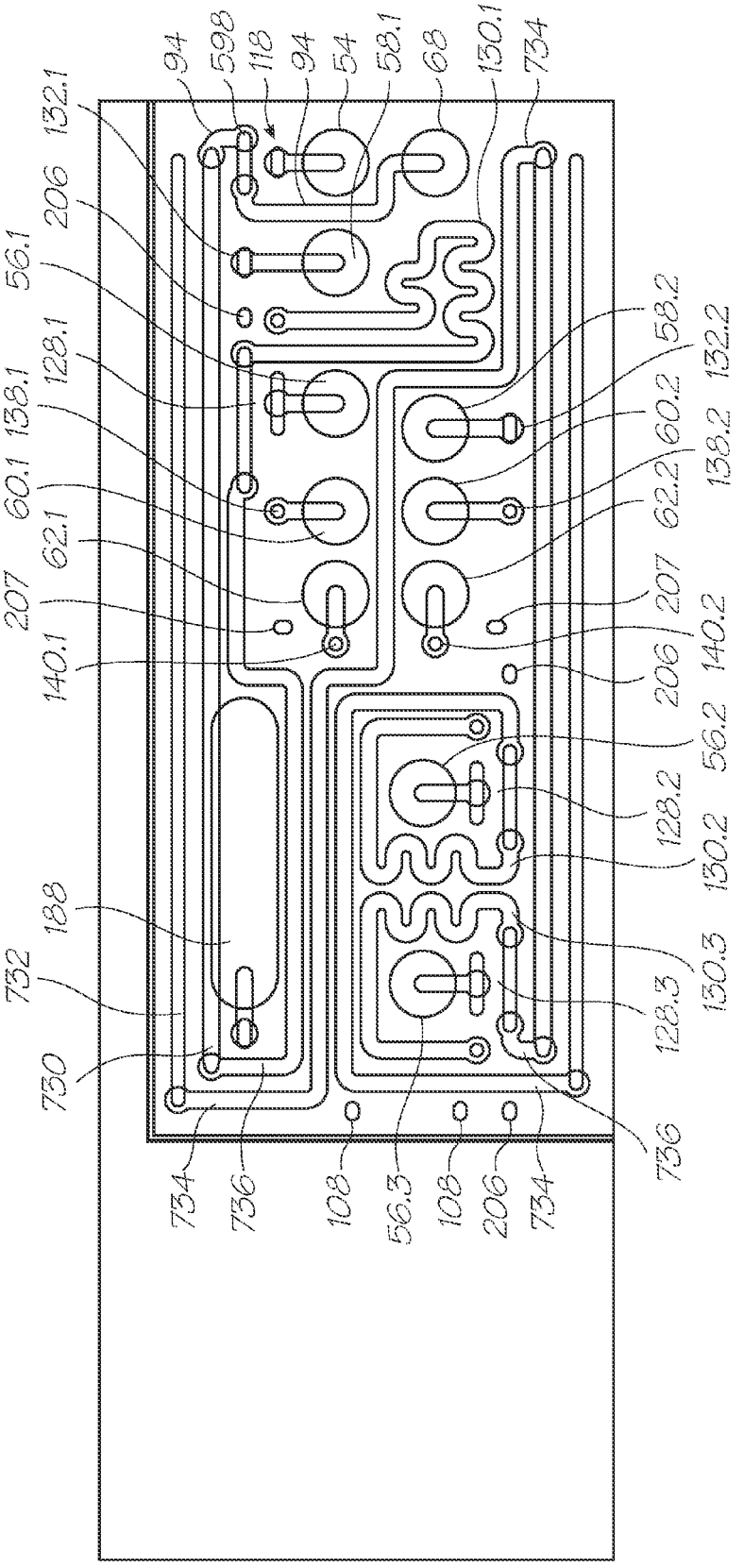

94
598
118
94
54
58.1
68
150.1
734
132.1
206
56.1
58.2
132.2
128.1
138.1
60.2
138.2
60.1
62.2
62.1
207
207
140.1
140.2
206
56.2
128.2
150.2
130.3
128.3
188
732
730
736
734
736
108
56.3
108
206
734

FIG. 80

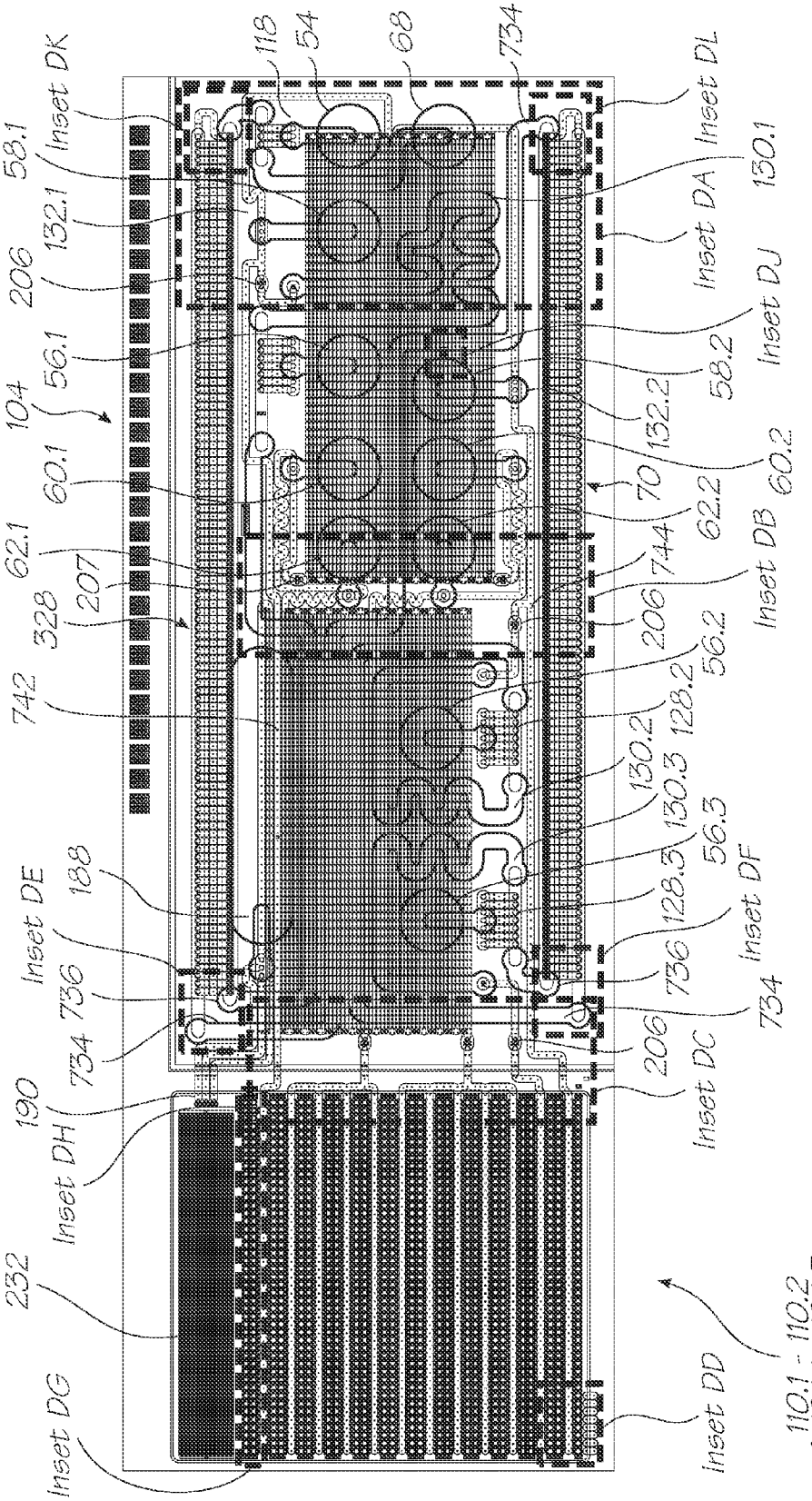

Inset DK
58.1
132.1
206
56.1
104
60.1
62.1
207
328
742
Inset DE
188
736
734
190
Inset DH
232
Inset DG
118
54
68
734
Inset DL
130.1
Inset DA
Inset DJ
58.2
132.2
70
62.2
60.2
Inset DB
744
206
56.2
128.2
130.2
130.3
56.3
128.3
Inset DF
736
734
206
Inset DC
Inset DD
110.1 - 110.2
& 124.1 - 124.3

FIG. 81

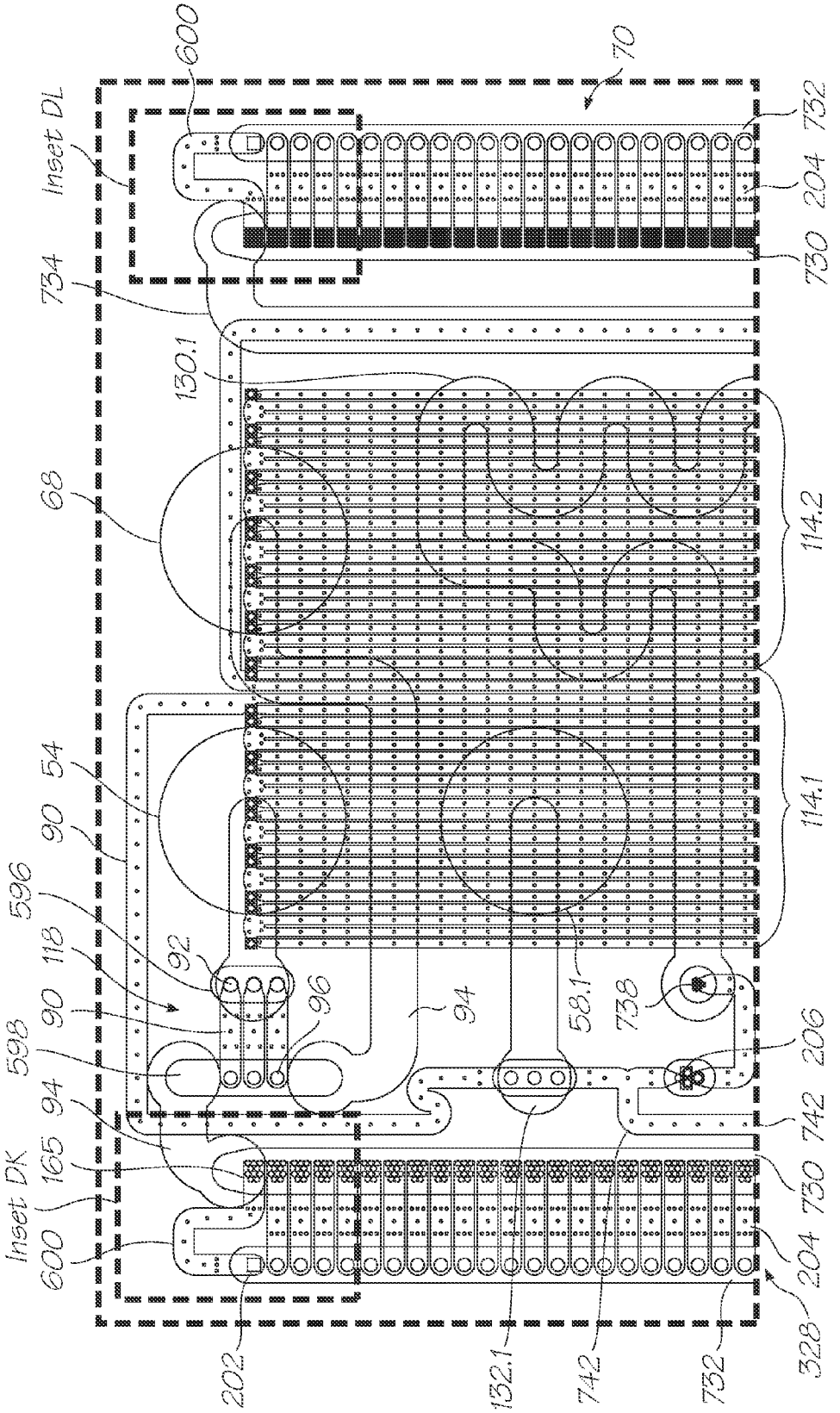


FIG. 82 (Inset DA)

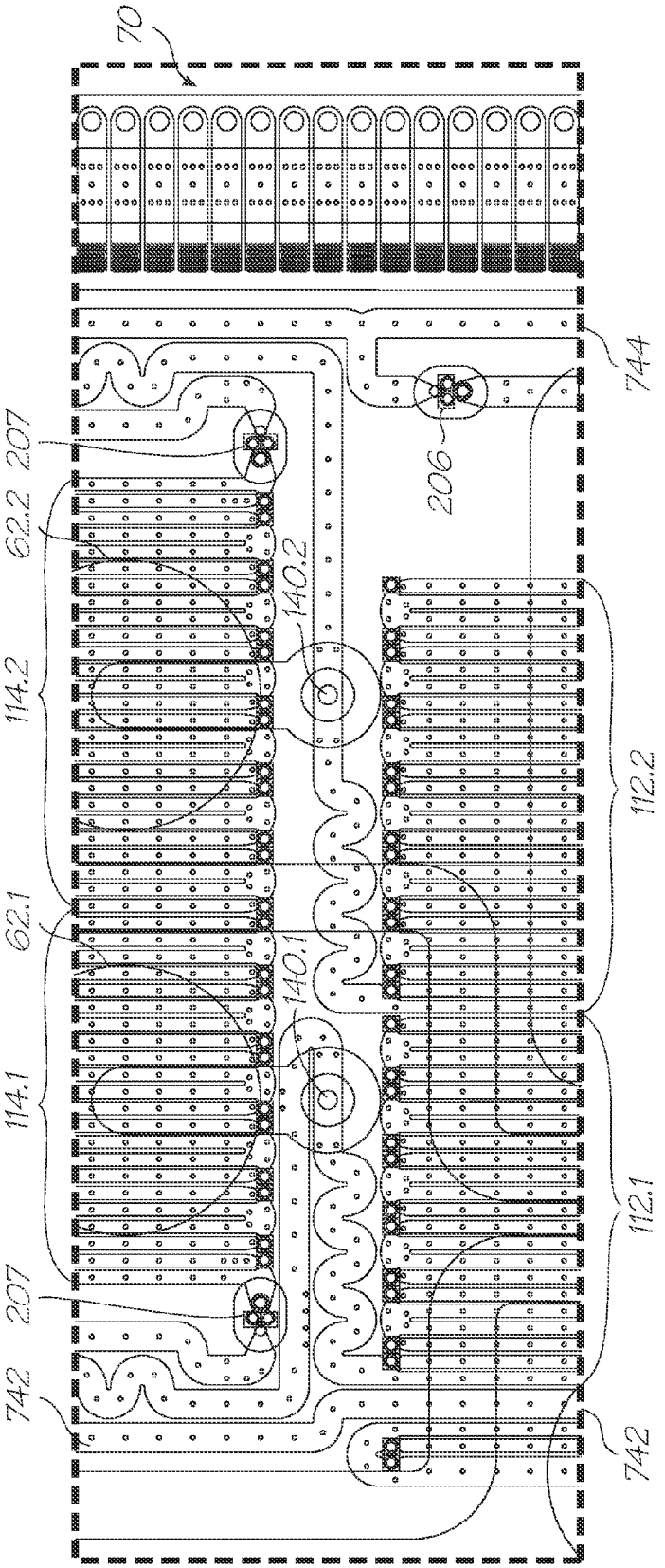


FIG. 83 (Inset DB)

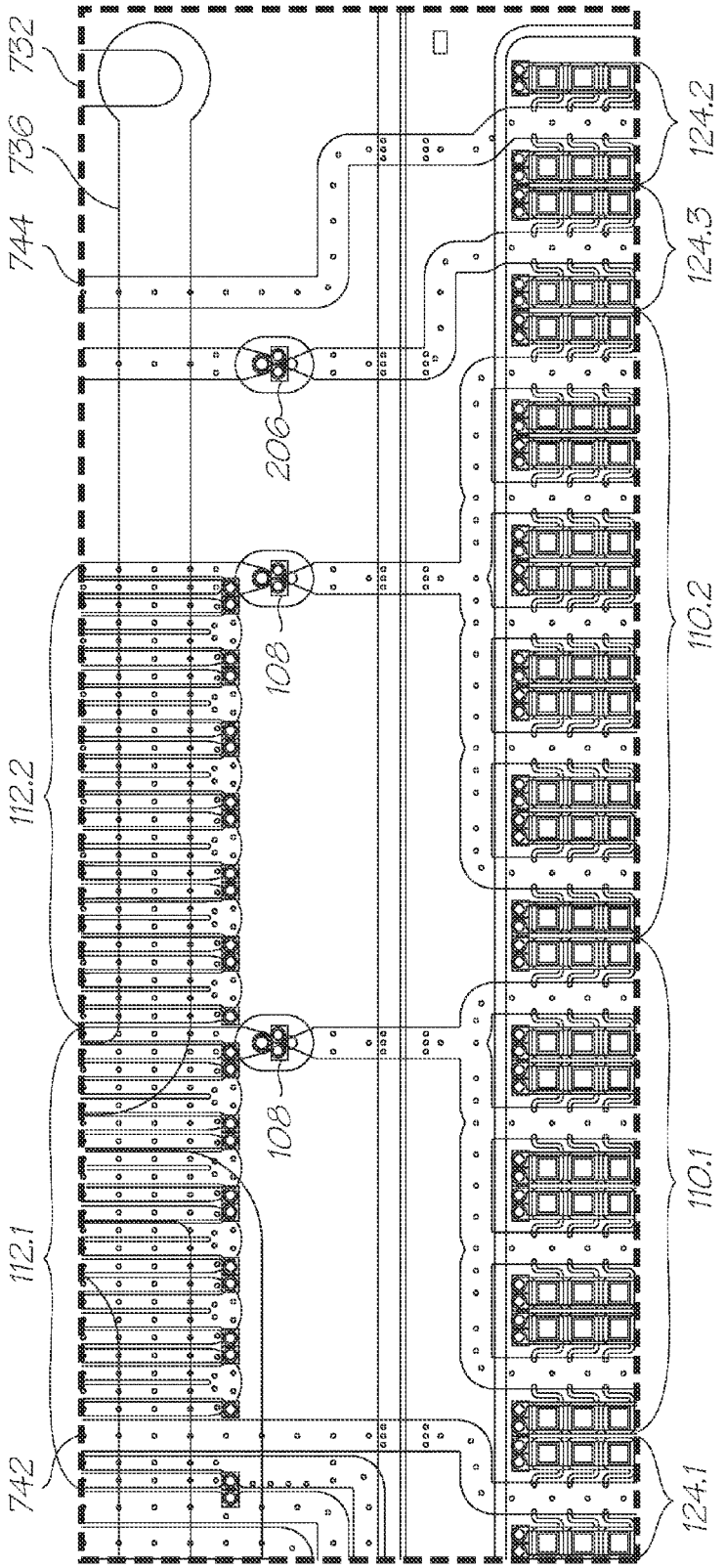


FIG. 84 (Inset DC)

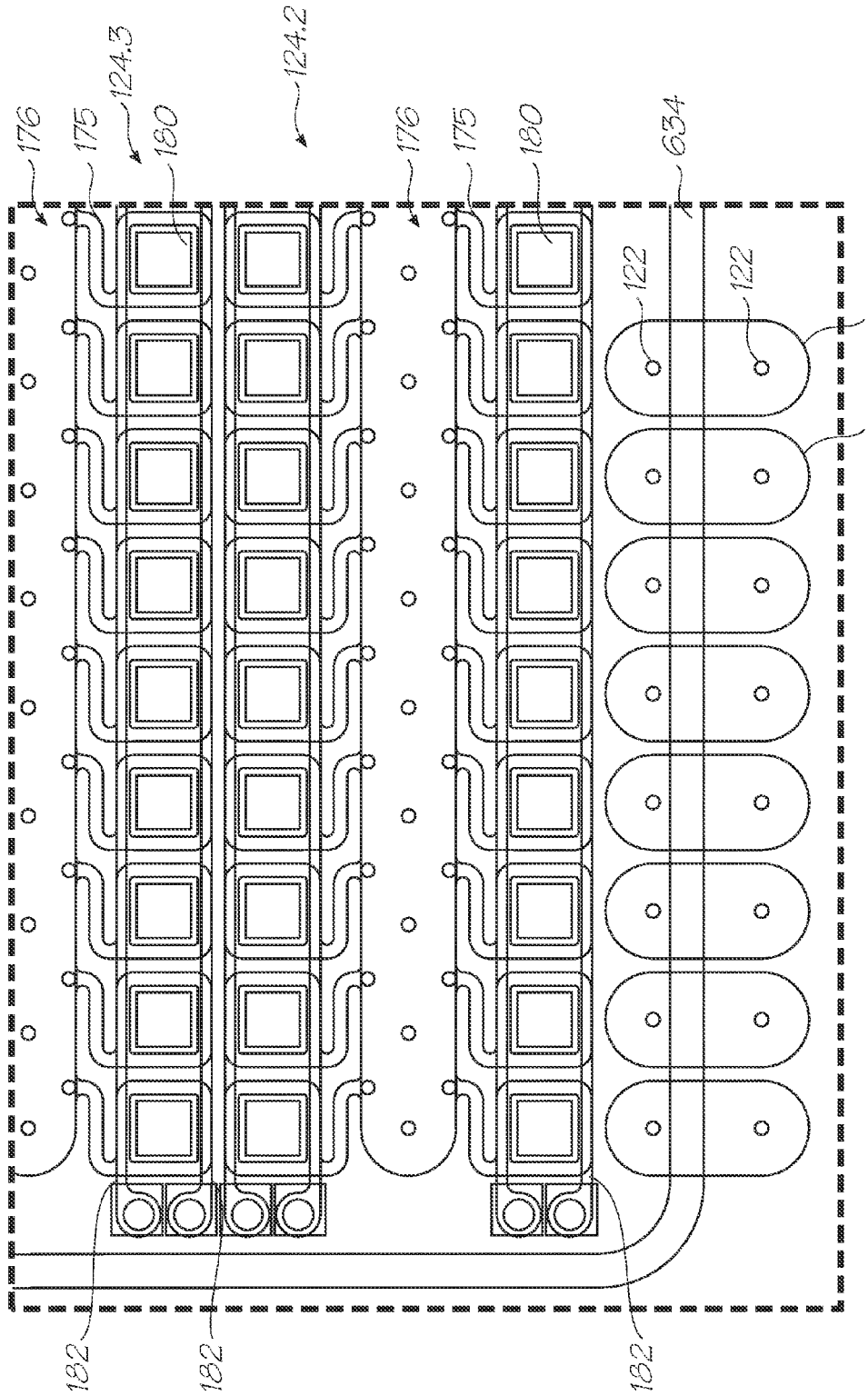


FIG. 85 (Inset DD)

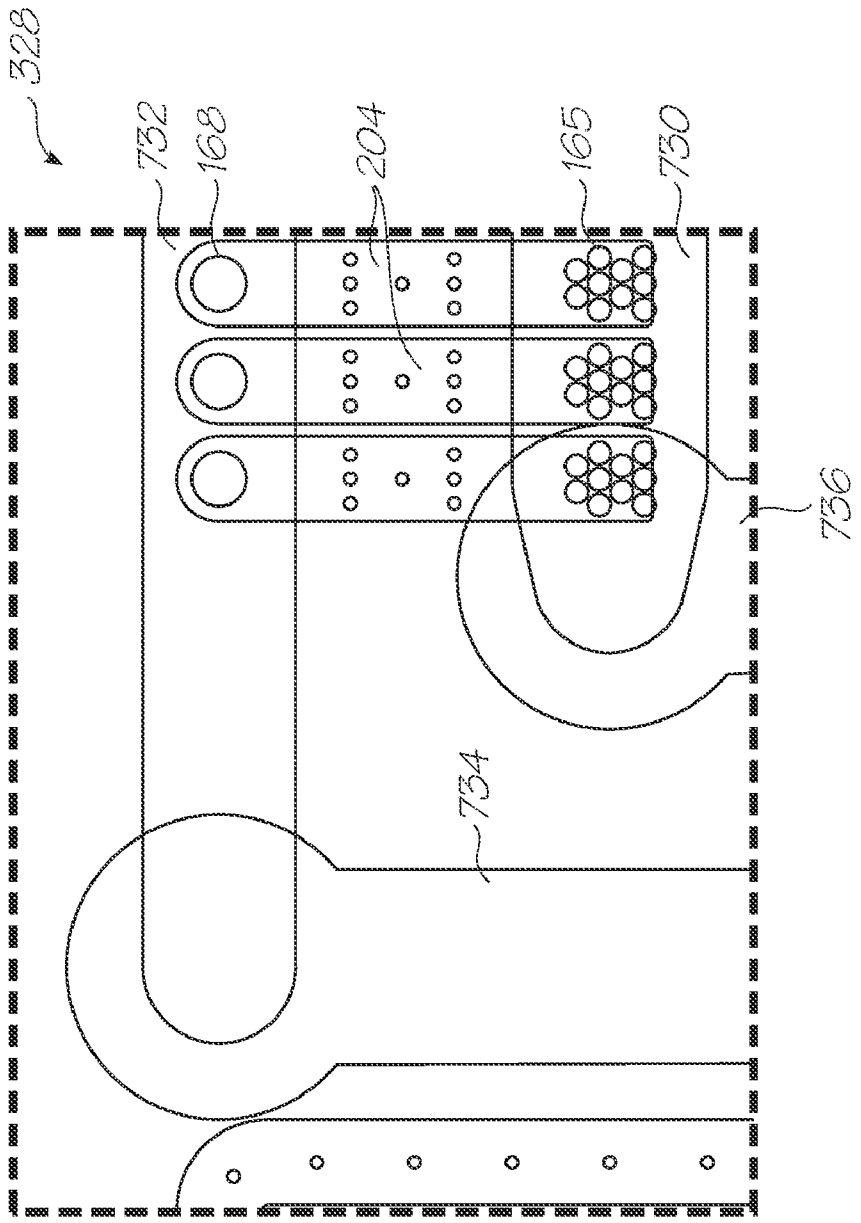


FIG. 86 (Inset DE)

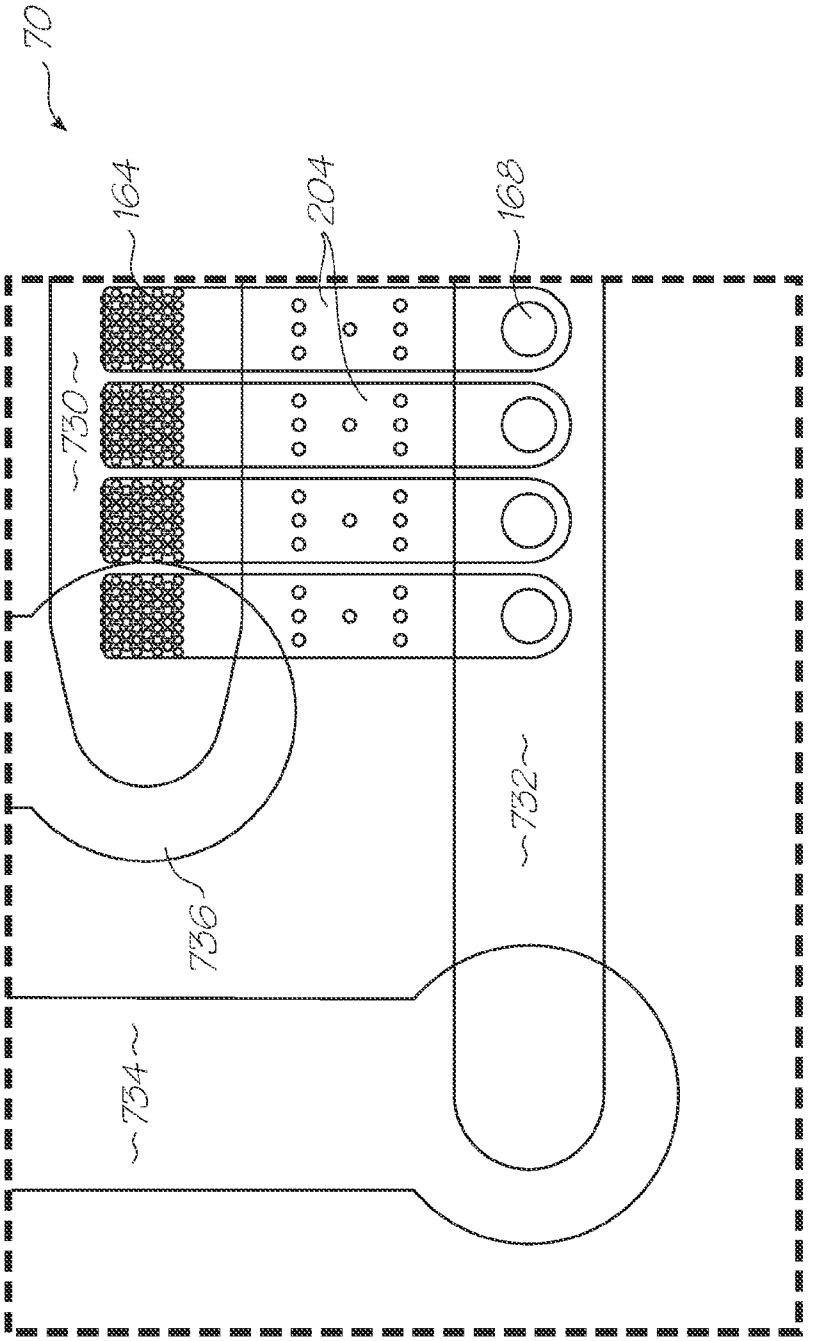


FIG. 87 (Inset DF)

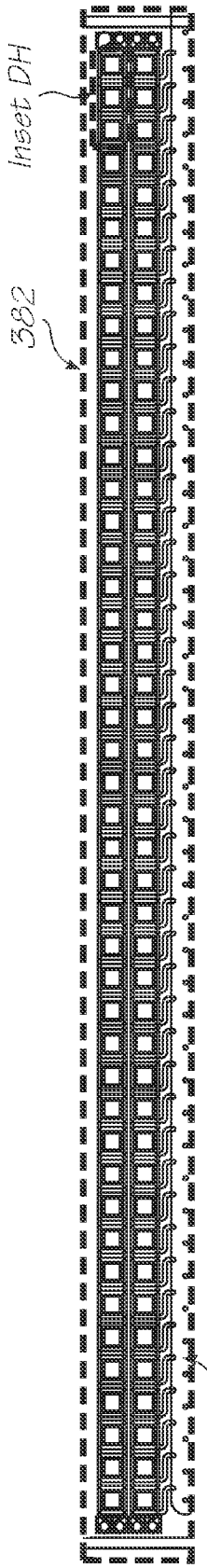


FIG. 88 (Inset DG)

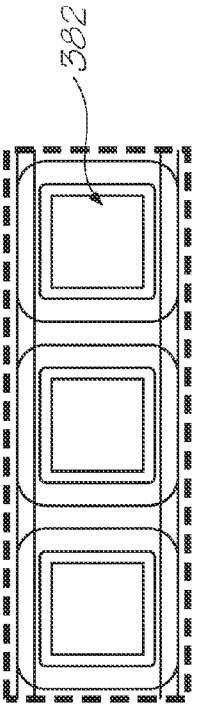


FIG. 89 (Inset DH)

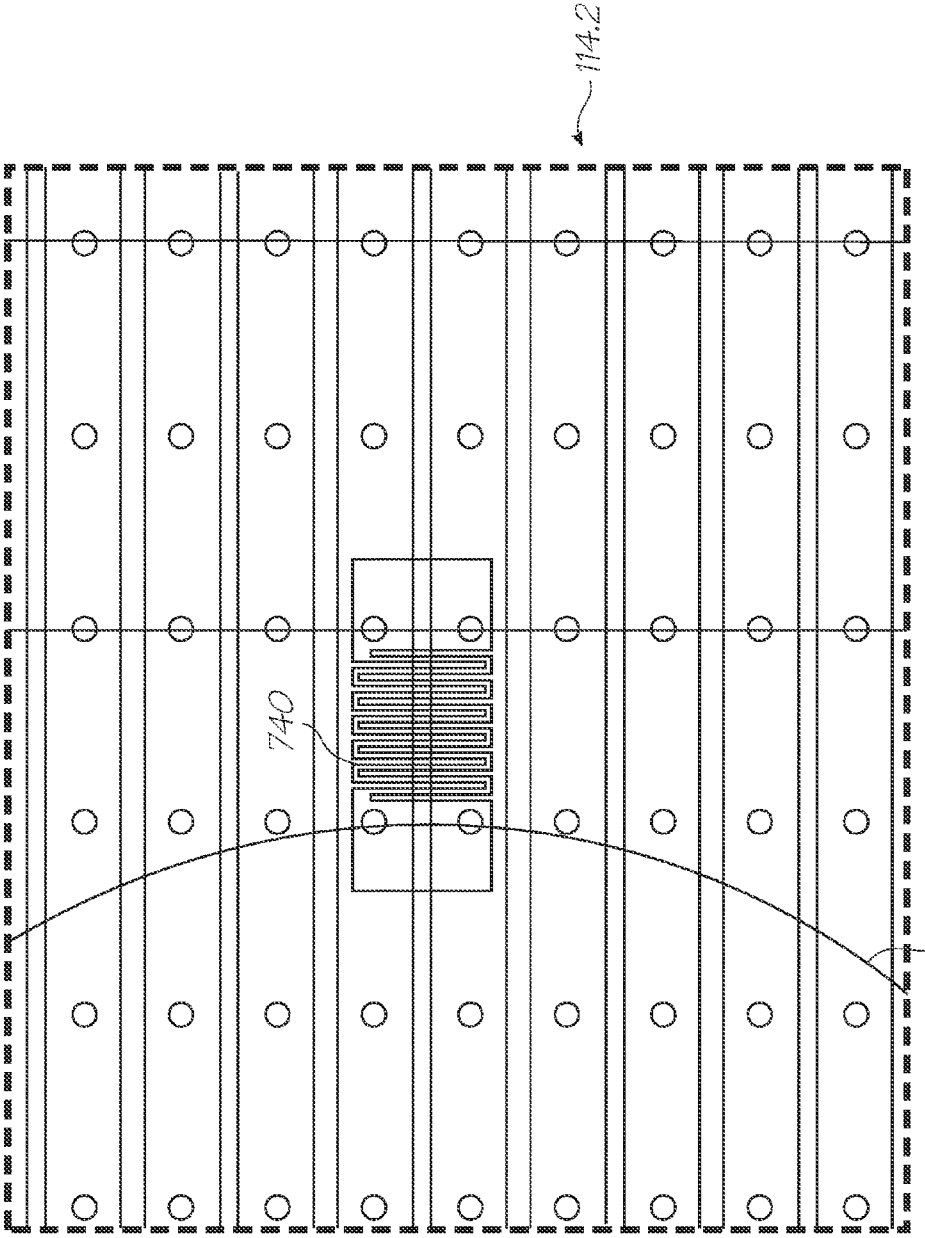


FIG. 90 (Inset DJ)

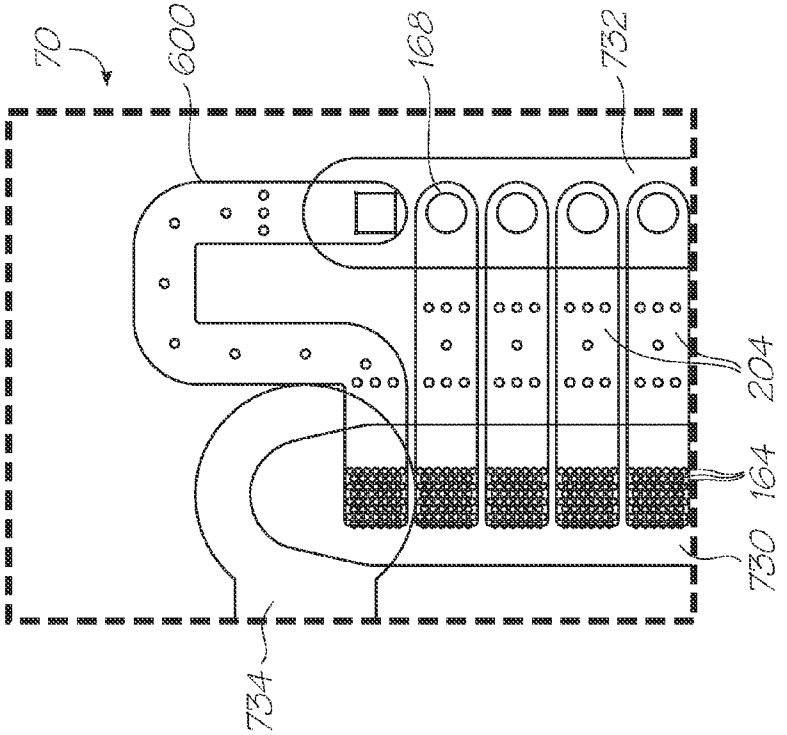


FIG. 92 (Inset DL)

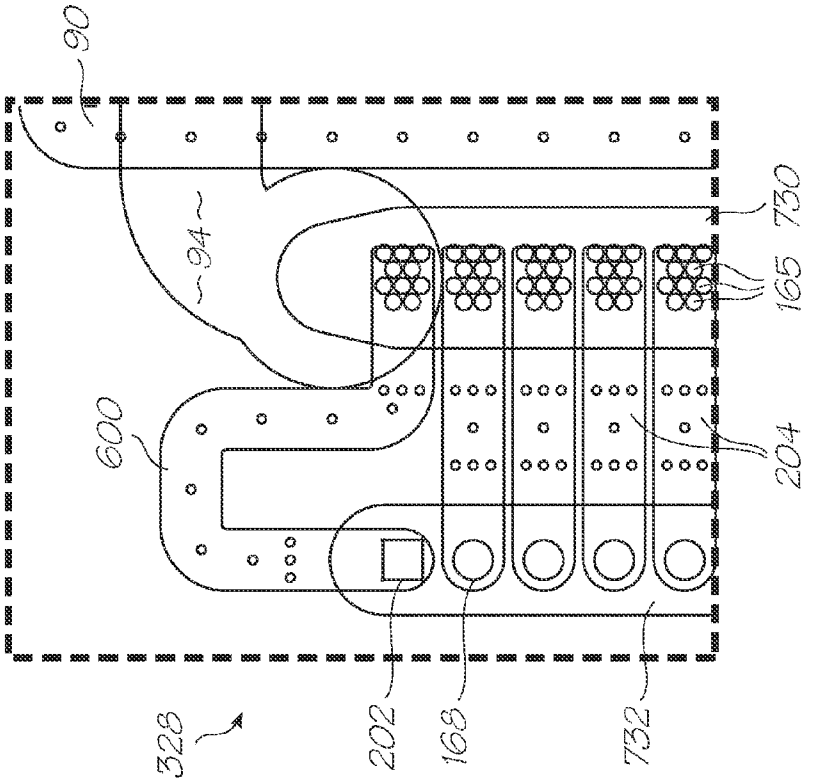


FIG. 91 (Inset DK)

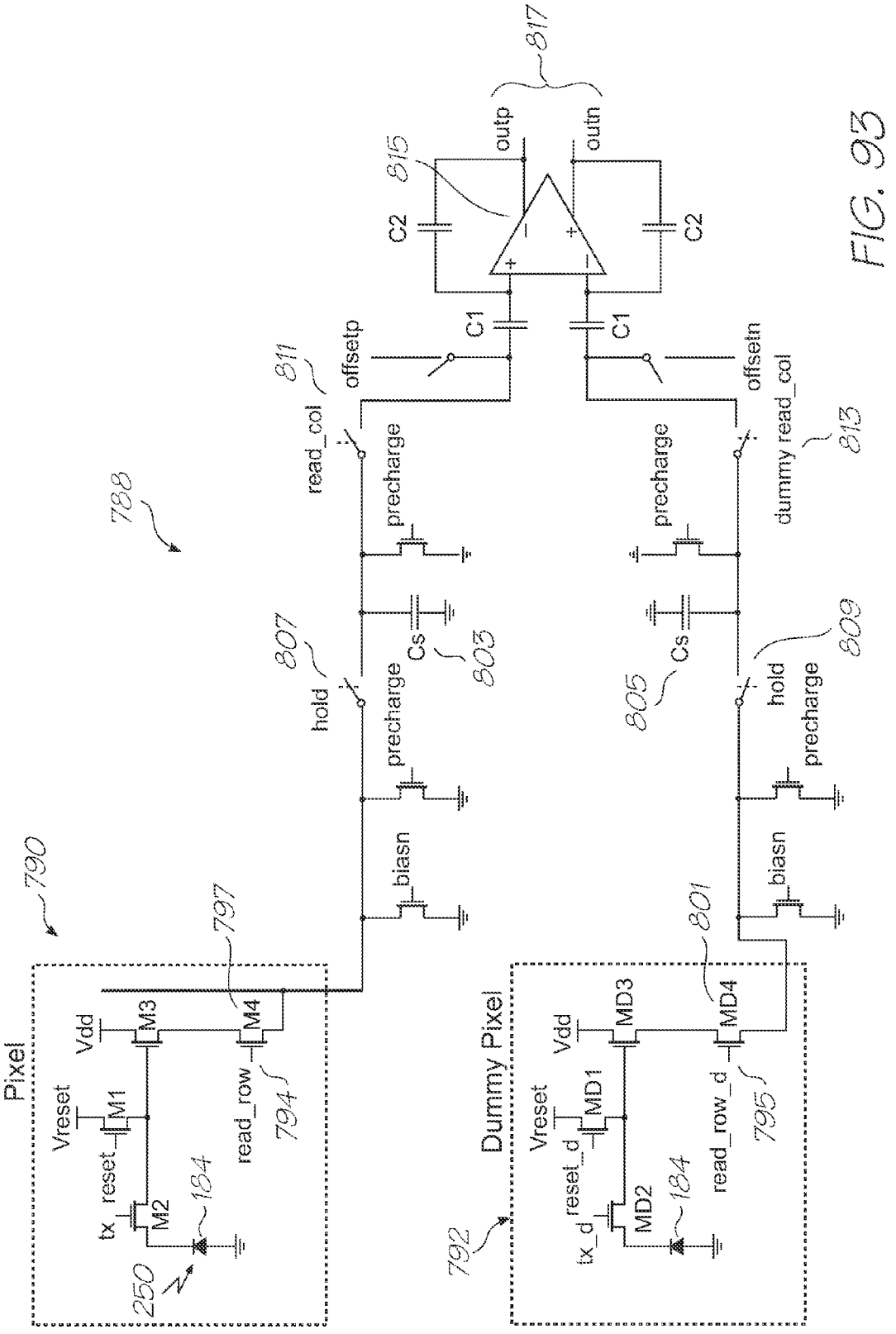

788
790
Pixel
Vreset
M1
reset
tx
M2
184
250
Vdd
M3
M4
read_row
794
797
792
Dummy Pixel
Vreset
MD1
reset_d
ix_d
MD2
184
Vdd
MD3
MD4
read_row_d
795
801
biasn
precharge
hold
Cs
803
805
807
809
read_col
offsetp
811
dummy read_col
offsetn
813
C1
C2
815
outp
outn
817

FIG. 93

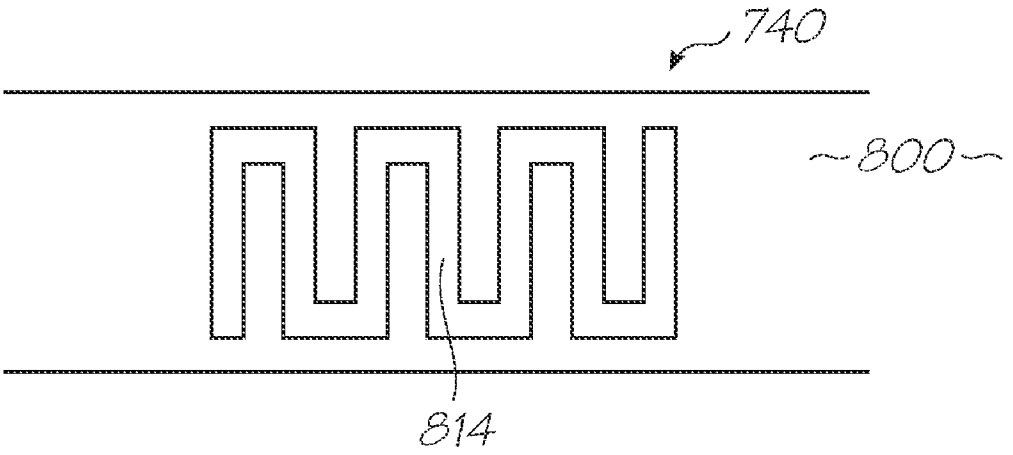


FIG. 94

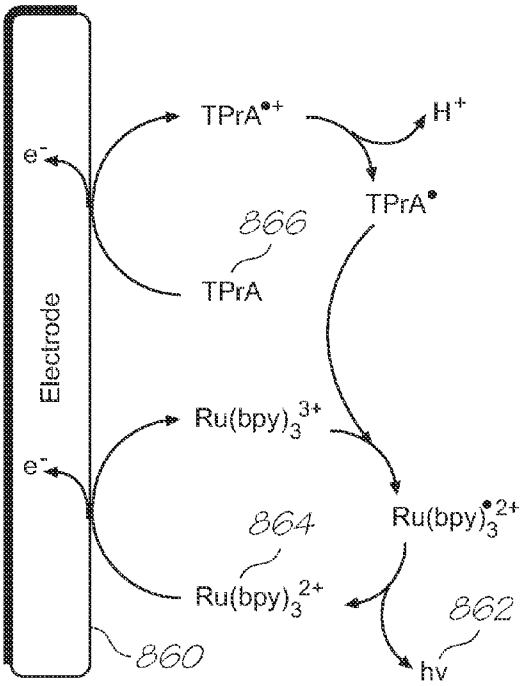


FIG. 95
(PRIOR ART)

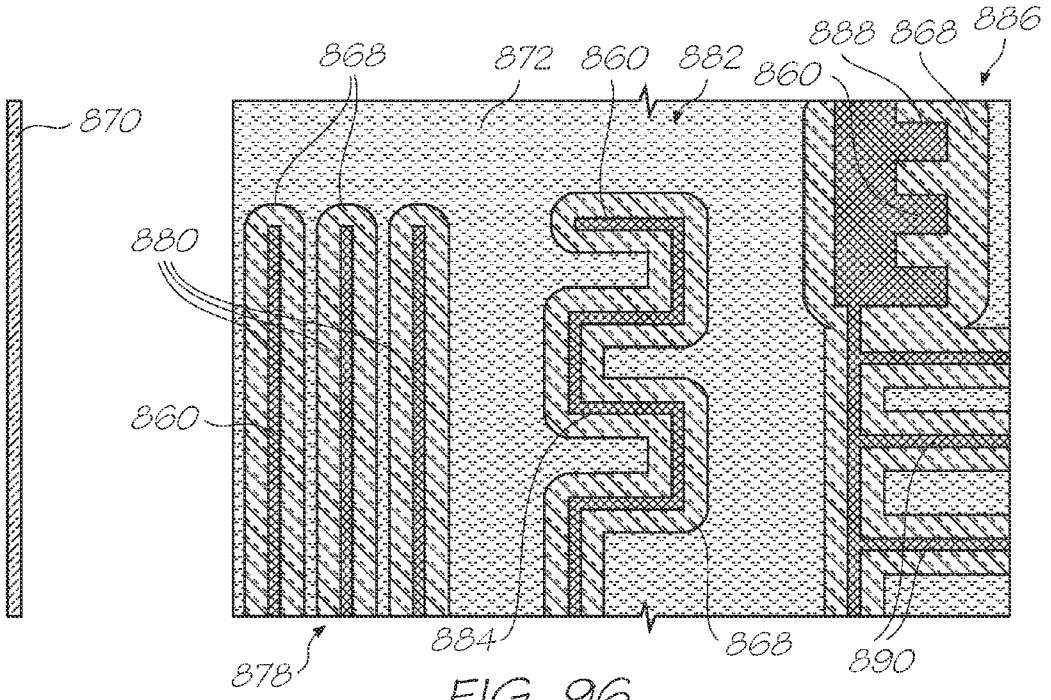


FIG. 96

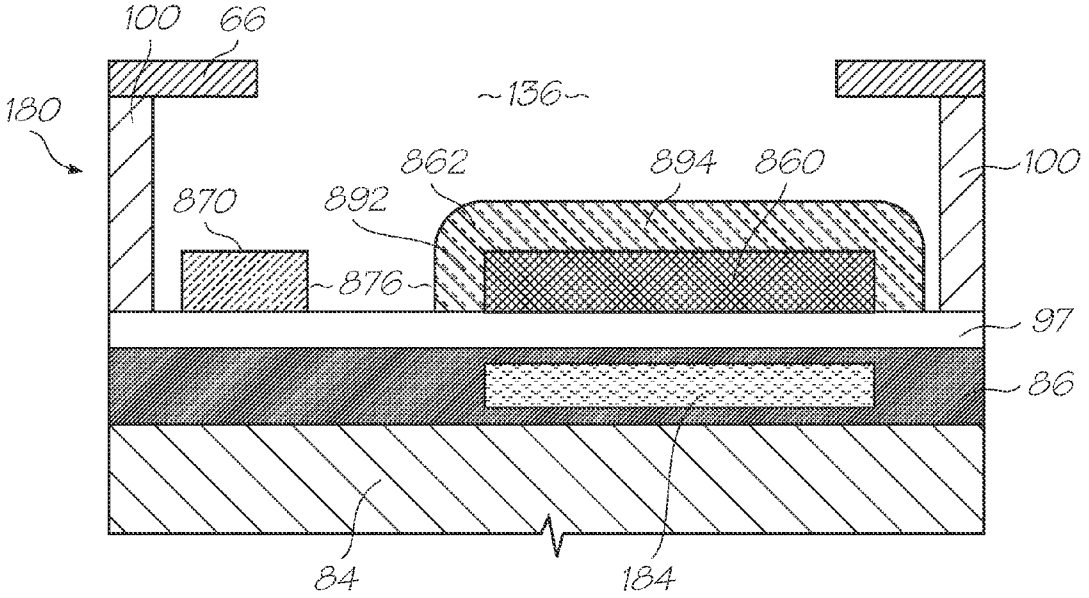

100
66
180
136
862
894
860
100
870
892
876
97
86
84
184

FIG. 97

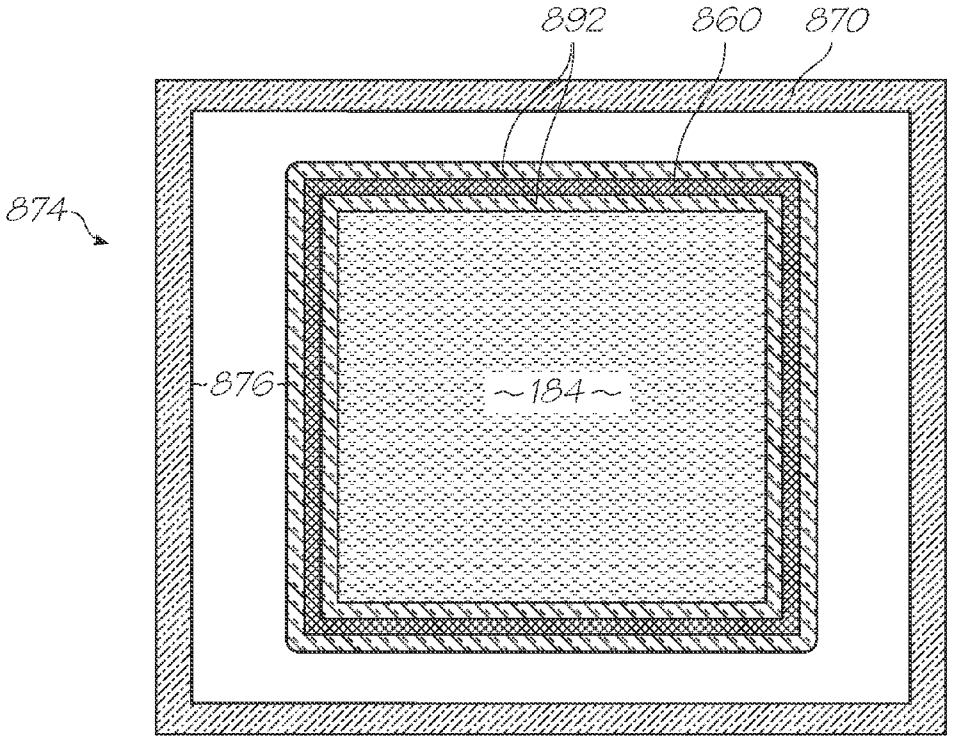

892
860
870
874
876
184

FIG. 98

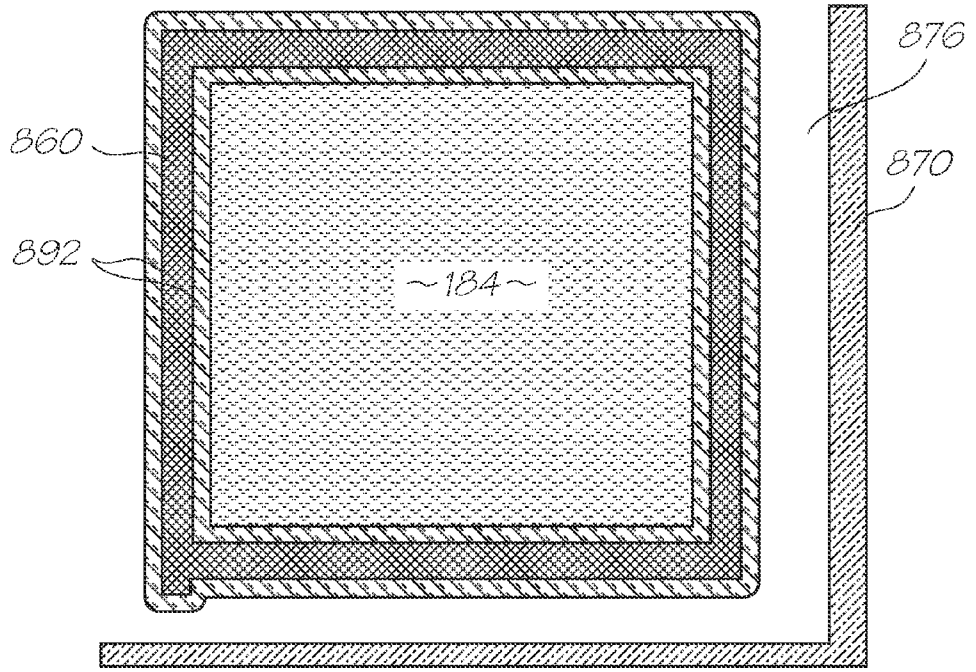


FIG. 99

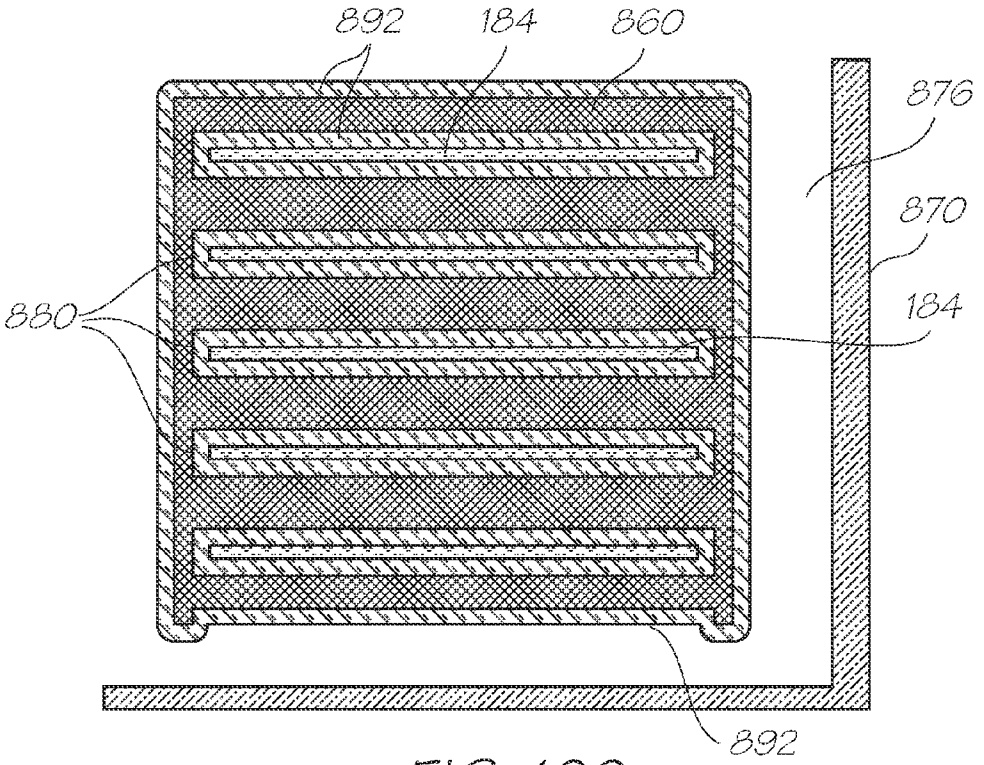


FIG. 100

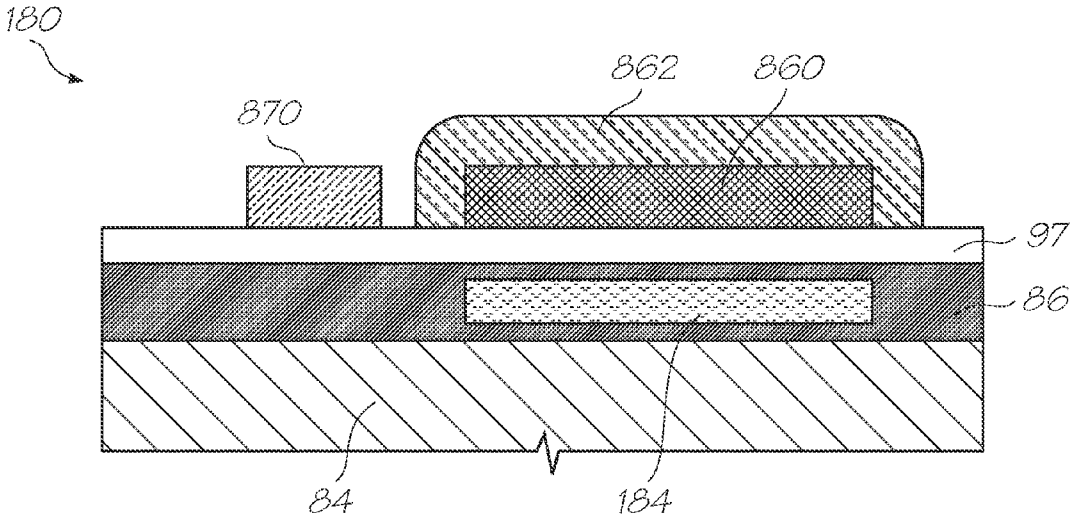


FIG. 101

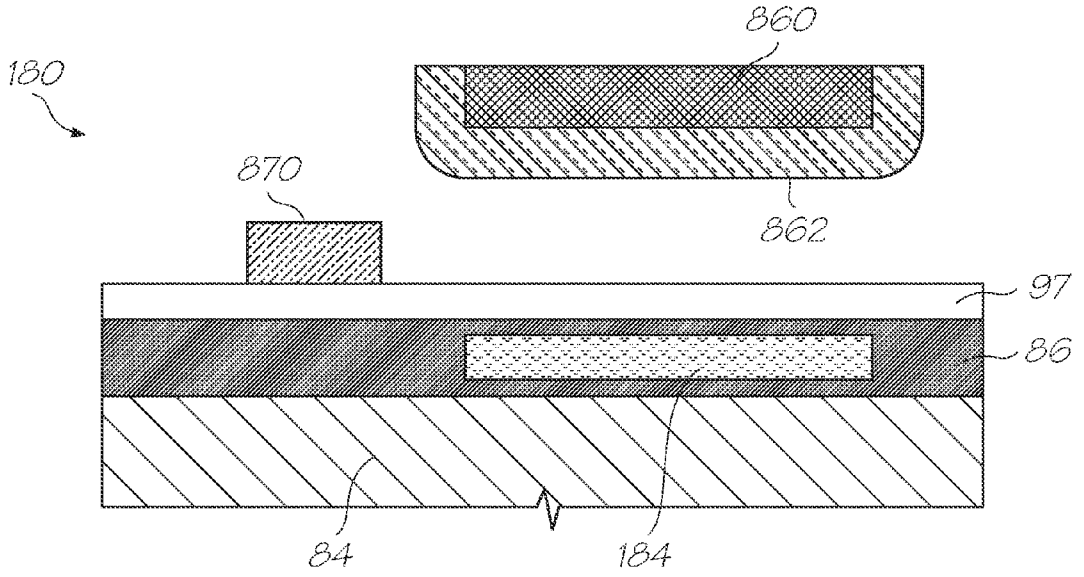


FIG. 102

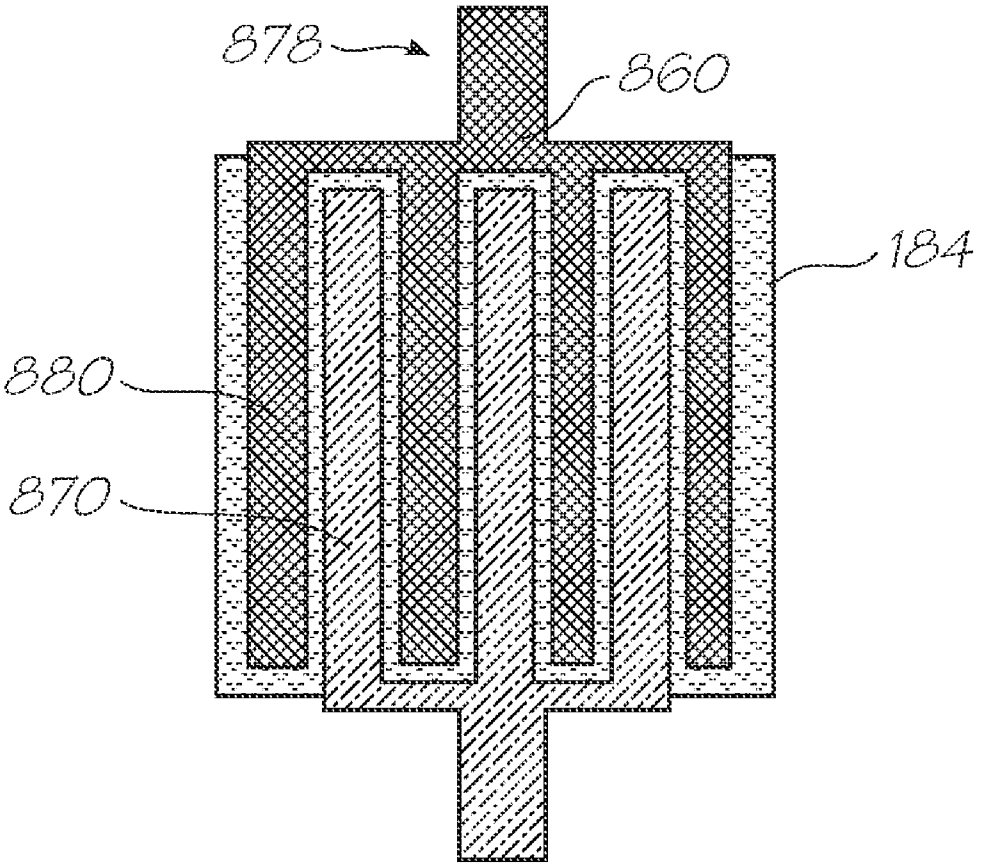


FIG. 103

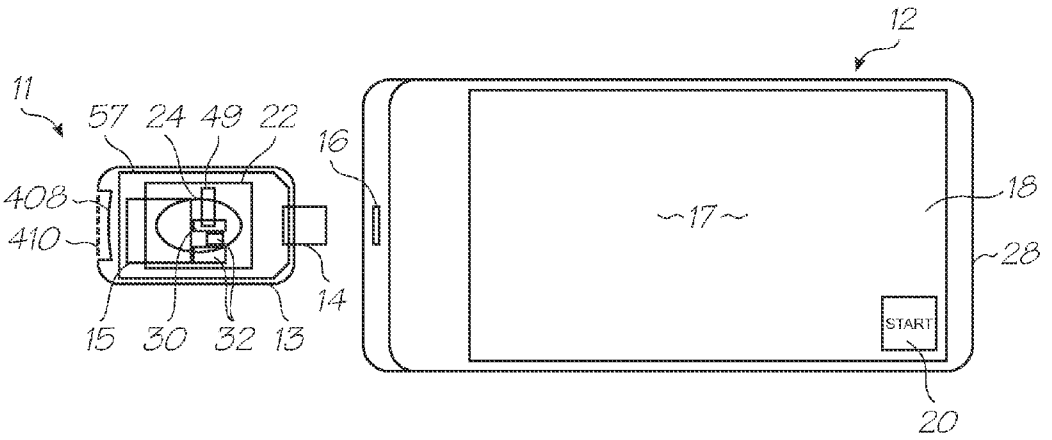


FIG. 104

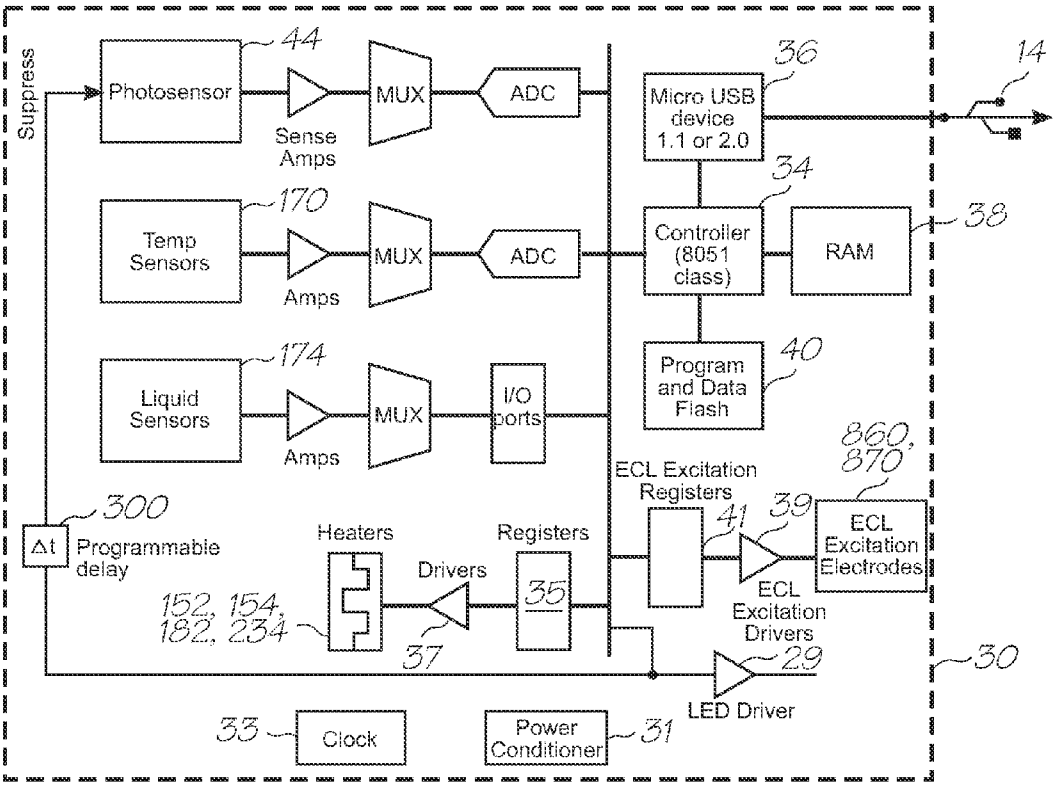


FIG. 105

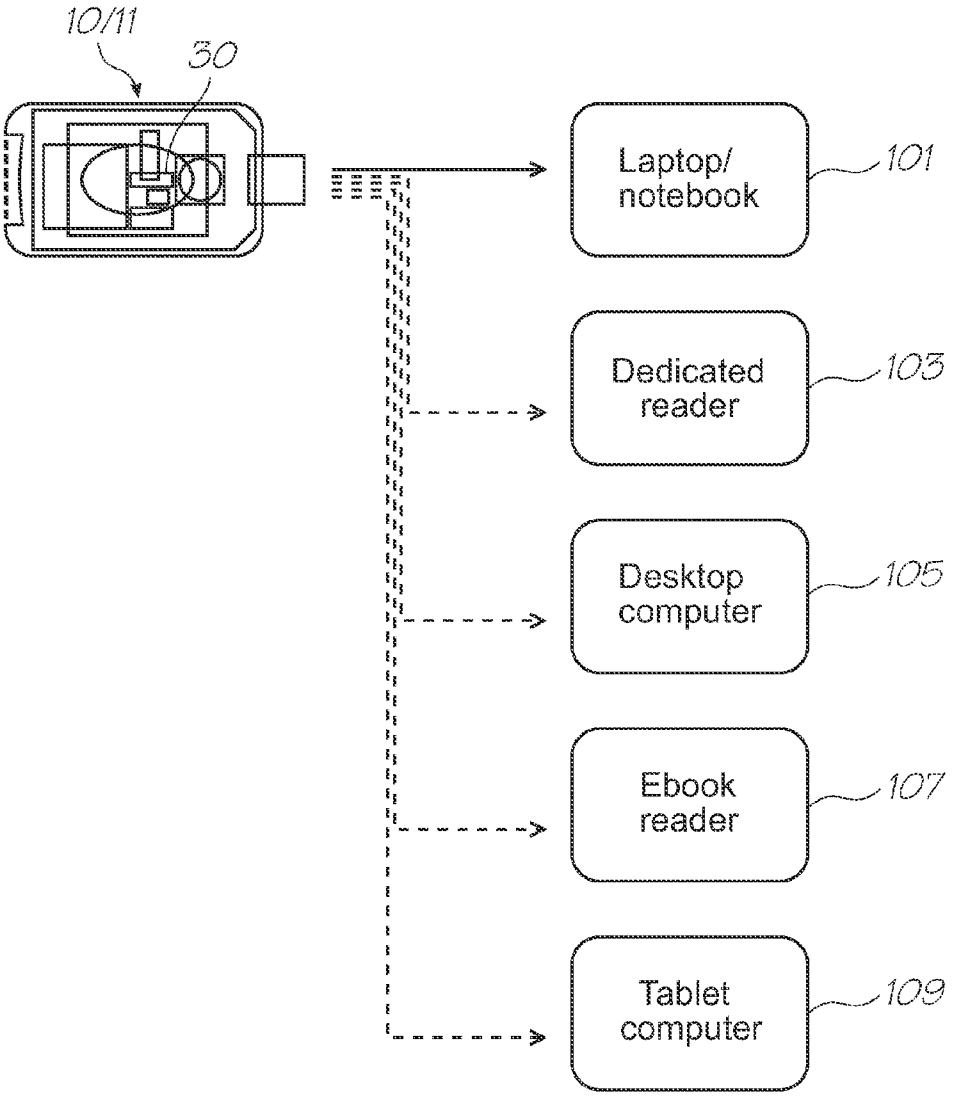

10/11
30
Laptop/ notebook
101
Dedicated reader
103
Desktop computer
105
Ebook reader
107
Tablet computer
109

FIG. 106

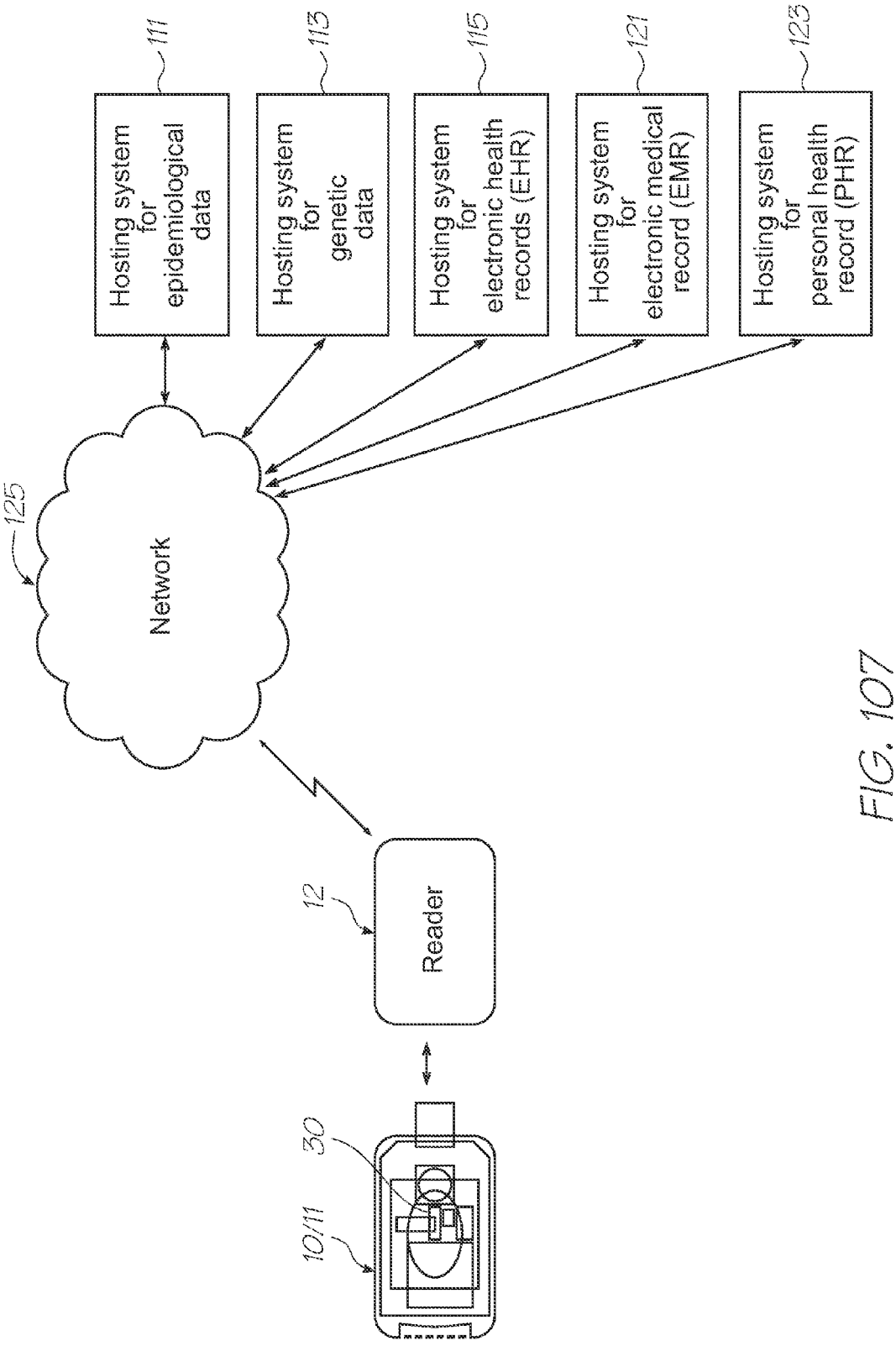

111
Hosting system for epidemiological data
113
Hosting system for genetic data
115
Hosting system for electronic health records (EHR)
121
Hosting system for electronic medical record (EMR)
123
Hosting system for personal health record (PHR)
125
Network
12
Reader
30
10/11

FIG. 107

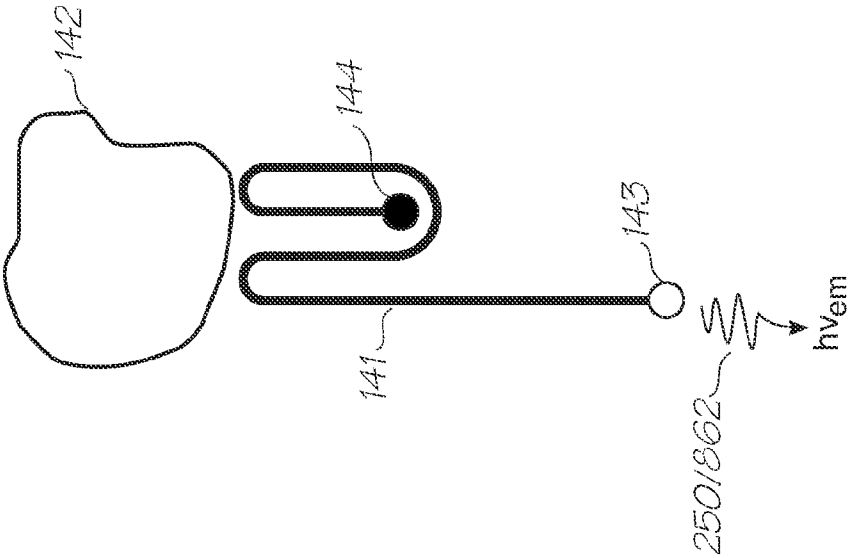


FIG. 108B
(PRIOR ART)

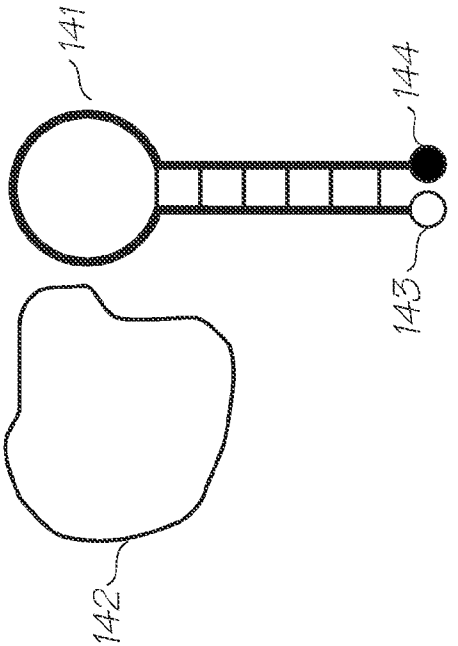


FIG. 108A
(PRIOR ART)

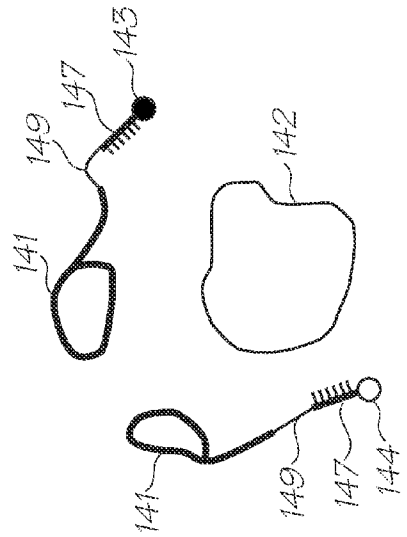


FIG. 109A
(PRIOR ART)

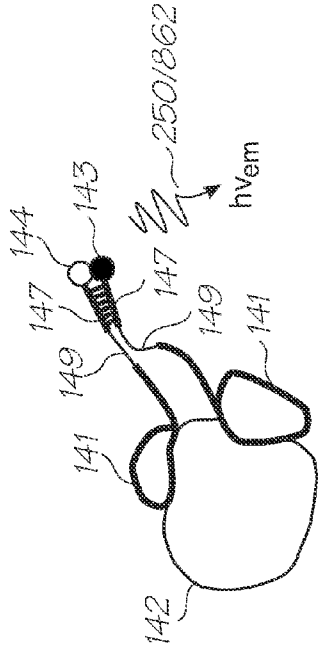


FIG. 109B
(PRIOR ART)

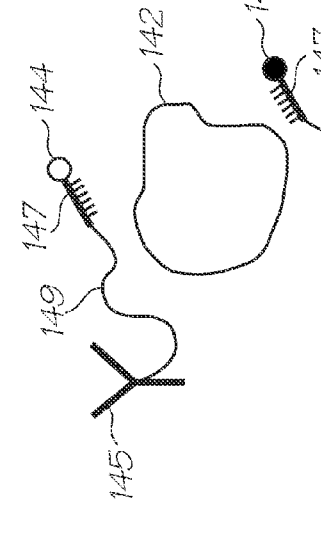


FIG. 110A
(PRIOR ART)

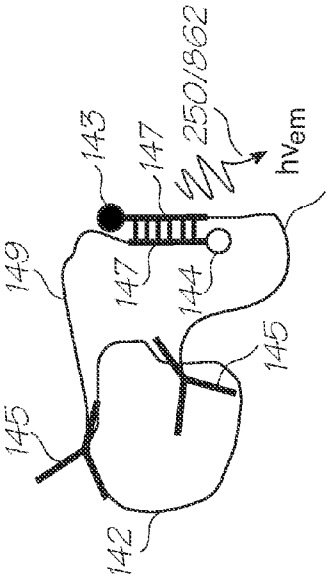


FIG. 110B
(PRIOR ART)

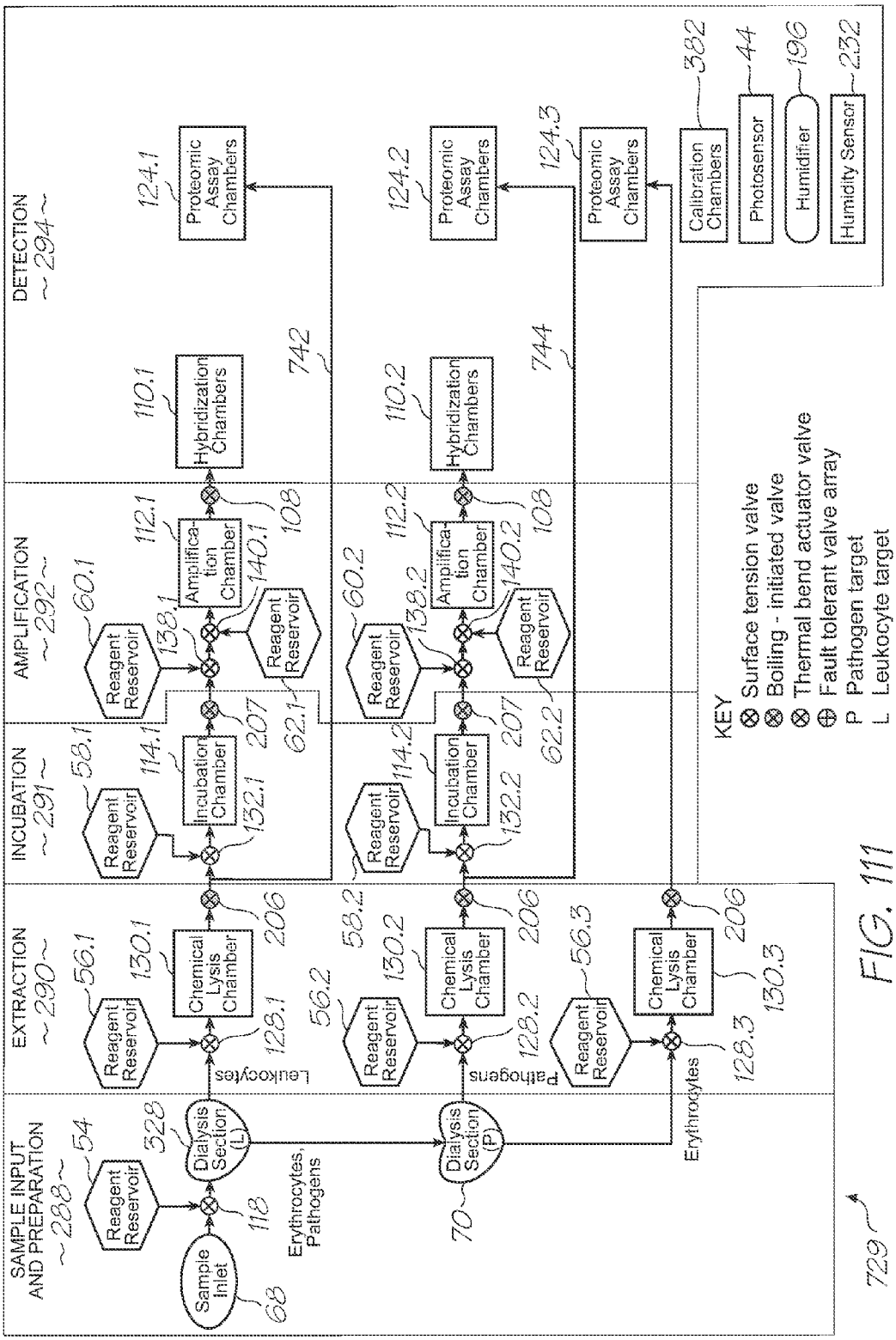

SAMPLE INPUT AND PREPARATION
~288~
EXTRACTION
~290~
INCUBATION
~291~
AMPLIFICATION
~292~
DETECTION
~294~
Reagent Reservoir
Sample Inlet
Dialysis Section (L)
Dialysis Section (P)
Chemical Lysis Chamber
Incubation Chamber
Amplification Chamber
Hybridization Chambers
Proteomic Assay Chambers
Calibration Chambers
Photosensor
Humidifier
Humidity Sensor
Erythrocytes, Pathogens
Leukocytes
Pathogens
Erythrocytes
KEY
Surface tension valve
Boiling - initiated valve
Thermal bend actuator valve
Fault tolerant valve array
P Pathogen target
L Leukocyte target

FIG. 111

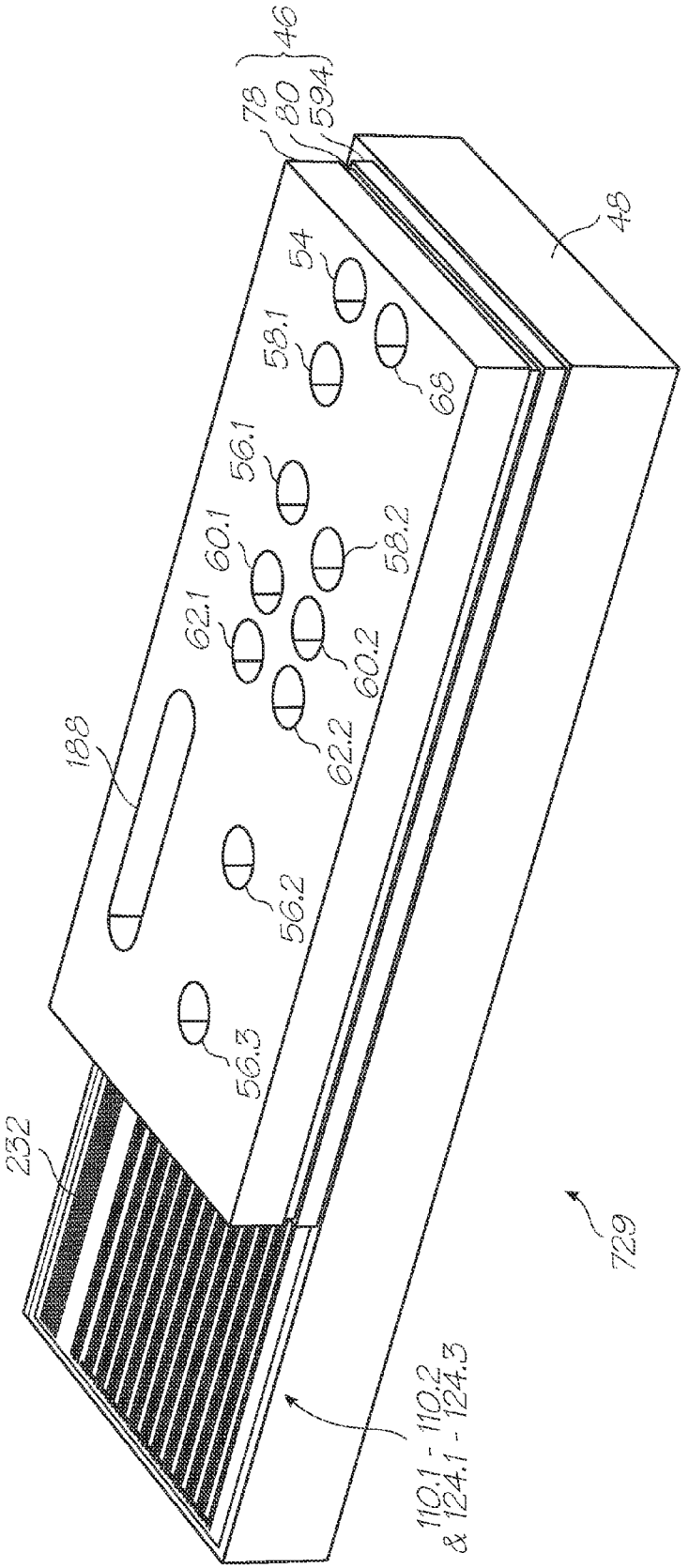

46
78
80
594
48
54
58.1
66
56.1
60.1
58.2
62.1
60.2
62.2
188
56.2
56.3
232
729
110.1 - 110.2
& 124.1 - 124.3

FIG. 112

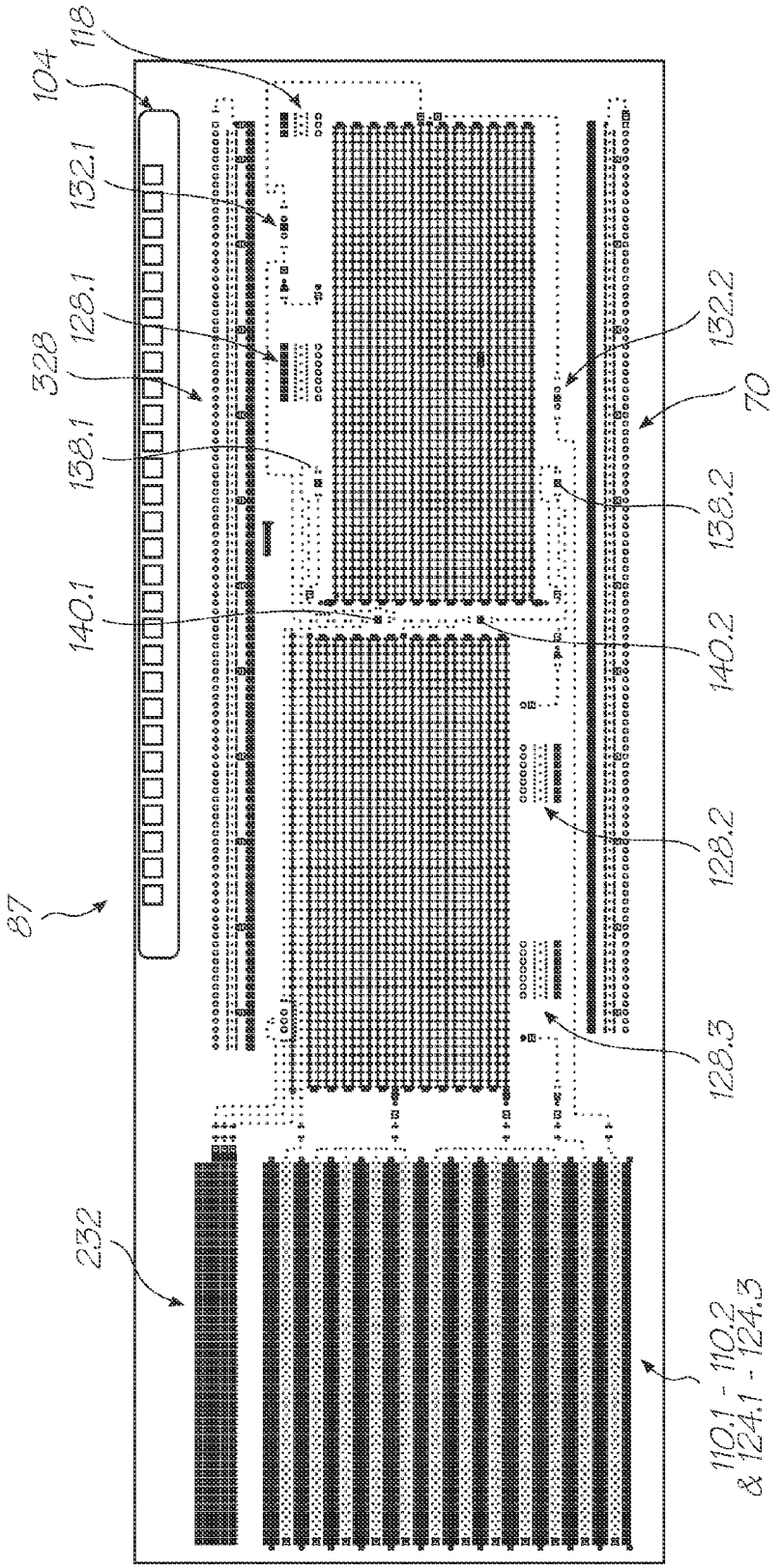

87
104
118
132.1
328
128.1
138.1
140.1
132.2
70
138.2
140.2
128.2
128.3
232
110.1 - 110.2
& 124.1 - 124.3

FIG. 113

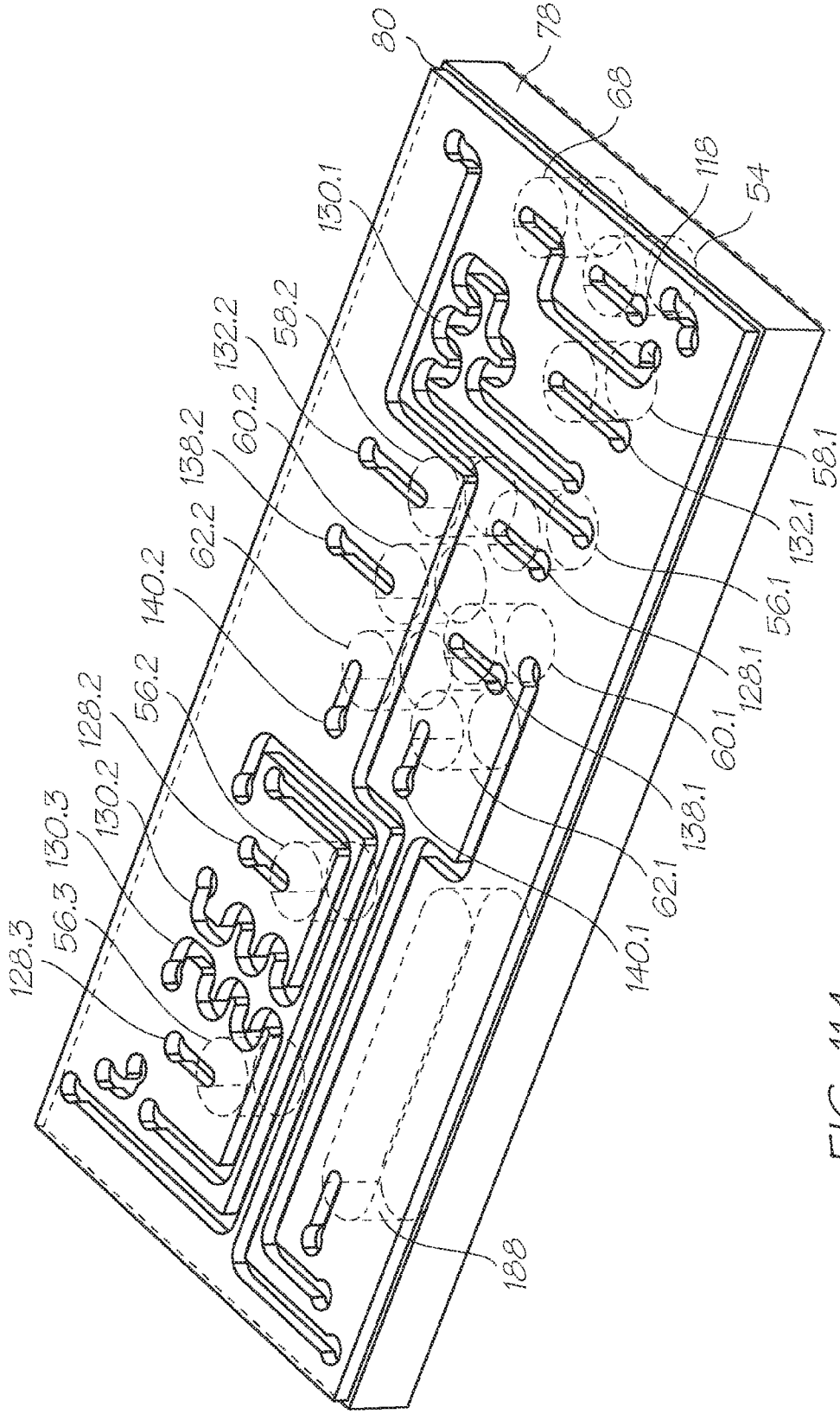

80
78
68
118
54
130.1
58.2
132.2
60.2
158.2
62.2
140.2
56.2
128.2
130.2
130.3
56.3
128.3
58.1
132.1
56.1
128.1
60.1
138.1
62.1
140.1
188

FIG. 114

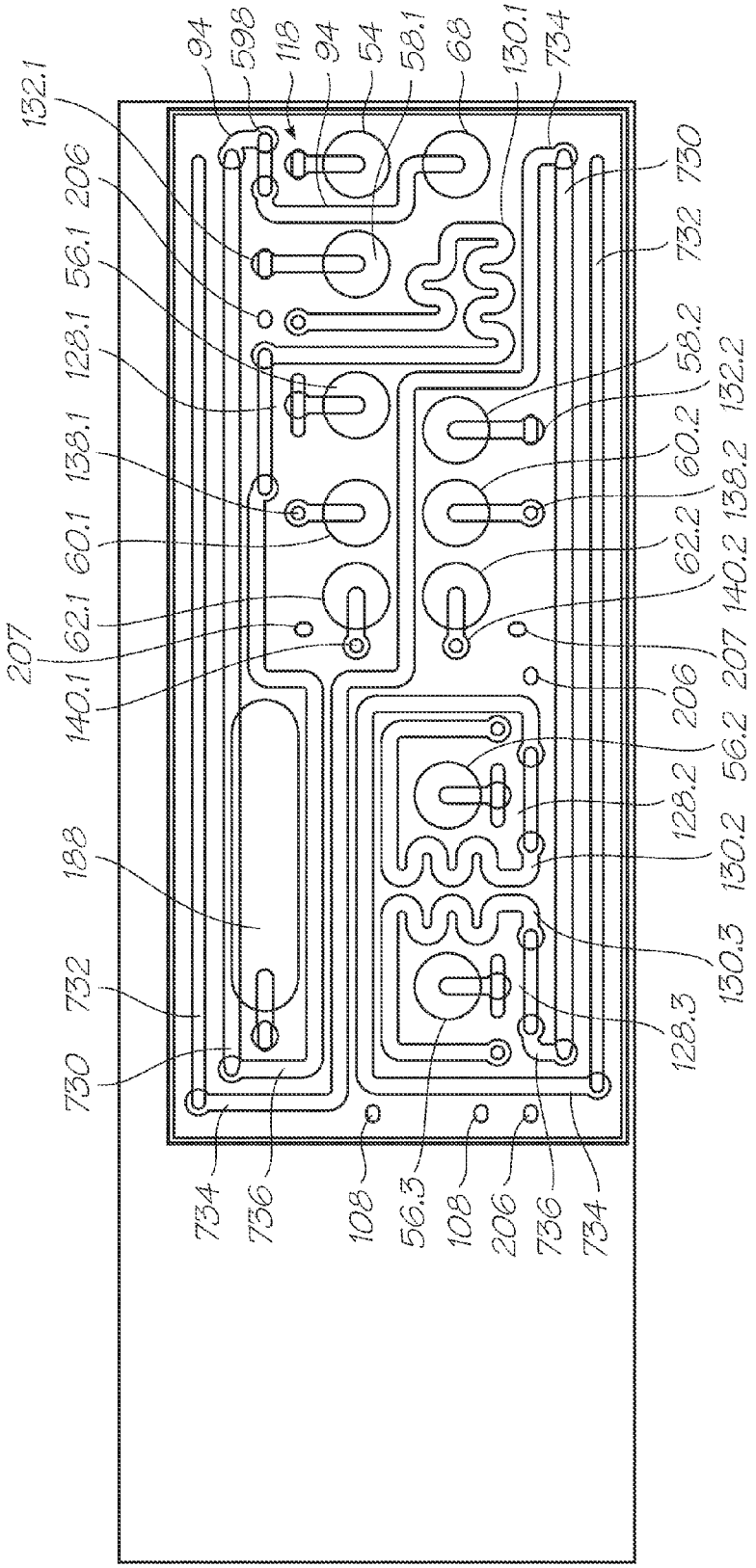

94
598
118
94
54
58.1
68
130.1
734
132.1
206
56.1
128.1
138.1
60.1
62.1
140.1
207
188
732
730
730
732
58.2
132.2
60.2
138.2
62.2
140.2
207
206
56.2
128.2
130.2
130.3
128.3
734
736
108
56.3
108
206
736
734

FIG. 115

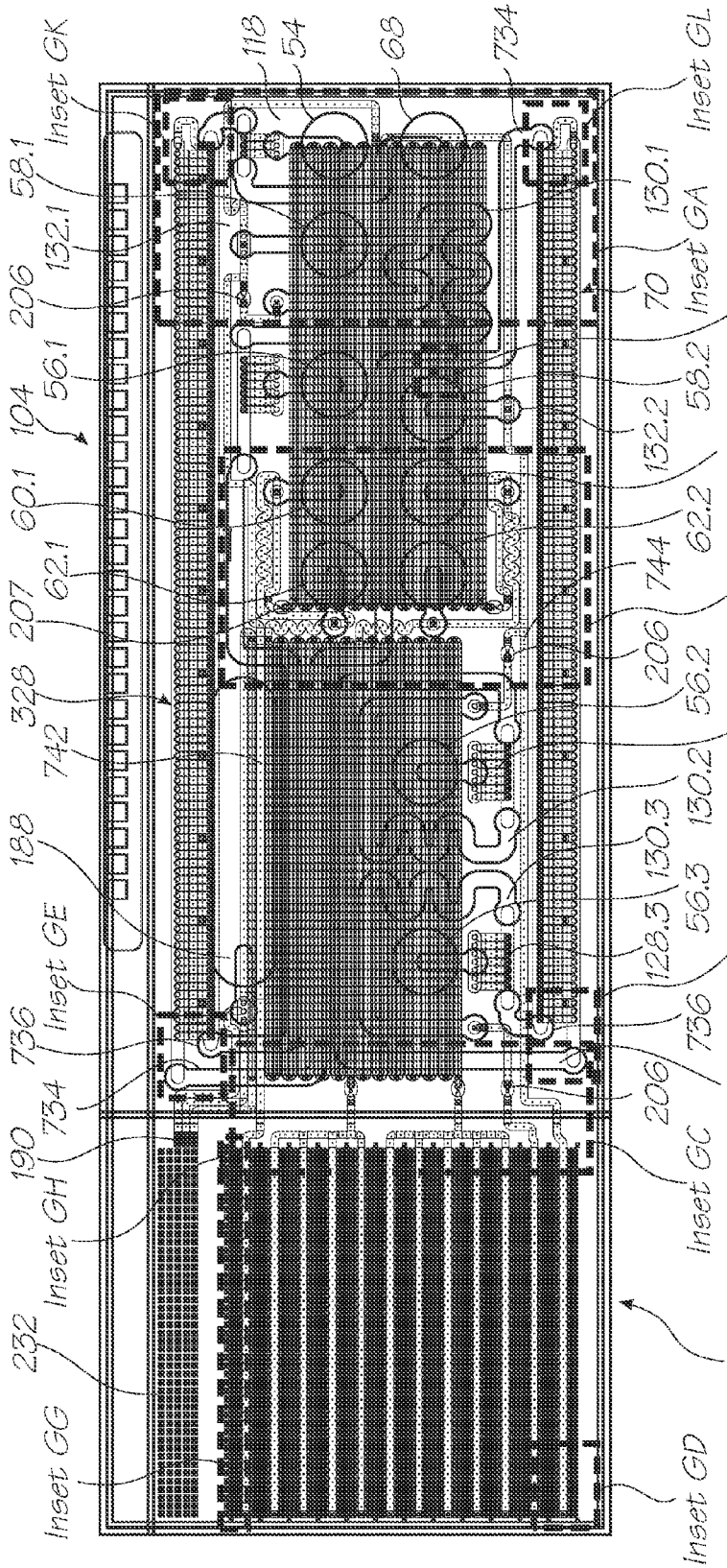

Inset GK
58.1
132.1
206
56.1
104
60.1
62.1
207
328
742
188
Inset GE
736
734
190
Inset GH
232
Inset GG
118
54
68
734
Inset GL
150.1
Inset GA
70
Inset GJ
58.2
132.2
60.2
62.2
744
Inset GB
206
56.2
128.2
130.2
130.3
56.3
128.3
Inset GF
736
734
206
Inset GC
Inset GD
110.1 - 110.2
& 124.1 - 124.3

FIG. 116

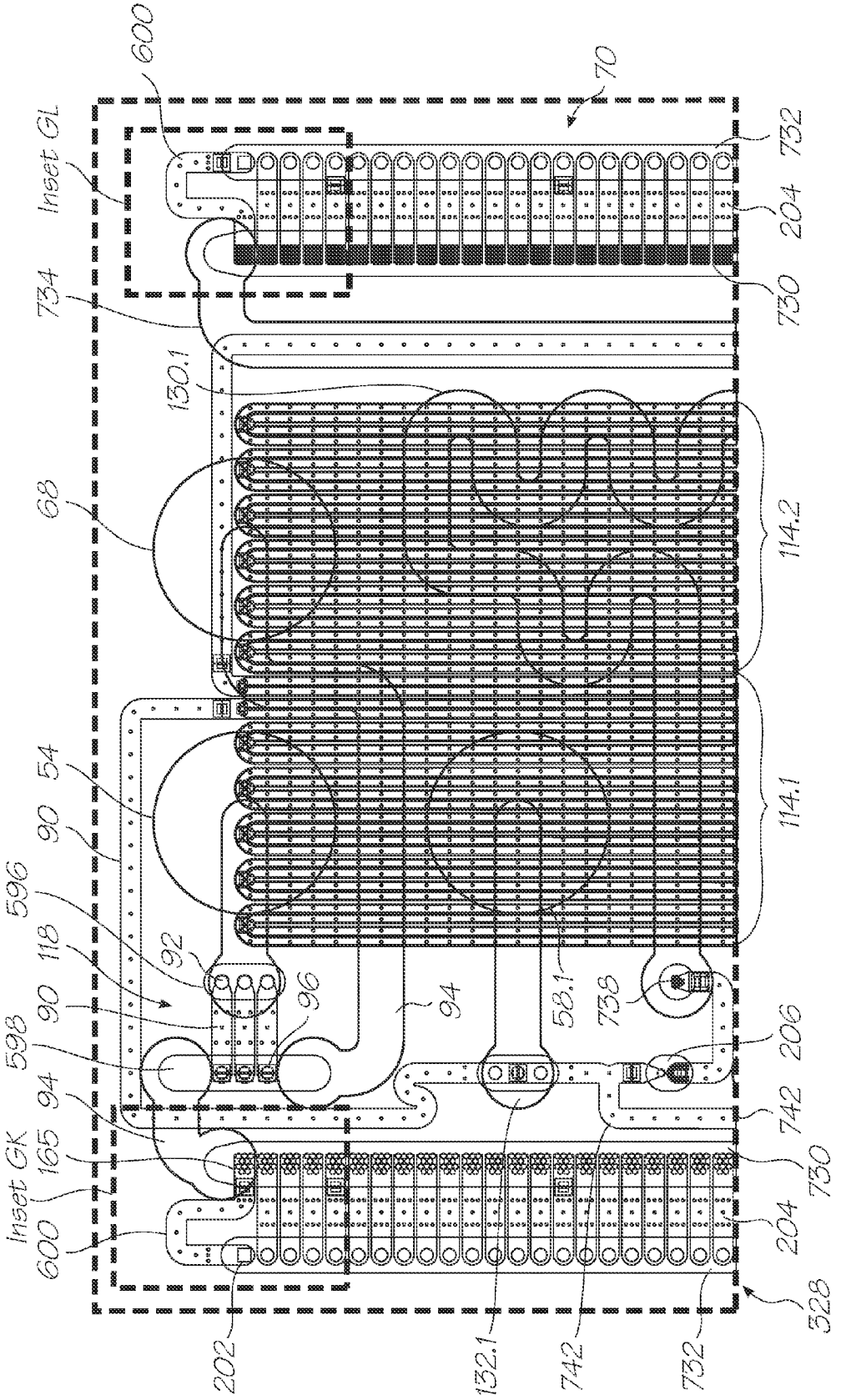


FIG. 117 (Inset GA)

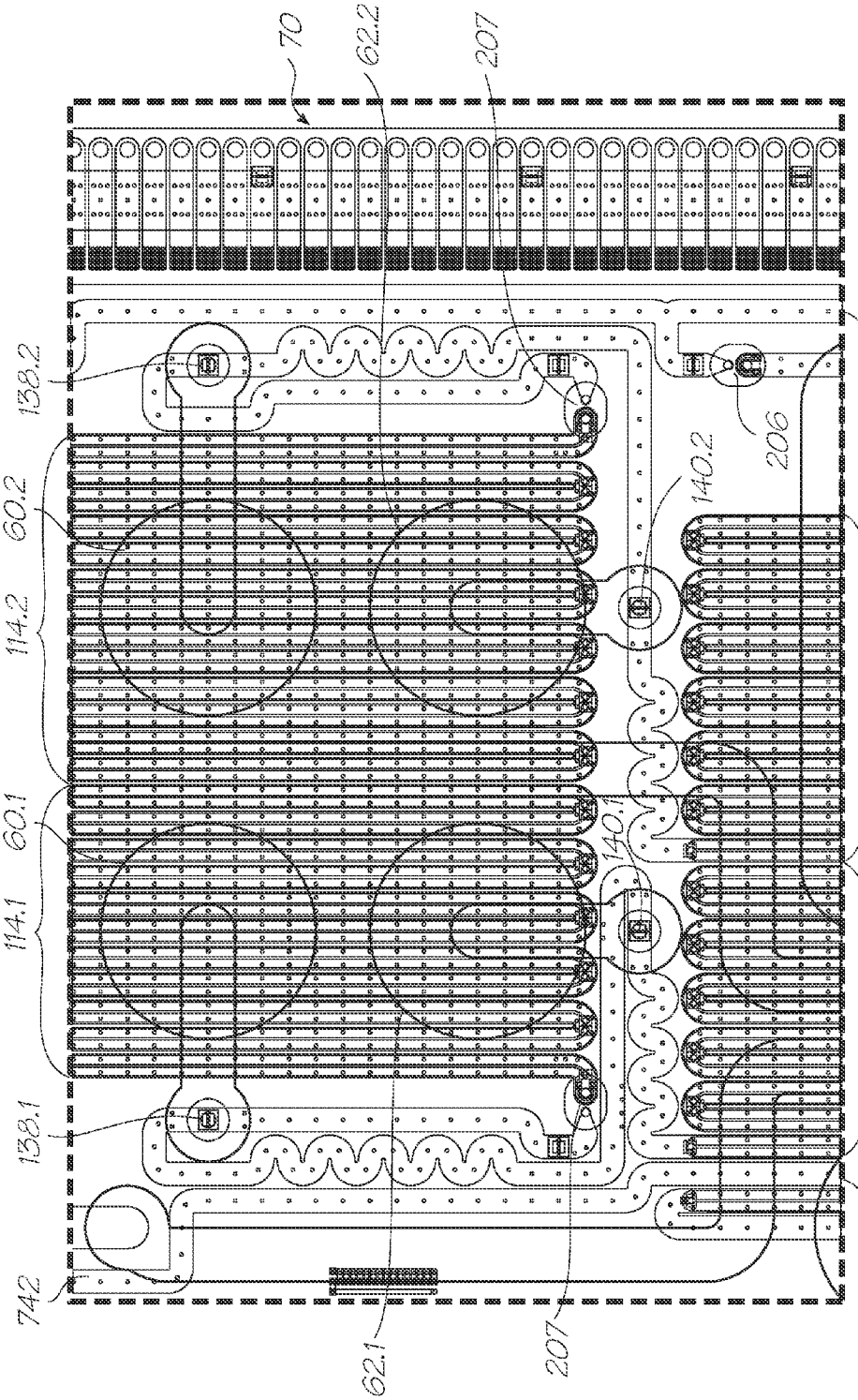


FIG. 118 (Inset GB)

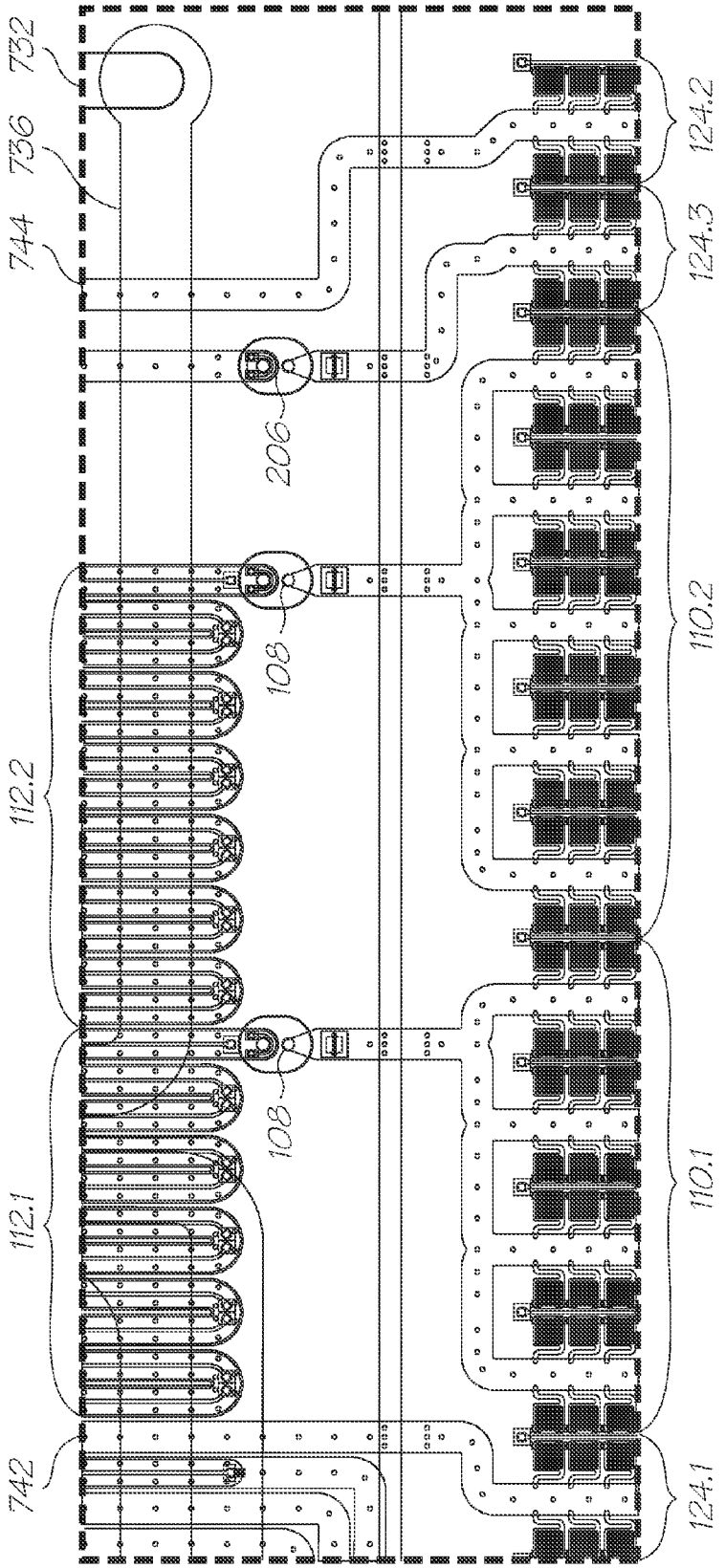


FIG. 119 (Inset GC)

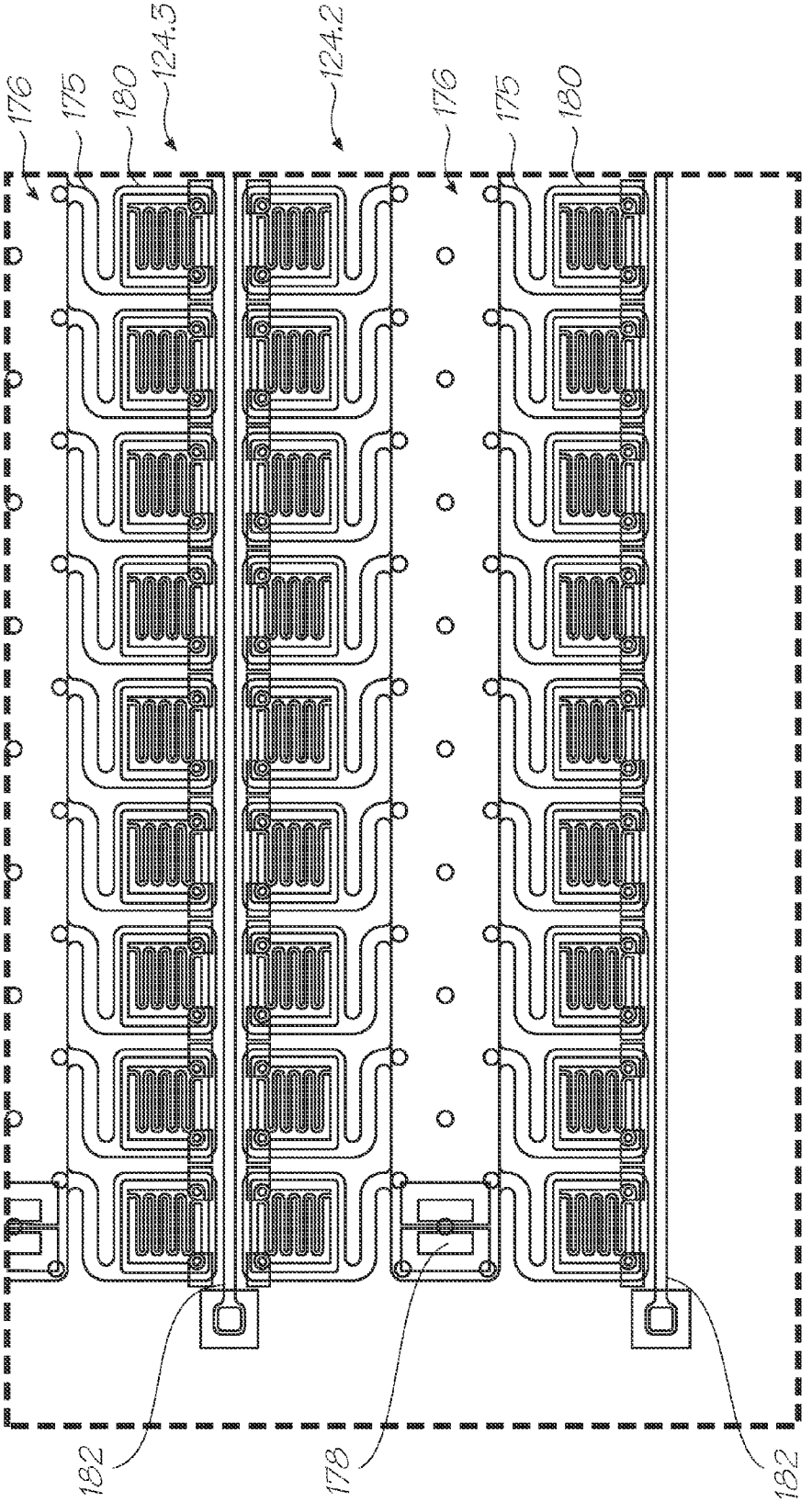


FIG. 120 (Inset GD)

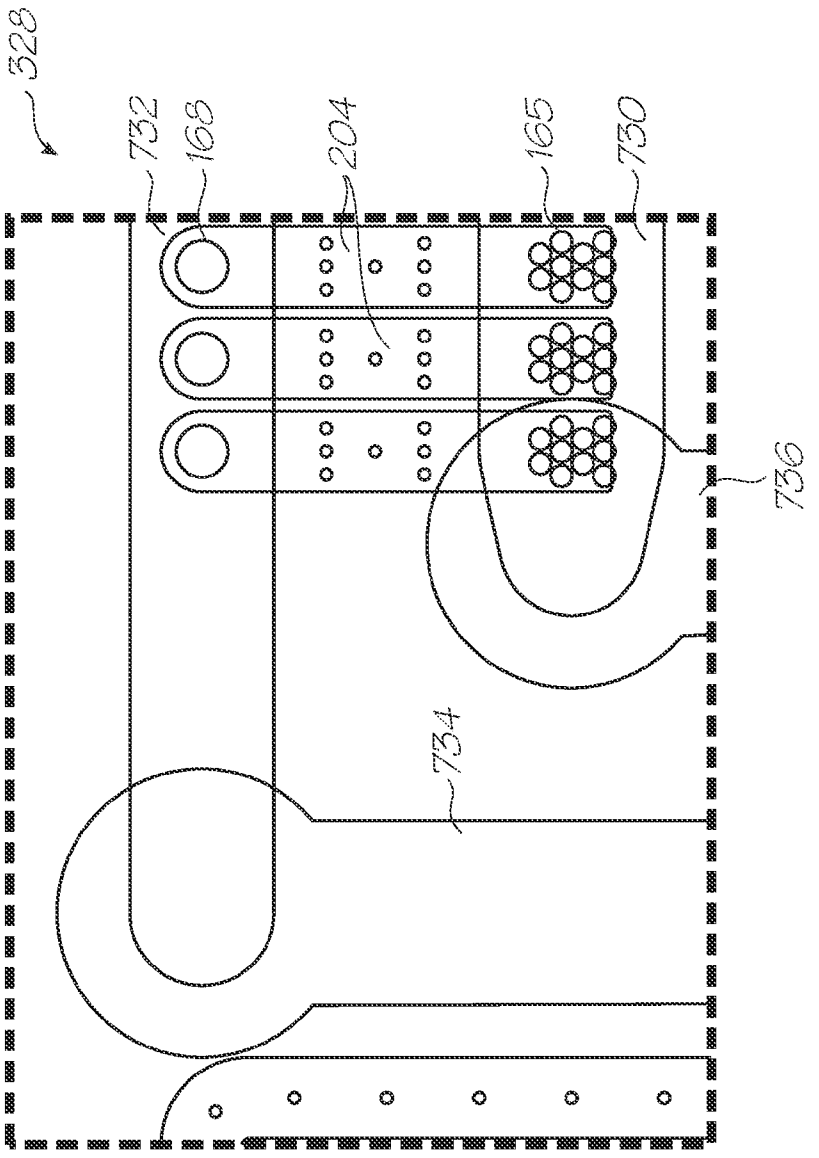


FIG. 121 (Inset GE)

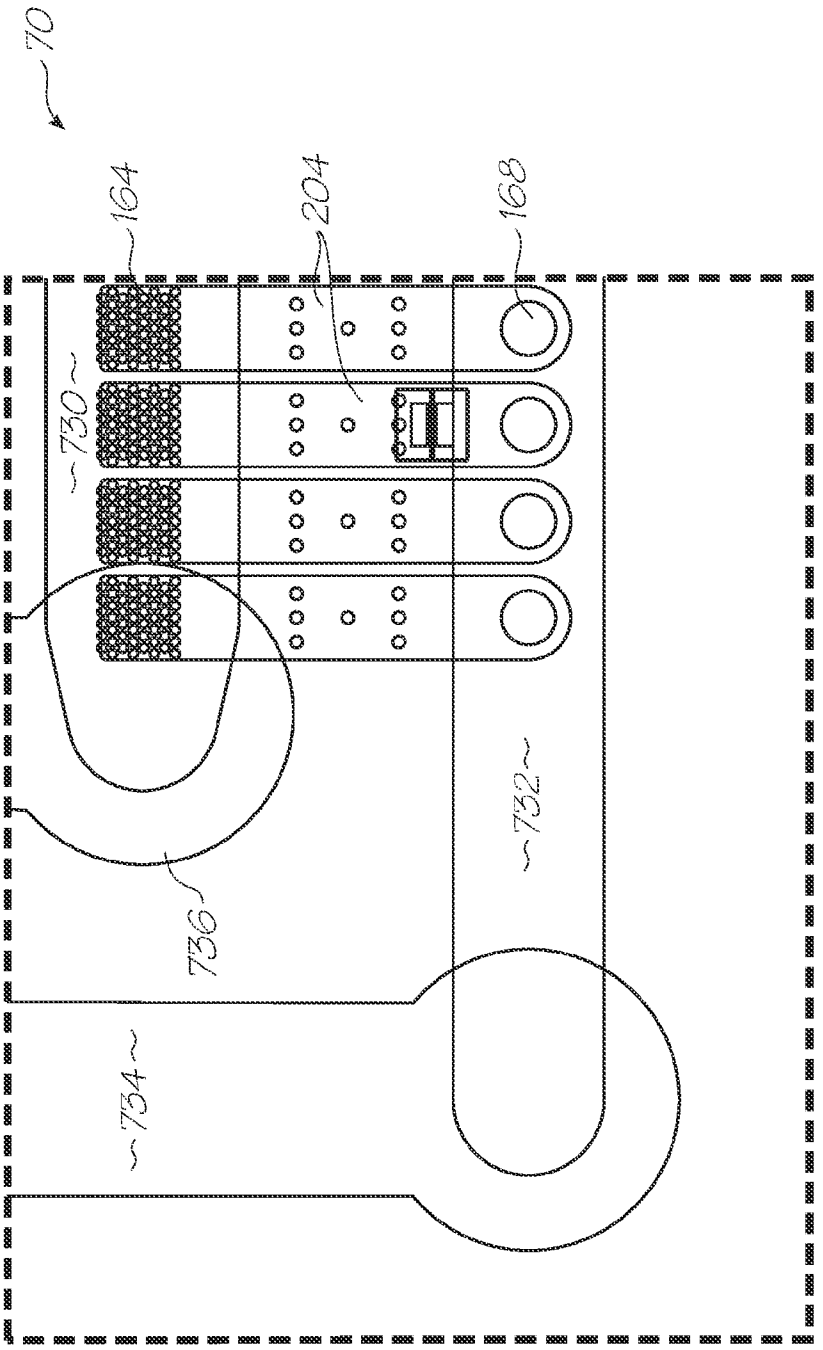


FIG. 122 (Inset GF)

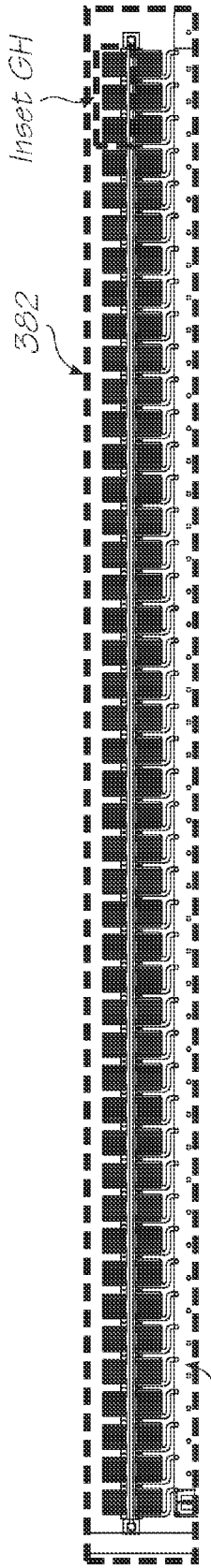


FIG. 123 (Inset GG)

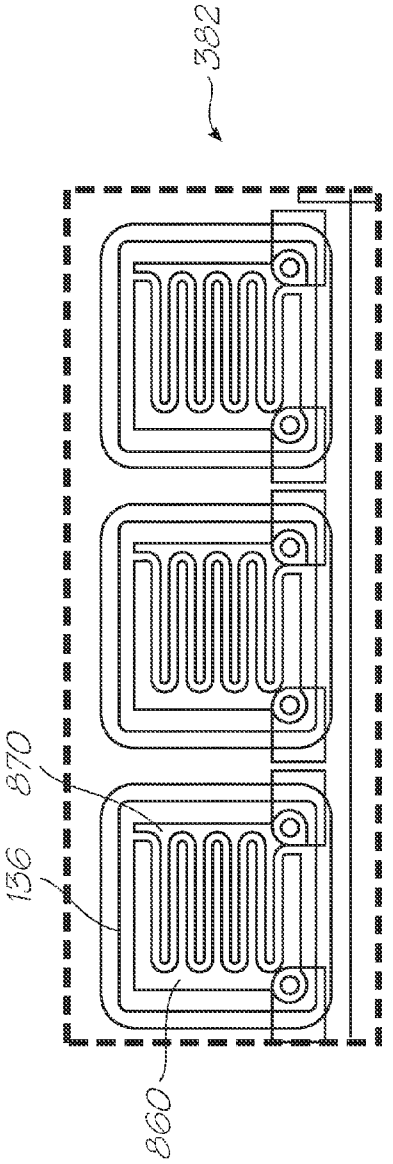


FIG. 124 (Inset GH)

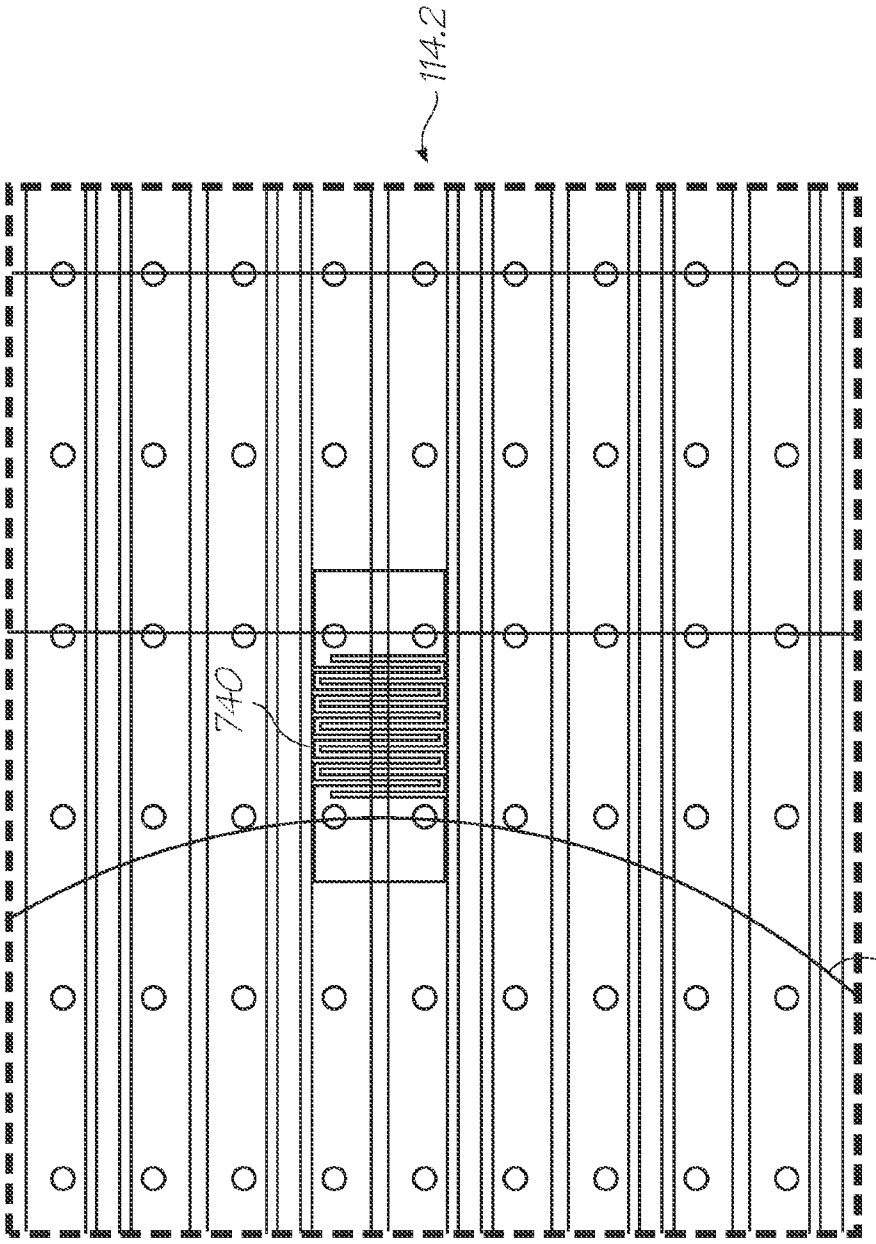


FIG. 125 (Inset GJ)

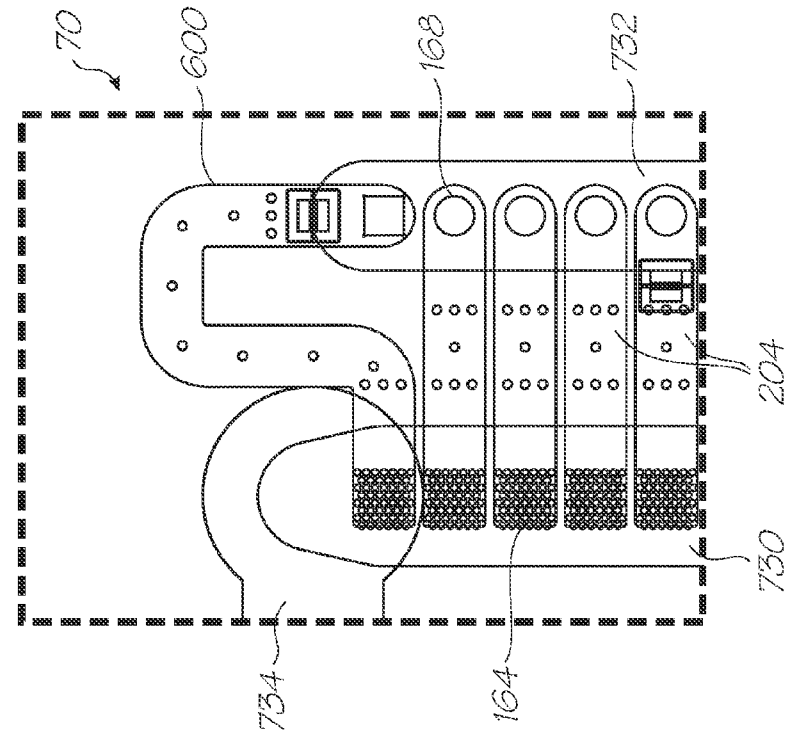


FIG. 127 (Inset GL)

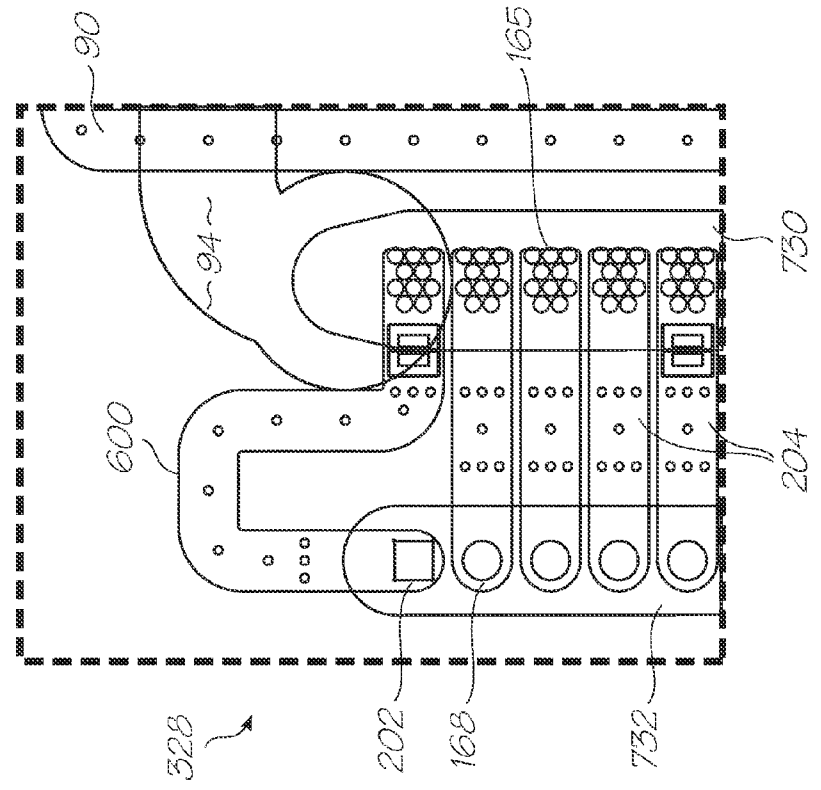


FIG. 126 (Inset GK)

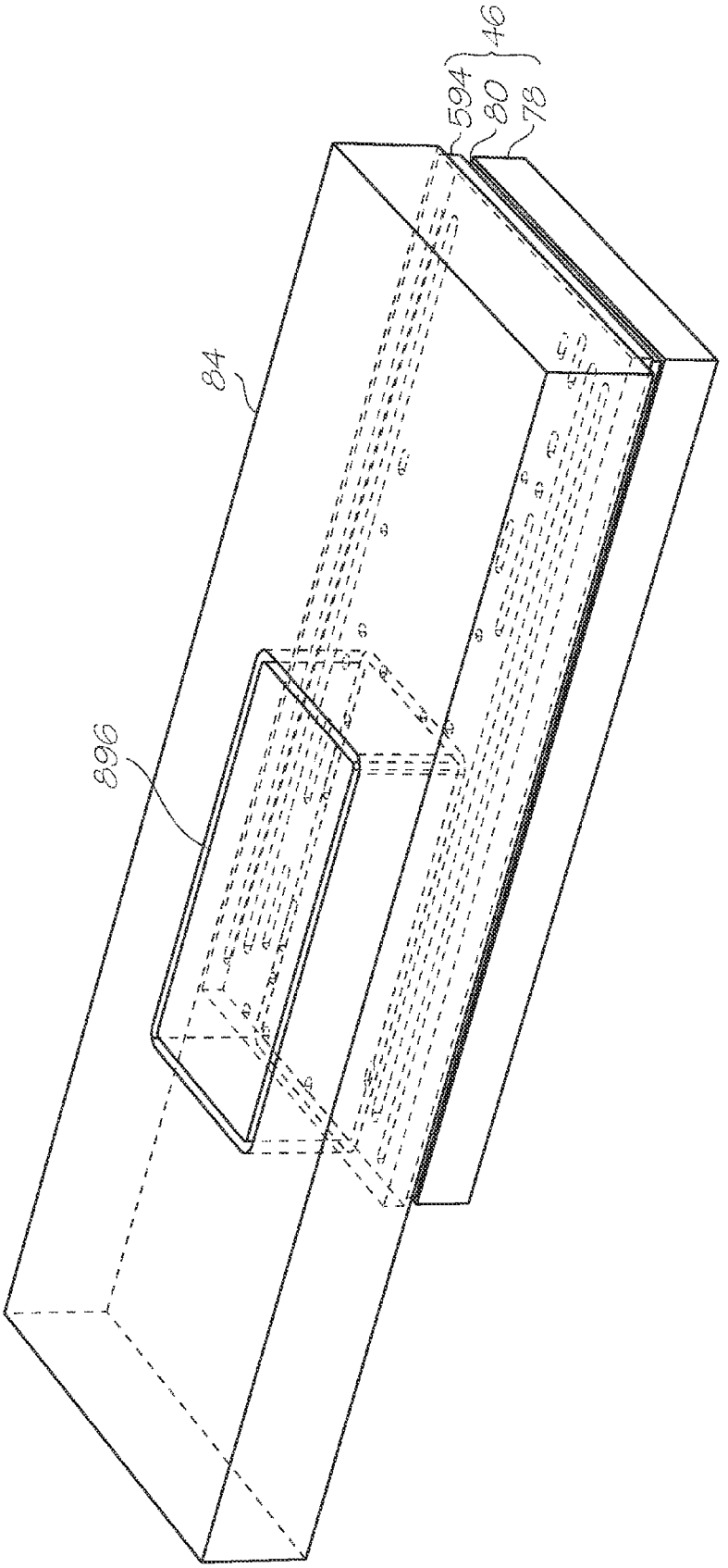


FIG. 128

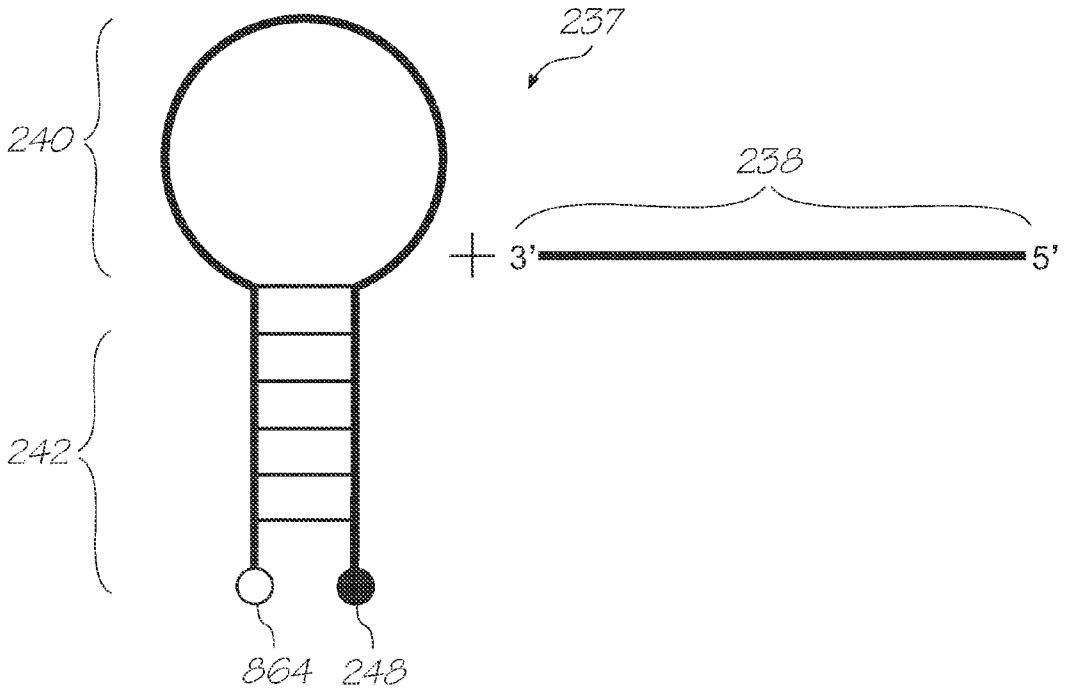


FIG. 129
(PRIOR ART)

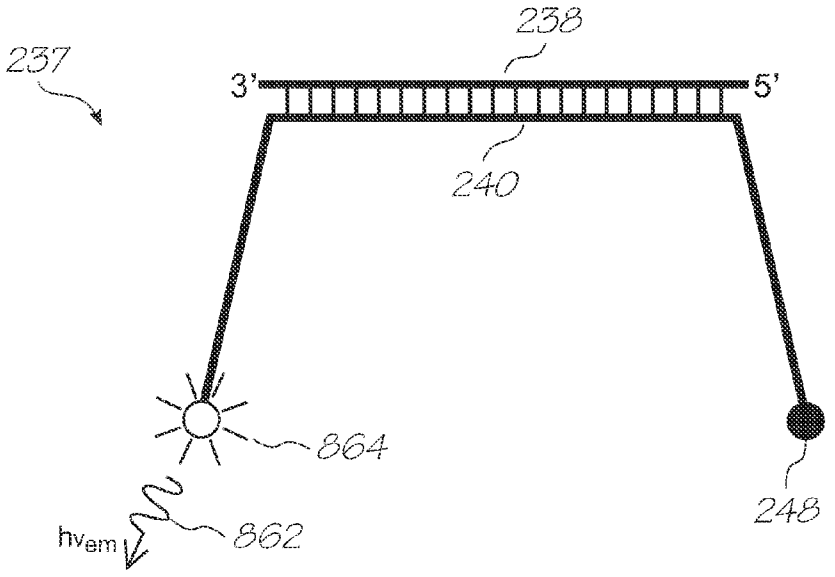


FIG. 130
(PRIOR ART)

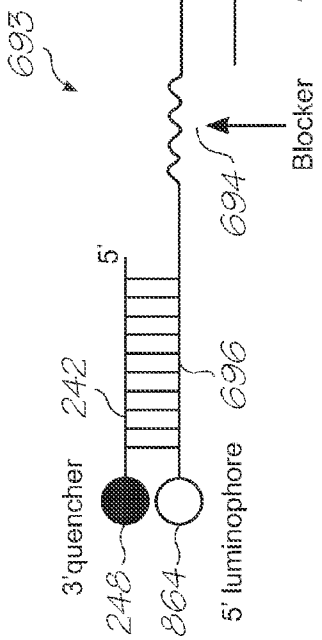


FIG. 131
(PRIOR ART)

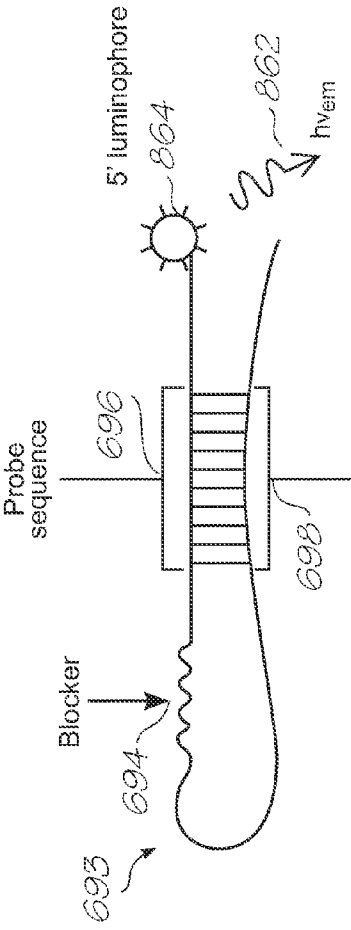


FIG. 132
(PRIOR ART)

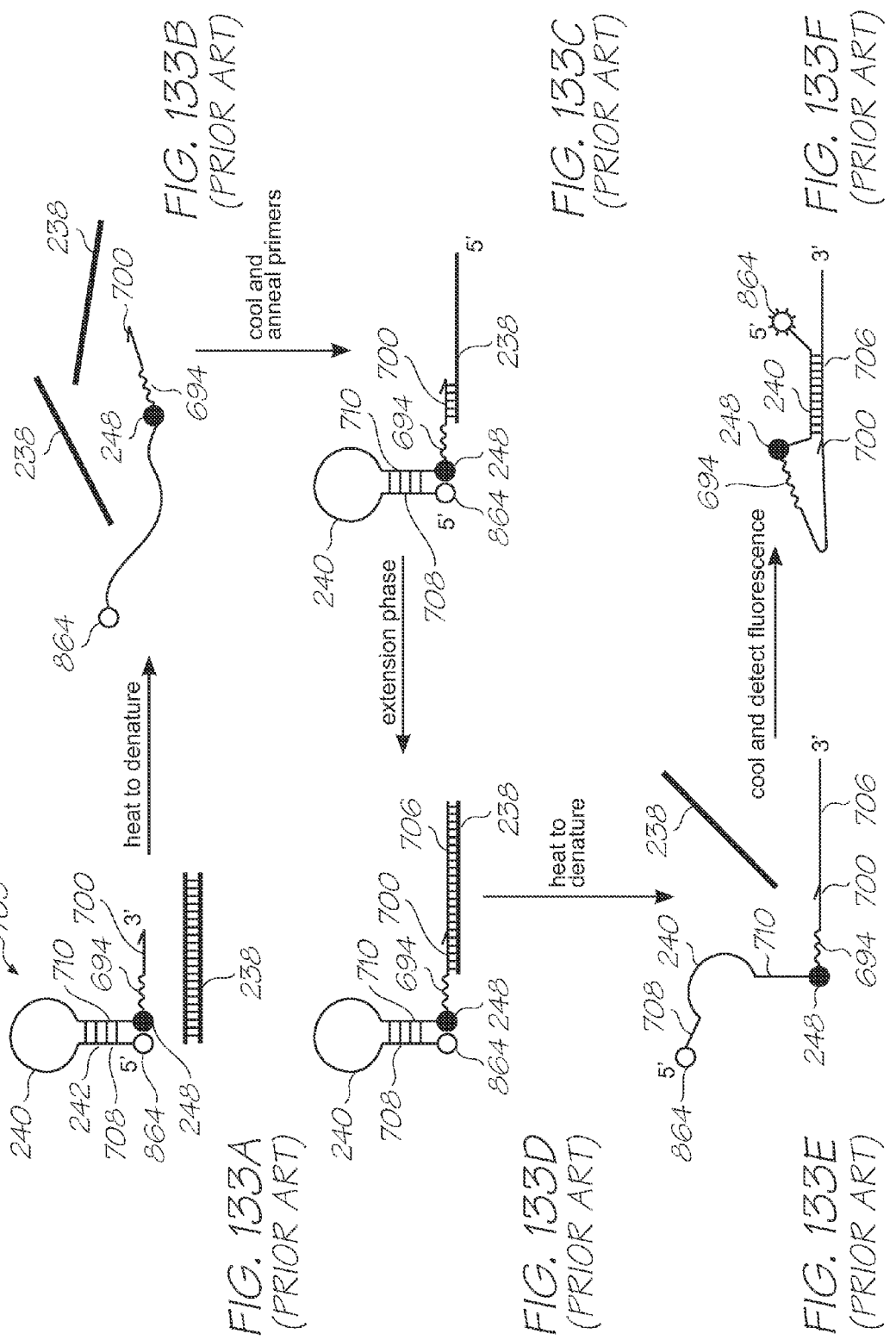


FIG. 133A (PRIOR ART)

FIG. 133B (PRIOR ART)

FIG. 133C (PRIOR ART)

FIG. 133D (PRIOR ART)

FIG. 133E (PRIOR ART)

FIG. 133F (PRIOR ART)

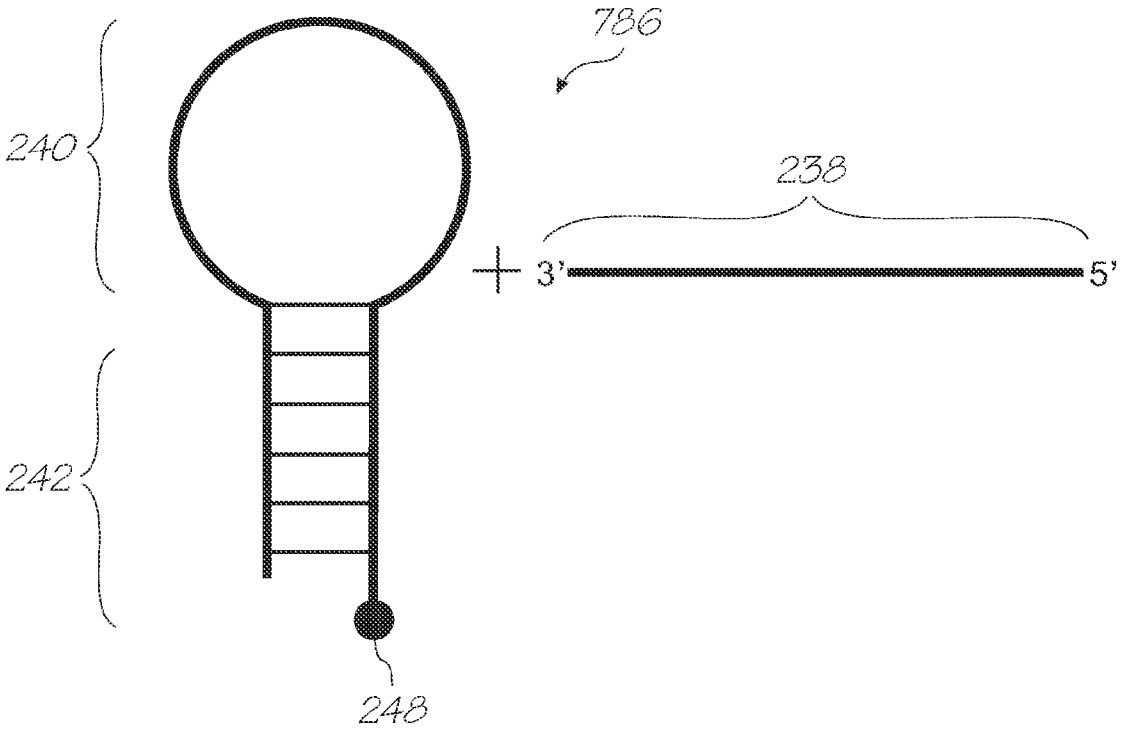


FIG. 134

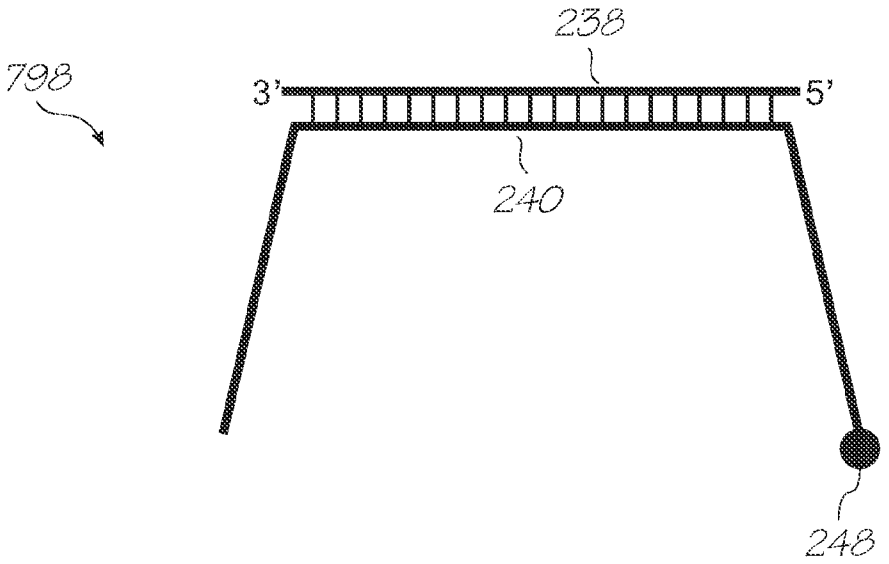


FIG. 135

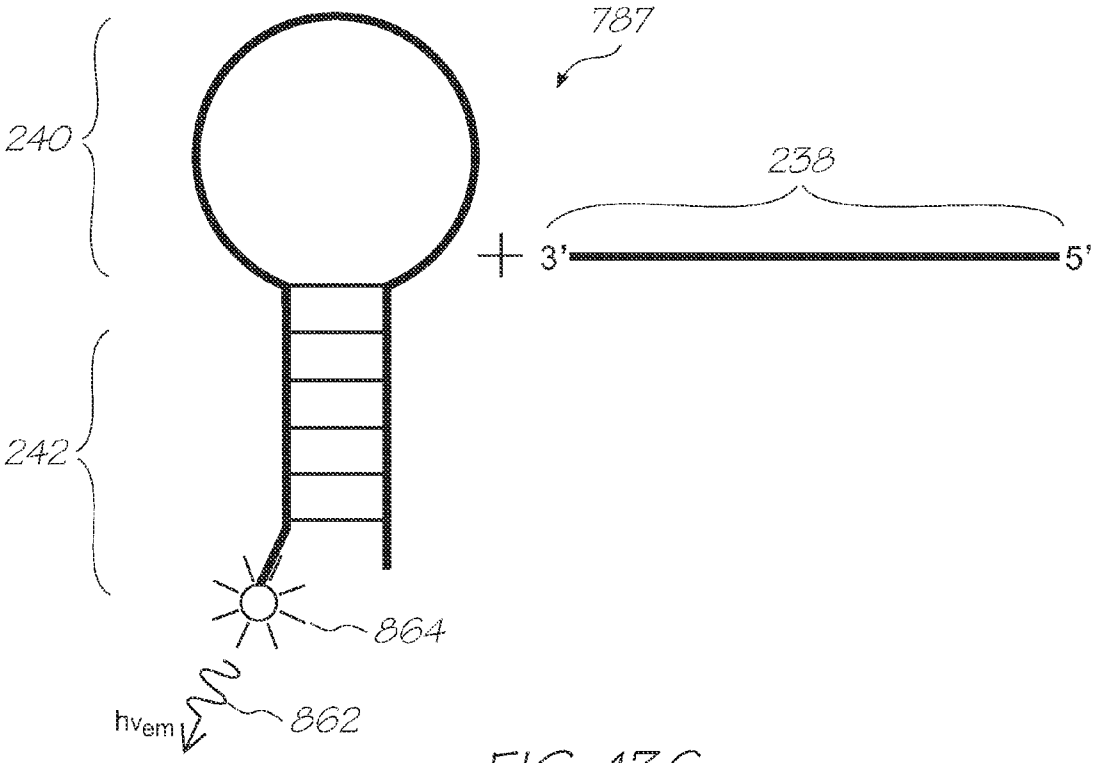


FIG. 136

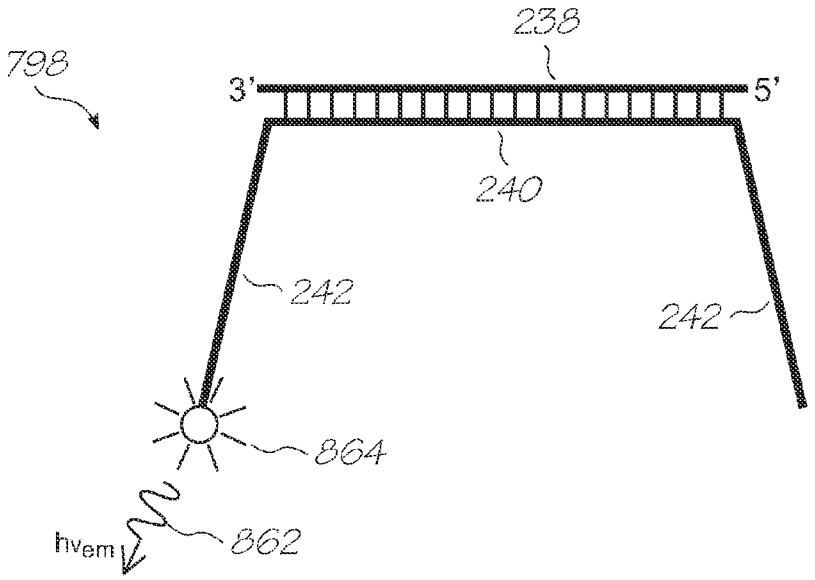


FIG. 137

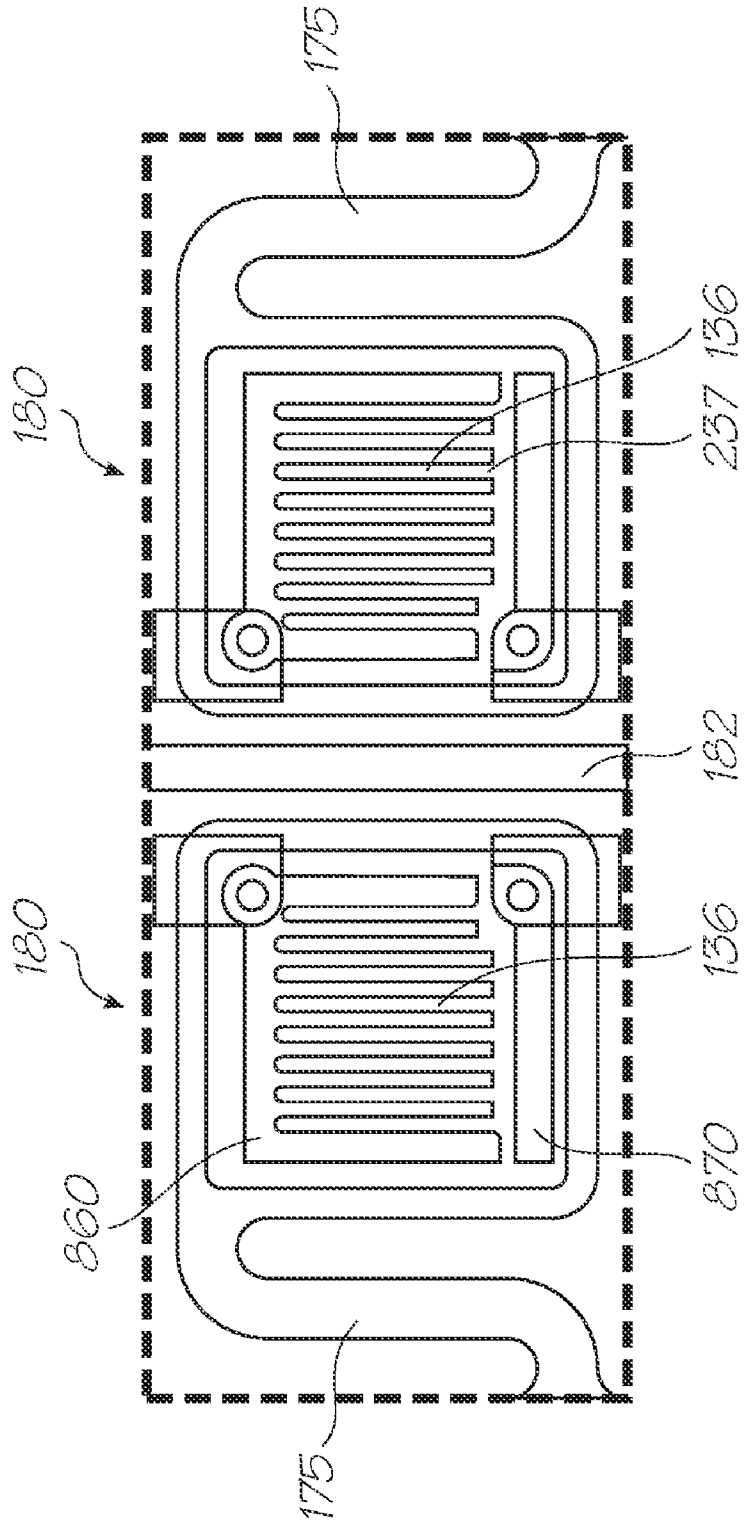


FIG. 138

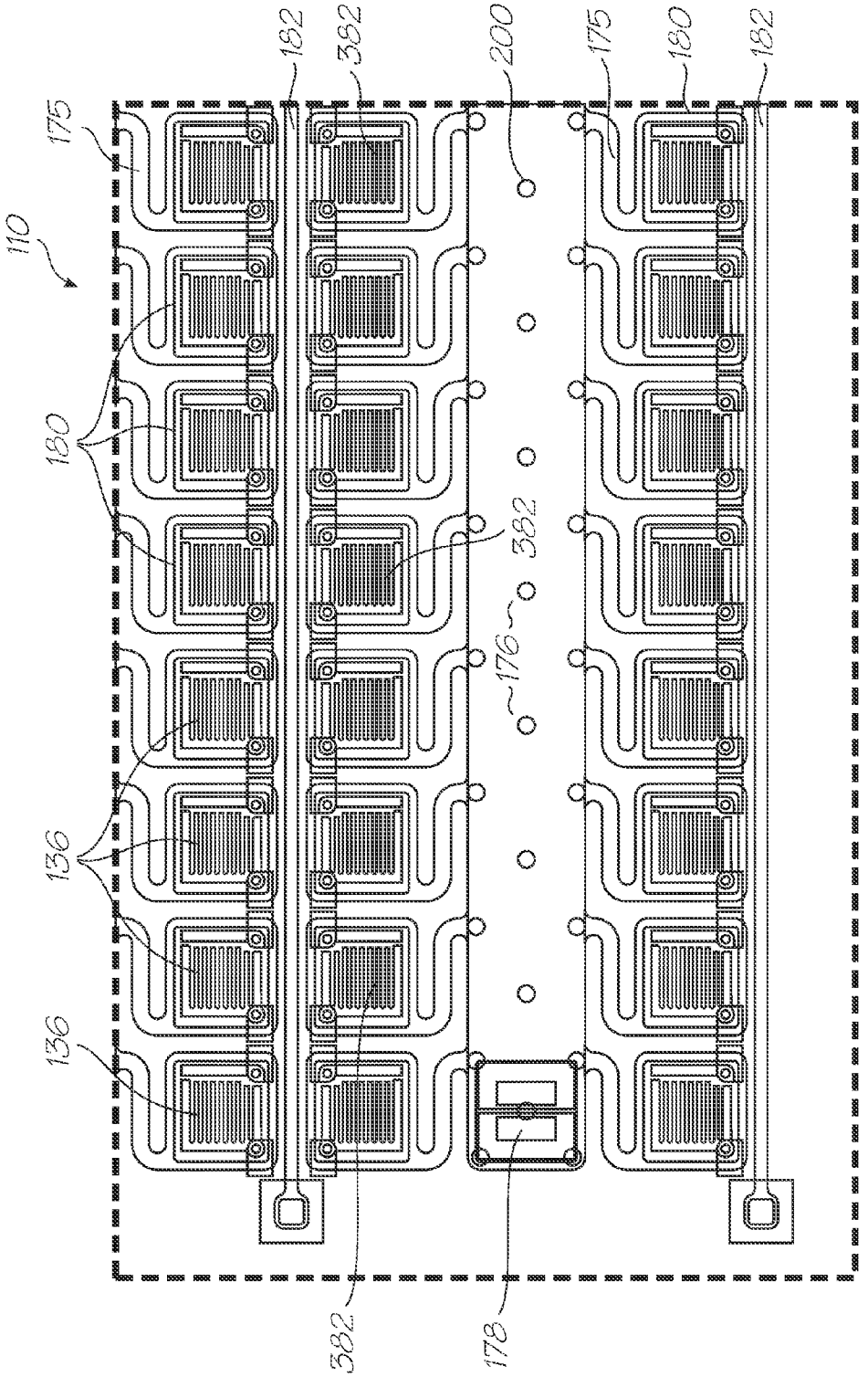


FIG. 139

TEST MODULE WITH CHEMICAL LYSIS SECTION

FIELD OF THE INVENTION

[0001] The present invention relates to diagnostic devices that use microsystems technologies (MST). In particular, the invention relates to microfluidic and biochemical processing and analysis for molecular diagnostics.

CO-PENDING APPLICATIONS

[0002] The following applications have been filed by the Applicant which relate to the present application:

GBS001US	GBS002US	GBS003US	GBS005US	GBS006US
GSR001US	GSR002US	GAS001US	GAS002US	GAS003US
GAS004US	GAS006US	GAS007US	GAS008US	GAS009US
GAS010US	GAS012US	GAS013US	GAS014US	GAS015US
GAS016US	GAS017US	GAS018US	GAS019US	GAS020US
GAS021US	GAS022US	GAS023US	GAS024US	GAS025US
GAS026US	GAS027US	GAS028US	GAS030US	GAS031US
GAS032US	GAS033US	GAS034US	GAS035US	GAS036US
GAS037US	GAS038US	GAS039US	GAS040US	GAS041US
GAS042US	GAS043US	GAS044US	GAS045US	GAS046US
GAS047US	GAS048US	GAS049US	GAS050US	GAS054US
GAS055US	GAS056US	GAS057US	GAS058US	GAS059US
GAS060US	GAS061US	GAS062US	GAS063US	GAS065US
GAS066US	GAS067US	GAS068US	GAS069US	GAS070US
GAS080US	GAS081US	GAS082US	GAS083US	GAS084US
GAS085US	GAS086US	GAS087US	GAS088US	GAS089US
GAS090US	GAS091US	GAS092US	GAS093US	GAS094US
GAS095US	GAS096US	GAS097US	GAS098US	GAS099US
GAS100US	GAS101US	GAS102US	GAS103US	GAS104US
GAS105US	GAS106US	GAS108US	GAS109US	GAS110US
GAS111US	GAS112US	GAS113US	GAS114US	GAS115US
GAS117US	GAS118US	GAS119US	GAS120US	GAS121US
GAS122US	GAS123US	GAS124US	GAS125US	GAS126US
GAS127US	GAS128US	GAS129US	GAS130US	GAS131US
GAS132US	GAS133US	GAS134US	GAS135US	GAS136US
GAS137US	GAS138US	GAS139US	GAS140US	GAS141US
GAS142US	GAS143US	GAS144US	GAS146US	GAS147US
GRR001US	GRR002US	GRR003US	GRR004US	GRR005US
GRR006US	GRR007US	GRR008US	GRR009US	GRR010US
GVA001US	GVA002US	GVA004US	GVA005US	GVA006US
GVA007US	GVA008US	GVA009US	GVA010US	GVA011US
GVA012US	GVA013US	GVA014US	GVA015US	GVA016US
GVA017US	GVA018US	GVA019US	GVA020US	GVA021US
GVA022US	GHU001US	GHU002US	GHU003US	GHU004US
GHU006US	GHU007US	GHU008US	GWM001US	GWM002US
GDI001US	GDI002US	GDI003US	GDI004US	GDI005US
GDI006US	GDI007US	GDI009US	GDI010US	GDI011US
GDI013US	GDI014US	GDI015US	GDI016US	GDI017US
GDI019US	GDI023US	GDI028US	GDI030US	GDI039US
GDI040US	GDI041US	GPC001US	GPC002US	GPC003US
GPC004US	GPC005US	GPC006US	GPC007US	GPC008US
GPC009US	GPC010US	GPC011US	GPC012US	GPC014US
GPC017US	GPC018US	GPC019US	GPC023US	GPC027US
GPC028US	GPC029US	GPC030US	GPC031US	GPC033US
GPC034US	GPC035US	GPC036US	GPC037US	GPC038US
GPC039US	GPC040US	GPC041US	GPC042US	GPC043US
GLY001US	GLY002US	GLY003US	GLY005US	GLY006US
GIN001US	GIN002US	GIN003US	GIN004US	GIN005US
GIN006US	GIN007US	GIN008US	GMI001US	GMI002US
GMI005US	GMI008US	GLE001US	GLE002US	GLE003US
GLE004US	GLE005US	GLE006US	GLE007US	GLE008US
GLE009US	GLE010US	GLE011US	GLE012US	GLE013US
GLE014US	GLA001US	GGA001US	GGA003US	GRE001US
GRE002US	GRE003US	GRE004US	GRE005US	GRE006US
GRE007US	GCF001US	GCF002US	GCF003US	GCF004US
GCF005US	GCF006US	GCF007US	GCF008US	GCF009US
GCF010US	GCF011US	GCF012US	GCF013US	GCF014US
GCF015US	GCF016US	GCF020US	GCF021US	GCF022US
GCF023US	GCF024US	GCF025US	GCF027US	GCF028US
GCF029US	GCF030US	GCF031US	GCF032US	GCF033US

-continued

GCF034US	GCF035US	GCF036US	GCF037US	GSA001US
GSA002US	GSE001US	GSE002US	GSE003US	GSE004US
GDA001US	GDA002US	GDA003US	GDA004US	GDA005US
GDA006US	GDA007US	GPK001US	GMO001US	GMV001US
GMV002US	GMV003US	GMV004US	GRD001US	GRD002US
GRD003US	GRD004US	GPD001US	GPD003US	GPD004US
GPD005US	GPD006US	GPD007US	GPD008US	GPD009US
GPD010US	GPD011US	GPD012US	GPD013US	GPD014US
GPD015US	GPD016US	GPD017US	GAL001US	GPA001US
GPA003US	GPA004US	GPA005US	GSS001US	GSL001US
GCA001US	GCA002US	GCA003US		

[0003] The disclosures of these co-pending applications are incorporated herein by reference. The above applications have been identified by their filing docket number, which will be substituted with the corresponding application number, once assigned.

BACKGROUND OF THE INVENTION

[0004] Molecular diagnostics has emerged as a field that offers the promise of early disease detection, potentially before symptoms have manifested. Molecular diagnostic testing is used to detect:

[0005] Inherited disorders

[0006] Acquired disorders

[0007] Infectious diseases

[0008] Genetic predisposition to health-related conditions.

[0009] With high accuracy and fast turnaround times, molecular diagnostic tests have the potential to reduce the occurrence of ineffective health care services, enhance patient outcomes, improve disease management and individualize patient care. Many of the techniques in molecular diagnostics are based on the detection and identification of specific nucleic acids, both deoxyribonucleic acid (DNA) and ribonucleic acid (RNA), extracted and amplified from a biological specimen (such as blood or saliva). The complementary nature of the nucleic acid bases allows short sequences of synthesized DNA (oligonucleotides) to bond (hybridize) to specific nucleic acid sequences for use in nucleic acid tests. If hybridization occurs, then the complementary sequence is present in the sample. This makes it possible, for example, to predict the disease a person will contract in the future, determine the identity and virulence of an infectious pathogen, or determine the response a person will have to a drug.

Nucleic Acid Based Molecular Diagnostic Test

[0010] A nucleic acid based test has four distinct steps:

[0011] 1. Sample preparation

[0012] 2. Nucleic acid extraction

[0013] 3. Nucleic acid amplification (optional)

[0014] 4. Detection

[0015] Many sample types are used for genetic analysis, such as blood, urine, sputum and tissue samples. The diagnostic test determines the type of sample required as not all samples are representative of the disease process. These samples have a variety of constituents, but usually only one of these is of interest. For example, in blood, high concentrations of erythrocytes can inhibit the detection of a pathogenic organism. Therefore a purification and/or concentration step at the beginning of the nucleic acid test is often required.

[0016] Blood is one of the more commonly sought sample types. It has three major constituents: leukocytes (white blood cells), erythrocytes (red blood cells) and thrombocytes (platelets). The thrombocytes facilitate clotting and remain active in vitro. To inhibit coagulation, the specimen is mixed with an agent such as ethylenediaminetetraacetic acid (EDTA) prior to purification and concentration. Erythrocytes are usually removed from the sample in order to concentrate the target cells. In humans, erythrocytes account for approximately 99% of the cellular material but do not carry DNA as they have no nucleus. Furthermore, erythrocytes contain components such as haemoglobin that can interfere with the downstream nucleic acid amplification process (described below). Removal of erythrocytes can be achieved by differentially lysing the erythrocytes in a lysis solution, leaving remaining cellular material intact which can then be separated from the sample using centrifugation. This provides a concentration of the target cells from which the nucleic acids are extracted.

[0017] The exact protocol used to extract nucleic acids depends on the sample and the diagnostic assay to be performed. For example, the protocol for extracting viral RNA will vary considerably from the protocol to extract genomic DNA. However, extracting nucleic acids from target cells usually involves a cell lysis step followed by nucleic acid purification. The cell lysis step disrupts the cell and nuclear membranes, releasing the genetic material. This is often accomplished using a lysis detergent, such as sodium dodecyl sulfate, which also denatures the large amount of proteins present in the cells.

[0018] The nucleic acids are then purified with an alcohol precipitation step, usually ice-cold ethanol or isopropanol, or via a solid phase purification step, typically on a silica matrix in a column, resin or on paramagnetic beads in the presence of high concentrations of a chaotropic salt, prior to washing and then elution in a low ionic strength buffer. An optional step prior to nucleic acid precipitation is the addition of a protease which digests the proteins in order to further purify the sample.

[0019] Other lysis methods include mechanical lysis via ultrasonic vibration and thermal lysis where the sample is heated to 94° C. to disrupt cell membranes.

[0020] The target DNA or RNA may be present in the extracted material in very small amounts, particularly if the target is of pathogenic origin. Nucleic acid amplification provides the ability to selectively amplify (that is, replicate) specific targets present in low concentrations to detectable levels.

[0021] The most commonly used nucleic acid amplification technique is the polymerase chain reaction (PCR). PCR is well known in this field and comprehensive description of this type of reaction is provided in E. van Pelt-Verkuil et al., Principles and Technical Aspects of PCR Amplification, Springer, 2008.

[0022] PCR is a powerful technique that amplifies a target DNA sequence against a background of complex DNA. If RNA is to be amplified (by PCR), it must be first transcribed into cDNA (complementary DNA) using an enzyme called reverse transcriptase. Afterwards, the resulting cDNA is amplified by PCR.

[0023] PCR is an exponential process that proceeds as long as the conditions for sustaining the reaction are acceptable. The components of the reaction are:

[0024] 1. pair of primers—short single strands of DNA with around 10-30 nucleotides complementary to the regions flanking the target sequence

[0025] 2. DNA polymerase—a thermostable enzyme that synthesizes DNA

[0026] 3. deoxyribonucleoside triphosphates (dNTPs)—provide the nucleotides that are incorporated into the newly synthesized DNA strand

[0027] 4. buffer—to provide the optimal chemical environment for DNA synthesis

[0028] PCR typically involves placing these reactants in a small tube (~10-50 microlitres) containing the extracted nucleic acids. The tube is placed in a thermal cycler; an instrument that subjects the reaction to a series of different temperatures for varying amounts of time. The standard protocol for each thermal cycle involves a denaturation phase, an annealing phase, and an extension phase. The extension phase is sometimes referred to as the primer extension phase. In addition to such three-step protocols, two-step thermal protocols can be employed, in which the annealing and extension phases are combined. The denaturation phase typically involves raising the temperature of the reaction to 90-95° C. to denature the DNA strands; in the annealing phase, the temperature is lowered to ~50-60° C. for the primers to anneal; and then in the extension phase the temperature is raised to the optimal DNA polymerase activity temperature of 60-72° C. for primer extension. This process is repeated cyclically around 20-40 times, the end result being the creation of millions of copies of the target sequence between the primers.

[0029] There are a number of variants to the standard PCR protocol such as multiplex PCR, linker-primed PCR, direct PCR, tandem PCR, real-time PCR and reverse-transcriptase PCR, amongst others, which have been developed for molecular diagnostics.

[0030] Multiplex PCR uses multiple primer sets within a single PCR mixture to produce amplicons of varying sizes that are specific to different DNA sequences. By targeting multiple genes at once, additional information may be gained from a single test-run that otherwise would require several experiments. Optimization of multiplex PCR is more difficult though and requires selecting primers with similar annealing temperatures, and amplicons with similar lengths and base composition to ensure the amplification efficiency of each amplicon is equivalent.

[0031] Linker-primed PCR, also known as ligation adaptor PCR, is a method used to enable nucleic acid amplification of essentially all DNA sequences in a complex DNA mixture without the need for target-specific primers. The method firstly involves digesting the target DNA population with a suitable restriction endonuclease (enzyme). Double-stranded oligonucleotide linkers (also called adaptors) with a suitable overhanging end are then ligated to the ends of target DNA fragments using a ligase enzyme. Nucleic acid amplification is subsequently performed using oligonucleotide primers which are specific for the linker sequences. In this way, all fragments of the DNA source which are flanked by linker oligonucleotides can be amplified.

[0032] Direct PCR describes a system whereby PCR is performed directly on a sample without any, or with minimal, nucleic acid extraction. It has long been accepted that PCR reactions are inhibited by the presence of many components of unpurified biological samples, such as the haem component in blood. Traditionally, PCR has required extensive purification of the target nucleic acid prior to preparation of the

reaction mixture. With appropriate changes to the chemistry and sample concentration, however, it is possible to perform PCR with minimal DNA purification, or direct PCR. Adjustments to the PCR chemistry for direct PCR include increased buffer strength, the use of polymerases which have high activity and processivity, and additives which chelate with potential polymerase inhibitors.

[0033] Tandem PCR utilises two distinct rounds of nucleic acid amplification to increase the probability that the correct amplicon is amplified. One form of tandem PCR is nested PCR in which two pairs of PCR primers are used to amplify a single locus in separate rounds of nucleic acid amplification. The first pair of primers hybridize to the nucleic acid sequence at regions external to the target nucleic acid sequence. The second pair of primers (nested primers) used in the second round of amplification bind within the first PCR product and produce a second PCR product containing the target nucleic acid, that will be shorter than the first one. The logic behind this strategy is that if the wrong locus were amplified by mistake during the first round of nucleic acid amplification, the probability is very low that it would also be amplified a second time by a second pair of primers and thus ensures specificity.

[0034] Real-time PCR, or quantitative PCR, is used to measure the quantity of a PCR product in real time. By using a fluorophore-containing probe or fluorescent dyes along with a set of standards in the reaction, it is possible to quantitate the starting amount of nucleic acid in the sample. This is particularly useful in molecular diagnostics where treatment options may differ depending on the pathogen load in the sample.

[0035] Reverse-transcriptase PCR (RT-PCR) is used to amplify DNA from RNA. Reverse transcriptase is an enzyme that reverse transcribes RNA into complementary DNA (cDNA), which is then amplified by PCR. RT-PCR is widely used in expression profiling, to determine the expression of a gene or to identify the sequence of an RNA transcript, including transcription start and termination sites. It is also used to amplify RNA viruses such as human immunodeficiency virus or hepatitis C virus.

[0036] Isothermal amplification is another form of nucleic acid amplification which does not rely on the thermal denaturation of the target DNA during the amplification reaction and hence does not require sophisticated machinery. Isothermal nucleic acid amplification methods can therefore be carried out in primitive sites or operated easily outside of a laboratory environment. A number of isothermal nucleic acid amplification methods have been described, including Strand Displacement Amplification, Transcription Mediated Amplification, Nucleic Acid Sequence Based Amplification, Recombinase Polymerase Amplification, Rolling Circle Amplification, Ramification Amplification, Helicase-Dependent Isothermal DNA Amplification and Loop-Mediated Isothermal Amplification.

[0037] Isothermal nucleic acid amplification methods do not rely on the continuing heat denaturation of the template DNA to produce single stranded molecules to serve as templates for further amplification, but instead rely on alternative methods such as enzymatic nicking of DNA molecules by specific restriction endonucleases, or the use of an enzyme to separate the DNA strands, at a constant temperature.

[0038] Strand Displacement Amplification (SDA) relies on the ability of certain restriction enzymes to nick the unmodified strand of hemi-modified DNA and the ability of a 5'-3' exonuclease-deficient polymerase to extend and displace the downstream strand. Exponential nucleic acid amplification is then achieved by coupling sense and antisense reactions in which strand displacement from the sense reaction serves as a template for the antisense reaction. The use of nickase enzymes which do not cut DNA in the traditional manner but produce a nick on one of the DNA strands, such as N. A1w1, N. BstNB1 and M1y1, are useful in this reaction. SDA has been improved by the use of a combination of a heat-stable restriction enzyme (Ava1) and heat-stable Exo-polymerase (Bst polymerase). This combination has been shown to increase amplification efficiency of the reaction from 10^8 fold amplification to 10^{10} fold amplification so that it is possible using this technique to amplify unique single copy molecules.

[0039] Transcription Mediated Amplification (TMA) and Nucleic Acid Sequence Based Amplification (NASBA) use an RNA polymerase to copy RNA sequences but not corresponding genomic DNA. The technology uses two primers and two or three enzymes, RNA polymerase, reverse transcriptase and optionally RNase H (if the reverse transcriptase does not have RNase activity). One primer contains a promoter sequence for RNA polymerase. In the first step of nucleic acid amplification, this primer hybridizes to the target ribosomal RNA (rRNA) at a defined site. Reverse transcriptase creates a DNA copy of the target rRNA by extension from the 3' end of the promoter primer. The RNA in the resulting RNA:DNA duplex is degraded by the RNase activity of the reverse transcriptase if present or the additional RNase H. Next, a second primer binds to the DNA copy. A new strand of DNA is synthesized from the end of this primer by reverse transcriptase, creating a double-stranded DNA molecule. RNA polymerase recognizes the promoter sequence in the DNA template and initiates transcription. Each of the newly synthesized RNA amplicons re-enters the process and serves as a template for a new round of replication.

[0040] In Recombinase Polymerase Amplification (RPA), the isothermal amplification of specific DNA fragments is achieved by the binding of opposing oligonucleotide primers to template DNA and their extension by a DNA polymerase. Heat is not required to denature the double-stranded DNA (dsDNA) template. Instead, RPA employs recombinase-primer complexes to scan dsDNA and facilitate strand exchange at cognate sites. The resulting structures are stabilised by single-stranded DNA binding proteins interacting with the displaced template strand, thus preventing the ejection of the primer by branch migration. Recombinase disassembly leaves the 3' end of the oligonucleotide accessible to a strand displacing DNA polymerase, such as the large fragment of Bacillus subtilis Pol I (Bsu), and primer extension ensues. Exponential nucleic acid amplification is accomplished by the cyclic repetition of this process.

[0041] Helicase-dependent amplification (HDA) mimics the in vivo system in that it uses a DNA helicase enzyme to generate single-stranded templates for primer hybridization and subsequent primer extension by a DNA polymerase. In the first step of the HDA reaction, the helicase enzyme traverses along the target DNA, disrupting the hydrogen bonds linking the two strands which are then bound by single-stranded binding proteins. Exposure of the single-stranded target region by the helicase allows primers to anneal. The DNA polymerase then extends the 3' ends of each primer using free deoxyribonucleoside triphosphates (dNTPs) to produce two DNA replicates. The two replicated dsDNA

strands independently enter the next cycle of HDA, resulting in exponential nucleic acid amplification of the target sequence.

[0042] Other DNA-based isothermal techniques include Rolling Circle Amplification (RCA) in which a DNA polymerase extends a primer continuously around a circular DNA template, generating a long DNA product that consists of many repeated copies of the circle. By the end of the reaction, the polymerase generates many thousands of copies of the circular template, with the chain of copies tethered to the original target DNA. This allows for spatial resolution of target and rapid nucleic acid amplification of the signal. Up to 10^{12} copies of template can be generated in 1 hour. Ramification amplification is a variation of RCA and utilizes a closed circular probe (C-probe) or padlock probe and a DNA polymerase with a high processivity to exponentially amplify the C-probe under isothermal conditions.

[0043] Loop-mediated isothermal amplification (LAMP), offers high selectivity and employs a DNA polymerase and a set of four specially designed primers that recognize a total of six distinct sequences on the target DNA. An inner primer containing sequences of the sense and antisense strands of the target DNA initiates LAMP. The following strand displacement DNA synthesis primed by an outer primer releases a single-stranded DNA. This serves as template for DNA synthesis primed by the second inner and outer primers that hybridize to the other end of the target, which produces a stem-loop DNA structure. In subsequent LAMP cycling one inner primer hybridizes to the loop on the product and initiates displacement DNA synthesis, yielding the original stem-loop DNA and a new stem-loop DNA with a stem twice as long. The cycling reaction continues with accumulation of 10^9 copies of target in less than an hour. The final products are stem-loop DNAs with several inverted repeats of the target and cauliflower-like structures with multiple loops formed by annealing between alternately inverted repeats of the target in the same strand.

[0044] After completion of the nucleic acid amplification, the amplified product must be analysed to determine whether the anticipated amplicon (the amplified quantity of target nucleic acids) was generated. The methods of analyzing the product range from simply determining the size of the amplicon through gel electrophoresis, to identifying the nucleotide composition of the amplicon using DNA hybridization.

[0045] Gel electrophoresis is one of the simplest ways to check whether the nucleic acid amplification process generated the anticipated amplicon. Gel electrophoresis uses an electric field applied to a gel matrix to separate DNA fragments. The negatively charged DNA fragments will move through the matrix at different rates, determined largely by their size. After the electrophoresis is complete, the fragments in the gel can be stained to make them visible. Ethidium bromide is a commonly used stain which fluoresces under UV light.

[0046] The size of the fragments is determined by comparison with a DNA size marker (a DNA ladder), which contains DNA fragments of known sizes, run on the gel alongside the amplicon. Because the oligonucleotide primers bind to specific sites flanking the target DNA, the size of the amplified product can be anticipated and detected as a band of known size on the gel. To be certain of the identity of the amplicon, or if several amplicons have been generated, DNA probe hybridization to the amplicon is commonly employed.

[0047] DNA hybridization refers to the formation of double-stranded DNA by complementary base pairing. DNA hybridization for positive identification of a specific amplification product requires the use of a DNA probe around 20 nucleotides in length. If the probe has a sequence that is complementary to the amplicon (target) DNA sequence, hybridization will occur under favourable conditions of temperature, pH and ionic concentration. If hybridization occurs, then the gene or DNA sequence of interest was present in the original sample.

[0048] Optical detection is the most common method to detect hybridization. Either the amplicons or the probes are labelled to emit light through fluorescence or electrochemiluminescence. These processes differ in the means of producing excited states of the light-producing moieties, but both enable covalent labelling of nucleotide strands. In electrochemiluminescence (ECL), light is produced by luminophore molecules or complexes upon stimulation with an electric current. In fluorescence, it is illumination with excitation light which leads to emission.

[0049] Fluorescence is detected using an illumination source which provides excitation light at a wavelength absorbed by the fluorescent molecule, and a detection unit. The detection unit comprises a photosensor (such as a photomultiplier tube or charge-coupled device (CCD) array) to detect the emitted signal, and a mechanism (such as a wavelength-selective filter) to prevent the excitation light from being included in the photosensor output. The fluorescent molecules emit Stokes-shifted light in response to the excitation light, and this emitted light is collected by the detection unit. Stokes shift is the frequency difference or wavelength difference between emitted light and absorbed excitation light.

[0050] ECL emission is detected using a photosensor which is sensitive to the emission wavelength of the ECL species being employed. For example, transition metal-ligand complexes emit light at visible wavelengths, so conventional photodiodes and CCDs are employed as photosensors. An advantage of ECL is that, if ambient light is excluded, the ECL emission can be the only light present in the detection system, which improves sensitivity.

[0051] Microarrays allow for hundreds of thousands of DNA hybridization experiments to be performed simultaneously. Microarrays are powerful tools for molecular diagnostics with the potential to screen for thousands of genetic diseases or detect the presence of numerous infectious pathogens in a single test. A microarray consists of many different DNA probes immobilized as spots on a substrate. The target DNA (amplicon) is first labelled with a fluorescent or luminescent molecule (either during or after nucleic acid amplification) and then applied to the array of probes. The microarray is incubated in a temperature controlled, humid environment for a number of hours or days while hybridization between the probe and amplicon takes place. Following incubation, the microarray must be washed in a series of buffers to remove unbound strands. Once washed, the microarray surface is dried using a stream of air (often nitrogen). The stringency of the hybridization and washes is critical. Insufficient stringency can result in a high degree of nonspecific binding. Excessive stringency can lead to a failure of appropriate binding, which results in diminished sensitivity. Hybridization is recognized by detecting light emission from the labelled amplicons which have formed a hybrid with complementary probes.

[0052] Fluorescence from microarrays is detected using a microarray scanner which is generally a computer controlled inverted scanning fluorescence confocal microscope which typically uses a laser for excitation of the fluorescent dye and a photosensor (such as a photomultiplier tube or CCD) to detect the emitted signal. The fluorescent molecules emit Stokes-shifted light (described above) which is collected by the detection unit.

[0053] The emitted fluorescence must be collected, separated from the unabsorbed excitation wavelength, and transported to the detector. In microarray scanners, a confocal arrangement is commonly used to eliminate out-of-focus information by means of a confocal pinhole situated at an image plane. This allows only the in-focus portion of the light to be detected. Light from above and below the plane of focus of the object is prevented from entering the detector, thereby increasing the signal to noise ratio. The detected fluorescent photons are converted into electrical energy by the detector which is subsequently converted to a digital signal. This digital signal translates to a number representing the intensity of fluorescence from a given pixel. Each feature of the array is made up of one or more such pixels. The final result of a scan is an image of the array surface. The exact sequence and position of every probe on the microarray is known, and so the hybridized target sequences can be identified and analysed simultaneously.

[0054] More information regarding fluorescent probes can be found at: http://www.premierbiosoft.com/tech_notes/FRET_probe.html and http://www.invitrogen.com/site/us/en/home/References/Molecular-Probes-The- Handbook/Technical-Notes-and-Product-Highlights/Fluorescence-Resonance-Energy-Transfer-FRET. html

Point-of-Care Molecular Diagnostics

[0055] Despite the advantages that molecular diagnostic tests offer, the growth of this type of testing in the clinical laboratory has been slower than expected and remains a minor part of the practice of laboratory medicine. This is primarily due to the complexity and costs associated with nucleic acid testing compared with tests based on methods not involving nucleic acids. The widespread adaptation of molecular diagnostics testing to the clinical setting is intimately tied to the development of instrumentation that significantly reduces the cost, provides a rapid and automated assay from start (specimen processing) to finish (generating a result) and operates without major intervention by personnel.

[0056] A point-of-care technology serving the physician's office, the hospital bedside or even consumer-based, at home, would offer many advantages including:

[0057] rapid availability of results enabling immediate facilitation of treatment and improved quality of care.

[0058] ability to obtain laboratory values from testing very small samples.

[0059] reduced clinical workload.

[0060] reduced laboratory workload and improved office efficiency by reducing administrative work.

[0061] improved cost per patient through reduced length of stay of hospitalization, conclusion of outpatient consultation at the first visit, and reduced handling, storing and shipping of specimens.

[0062] facilitation of clinical management decisions such as infection control and antibiotic use.

Lab-on-a-Chip (LOC) Based Molecular Diagnostics

[0063] Molecular diagnostic systems based on microfluidic technologies provide the means to automate and speed up molecular diagnostic assays. The quicker detection times are primarily due to the extremely low volumes involved, automation, and the low-overhead inbuilt cascading of the diagnostic process steps within a microfluidic device. Volumes in the nanoliter and microliter scale also reduce reagent consumption and cost. Lab-on-a-chip (LOC) devices are a common form of microfluidic device. LOC devices have MST structures within a MST layer for fluid processing integrated onto a single supporting substrate (usually silicon). Fabrication using the VLSI (very large scale integrated) lithographic techniques of the semiconductor industry keeps the unit cost of each LOC device very low. However, controlling fluid flow through the LOC device, adding reagents, controlling reaction conditions and so on necessitate bulky external plumbing and electronics. Connecting a LOC device to these external devices effectively restricts the use of LOC devices for molecular diagnostics to the laboratory setting. The cost of the external equipment and complexity of its operation precludes LOC-based molecular diagnostics as a practical option for point-of-care settings.

[0064] In view of the above, there is a need for a molecular diagnostic system based on a LOC device for use at point-of-care.

SUMMARY OF THE INVENTION

[0065] Accordingly, the present invention provides a test module for lysing cells in a fluid, the test module comprising:

[0066] an outer casing with receptacle for receiving a fluid containing cells;

[0067] a lysis reagent reservoir containing a lysis reagent and having an outlet valve; and,

[0068] a lysis section in fluid communication with the receptacle for holding the fluid during lysis of the cells; wherein,

[0069] the outlet valve is upstream of the lysis section and configured to open as the fluid flows into the lysis section thereby adding the lysis reagent to the fluid.

[0070] Preferably, the outlet valve is a surface tension valve with an aperture configured to pin a meniscus that retains the lysis reagent therein until contact with the fluid removes the meniscus and the lysis reagent is added to the fluid flow into the lysis section.

[0071] Preferably, the lysis section is configured as a lysis microchannel to draw the fluid from the receptacle by capillary action, the lysis section having an active valve at a downstream end of the lysis microchannel for retaining the fluid during lysis of the cells.

[0072] Preferably, the active valve is a boiling-initiated valve with a meniscus anchor for retaining the fluid in the lysis section, the boiling-initiated valve also having a valve heater for boiling the liquid such that the meniscus unpins from the meniscus anchor and capillary driven flow out of the lysis section resumes.

[0073] Preferably, the microchannel has a cross sectional area transverse to the flow of between 8 square microns and 20,000 square microns.

[0074] Preferably, the test module also has a supporting substrate wherein the lysis section and the lysis reagent reservoir are supported on the supporting substrate and configured as a lab-on-a-chip (LOC) device.

[0075] Preferably, the test module also has CMOS circuitry between the supporting substrate and the lysis section, the CMOS circuitry being configured for operative control of the valve heater at the downstream end of the microchannel.

[0076] Preferably, the test module also has a polymerase chain reaction (PCR) section with at least one heater for thermally cycling the fluid to amplify nucleic acid sequences released from the cells.

[0077] Preferably, the test module also has at least one sensor wherein the CMOS circuitry is configured to use the sensor for feedback control of the at least one PCR heater.

[0078] Preferably, the test module also has a plurality of heaters and at least one temperature sensor and at least one liquid sensor such that the CMOS circuitry controls initial activation of the heaters in response to the at least one liquid sensor and heater power in response to the at least one temperature sensor.

[0079] Preferably, each of the plurality of heaters is independently operable.

[0080] Preferably, the PCR section is configured as a PCR microchannel with the same cross section as the lysis microchannel, the PCR section also having an active valve at a downstream end of the PCR microchannel for retaining the fluid during amplification of the nucleic acid sequences.

[0081] Preferably, the test module also has a PCR mix reservoir and a polymerase reservoir wherein the PCR mix reservoir contains dNTPs, primers and buffer solution and the polymerase reservoir contains polymerase enzymes.

[0082] Preferably, the test module also has a cap which defines the lysis reagent reservoir, the PCR mix reservoir and the polymerase reservoir, wherein the lysis section and the PCR section are between the cap and the supporting substrate.

[0083] Preferably, the test module also has a dialysis section wherein the cells in the fluid are of different sizes, the dialysis section being configured for separating cells larger than a predetermined threshold into a portion of the sample which is processed separately from the remainder of the sample containing only cells smaller than the predetermined threshold.

[0084] Preferably, the nucleic acid sequences are from the cells larger than the predetermined threshold.

[0085] Preferably, the test module also has an anticoagulant reservoir wherein the fluid is a whole blood sample such that anticoagulant is added to the whole blood upstream of the dialysis section and the dialysis section is configured to concentrate the leukocytes into a portion of the whole blood sample.

[0086] Preferably, the test module also has a hybridization section downstream of the PCR section, the hybridization section having an array of probes for hybridization with predetermined target nucleic acid sequences in the amplicon from the PCR section; and,

[0087] a photosensor for detecting hybridization of probes within the array of probes.

[0088] Preferably, the hybridization section has electrodes positioned for receiving an electrical pulse, and the probes are electrochemiluminescent (ECL) probes for hybridization with the target nucleic acid sequences to form probe-target hybrids, the probe-target hybrids being configured to emit a photon of light when excited by current between the electrodes.

[0089] Preferably, the photosensor is an array of photodiodes positioned in registration with the ECL probes respectively.

[0090] The easily usable, mass-producible, inexpensive, and portable genetic test module accepts a biochemical sample, uses a chemical lysis subunit for lysing cells or cell organelles, and processes the lysates.

[0091] The lysing process extracts analytical and diagnostic targets from cells in the sample and provides for follow-on processing and analysis of the targets. The lysis subunit being integral to the module, provides for simple assay procedures, low assay system complexity, leading into an inexpensive assay system.

BRIEF DESCRIPTION OF THE DRAWINGS

[0092] Preferred embodiments of the present invention will now be described by way of example only with reference to the accompanying drawings, in which:

[0093] FIG. **1** shows a test module and test module reader configured for fluorescence detection;

[0094] FIG. **2** is a schematic overview of the electronic components in the test module configured for fluorescence detection;

[0095] FIG. **3** is a schematic overview of the electronic components in the test module reader;

[0096] FIG. **4** is a schematic representation of the architecture of the LOC device;

[0097] FIG. **5** is a perspective of the LOC device;

[0098] FIG. **6** is a plan view of the LOC device with features and structures from all layers superimposed on each other;

[0099] FIG. **7** is a plan view of the LOC device with the structures of the cap shown in isolation;

[0100] FIG. **8** is a top perspective of the cap with internal channels and reservoirs shown in dotted line;

[0101] FIG. **9** is an exploded top perspective of the cap with internal channels and reservoirs shown in dotted line;

[0102] FIG. **10** is a bottom perspective of the cap showing the configuration of the top channels;

[0103] FIG. **11** is a plan view of the LOC device showing the structures of the CMOS+MST device in isolation;

[0104] FIG. **12** is a schematic section view of the LOC device at the sample inlet;

[0105] FIG. **13** is an enlarged view of Inset AA shown in FIG. **6**;

[0106] FIG. **14** is an enlarged view of Inset AB shown in FIG. **6**;

[0107] FIG. **15** is an enlarged view of Inset AE shown in FIG. **13**;

[0108] FIG. **16** is a partial perspective illustrating the laminar structure of the LOC device within Inset AE;

[0109] FIG. **17** is a partial perspective illustrating the laminar structure of the LOC device within Inset AE;

[0110] FIG. **18** is a partial perspective illustrating the laminar structure of the LOC device within Inset AE;

[0111] FIG. **19** is a partial perspective illustrating the laminar structure of the LOC device within Inset AE;

[0112] FIG. **20** is a partial perspective illustrating the laminar structure of the LOC device within Inset AE;

[0113] FIG. **21** is a partial perspective illustrating the laminar structure of the LOC device within Inset AE;

[0114] FIG. **22** is schematic section view of the lysis reagent reservoir shown in FIG. **21**;

[0115] FIG. **23** is a partial perspective illustrating the laminar structure of the LOC device within Inset AB;

[0116] FIG. **24** is a partial perspective illustrating the laminar structure of the LOC device within Inset AB;

[0117] FIG. **25** is a partial perspective illustrating the laminar structure of the LOC device within Inset AI;

[0118] FIG. **26** is a partial perspective illustrating the laminar structure of the LOC device within Inset AB;

[0119] FIG. **27** is a partial perspective illustrating the laminar structure of the LOC device within Inset AB;

[0120] FIG. **28** is a partial perspective illustrating the laminar structure of the LOC device within Inset AB;

[0121] FIG. **29** is a partial perspective illustrating the laminar structure of the LOC device within Inset AB;

[0122] FIG. **30** is a schematic section view of the amplification mix reservoir and the polymerase reservoir;

[0123] FIG. **31** show the features of a boiling-initiated valve in isolation;

[0124] FIG. **32** is a schematic section view of the boiling-initiated valve taken through line **33-33** shown in FIG. **31**;

[0125] FIG. **33** is an enlarged view of Inset AF shown in FIG. **15**;

[0126] FIG. **34** is a schematic section view of the upstream end of the dialysis section taken through line **35-35** shown in FIG. **33**;

[0127] FIG. **35** is an enlarged view of Inset AC shown in FIG. **6**;

[0128] FIG. **36** is a further enlarged view within Inset AC showing the amplification section;

[0129] FIG. **37** is a further enlarged view within Inset AC showing the amplification section;

[0130] FIG. **38** is a further enlarged view within Inset AC showing the amplification section;

[0131] FIG. **39** is a further enlarged view within Inset AK shown in FIG. **38**;

[0132] FIG. **40** is a further enlarged view within Inset AC showing the amplification chamber;

[0133] FIG. **41** is a further enlarged view within Inset AC showing the amplification section;

[0134] FIG. **42** is a further enlarged view within Inset AC showing the amplification chamber;

[0135] FIG. **43** is a further enlarged view within Inset AL shown in FIG. **42**;

[0136] FIG. **44** is a further enlarged view within Inset AC showing the amplification section;

[0137] FIG. **45** is a further enlarged view within Inset AM shown in FIG. **44**;

[0138] FIG. **46** is a further enlarged view within Inset AC showing the amplification chamber;

[0139] FIG. **47** is a further enlarged view within Inset AN shown in FIG. **46**;

[0140] FIG. **48** is a further enlarged view within Inset AC showing the amplification chamber;

[0141] FIG. **49** is a further enlarged view within Inset AC showing the amplification chamber;

[0142] FIG. **50** is a further enlarged view within Inset AC showing the amplification section;

[0143] FIG. **51** is a schematic section view of the amplification section;

[0144] FIG. **52** is an enlarged plan view of the hybridization section;

[0145] FIG. **53** is a further enlarged plan view of two hybridization chambers in isolation;

[0146] FIG. **54** is schematic section view of a single hybridization chamber;

[0147] FIG. **55** is an enlarged view of the humidifier illustrated in Inset AG shown in FIG. **6**;

[0148] FIG. **56** is an enlarged view of Inset AD shown in FIG. **52**;

[0149] FIG. **57** is an exploded perspective view of the LOC device within Inset AD;

[0150] FIG. **58** is an enlarged plan view of the humidity sensor shown in Inset AH of FIG. **6**;

[0151] FIG. **59** is a schematic section view of a leukocyte target dialysis section;

[0152] FIG. **60** is a schematic showing part of the photodiode array of the photo sensor;

[0153] FIG. **61** is an enlarged view of the evaporator shown in Inset AP of FIG. **55**;

[0154] FIG. **62** is a diagram of linker-primed PCR;

[0155] FIG. **63** is a schematic representation of a test module with a lancet;

[0156] FIG. **64** is a diagrammatic representation of the architecture of LOC variant VII;

[0157] FIG. **65** is a plan view of LOC variant VIII with features and structures from all layers superimposed on each other;

[0158] FIG. **66** is an enlarged view of Inset CA shown in FIG. **65**;

[0159] FIG. **67** is a partial perspective illustrating the laminar structure of LOC variant VIII within Inset CA shown in FIG. **65**;

[0160] FIG. **68** is an enlarged view of Inset CE shown in FIG. **66**;

[0161] FIG. **69** is a diagrammatic representation of the architecture of LOC variant VIII;

[0162] FIG. **70** is a schematic illustration of the architecture of LOC variant XIV;

[0163] FIG. **71** is a schematic illustration of the architecture of LOC variant XLI;

[0164] FIG. **72** is a schematic illustration of the architecture of LOC variant XLII;

[0165] FIG. **73** is a schematic illustration of the architecture of LOC variant XLIII;

[0166] FIG. **74** is a schematic illustration of the architecture of LOC variant XLIV;

[0167] FIG. **75** is a schematic illustration of the architecture of LOC variant XLVII;

[0168] FIG. **76** is a diagrammatic representation of the architecture of LOC variant X;

[0169] FIG. **77** is a perspective view of LOC variant X;

[0170] FIG. **78** is a plan view of LOC variant X showing the structures of the CMOS+MST device in isolation;

[0171] FIG. **79** is a perspective view of the underside of the cap with the reagent reservoirs shown in dotted line;

[0172] FIG. **80** is a plan view showing only the features of the cap in isolation;

[0173] FIG. **81** is a plan view showing all the features superimposed on each other, and showing the location of Insets DA to DK;

[0174] FIG. **82** is an enlarged view of Inset DA shown in FIG. **81**;

[0175] FIG. **83** is an enlarged view of Inset DB shown in FIG. **81**;

[0176] FIG. **84** is an enlarged view of Inset DC shown in FIG. **81**;

[0177] FIG. **85** is an enlarged view of Inset DD shown in FIG. **81**;

[0178] FIG. **86** is an enlarged view of Inset DE shown in FIG. **81**;

[0179] FIG. **87** is an enlarged view of Inset DF shown in FIG. **81**;

[0180] FIG. **88** is an enlarged view of Inset DG shown in FIG. **81**;

[0181] FIG. **89** is an enlarged view of Inset DH shown in FIG. **81**;

[0182] FIG. **90** is an enlarged view of Inset DJ shown in FIG. **81**;

[0183] FIG. **91** is an enlarged view of Inset DK shown in FIG. **81**;

[0184] FIG. **92** is an enlarged view of Inset DL shown in FIG. **81**;

[0185] FIG. **93** is a circuit diagram of the differential imager;

[0186] FIG. **94** schematically illustrates a CMOS-controlled flow rate sensor;

[0187] FIG. **95** illustrates the reactions occurring during an electrochemiluminescence (ECL) process;

[0188] FIG. **96** schematically illustrates three different anode configurations;

[0189] FIG. **97** is a schematic partial cross-section of the anode and cathode in the hybridization chamber;

[0190] FIG. **98** schematically illustrates an anode in a ring geometry around the peripheral edge of a photodiode;

[0191] FIG. **99** schematically illustrates an anode in a ring geometry within the peripheral edge of a photodiode;

[0192] FIG. **100** schematically illustrates an anode with a series of fingers to increase the length of its lateral edges;

[0193] FIG. **101** schematically illustrates the use of a transparent anode to maximise surface area coupling and ECL signal detection;

[0194] FIG. **102** schematically illustrates the use of an anode affixed to the roof of the hybridization chamber to maximise surface area coupling and ECL signal detection;

[0195] FIG. **103** schematically illustrates an anode interdigitated with a cathode;

[0196] FIG. **104** shows a test module and test module reader configured for use with ECL detection;

[0197] FIG. **105** is a schematic overview of the electronic components in the test module configured for use with ECL detection;

[0198] FIG. **106** shows a test module and alternative test module readers;

[0199] FIG. **107** shows a test module and test module reader along with the hosting system housing various databases;

[0200] FIGS. **108**A and **108**B is a diagram illustrating binding of an aptamer to a protein to produce a detectable signal;

[0201] FIGS. **109**A and **109**B are diagrams illustrating binding of two aptamers to a protein to produce a detectable signal;

[0202] FIGS. **110**A and **110**B are diagrams illustrating binding of two antibodies to a protein to produce a detectable signal;

[0203] FIG. **111** is a diagrammatic representation of the architecture of LOC variant L with ECL detection;

[0204] FIG. **112** is a perspective view of LOC variant L;

[0205] FIG. **113** is a plan view of LOC variant L showing the structures of the CMOS+MST device in isolation;

[0206] FIG. **114** is a perspective view of the underside of the cap of LOC variant L with the reagent reservoirs shown in dotted lines;

[0207] FIG. **115** is a plan view of LOC variant L showing the features of the cap in isolation;

[0208] FIG. **116** is a plan view of LOC variant L showing all the features superimposed on each other and showing the locations of Insets GA to GL;

[0209] FIG. **117** is an enlarged view of Inset GA shown in FIG. **116**;

[0210] FIG. **118** is an enlarged view of Inset GB shown in FIG. **116**;

[0211] FIG. **119** is an enlarged view of Inset GC shown in FIG. **116**;

[0212] FIG. **120** is an enlarged view of Inset GD shown in FIG. **116**;

[0213] FIG. **121** is an enlarged view of Inset GE shown in FIG. **116**;

[0214] FIG. **122** is an enlarged view of Inset GF shown in FIG. **116**;

[0215] FIG. **123** is an enlarged view of Inset GG shown in FIG. **116**;

[0216] FIG. **124** is an enlarged view of Inset GH shown in FIG. **116**;

[0217] FIG. **125** is an enlarged view of Inset GJ shown in FIG. **116**;

[0218] FIG. **126** is an enlarged view of Inset GK shown in FIG. **116**;

[0219] FIG. **127** is an enlarged view of Inset GL shown in FIG. **116**;

[0220] FIG. **128** is a diagrammatic representation of a LOC device with thermal insulation trench;

[0221] FIG. **129** is a diagram of an electrochemiluminescence resonance energy transfer probe in a closed configuration;

[0222] FIG. **130** is a diagram of an electrochemiluminescence resonance energy transfer probe in an open and hybridized configuration;

[0223] FIG. **131** is a diagram of a primer-linked, luminescent linear probe during the initial round of amplification;

[0224] FIG. **132** is a diagram of a primer-linked, luminescent linear probe during a subsequent amplification cycle;

[0225] FIGS. **133**A to **133**F diagrammatically illustrate thermal cycling of a luminescent primer-linked stem-and-loop probe;

[0226] FIG. **134** schematically illustrates a negative control luminescent probe in its stem-and-loop configuration;

[0227] FIG. **135** schematically illustrates the negative control luminescent probe of FIG. **134** in its open configuration;

[0228] FIG. **136** schematically illustrates a positive control luminescent probe in its stem-and-loop configuration;

[0229] FIG. **137** schematically illustrates the positive control luminescent probe of FIG. **136** in its open configuration;

[0230] FIG. **138** is an enlarged view of the hybridization chamber of LOC variant L;

[0231] FIG. **139** is an enlarged view of the hybridization chamber array of LOC variant L showing the distribution of calibration chambers;

DETAILED DESCRIPTION OF THE PREFERRED EMBODIMENTS

Overview

[0232] This overview identifies the main components of a molecular diagnostic system that incorporates embodiments of the present invention. Comprehensive details of the system architecture and operation are set out later in the specification.

[0233] Referring to FIGS. **1**, **2**, **3**, **104** and **105**, the system has the following top level components:

[0234] Test modules **10** and **11** are the size of a typical USB memory key and very cheap to produce. Test modules **10** and **11** each contain a microfluidic device, typically in the form of a lab-on-a-chip (LOC) device **30** preloaded with reagents and typically more than 1000 probes for the molecular diagnostic assay (see FIGS. **1** and **104**). Test module **10** schematically shown in FIG. **1** uses a fluorescence-based detection technique to identify target molecules, while test module **11** in FIG. **104** uses an electrochemiluminescence-based detection technique. The LOC device **30** has an integrated photosensor **44** for fluorescence or electrochemiluminescence detection (described in detail below). Both test modules **10** and **11** use a standard Micro-USB plug **14** for power, data and control, both have a printed circuit board (PCB) **57**, and both have external power supply capacitors **32** and an inductor **15**. The test modules **10** and **11** are both single-use only for mass production and distribution in sterile packaging ready for use.

[0235] The outer casing **13** has a macroreceptacle **24** for receiving the biological sample and a removable sterile sealing tape **22**, preferably with a low tack adhesive, to cover the macroreceptacle prior to use. A membrane seal **408** with a membrane guard **410** forms part of the outer casing **13** to reduce dehumidification within the test module while providing pressure relief from small air pressure fluctuations. The membrane guard **410** protects the membrane seal **408** from damage.

[0236] Test module reader **12** powers the test module **10** or **11** via Micro-USB port **16**. The test module reader **12** can adopt many different forms and a selection of these are described later. The version of the reader **12** shown in FIGS. **1**, **3** and **104** is a smart phone embodiment. A block diagram of this reader **12** is shown in FIG. **3**. Processor **42** runs application software from program storage **43**. The processor **42** also interfaces with the display screen **18** and user interface (UI) touch screen **17** and buttons **19**, a cellular radio **21**, wireless network connection **23**, and a satellite navigation system **25**. The cellular radio **21** and wireless network connection **23** are used for communications. Satellite navigation system **25** is used for updating epidemiological databases with location data. The location data can, alternatively, be entered manually via the touch screen **17** or buttons **19**. Data storage **27** holds genetic and diagnostic information, test results, patient information, assay and probe data for identifying each probe and its array position. Data storage **27** and program storage **43** may be shared in a common memory facility. Application software installed on the test module reader **12** provides analysis of results, along with additional test and diagnostic information.

[0237] To conduct a diagnostic test, the test module **10** (or test module **11**) is inserted into the Micro-USB port **16** on the test module reader **12**. The sterile sealing tape **22** is peeled back and the biological sample (in a liquid form) is loaded into the sample macroreceptacle **24**. Pressing start button **20** initiates testing via the application software. The sample flows into the LOC device **30** and the on-board assay extracts, incubates, amplifies and hybridizes the sample nucleic acids (the target) with presynthesized hybridization-responsive oligonucleotide probes. In the case of test module **10** (which uses fluorescence-based detection), the probes are fluorescently labelled and the LED **26** housed in the casing **13** provides the necessary excitation light to induce fluorescence emission from the hybridized probes (see FIGS. **1** and **2**). In test module **11** (which uses electrochemiluminescence (ECL) detection), the LOC device **30** is loaded with ECL probes (discussed above) and the LED **26** is not necessary for generating the luminescent emission. Instead, electrodes **860** and **870** provide the excitation electrical current (see FIG. **105**). The emission (fluorescent or luminescent) is detected using a photosensor **44** integrated into CMOS circuitry of each LOC device. The detected signal is amplified and converted to a digital output which is analyzed by the test module reader **12**. The reader then displays the results.

[0238] The data may be saved locally and/or uploaded to a network server containing patient records. The test module **10** or **11** is removed from the test module reader **12** and disposed of appropriately.

[0239] FIGS. **1**, **3** and **104** show the test module reader **12** configured as a mobile phone/smart phone **28**. In other forms, the test module reader is a laptop/notebook **101**, a dedicated reader **103**, an ebook reader **107**, a tablet computer **109** or desktop computer **105** for use in hospitals, private practices or laboratories (see FIG. **106**). The reader can interface with a range of additional applications such as patient records, billing, online databases and multi-user environments. It can also be interfaced with a range of local or remote peripherals such as printers and patient smart cards.

[0240] Referring to FIG. **107**, the data generated by the test module **10** can be used to update, via the reader **12** and network **125**, the epidemiological databases hosted on the hosting system for epidemiological data **111**, the genetic databases hosted on the hosting system for genetic data **113**, the electronic health records hosted on the hosting system for electronic health records (EHR) **115**, the electronic medical records hosted on the hosting system for electronic medical records (EMR) **121**, and the personal health records hosted on the hosting system for personal health records (PHR) **123**. Conversely, the epidemiological data hosted on the hosting system for epidemiological data **111**, the genetic data hosted on the hosting system for genetic data **113**, the electronic health records hosted on the hosting system for electronic health records (EHR) **115**, the electronic medical records hosted on the hosting system for electronic medical records (EMR) **121**, and the personal health records hosted on the hosting system for personal health records (PHR) **123**, can be used to update, via network **125** and the reader **12**, the digital memory in the LOC **30** of the test module **10**.

[0241] Referring back to FIGS. **1**, **2**, **104** and **105** the reader **12** uses battery power in the mobile phone configuration. The mobile phone reader contains all test and diagnostic information preloaded. Data can also be loaded or updated via a number of wireless or contact interfaces to enable communications with peripheral devices, computers or online servers. A Micro-USB port **16** is provided for connection to a computer or mains power supply for battery recharge.

[0242] FIG. **63** shows an embodiment of the test module **10** used for tests that only require a positive or negative result for a particular target, such as testing whether a person is infected with, for example, H1N1 Influenza A virus. Only a purpose built USB power/indicator-only module **47** is adequate. No other reader or application software is necessary. An indicator **45** on the USB power/indicator-only module **47** signals positive or negative results. This configuration is well suited to mass screening.

[0243] Additional items supplied with the system may include a test tube containing reagents for pre-treatment of certain samples, along with spatula and lancet for sample collection. FIG. **63** shows an embodiment of the test module incorporating a spring-loaded, retractable lancet **390** and lancet release button **392** for convenience. A satellite phone can be used in remote areas.

Test Module Electronics

[0244] FIGS. **2** and **105** are block diagrams of the electronic components in the test modules **10** and **11**, respectively. The CMOS circuitry integrated in the LOC device **30** has a USB device driver **36**, a controller **34**, a USB-compatible LED driver **29**, clock **33**, power conditioner **31**, RAM **38** and program and data flash memory **40**. These provide the control and memory for the entire test module **10** or **11** including the photosensor **44**, the temperature sensors **170**, the liquid sensors **174**, and the various heaters **152**, **154**, **182**, **234**, together with associated drivers **37** and **39** and registers **35** and **41**. Only the LED **26** (in the case of test module **10**), external power supply capacitors **32** and the Micro-USB plug **14** are external to the LOC device **30**. The LOC devices **30** include bond-pads for making connections to these external components. The RAM **38** and the program and data flash memory **40** have the application software and the diagnostic and test information (Flash/Secure storage, e.g. via encryption) for over 1000 probes. In the case of test module **11** configured for ECL detection, there is no LED **26** (see FIGS. **104** and **105**). Data is encrypted by the LOC device **30** for secure storage and secure communication with an external device. The LOC devices **30** are loaded with electrochemiluminescent probes and the hybridization chambers each have a pair of ECL excitation electrodes **860** and **870**.

[0245] Many types of test modules **10** are manufactured in a number of test forms, ready for off-the-shelf use. The differences between the test forms lie in the on board assay of reagents and probes.

[0246] Some examples of infectious diseases rapidly identified with this system include:

[0247] Influenza—Influenza virus A, B, C, Isavirus, Thogotovirus

[0248] Pneumonia—respiratory syncytial virus (RSV), adenovirus, metapneumovirus, *Streptococcus pneumoniae, Staphylococcus aureus*

[0249] Tuberculosis—*Mycobacterium tuberculosis, bovis, africanum, canetti,* and *microti*

[0250] *Plasmodium falciparum, Toxoplasma gondii* and other protozoan parasites

[0251] Typhoid—*Salmonella enterica* serovar typhi

[0252] Ebola virus

[0253] Human immunodeficiency virus (HIV)

[0254] Dengue Fever—Flavivirus

[0255] Hepatitis (A through E)

[0256] Hospital acquired infections—for example *Clostridium difficile,* Vancomycin resistant *Enterococcus,* and Methicillin resistant *Staphylococcus aureus*

[0257] Herpes simplex virus (HSV)

[0258] Cytomegalovirus (CMV)

[0259] Epstein-Ban virus (EBV)

[0260] Encephalitis—Japanese Encephalitis virus, Chandipura virus

[0261] Whooping cough—*Bordetella pertussis*

[0262] Measles—paramyxovirus

[0263] Meningitis—*Streptococcus pneumoniae* and *Neisseria meningitidis*

[0264] Anthrax—*Bacillus anthracis*

[0265] Some examples of genetic disorders identified with this system include:

[0266] Cystic fibrosis

[0267] Haemophilia

[0268] Sickle cell disease

[0269] Tay-Sachs disease

[0270] Haemochromatosis

[0271] Cerebral arteriopathy

[0272] Crohn's disease

[0273] Polycistic kidney disease

[0274] Congential heart disease

[0275] Rett syndrome

[0276] A small selection of cancers identified by the diagnostic system include:

[0277] Ovarian

[0278] Colon carcinoma

[0279] Multiple endocrine neoplasia

[0280] Retinoblastoma

[0281] Turcot syndrome

[0282] The above lists are not exhaustive and the diagnostic system can be configured to detect a much greater variety of diseases and conditions using nucleic acid and proteomic analysis.

Detailed Architecture of System Components

LOC Device

[0283] The LOC device **30** is central to the diagnostic system. It rapidly performs the four major steps of a nucleic acid based molecular diagnostic assay, i.e. sample preparation, nucleic acid extraction, nucleic acid amplification, and detection, using a microfluidic platform. The LOC device also has alternative uses, and these are detailed later. As discussed above, test modules **10** and **11** can adopt many different configurations to detect different targets Likewise, the LOC device **30** has numerous different embodiments tailored to the target(s) of interest. One form of the LOC device **30** is LOC device **301** for fluorescent detection of target nucleic acid sequences in the pathogens of a whole blood sample. For the purposes of illustration, the structure and operation of LOC device **301** is now described in detail with reference to FIGS. **4** to **26** and **27** to **57**.

[0284] FIG. **4** is a schematic representation of the architecture of the LOC device **301**. For convenience, process stages shown in FIG. **4** are indicated with the reference numeral corresponding to the functional sections of the LOC device **301** that perform that process stage. The process stages associated with each of the major steps of a nucleic acid based molecular diagnostic assay are also indicated: sample input and preparation **288**, extraction **290**, incubation **291**, amplification **292** and detection **294**. The various reservoirs, cham-

bers, valves and other components of the LOC device **301** will be described in more detail later.

[0285] FIG. **5** is a perspective view of the LOC device **301**. It is fabricated using high volume CMOS and MST (microsystems technology) manufacturing techniques. The laminar structure of the LOC device **301** is illustrated in the schematic (not to scale) partial section view of FIG. **12**. The LOC device **301** has a silicon substrate **84** which supports the CMOS+MST chip **48**, comprising CMOS circuitry **86** and an MST layer **87**, with a cap **46** overlaying the MST layer **87**. For the purposes of this patent specification, the term 'MST layer' is a reference to a collection of structures and layers that process the sample with various reagents. Accordingly, these structures and components are configured to define flow-paths with characteristic dimensions that will support capillary driven flow of liquids with physical characteristics similar to those of the sample during processing. In light of this, the MST layer and components are typically fabricated using surface micromachining techniques and/or bulk micromachining techniques. However, other fabrication methods can also produce structures and components dimensioned for capillary driven flows and processing very small volumes. The specific embodiments described in this specification show the MST layer as the structures and active components supported on the CMOS circuitry **86**, but excluding the features of the cap **46**. However, the skilled addressee will appreciate that the MST layer need not have underlying CMOS or indeed an overlying cap in order for it to process the sample.

[0286] The overall dimensions of the LOC device shown in the following figures are 1760 μm×5824 μm. Of course, LOC devices fabricated for different applications may have different dimensions.

[0287] FIG. **6** shows the features of the MST layer **87** superimposed with the features of the cap. Insets AA to AD, AG and AH shown in FIG. **6** are enlarged in FIGS. **13**, **14**, **35**, **56**, **55** and **58**, respectively, and described in detail below for a comprehensive understanding of each structure within the LOC device **301**. FIGS. **7** to **10** show the features of the cap **46** in isolation while FIG. **11** shows the CMOS+MST device **48** structures in isolation.

Laminar Structure

[0288] FIGS. **12** and **22** are sketches that diagrammatically show the laminar structure of the CMOS+MST device **48**, the cap **46** and the fluidic interaction between the two. The figures are not to scale for the purposes of illustration. FIG. **12** is a schematic section view through the sample inlet **68** and FIG. **22** is a schematic section through the reservoir **54**. As best shown in FIG. **12**, the CMOS+MST device **48** has a silicon substrate **84** which supports the CMOS circuitry **86** that operates the active elements within the MST layer **87** above. A passivation layer **88** seals and protects the CMOS layer **86** from the fluid flows through the MST layer **87**.

[0289] Fluid flows through both the cap channels **94** and the MST channels **90** (see for example FIGS. **7** and **16**) in the cap layer **46** and MST channel layer **100**, respectively. Cell transport occurs in the larger channels **94** fabricated in the cap **46**, while biochemical processes are carried out in the smaller MST channels **90**. Cell transport channels are sized so as to be able to transport cells in the sample to predetermined sites in the MST channels **90**. Transportation of cells with sizes greater than 20 microns (for example, certain leukocytes) requires channel dimensions greater than 20 microns, and therefore a cross sectional area transverse to the flow of greater than 400 square microns. MST channels, particularly at locations in the LOC where transport of cells is not required, can be significantly smaller.

[0290] It will be appreciated that cap channel **94** and MST channel **90** are generic references and particular MST channels **90** may also be referred to as (for example) heated microchannels or dialysis MST channels in light of their particular function. MST channels **90** are formed by etching through a MST channel layer **100** deposited on the passivation layer **88** and patterned with photoresist. The MST channels **90** are enclosed by a roof layer **66** which forms the top (with respect to the orientation shown in the figures) of the CMOS+MST device **48**.

[0291] Despite sometimes being shown as separate layers, the cap channel layer **80** and the reservoir layer **78** are formed from a unitary piece of material. Of course, the piece of material may also be non-unitary. This piece of material is etched from both sides in order to form a cap channel layer **80** in which the cap channels **94** are etched and the reservoir layer **78** in which the reservoirs **54**, **56**, **58**, **60** and **62** are etched. Alternatively, the reservoirs and the cap channels are formed by a micromolding process. Both etching and micromolding techniques are used to produce channels with cross sectional areas transverse to the flow as large as 20,000 square microns, and as small as 8 square microns.

[0292] At different locations in the LOC device, there can be a range of appropriate choices for the cross sectional area of the channel transverse to the flow. Where large quantities of sample, or samples with large constituents, are contained in the channel, a cross-sectional area of up to 20,000 square microns (for example, a 200 micron wide channel in a 100 micron thick layer) is suitable. Where small quantities of liquid, or mixtures without large cells present, are contained in the channel, a very small cross sectional area transverse to the flow is preferable.

[0293] A lower seal **64** encloses the cap channels **94** and the upper seal layer **82** encloses the reservoirs **54**, **56**, **58**, **60** and **62**.

[0294] The five reservoirs **54**, **56**, **58**, **60** and **62** are preloaded with assay-specific reagents. In the embodiment described here, the reservoirs are preloaded with the following reagents, but other reagents can easily be substituted:

[0295] reservoir **54**: anticoagulant with option to include erythrocyte lysis buffer

[0296] reservoir **56**: lysis reagent

[0297] reservoir **58**: restriction enzymes, ligase and linkers (for linker-primed PCR (see FIG. **62**, extracted from T. Stachan et al., Human Molecular Genetics 2, Garland Science, NY and London, 1999))

[0298] reservoir **60**: amplification mix (dNTPs, primers, buffer) and

[0299] reservoir **62**: DNA polymerase.

[0300] The cap **46** and the CMOS+MST layers **48** are in fluid communication via corresponding openings in the lower seal **64** and the roof layer **66**. These openings are referred to as uptakes **96** and downtakes **92** depending on whether fluid is flowing from the MST channels **90** to the cap channels **94** or vice versa.

LOC Device Operation

[0301] The operation of the LOC device **301** is described below in a step-wise fashion with reference to analysing pathogenic DNA in a blood sample. Of course, other types of biological or non-biological fluid are also analysed using an

appropriate set, or combination, of reagents, test protocols, LOC variants and detection systems. Referring back to FIG. **4**, there are five major steps involved in analysing a biological sample, comprising sample input and preparation **288**, nucleic acid extraction **290**, nucleic acid incubation **291**, nucleic acid amplification **292** and detection and analysis **294**.

[0302] The sample input and preparation step **288** involves mixing the blood with an anticoagulant **116** and then separating pathogens from the leukocytes and erythrocytes with the pathogen dialysis section **70**. As best shown in FIGS. **7** and **12**, the blood sample enters the device via the sample inlet **68**. Capillary action draws the blood sample along the cap channel **94** to the reservoir **54**. Anticoagulant is released from the reservoir **54** as the sample blood flow opens its surface tension valve **118** (see FIGS. **15** and **22**). The anticoagulant prevents the formation of clots which would block the flow.

[0303] As best shown in FIG. **22**, the anticoagulant **116** is drawn out of the reservoir **54** by capillary action and into the MST channel **90** via the downtake **92**. The downtake **92** has a capillary initiation feature (CIF) **102** to shape the geometry of the meniscus such that it does not anchor to the rim of the downtake **92**. Vent holes **122** in the upper seal **82** allows air to replace the anticoagulant **116** as it is drawn out of the reservoir **54**.

[0304] The MST channel **90** shown in FIG. **22** is part of a surface tension valve **118**. The anticoagulant **116** fills the surface tension valve **118** and pins a meniscus **120** to the uptake **96** to a meniscus anchor **98**. Prior to use, the meniscus **120** remains pinned at the uptake **96** so the anticoagulant does not flow into the cap channel **94**. When the blood flows through the cap channel **94** to the uptake **96**, the meniscus **120** is removed and the anticoagulant is drawn into the flow.

[0305] FIGS. **15** to **21** show Inset AE which is a portion of Inset AA shown in FIG. **13**. As shown in FIGS. **15**, **16** and **17**, the surface tension valve **118** has three separate MST channels **90** extending between respective downtakes **92** and uptakes **96**. The number of MST channels **90** in a surface tension valve can be varied to change the flow rate of the reagent into the sample mixture. As the sample mixture and the reagents mix together by diffusion, the flow rate out of the reservoir determines the concentration of the reagent in the sample flow. Hence, the surface tension valve for each of the reservoirs is configured to match the desired reagent concentration.

[0306] The blood passes into a pathogen dialysis section **70** (see FIGS. **4** and **15**) where target cells are concentrated from the sample using an array of apertures **164** sized according to a predetermined threshold. Cells smaller than the threshold pass through the apertures while larger cells do not pass through the apertures. Unwanted cells, which may be either the larger cells withheld by the array of apertures **164** or the smaller cells that pass through the apertures, are redirected to a waste unit **76** while the target cells continue as part of the assay.

[0307] In the pathogen dialysis section **70** described here, the pathogens from the whole blood sample are concentrated for microbial DNA analysis. The array of apertures is formed by a multitude of 3 micron diameter holes **164** fluidically connecting the input flow in the cap channel **94** to a target channel **74**. The 3 micron diameter apertures **164** and the dialysis uptake holes **168** for the target channel **74** are connected by a series of dialysis MST channels **204** (best shown in FIGS. **15** and **21**). Pathogens are small enough to pass through the 3 micron diameter apertures **164** and fill the target channel **74** via the dialysis MST channels **204**. Cells larger than 3 microns, such as erythrocytes and leukocytes, stay in the waste channel **72** in the cap **46** which leads to a waste reservoir **76** (see FIG. **7**).

[0308] Other aperture shapes, sizes and aspect ratios can be used to isolate specific pathogens or other target cells such as leukocytes for human DNA analysis. Greater detail on the dialysis section and dialysis variants is provided later.

[0309] Referring again to FIGS. **6** and **7**, the flow is drawn through the target channel **74** to the surface tension valve **128** of the lysis reagent reservoir **56**. The surface tension valve **128** has seven MST channels **90** extending between the lysis reagent reservoir **56** and the target channel **74**. When the menisci are unpinned by the sample flow, the flow rate from all seven of the MST channels **90** will be greater than the flow rate from the anticoagulant reservoir **54** where the surface tension valve **118** has three MST channels **90** (assuming the physical characteristics of the fluids are roughly equivalent). Hence the proportion of lysis reagent in the sample mixture is greater than that of the anticoagulant.

[0310] The lysis reagent and target cells mix by diffusion in the target channel **74** within the chemical lysis section **130**. A boiling-initiated valve **126** stops the flow until sufficient time has passed for diffusion and lysis to take place, releasing the genetic material from the target cells (see FIGS. **6** and **7**). The structure and operation of the boiling-initiated valves are described in greater detail below with reference to FIGS. **31** and **32**. Other active valve types (as opposed to passive valves such as the surface tension valve **118**) have also been developed by the Applicant which may be used here instead of the boiling-initiated valve. These alternative valve designs are also described later.

[0311] When the boiling-initiated valve **126** opens, the lysed cells flow into a mixing section **131** for pre-amplification restriction digestion and linker ligation.

[0312] Referring to FIG. **13**, restriction enzymes, linkers and ligase are released from the reservoir **58** when the flow unpins the menisci at the surface tension valve **132** at the start of the mixing section **131**. The mixture flows the length of the mixing section **131** for diffusion mixing. At the end of the mixing section **131** is downtake **134** leading into the incubator inlet channel **133** of the incubation section **114** (see FIG. **13**). The incubator inlet channel **133** feeds the mixture into a serpentine configuration of heated microchannels **210** which provides an incubation chamber for holding the sample during restriction digestion and ligation of the linkers (see FIGS. **13** and **14**).

[0313] FIGS. **23**, **24**, **25**, **26**, **27**, **28** and **29** show the layers of the LOC device **301** within Inset AB of FIG. **6**. Each figure shows the sequential addition of layers forming the structures of the CMOS+MST layer **48** and the cap **46**. Inset AB shows the end of the incubation section **114** and the start of the amplification section **112**. As best shown in FIGS. **14** and **23**, the flow fills the microchannels **210** of the incubation section **114** until reaching the boiling-initiated valve **106** where the flow stops while diffusion takes place. As discussed above, the microchannel **210** upstream of the boiling-initiated valve **106** becomes an incubation chamber containing the sample, restriction enzymes, ligase and linkers. The heaters **154** are then activated and held at constant temperature for a specified time for restriction digestion and linker ligation to occur.

[0314] The skilled worker will appreciate that this incubation step **291** (see FIG. **4**) is optional and only required for

some nucleic acid amplification assay types. Furthermore, in some instances, it may be necessary to have a heating step at the end of the incubation period to spike the temperature above the incubation temperature. The temperature spike inactivates the restriction enzymes and ligase prior to entering the amplification section **112**. Inactivation of the restriction enzymes and ligase has particular relevance when isothermal nucleic acid amplification is being employed.

[0315] Following incubation, the boiling-initiated valve **106** is activated (opened) and the flow resumes into the amplification section **112**. Referring to FIGS. **31** and **32**, the mixture fills the serpentine configuration of heated microchannels **158**, which form one or more amplification chambers, until it reaches the boiling-initiated valve **108**. As best shown in the schematic section view of FIG. **30**, amplification mix (dNTPs, primers, buffer) is released from reservoir **60** and polymerase is subsequently released from reservoir **62** into the intermediate MST channel **212** connecting the incubation and amplification sections (**114** and **112** respectively).

[0316] FIGS. **35** to **51** show the layers of the LOC device **301** within Inset AC of FIG. **6**. Each figure shows the sequential addition of layers forming the structures of the CMOS+ MST device **48** and the cap **46**. Inset AC is at the end of the amplification section **112** and the start of the hybridization and detection section **52**. The incubated sample, amplification mix and polymerase flow through the microchannels **158** to the boiling-initiated valve **108**. After sufficient time for diffusion mixing, the heaters **154** in the microchannels **158** are activated for thermal cycling or isothermal amplification. The amplification mix goes through a predetermined number of thermal cycles or a preset amplification time to amplify sufficient target DNA. After the nucleic acid amplification process, the boiling-initiated valve **108** opens and flow resumes into the hybridization and detection section **52**. The operation of boiling-initiated valves is described in more detail later.

[0317] As shown in FIG. **52**, the hybridization and detection section **52** has an array of hybridization chambers **110**. FIGS. **52**, **53**, **54** and **56** show the hybridization chamber array **110** and individual hybridization chambers **180** in detail. At the entrance to the hybridization chamber **180** is a diffusion barrier **175** which prevents diffusion of the target nucleic acid, probe strands and hybridized probes between the hybridization chambers **180** during hybridization so as to prevent erroneous hybridization detection results. The diffusion barriers **175** present a flow-path-length that is long enough to prevent the target sequences and probes diffusing out of one chamber and contaminating another chamber within the time taken for the probes and nucleic acids to hybridize and the signal to be detected, thus avoiding an erroneous result.

[0318] Another mechanism to prevent erroneous readings is to have identical probes in a number of the hybridization chambers. The CMOS circuitry **86** derives a single result from the photodiodes **184** corresponding to the hybridization chambers **180** that contain identical probes. Anomalous results can be disregarded or weighted differently in the derivation of the single result.

[0319] The thermal energy required for hybridization is provided by CMOS-controlled heaters **182** (described in more detail below). After the heater is activated, hybridization occurs between complementary target-probe sequences. The LED driver **29** in the CMOS circuitry **86** signals the LED **26** located in the test module **10** to illuminate. These probes only fluoresce when hybridization has occurred thereby avoiding washing and drying steps that are typically required to remove unbound strands. Hybridization forces the stem-and-loop structure of the FRET probes **186** to open, which allows the fluorophore to emit fluorescent energy in response to the LED excitation light, as discussed in greater detail later. Fluorescence is detected by a photodiode **184** in the CMOS circuitry **86** underlying each hybridization chamber **180** (see hybridization chamber description below). The photodiodes **184** for all hybridization chambers and associated electronics collectively form the photosensor **44** (see FIG. **60**). In other embodiments, the photosensor may be an array of charge coupled devices (CCD array). The detected signal from the photodiodes **184** is amplified and converted to a digital output which is analyzed by the test module reader **12**. Further details of the detection method are described later.

Additional Details for the LOC Device

Modularity of the Design

[0320] The LOC device **301** has many functional sections, including the reagent reservoirs **54**, **56**, **58**, **60** and **62**, the dialysis section **70**, lysis section **130**, incubation section **114**, and amplification section **112**, valve types, the humidifier and humidity sensor. In other embodiments of the LOC device, these functional sections can be omitted, additional functional sections can be added or the functional sections can be used for alternative purposes to those described above.

[0321] For example, the incubation section **114** can be used as the first amplification section **112** of a tandem amplification assay system, with the chemical lysis reagent reservoir **56** being used to add the first amplification mix of primers, dNTPs and buffer and reagent reservoir **58** being used for adding the reverse transcriptase and/or polymerase. A chemical lysis reagent can also be added to the reservoir **56** along with the amplification mix if chemical lysis of the sample is desired or, alternatively, thermal lysis can occur in the incubation section by heating the sample for a predetermined time. In some embodiments, an additional reservoir can be incorporated immediately upstream of reservoir **58** for the mix of primers, dNTPs and buffer if there is a requirement for chemical lysis and a separation of this mix from the chemical lysis reagent is desired.

[0322] In some circumstances it may be desirable to omit a step, such as the incubation step **291**. In this case, a LOC device can be specifically fabricated to omit the reagent reservoir **58** and incubation section **114**, or the reservoir can simply not be loaded with reagents or the active valves, if present, not activated to dispense the reagents into the sample flow, and the incubation section then simply becomes a channel to transport the sample from the lysis section **130** to the amplification section **112**. The heaters are independently operable and therefore, where reactions are dependent on heat, such as thermal lysis, programming the heaters not to activate during this step ensures thermal lysis does not occur in LOC devices that do not require it. The dialysis section **70** can be located at the beginning of the fluidic system within the microfluidic device as shown in FIG. **4** or can be located anywhere else within the microfluidic device. For example, dialysis after the amplification phase **292** to remove cellular debris prior to the hybridization and detection step **294** may be beneficial in some circumstances. Alternatively, two or more dialysis sections can be incorporated at any location throughout the LOC device. Similarly, it is possible to incor-

porate additional amplification sections **112** to enable multiple targets to be amplified in parallel or in series prior to being detected in the hybridization chamber arrays **110** with specific nucleic acid probes. For analysis of samples like whole blood, in which dialysis is not required, the dialysis section **70** is simply omitted from the sample input and preparation section **288** of the LOC design. In some cases, it is not necessary to omit the dialysis section **70** from the LOC device even if the analysis does not require dialysis. If there is no geometric hindrance to the assay by the existence of a dialysis section, a LOC with the dialysis section **70** in the sample input and preparation section can still be used without a loss of the required functionality.

[0323] Furthermore, the detection section **294** may encompass proteomic chamber arrays which are identical to the hybridization chamber arrays but are loaded with probes designed to conjugate or hybridize with sample target proteins present in non-amplified sample instead of nucleic acid probes designed to hybridize to target nucleic acid sequences.

[0324] It will be appreciated that the LOC devices fabricated for use in this diagnostic system are different combinations of functional sections selected in accordance with the particular LOC application. The vast majority of functional sections are common to many of the LOC devices and the design of additional LOC devices for new application is a matter of compiling an appropriate combination of functional sections from the extensive selection of functional sections used in the existing LOC devices.

[0325] Only a small number of the LOC devices are shown in this description and some more are shown schematically to illustrate the design flexibility of the LOC devices fabricated for this system. The person skilled in the art will readily recognise that the LOC devices shown in this description are not an exhaustive list and many additional LOC designs are a matter of compiling the appropriate combination of functional sections.

Sample Types

[0326] LOC variants can accept and analyze the nucleic acid or protein content of a variety of sample types in liquid form including, but not limited to, blood and blood products, saliva, cerebrospinal fluid, urine, semen, amniotic fluid, umbilical cord blood, breast milk, sweat, pleural effusion, tear, pericardial fluid, peritoneal fluid, environmental water samples and drink samples. Amplicon obtained from macroscopic nucleic acid amplification can also be analysed using the LOC device; in this case, all the reagent reservoirs will be empty or configured not to release their contents, and the dialysis, lysis, incubation and amplification sections will be used solely to transport the sample from the sample inlet **68** to the hybridization chambers **180** for nucleic acid detection, as described above.

[0327] For some sample types, a pre-processing step is required, for example semen may need to be liquefied and mucus may need to be pre-treated with an enzyme to reduce the viscosity prior to input into the LOC device.

Sample Input

[0328] Referring to FIGS. **1** and **12**, the sample is added to the macroreceptacle **24** of the test module **10**. The macroreceptacle **24** is a truncated cone which feeds into the inlet **68** of the LOC device **301** by capillary action. Here it flows into the 64 μm wide×60 μm deep cap channel **94** where it is drawn towards the anticoagulant reservoir **54**, also by capillary action.

Reagent Reservoirs

[0329] The small volumes of reagents required by the assay systems using microfluidic devices, such as LOC device **301**, permit the reagent reservoirs to contain all reagents necessary for the biochemical processing with each of the reagent reservoirs having a small volume. This volume is easily less than 1,000,000,000 cubic microns, in the vast majority of cases less than 300,000,000 cubic microns, typically less than 70,000,000 cubic microns and in the case of the LOC device **301** shown in the drawings, less than 20,000,000 cubic microns.

Dialysis Section

[0330] Referring to FIGS. **15** to **21**, **33** and **34**, the pathogen dialysis section **70** is designed to concentrate pathogenic target cells from the sample. As previously described, a plurality of apertures in the form of 3 micron diameter holes **164** in the roof layer **66** filter the target cells from the bulk of the sample. As the sample flows past the 3 micron diameter apertures **164**, microbial pathogens pass through the holes into a series of dialysis MST channels **204** and flow back up into the target channel **74** via 16 μm dialysis uptake holes **168** (see FIGS. **33** and **34**). The remainder of the sample (erythrocytes and so on) stay in the cap channel **94**. Downstream of the pathogen dialysis section **70**, the cap channel **94** becomes the waste channel **72** leading to the waste reservoir **76**. For biological samples of the type that generate a substantial amount of waste, a foam insert or other porous element **49** within the outer casing **13** of the test module **10** is configured to be in fluid communication with the waste reservoir **76** (see FIG. **1**).

[0331] The pathogen dialysis section **70** functions entirely on capillary action of the fluid sample. The 3 micron diameter apertures **164** at the upstream end of the pathogen dialysis section **70** have capillary initiation features (CIFs) **166** (see FIG. **33**) so that the fluid is drawn down into the dialysis MST channel **204** beneath. The first uptake hole **198** for the target channel **74** also has a CIF **202** (see FIG. **15**) to avoid the flow simply pinning a meniscus across the dialysis uptake holes **168**.

[0332] The small constituents dialysis section **682** schematically shown in FIG. **71** can have a similar structure to the pathogen dialysis section **70**. The small constituents dialysis section separates any small target cells or molecules from a sample by sizing (and, if necessary, shaping) apertures suitable for allowing the small target cells or molecules to pass into the target channel and continue for further analysis. Larger sized cells or molecules are removed to a waste reservoir **766**. Thus, the LOC device **30** (see FIGS. **1** and **104**) is not limited to separating pathogens that are less than 3 μm in size, but can be used to separate cells or molecules of any size desired.

Lysis Section

[0333] Referring back to FIGS. **7**, **11** and **13**, the genetic material in the sample is released from the cells by a chemical lysis process. As described above, a lysis reagent from the lysis reservoir **56** mixes with the sample flow in the target channel **74** downstream of the surface tension valve **128** for

the lysis reservoir **56**. However, some diagnostic assays are better suited to a thermal lysis process, or even a combination of chemical and thermal lysis of the target cells. The LOC device **301** accommodates this with the heated microchannels **210** of the incubation section **114**. The sample flow fills the incubation section **114** and stops at the boiling-initiated valve **106**. The incubation microchannels **210** heat the sample to a temperature at which the cellular membranes are disrupted.

[0334] In some thermal lysis applications, an enzymatic reaction in the chemical lysis section **130** is not necessary and the thermal lysis completely replaces the enzymatic reaction in the chemical lysis section **130**.

Boiling-Initiated Valve

[0335] As discussed above, the LOC device **301** has three boiling-initiated valves **126**, **106** and **108**. The location of these valves is shown in FIG. **6**. FIG. **31** is an enlarged plan view of the boiling-initiated valve **108** in isolation at the end of the heated microchannels **158** of the amplification section **112**.

[0336] The sample flow **119** is drawn along the heated microchannels **158** by capillary action until it reaches the boiling-initiated valve **108**. The leading meniscus **120** of the sample flow pins at a meniscus anchor **98** at the valve inlet **146**. The geometry of the meniscus anchor **98** stops the advancing meniscus to arrest the capillary flow. As shown in FIGS. **31** and **32**, the meniscus anchor **98** is an aperture provided by an uptake opening from the MST channel **90** to the cap channel **94**. Surface tension in the meniscus **120** keeps the valve closed. An annular heater **152** is at the periphery of the valve inlet **146**. The annular heater **152** is CMOS-controlled via the boiling-initiated valve heater contacts **153**.

[0337] To open the valve, the CMOS circuitry **86** sends an electrical pulse to the valve heater contacts **153**. The annular heater **152** resistively heats until the liquid sample **119** boils. The boiling unpins the meniscus **120** from the valve inlet **146** and initiates wetting of the cap channel **94**. Once wetting the cap channel **94** begins, capillary flow resumes. The fluid sample **119** fills the cap channel **94** and flows through the valve downtake **150** to the valve outlet **148** where capillary driven flow continues along the amplification section exit channel **160** into the hybridization and detection section **52**. Liquid sensors **174** are placed before and after the valve for diagnostics.

[0338] It will be appreciated that once the boiling-initiated valves are opened, they cannot be re-closed. However, as the LOC device **301** and the test module **10** are single-use devices, re-closing the valves is unnecessary.

Incubation Section and Nucleic Acid Amplification Section

[0339] FIGS. **6**, **7**, **13**, **14**, **23**, **24**, **25**, **35** to **45**, **50** and **51** show the incubation section **114** and the amplification section **112**. The incubation section **114** has a single, heated incubation microchannel **210** etched in a serpentine pattern in the MST channel layer **100** from the downtake opening **134** to the boiling-initiated valve **106** (see FIGS. **13** and **14**). Control over the temperature of the incubation section **114** enables enzymatic reactions to take place with greater efficiency. Similarly, the amplification section **112** has a heated amplification microchannel **158** in a serpentine configuration leading from the boiling-initiated valve **106** to the boiling-initiated valve **108** (see FIGS. **6** and **14**). These valves arrest the flow to retain the target cells in the heated incubation or amplification microchannels **210** or **158** while mixing, incubation and nucleic acid amplification takes place. The serpentine pattern of the microchannels also facilitates (to some extent) mixing of the target cells with reagents.

[0340] In the incubation section **114** and the amplification section **112**, the sample cells and the reagents are heated by the heaters **154** controlled by the CMOS circuitry **86** using pulse width modulation (PWM). Each meander of the serpentine configuration of the heated incubation microchannel **210** and amplification microchannel **158** has three separately operable heaters **154** extending between their respective heater contacts **156** (see FIG. **14**) which provides for the two-dimensional control of input heat flux density. As best shown in FIG. **51**, the heaters **154** are supported on the roof layer **66** and embedded in the lower seal **64**. The heater material is TiAl but many other conductive metals would be suitable. The elongate heaters **154** are parallel with the longitudinal extent of each channel section that forms the wide meanders of the serpentine shape. In the amplification section **112**, each of the wide meanders can operate as separate PCR chambers via individual heater control.

[0341] The small volumes of amplicon required by the assay systems using microfluidic devices, such as LOC device **301**, permit low amplification mixture volumes for amplification in amplification section **112**. This volume is easily less than 400 nanoliters, in the vast majority of cases less than 170 nanoliters, typically less than 70 nanoliters and in the case of the LOC device **301**, between 2 nanoliters and 30 nanoliters.

Increased Rates of Heating and Greater Diffusive Mixing

[0342] The small cross section of each channel section increases the heating rate of the amplification fluid mix. All the fluid is kept a relatively short distance from the heater **154**. Reducing the channel cross section (that is the amplification microchannel **158** cross section) to less than 100,000 square microns achieves appreciably higher heating rates than that provided by more 'macro-scale' equipment. Lithographic fabrication techniques allow the amplification microchannel **158** to have a cross sectional area transverse to the flow-path less than 16,000 square microns which gives substantially higher heating rates. Feature sizes on the order of 1 micron are readily achievable with lithographic techniques. If very little amplicon is needed (as is the case in the LOC device **301**), the cross sectional area can be reduced to less than 2,500 square microns. For diagnostic assays with 1,000 to 2,000 probes on the LOC device, and a requirement of 'sample-in, answer out' in less than 1 minute, a cross sectional area transverse to the flow of between 400 square microns and 1 square micron is adequate.

[0343] The heater element in the amplification microchannel **158** heats the nucleic acid sequences at a rate more than 80 Kelvin (K) per second, in the vast majority of cases at a rate greater than 100 K per second. Typically, the heater element heats the nucleic acid sequences at a rate more than 1,000 K per second and in many cases, the heater element heats the nucleic acid sequences at a rate more than 10,000 K per second. Commonly, based on the demands of the assay system, the heater element heats the nucleic acid sequences at a rate more than 100,000 K per second, more than 1,000,000 K per second more than 10,000,000 K per second, more than 20,000,000 K per second, more than 40,000,000 K per second, more than 80,000,000 K per second and more than 160,000,000 K per second.

[0344] A small cross-sectional area channel is also beneficial for diffusive mixing of any reagents with the sample fluid. Before diffusive mixing is complete, diffusion of one liquid into the other is greatest near the interface between the two. Concentration decreases with distance from the interface. Using microchannels with relatively small cross sections transverse to the flow direction, keeps both fluid flows close to the interface for more rapid diffusive mixing. Reducing the channel cross section to less than 100,000 square microns achieves appreciably higher mixing rates than that provided by more 'macro-scale' equipment. Lithographic fabrication techniques allows microchannels with a cross sectional area transverse to the flow-path less than 16000 square microns which gives significantly higher mixing rates. If small volumes are needed (as is the case in the LOC device **301**), the cross sectional area can be reduced to less than 2500 square microns. For diagnostic assays with 1000 to 2000 probes on the LOC device, and a requirement of 'sample-in, answer out' in less than 1 minute, a cross sectional area transverse to the flow of between 400 square microns and 1 square micron is adequate.

Short Thermal Cycle Times

[0345] Keeping the sample mixture proximate to the heaters, and using very small fluid volumes allows rapid thermal cycling during the nucleic acid amplification process. Each thermal cycle (i.e. denaturing, annealing and primer extension) is completed in less than 30 seconds for target sequences up to 150 base pairs (bp) long. In the vast majority of diagnostic assays, the individual thermal cycle times are less than 11 seconds, and a large proportion are less than 4 seconds. LOC devices **30** with some of the most common diagnostic assays have thermal cycles time between 0.45 seconds to 1.5 seconds for target sequences up to 150 by long. Thermal cycling at this rate allows the test module to complete the nucleic acid amplification process in much less than 10 minutes; often less than 220 seconds. For most assays, the amplification section generates sufficient amplicon in less than 80 seconds from the sample fluid entering the sample inlet. For a great many assays, sufficient amplicon is generated in 30 seconds. Upon completion of a preset number of amplification cycles, the amplicon is fed into the hybridization and detection section **52** via the boiling-initiated valve **108**.

Hybridization Chambers

[0346] FIGS. **52**, **53**, **54**, **56** and **57** show the hybridization chambers **180** in the hybridization chamber array **110**. The hybridization and detection section **52** has a 24×45 array **110** of hybridization chambers **180**, each with hybridization-responsive FRET probes **186**, heater element **182** and an integrated photodiode **184**. The photodiode **184** is incorporated for detection of fluorescence resulting from the hybridization of a target nucleic acid sequence or protein with the FRET probes **186**. Each photodiode **184** is independently controlled by the CMOS circuitry **86**. Any material between the FRET probes **186** and the photodiode **184** must be transparent to the emitted light. Accordingly, the wall section **97** between the probes **186** and the photodiode **184** is also optically transparent to the emitted light. In the LOC device **301**, the wall section **97** is a thin (approximately 0.5 micron) layer of silicon dioxide.

[0347] Incorporation of a photodiode **184** directly beneath each hybridization chamber **180** allows the volume of probe-target hybrids to be very small while still generating a detectable fluorescence signal (see FIG. **54**). The small amounts permit small volume hybridization chambers. A detectable amount of probe-target hybrid requires a quantity of probe, prior to hybridization, which is easily less than 270 picograms (corresponding to 900,000 cubic microns), in the vast majority of cases less than 60 picograms (corresponding to 200,000 cubic microns), typically less than 12 picograms (corresponding to 40,000 cubic microns) and in the case of the LOC device **301** shown in the accompanying figures, less than 2.7 picograms (corresponding to a chamber volume of 9,000 cubic microns). Of course, reducing the size of the hybridization chambers allows a higher density of chambers and therefore more probes on the LOC device. In LOC device **301**, the hybridization section has more than 1,000 chambers in an area of 1,500 microns by 1,500 microns (i.e. less than 2,250 square microns per chamber). Smaller volumes also reduce the reaction times so that hybridization and detection is faster. An additional advantage of the small amount of probe required in each chamber is that only very small quantities of probe solution need to be spotted into each chamber during production of the LOC device. Embodiments of the LOC device according to the invention can be spotted using a probe solution volume of 1 picoliter or less.

[0348] After nucleic acid amplification, boiling-initiated valve **108** is activated and the amplicon flows along the flow-path **176** and into each of the hybridization chambers **180** (see FIGS. **52** and **56**). An end-point liquid sensor **178** indicates when the hybridization chambers **180** are filled with amplicon and the heaters **182** can be activated.

[0349] After sufficient hybridization time, the LED **26** (see FIG. **2**) is activated. The opening in each of the hybridization chambers **180** provides an optical window **136** for exposing the FRET probes **186** to the excitation radiation (see FIGS. **52**, **54** and **56**). The LED **26** is illuminated for a sufficiently long time in order to induce a fluorescence signal from the probes with high intensity. During excitation, the photodiode **184** is shorted. After a pre-programmed delay **300** (see FIG. **2**), the photodiode **184** is enabled and fluorescence emission is detected in the absence of the excitation light. The incident light on the active area **185** of the photodiode **184** (see FIG. **54**) is converted into a photocurrent which can then be measured using CMOS circuitry **86**.

[0350] The hybridization chambers **180** are each loaded with probes for detecting a single target nucleic acid sequence. Each hybridization chambers **180** can be loaded with probes to detect over 1,000 different targets if desired. Alternatively, many or all the hybridization chambers can be loaded with the same probes to detect the same target nucleic acid repeatedly. Replicating the probes in this way throughout the hybridization chamber array **110** leads to increased confidence in the results obtained and the results can be combined by the photodiodes adjacent those hybridization chambers to provide a single result if desired. The person skilled in the art will recognise that it is possible to have from one to over 1,000 different probes on the hybridization chamber array **110**, depending on the assay specification.

Hybridization Chambers with Electrochemiluminescence Detection

[0351] FIGS. **97**, **120**, **138** and **139** show the hybridization chambers **180** used in an ECL variant of the LOC device, LOC variant L **729**. In this embodiment of the LOC device, a 24×45 array **110** of hybridization chambers **180**, each with hybridization-responsive ECL probes **237**, is positioned in

registration with a corresponding array of photodiodes **184** integrated into the CMOS. In a similar fashion to the LOC devices configured for fluorescence detection, each photodiode **184** is incorporated for detection of ECL resulting from the hybridization of a target nucleic acid sequence or protein with an ECL probe **237**. Each photodiode **184** is independently controlled by the CMOS circuitry **86**. Again, the transparent wall section **97** between the probes **186** and the photodiode **184** is transparent to the emitted light.

[0352] A photodiode **184** closely adjacent each hybridization chamber **180** allows the amount of probe-target hybrids to be very small while still generating a detectable ECL signal (see FIG. **97**). The small amounts permit small volume hybridization chambers. A detectable amount of probe-target hybrid requires a quantity of probe, prior to hybridization, which is easily less than 270 picograms (corresponding to a chamber volume of 900,000 cubic microns), in the vast majority of cases less than 60 picograms (corresponding to 200,000 cubic microns), typically less than 12 picograms (corresponding to 40,000 cubic microns) and in the case of the LOC device shown in the drawings less than 2.7 picograms (corresponding to a chamber volume of 9,000 cubic microns). Of course, reducing the size of the hybridization chambers allows a higher density of chambers and therefore more probes on the LOC device. In the LOC device shown, the hybridization section has more than 1,000 chambers in an area of 1,500 microns by 1,500 microns (i.e. less than 2,250 square microns per chamber). Smaller volumes also reduce the reaction times so that hybridization and detection is faster. An additional advantage of the small amount of probe required in each chamber is that only very small quantities of probe solution need be spotted into each chamber during production of the LOC device. In the case of the LOC device shown in the drawings, the required amount of probe can be spotted using a solution volume of 1 picoliter or less.

[0353] After nucleic acid amplification, the boiling-initiated valve **108** is activated and the amplicon flows along the flow-path **176** and into each of the hybridization chambers **180** (see FIGS. **52** and **139**). An end-point liquid sensor **178** indicates when the hybridization chambers **180** are filled with amplicon so that the heaters **182** can be activated.

[0354] After sufficient hybridization time, the photodiode **184** is enabled ready for collection of the ECL signal. Then the ECL excitation drivers **39** (see FIG. **105**) activate the ECL electrodes **860** and **870** for a predetermined length of time. The photodiode **184** remains active for a short time after cessation of the ECL excitation current to maximize the signal-to-noise ratio. For example, if the photodiode **184** remains active for five times the decay lifetime of the luminescent emission, then the signal will have decayed to less than one percent of the initial value. The incident light on the photodiode **184** is converted into a photocurrent which can then be measured using CMOS circuitry **86**.

Proteomic Assay Chambers

[0355] Some LOC variants, such as LOC variant L **729**, are configured to perform homogeneous protein assays on crude cell lysates within proteomic assay chamber arrays (see for example **124.1** to **124.3** of FIGS. **116** and **120**) for the detection of host cell and/or pathogenic proteins. The proteomic assay chamber arrays **124.1**-**124.3** are manufactured and configured in exactly the same manner as the hybridization chamber arrays **110** (see FIGS. **52**, **53**, **54** and **56**). Each proteomic assay chamber has a diffusion barrier **175** at the entrance to prevent diffusion of sample and reagents between chambers, thus avoiding an erroneous result (see FIGS. **84** and **85**, which are insets DC and DD of FIG. **81**). Where required for protein hybridization or conjugation, thermal energy is provided by CMOS-controlled heaters **182** in each chamber. In some embodiments, an end-point liquid sensor **178** is used to indicate when the proteomic assay chambers are filled with sample so that the heaters **182** can be activated. After sufficient time has elapsed, the fluorescent or electrochemiluminescent signal generated following protein recognition is detected by the photosensor **44**.

Humidifier and Humidity Sensor

[0356] Inset AG of FIG. **6** indicates the position of the humidifier **196**. The humidifier prevents evaporation of the reagents and probes during operation of the LOC device **301**. As best shown in the enlarged view of FIG. **55**, a water reservoir **188** is fluidically connected to three evaporators **190**. The water reservoir **188** is filled with molecular biology-grade water and sealed during manufacturing. As best shown in FIGS. **55** and **61**, water is drawn into three downtakes **194** and along respective water supply channels **192** by capillary action to a set of three uptakes **193** at the evaporators **190**. A meniscus pins at each uptake **193** to retain the water. The evaporators have annular shaped heaters **191** which encircle the uptakes **193**. The annular heaters **191** are connected to the CMOS circuitry **86** by the conductive columns **376** to the top metal layer **195** (see FIG. **37**). Upon activation, the annular heaters **191** heat the water causing evaporation and humidifying the device surrounds.

[0357] The position of the humidity sensor **232** is also shown in FIG. **6**. However, as best shown in the enlarged view of Inset AH in FIG. **58**, the humidity sensor has a capacitive comb structure. A lithographically etched first electrode **296** and a lithographically etched second electrode **298** face each other such that their teeth are interleaved. The opposed electrodes form a capacitor with a capacitance that can be monitored by the CMOS circuitry **86**. As the humidity increases, the permittivity of the air gap between the electrodes increases, so that the capacitance also increases. The humidity sensor **232** is adjacent the hybridization chamber array **110** where humidity measurement is most important to slow evaporation from the solution containing the exposed probes.

Feedback Sensors

[0358] Temperature and liquid sensors are incorporated throughout the LOC device **301** to provide feedback and diagnostics during device operation. Referring to FIG. **35**, nine temperature sensors **170** are distributed throughout the amplification section **112** Likewise, the incubation section **114** also has nine temperature sensors **170**. These sensors each use a 2×2 array of bipolar junction transistors (BJTs) to monitor the fluid temperature and provide feedback to the CMOS circuitry **86**. The CMOS circuitry **86** uses this to precisely control the thermal cycling during the nucleic acid amplification process and any heating during thermal lysis and incubation.

[0359] In the hybridization chambers **180**, the CMOS circuitry **86** uses the hybridization heaters **182** as temperature sensors (see FIG. **56**). The electrical resistance of the hybridization heaters **182** is temperature dependent and the CMOS circuitry **86** uses this to derive a temperature reading for each of the hybridization chambers **180**.

[0360] The LOC device **301** also has a number of MST channel liquid sensors **174** and cap channel liquid sensors **208**. FIG. **35** shows a line of MST channel liquid sensors **174** at one end of every other meander in the heated microchannel **158**. As best shown in FIG. **37**, the MST channel liquid sensors **174** are a pair of electrodes formed by exposed areas of the top metal layer **195** in the CMOS structure **86**. Liquid closes the circuit between the electrodes to indicate its presence at the sensor's location.

[0361] FIG. **25** shows an enlarged perspective of cap channel liquid sensors **208**. Opposing pairs of TiAl electrodes **218** and **220** are deposited on the roof layer **66**. Between the electrodes **218** and **220** is a gap **222** to hold the circuit open in the absence of liquid. The presence of liquid closes the circuit and the CMOS circuitry **86** uses this feedback to monitor the flow.

Gravitational Independence

[0362] The test modules **10** are orientation independent. They do not need to be secured to a flat stable surface in order to operate. Capillary driven fluid flows and a lack of external plumbing into ancillary equipment allow the modules to be truly portable and simply plugged into a similarly portable hand held reader such as a mobile telephone. Having a gravitationally independent operation means the test modules are also accelerationally independent to all practical extents. They are resistant to shock and vibration and will operate on moving vehicles or while the mobile telephone is being carried around.

Dialysis Variants

Leukocyte Target

[0363] The dialysis design described above in the LOC device **301** targets pathogens. FIG. **59** is a schematic section view of a dialysis section **328** designed to concentrate leukocytes from a blood sample for human DNA analysis. It will be appreciated that the structure is essentially the same as that of the pathogen target dialysis section **70** described above with the exception that apertures in the form of 7.5 micron diameter holes **165** restrict leukocytes from passing from the cap channel **94** to the dialysis MST channels **204**. In situations where the sample being analysed is a blood sample, and the presence of haemoglobin from the erythrocytes interferes with the subsequent reaction steps, addition of an erythrocyte lysis buffer along with the anticoagulant in the reservoir **54** (see FIG. **22**), will ensure that the majority of the lysed erythrocytes (and hence haemoglobin) will be removed from the sample during this dialysis step. A commonly used erythrocyte lysis buffer is 0.15M NH_4CL, 10 mM $KHCO_3$, 0.1 mM EDTA, pH 7.2-7.4, but a person skilled in the art will recognise that any buffer which efficiently lyses erythrocytes can be used.

[0364] Downstream of the leukocyte dialysis section **328**, the cap channel **94** becomes the target channel **74** such that the leukocytes continue as part of the assay. Furthermore, in this case, the dialysis uptake holes **168** lead to a waste channel **72** so that all smaller cells and components in the sample are removed. It should be noted that this dialysis variant only reduces the concentration of the unwanted specimens in the target channel **74**.

[0365] FIG. **72** schematically illustrates a large constituents dialysis section **686** which also separates any large target constituents from a sample. The apertures in this dialysis section are fabricated with a size and shape tailored to withhold the large target constituents of interest in the target channel for further analysis. As with the leukocyte dialysis section described above, most (but not all) smaller sized cells, organisms or molecules flow to a waste reservoir **768**. Thus, other embodiments of the LOC device are not limited to separating leukocytes that are larger than 7.5 μm in size, but can be used to separate cells, organisms or molecules of any size desired.

Dialysis Section with Flow Channel to Prevent Trapped Air Bubbles

[0366] Described below is an embodiment of the LOC device referred to as LOC variant VIII **518** and shown in FIGS. **65**, **66**, **67** and **68**. This LOC device has a dialysis section that fills with the fluid sample without leaving air bubbles trapped in the channels. LOC variant VIII **518** also has an additional layer of material referred to as an interface layer **594**. The interface layer **594** is positioned between the cap channel layer **80** and the MST channel layer **100** of the CMOS+MST device **48**. The interface layer **594** allows a more complex fluidic interconnection between the reagent reservoirs and the MST layer **87** without increasing the size of the silicon substrate **84**.

[0367] Referring to FIG. **66**, the bypass channel **600** is designed to introduce a time delay in the fluid sample flow from the interface waste channel **604** to the interface target channel **602**. This time delay allows the fluid sample to flow through the dialysis MST channel **204** to the dialysis uptake **168** where it pins a meniscus. With a capillary initiation feature (CIF) **202** at the uptake from the bypass channel **600** to the interface target channel **602**, the sample fluid fills the interface target channel **602** from a point upstream of all the dialysis uptakes **168** from the dialysis MST channels **204**.

[0368] Without the bypass channel **600**, the interface target channel **602** still starts filling from the upstream end, but eventually the advancing meniscus reaches and passes over an uptake belonging to an MST channel that has not yet filled, leading into air entrapment at that point. Trapped air reduces the sample flow rate through the leukocyte dialysis section **328**.

Nucleic Acid Amplification Variants

Direct PCR

[0369] Traditionally, PCR requires extensive purification of the target DNA prior to preparation of the reaction mixture. However, with appropriate changes to the chemistry and sample concentration, it is possible to perform nucleic acid amplification with minimal DNA purification, or direct amplification. When the nucleic acid amplification process is PCR, this approach is called direct PCR. In LOC devices where nucleic acid amplification is performed at a controlled, constant temperature, the approach is direct isothermal amplification. Direct nucleic acid amplification techniques have considerable advantages for use in LOC devices, particularly relating to simplification of the required fluidic design. Adjustments to the amplification chemistry for direct PCR or direct isothermal amplification include increased buffer strength, the use of polymerases which have high activity and processivity, and additives which chelate with potential polymerase inhibitors. Dilution of inhibitors present in the sample is also important.

[0370] To take advantage of direct nucleic acid amplification techniques, the LOC device designs incorporate two

additional features. The first feature is reagent reservoirs (for example reservoir **58** in FIG. **8**) which are appropriately dimensioned to supply a sufficient quantity of amplification reaction mix, or diluent, so that the final concentrations of sample components which might interfere with amplification chemistry are low enough to permit successful nucleic acid amplification. The desired dilution of non-cellular sample components is in the range of 5× to 20×. Different LOC structures, for example the pathogen dialysis section **70** in FIG. **4**, are used when appropriate to ensure that the concentration of target nucleic acid sequences is maintained at a high enough level for amplification and detection. In this embodiment, further illustrated in FIG. **6**, a dialysis section which effectively concentrates pathogens small enough to be passed into the amplification section **292** is employed upstream of the sample extraction section **290**, and rejects larger cells to a waste receptacle **76**. In another embodiment, a dialysis section is used to selectively deplete proteins and salts in blood plasma while retaining cells of interest.

[0371] The second LOC structural feature which supports direct nucleic acid amplification is design of channel aspect ratios to adjust the mixing ratio between the sample and the amplification mix components. For example, to ensure dilution of inhibitors associated with the sample in the preferred 5×-20× range through a single mixing step, the length and cross-section of the sample and reagent channels are designed such that the sample channel, upstream of the location where mixing is initiated, constitutes a flow impedance 4×-19× higher than the flow impedance of the channels through which the reagent mixture flows. Control over flow impedances in microchannels is readily achieved through control over the design geometry. The flow impedance of a microchannel increases linearly with the channel length, for a constant cross-section. Importantly for mixing designs, flow impedance in microchannels depends more strongly on the smallest cross-sectional dimension. For example, the flow impedance of a microchannel with rectangular cross-section is inversely proportional to the cube of the smallest perpendicular dimension, when the aspect ratio is far from unity.

Reverse-Transcriptase PCR (RT-PCR)

[0372] Where the sample nucleic acid species being analysed or extracted is RNA, such as from RNA viruses or messenger RNA, it is first necessary to reverse transcribe the RNA into complementary DNA (cDNA) prior to PCR amplification. The reverse transcription reaction can be performed in the same chamber as the PCR (one-step RT-PCR) or it can be performed as a separate, initial reaction (two-step RT-PCR). In the LOC variants described herein, a one-step RT-PCR can be performed simply by adding the reverse transcriptase to reagent reservoir **62** along with the polymerase and programming the heaters **154** to cycle firstly for the reverse transcription step and then progress onto the nucleic acid amplification step. A two-step RT-PCR could also be easily achieved by utilizing the reagent reservoir **58** to store and dispense the buffers, primers, dNTPs and reverse transcriptase and the incubation section **114** for the reverse transcription step followed by amplification in the normal way in the amplification section **112**.

Isothermal Nucleic Acid Amplification

[0373] For some applications, isothermal nucleic acid amplification is the preferred method of nucleic acid amplification, thus avoiding the need to repetitively cycle the reaction components through various temperature cycles but instead maintaining the amplification section at a constant temperature, typically around 37° C. to 41° C. A number of isothermal nucleic acid amplification methods have been described, including Strand Displacement Amplification (SDA), Transcription Mediated Amplification (TMA), Nucleic Acid Sequence Based Amplification (NASBA), Recombinase Polymerase Amplification (RPA), Helicase-Dependent isothermal DNA Amplification (HDA), Rolling Circle Amplification (RCA), Ramification Amplification (RAM) and Loop-mediated Isothermal Amplification (LAMP), and any of these, or other isothermal amplification methods, can be employed in particular embodiments of the LOC device described herein.

[0374] In order to perform isothermal nucleic acid amplification, the reagent reservoirs **60** and **62** adjoining the amplification section will be loaded with the appropriate reagents for the specified isothermal method instead of PCR amplification mix and polymerase. For example, for SDA, reagent reservoir **60** contains amplification buffer, primers and dNTPs and reagent reservoir **62** contains an appropriate nickase enzyme and Exo-DNA polymerase. For RPA, reagent reservoir **60** contains the amplification buffer, primers, dNTPs and recombinase proteins, with reagent reservoir **62** containing a strand displacing DNA polymerase such as Bsu. Similarly, for HDA, reagent reservoir **60** contains amplification buffer, primers and dNTPs and reagent reservoir **62** contains an appropriate DNA polymerase and a helicase enzyme to unwind the double stranded DNA strand instead of using heat. The skilled person will appreciate that the necessary reagents can be split between the two reagent reservoirs in any manner appropriate for the nucleic acid amplification process.

[0375] For amplification of viral nucleic acids from RNA viruses such as HIV or hepatitis C virus, NASBA or TMA is appropriate as it is unnecessary to first transcribe the RNA to cDNA. In this example, reagent reservoir **60** is filled with amplification buffer, primers and dNTPs and reagent reservoir **62** is filled with RNA polymerase, reverse transcriptase and, optionally, RNase H.

[0376] For some forms of isothermal nucleic acid amplification it may be necessary to have an initial denaturation cycle to separate the double stranded DNA template, prior to maintaining the temperature for the isothermal nucleic acid amplification to proceed. This is readily achievable in all embodiments of the LOC device described herein, as the temperature of the mix in the amplification section **112** can be carefully controlled by the heaters **154** in the amplification microchannels **158** (see FIG. **14**).

[0377] Isothermal nucleic acid amplification is more tolerant of potential inhibitors in the sample and, as such, is generally suitable for use where direct nucleic acid amplification from the sample is desired. Therefore, isothermal nucleic acid amplification is sometimes useful in LOC variant XLIII **673**, LOC variant XLIV **674** and LOC variant XLVII **677**, amongst others, shown in FIGS. **73**, **74** and **75**, respectively. Direct isothermal amplification may also be combined with one or more pre-amplification dialysis steps **70**, **686** or **682** as shown in FIGS. **73** and **75** and/or a pre-hybridization dialysis step **682** as indicated in FIG. **74** to help partially concentrate the target cells in the sample before nucleic acid amplification or remove unwanted cellular debris prior to the sample entering the hybridization chamber array **110**, respectively. The per-

son skilled in the art will appreciate that any combination of pre-amplification dialysis and pre-hybridization dialysis can be used.

[0378] Isothermal nucleic acid amplification can also be performed in parallel amplification sections such as those schematically represented in FIGS. **64**, **69** and **70**, multiplexed and some methods of isothermal nucleic acid amplification, such as LAMP, are compatible with an initial reverse transcription step to amplify RNA.

Other Design Variants

Flow Rate Sensor

[0379] In addition to temperature and liquid sensors, the LOC device can also incorporate CMOS-controlled flow rate sensors **740**, as schematically illustrated in FIG. **94** and in LOC Variant X **728** (see FIGS. **76** to **92**). The sensors are used to determine the flow rate in two steps. In the first step, the temperature of the serpentine heater element **814** is determined by applying a low current and measuring the voltage to determine the resistance of the serpentine heater element **814**, and therefore the temperature of the element **814** using the known relationship between resistance and the temperature of the heater element. At this stage, minimal heat is being dissipated in the element **814** and the temperature of the liquid in the channel is equal to the calculated temperature of the element **814**. In the second step, a higher current is applied to the serpentine heater element **814** such that the temperature of the element **814** increases and some heat is lost to the flowing liquid. By again measuring the voltage across the element **814** while the higher current is being applied, the new resistance of the element **814** is determined and the increased temperature is again calculated by the CMOS circuitry **86**. Using the new temperature of the serpentine heater element **814** and the known temperature of sample liquid calculated in the first step, the flow speed of the liquid is determined. From the known channel cross sectional geometry and the flow speed, the flow rate of the liquid in the channel is calculated.

Protein Detection Variants

[0380] Some embodiments of the LOC device use a homogeneous protein detection assay to detect specific proteins within a crude cell lysate. Numerous homogeneous protein detection assays have been developed for use in these embodiments of the LOC device. Commonly, these assays utilize antibodies or aptamers to capture the target protein.

[0381] In one type of assay, an aptamer **141** which binds to a particular protein **142** is labelled with two different fluorophores or luminophores **143** and **144** which can function as a donor and an acceptor in a fluorescence resonance energy transfer (FRET) or electrochemiluminescence resonance energy transfer (ERET) reaction (see FIGS. **108**A and **108**B). Both donor **143** and acceptor **144** are linked to the same aptamer **141**, and the change in separation is caused by a change in conformation upon binding to the target protein **142**. For example, an aptamer **141** in the absence of the target forms a conformation where the donor and acceptor are in close proximity (see FIG. **108**A); upon binding to the target, the new conformation results in a larger separation between the donor and acceptor (see FIG. **108**B). When the acceptor is a quencher and the donor is a luminophore, the effect of binding to the target is an increase in light emission **250** or **862** (see FIG. **108**B).

[0382] A second type of assay uses two antibodies **145** or two aptamers **141** that must independently bind to different, non-overlapping epitopes or regions of the target protein **142** (see FIGS. **109**A, **109**B, **110**A and **110**B). These antibodies **145** or aptamers **141** are labelled with different fluorophores or luminophores **143** and **144** which can function as a donor and an acceptor in a fluorescence resonance energy transfer (FRET) or electrochemiluminescence resonance energy transfer (ERET) reaction. The fluorophores or luminophores **143** and **144** form part of a pair of short complementary oligonucleotides **147** attached to the antibodies or aptamers via long, flexible linkers **149** (see FIGS. **109**A and **110**A). Once the antibodies **145** or aptamers **141** bind to the target protein **142**, the complementary oligonucleotides **147** find each other and hybridize to one another (see FIGS. **109**B and **110**B). This brings the donors and acceptors **143** and **144** in close proximity to one another resulting in efficient FRET **250** or ERET **862** that is used as a signal for target protein detection.

[0383] To ensure there is no, or very little, background signal as a result of the oligonucleotides **147** attached to the two antibodies **145** or aptamers **141** hybridizing to one another in the absence of their binding to the protein **142**, it is necessary to carefully choose the length and sequence of the complementary oligonucleotides **147** so that the dissociation constant (k_d) for the duplex is relatively high (~5 μM). Thus when free antibodies or aptamers labelled with these oligonucleotides are mixed at nanomolar concentrations, well below that of their k_d, the likelihood of duplex formation and a FRET **250** or ERET **862** signal being generated is negligible. However, when both antibodies **145** or both aptamers **141** bind to the target protein **142**, the local concentration of the oligonucleotides **147** will be much higher than their k_d resulting in almost complete hybridization and generation of a detectable FRET **250** or ERET **862** signal.

[0384] The choice of fluorophores and luminophores is an important consideration when designing a homogeneous protein detection assay. Crude cell lysates are often turbid and may contain substances which autofluoresce. In such cases, the use of molecules with long-lasting fluorescence or electrochemiluminescence and donor-acceptor pairs **143** and **144** which are optimized to give maximal FRET **250** or ERET **862** is desired. One such pair is europium chelate and Cy5, which has previously been shown to significantly improve signal-to-background ratio in such a system when compared with other donor-acceptor pairs, by allowing the signal to be read after interfering background fluorescence, electrochemiluminescence or scattered light has decayed. Europium chelate and AlexaFluor **647** or terbium chelate and Fluorescein FRET or ERET pairs also work well. The sensitivity and specificity of this approach is similar to that of enzyme-linked immunosorbent assays (ELISAs), but no sample manipulation is required.

[0385] In some embodiments of the LOC device, one of the antibodies **145** or one of the aptamers **141** is attached to the base of the proteomic assay chamber **124** (see for example FIGS. **116** and **120**) and the protein lysate is combined with the other antibody **145** or aptamer **141** during lysis within the chemical lysis section **130** to facilitate binding to the first antibody **145** or aptamer **141** prior to entering the proteomic assay chamber **124**. This increases the subsequent speed with

which a detectable signal is generated as only one conjugation or hybridization event is required within the proteomic assay chamber.

Photodiode

[0386] FIG. **54** shows the photodiode **184** integrated into the CMOS circuitry **86** of the LOC device **301**. The photodiode **184** is fabricated as part of the CMOS circuitry **86** without additional masks or steps. This is one significant advantage of a CMOS photodiode over a CCD, an alternate sensing technology which could be integrated on the same chip using non-standard processing steps, or fabricated on an adjacent chip. On-chip detection is low cost and reduces the size of the assay system. The shorter optical path length reduces noise from the surrounding environment for efficient collection of the fluorescence signal and eliminates the need for a conventional optical assembly of lenses and filters.

[0387] Quantum efficiency of the photodiode **184** is the fraction of photons impinging on its active area **185** that are effectively converted to photo-electrons. For standard silicon processes, the quantum efficiency is in the range of 0.3 to 0.5 for visible light, depending on process parameters such as the amount and absorption properties of the cover layers.

[0388] The detection threshold of the photodiode **184** determines the smallest intensity of the fluorescence signal that can be detected. The detection threshold also determines the size of the photodiode **184** and hence the number of hybridization chambers **180** in the hybridization and detection section **52** (see FIG. **52**). The size and number of chambers are technical parameters that are limited by the dimensions of the LOC device (in the case of the LOC device **301**, the dimensions are 1760 μm×5824 μm) and the real estate available after other functional modules such as the pathogen dialysis section **70** and amplification section(s) **112** are incorporated.

[0389] For standard silicon processes, the photodiode **184** detects a minimum of 5 photons. However, to ensure reliable detection, the minimum can be set to 10 photons. Therefore with the quantum efficiency range being 0.3 to 0.5 (as discussed above), the fluorescence emission from the probes should be a minimum of 17 photons but 30 photons would incorporate a suitable margin of error for reliable detection.

Electrochemiluminescence as an Alternative Detection Method

[0390] Electrochemiluminescence (ECL) involves the generation of species at electrode surfaces that then undergo electron-transfer reactions to form excited states that emit light. Electrochemiluminescence differs from normal chemiluminescence in that formation of the excited species relies on oxidation or reduction of the luminophore or a coreactant at an electrode. Coreactants, in this context, are additional reagents added to the ECL solution which enhance the efficiency of ECL emission. In normal chemiluminescence, the excited species form purely through mixing of suitable reagents. The emitting atom or complex is traditionally referred to as a luminophore. In brief, ECL relies on generating an excited state of the luminophore, at which point a photon will be emitted. As with any such process, it is possible for an alternate path to be taken from the excited state which does not lead to the desired light emission (i.e. quenching).

[0391] Embodiments of the test module that use ECL instead of fluorescence detection do not require an excitation LED. Electrodes are fabricated within the hybridization chambers to provide the electrical pulse for ECL generation and the photons are detected using the photosensor **44**. The duration and voltage of the electrical pulse are controlled; in some embodiments, control over the current is used as an alternative to controlling the voltage.

Luminophore and Quencher

[0392] The ruthenium complex, $[Ru(bpy)_3]^{2+}$, described previously for use as a fluorescent reporter in the probes, can also be used as a luminophore in an ECL reaction in the hybridization chambers, with TPrA (tri-n-propylamine $(CH_3CH_2—CH_2)_3N$) as the coreactant. Coreactant ECL has the benefit that luminophores are not consumed after photon emission and the reagents are available for the process to repeat. Furthermore, the $[Ru(bpy)_3]^{2+}$/TPrA ECL system provides good signal levels at physiologically relevant conditions of pH in aqueous solutions. Alternative coreactants which can produce equivalent or better results than TPrA with ruthenium complexes are N-butyldiethanolamine and 2-(dibutylamino)ethanol.

[0393] FIG. **95** illustrates the reactions occurring during an ECL process in which $[Ru(bpy)_3]^{2+}$ is the luminophore **864** and TPrA is the coreactant **866**. ECL emission **862** in the $[Ru(bpy)_3]^{2+}$/TPrA ECL system follows the oxidation of both $Ru(bpy)_3^{2+}$ and TPrA at the anode **860**. The reactions are as follows:

$$Ru(bpy)_3^{2+} - e^- \rightarrow Ru(bpy)_3^{3+} \quad (1)$$

$$TPrA - e^- \rightarrow [TPrA^{\bullet}]^+ \rightarrow TPrA^{\bullet} + H^+ \quad (2)$$

$$Ru(bpy)_3^{3+} + TPrA^{\bullet} \rightarrow Ru(bpy)_3^{\bullet 2+} + products \quad (3)$$

$$Ru(bpy)_3^{\bullet 2+} \rightarrow Ru(bpy)_3^{2+} + h\upsilon \quad (4)$$

[0394] The wavelength of the emitted light **862** is around 620 nm and the anode potential is around 1.1 V with respect to a Ag/AgCl reference electrode. For the $[Ru(bpy)_3]^{2+}$/TPrA ECL system, either the Black Hole Quencher, BHQ **2**, or Iowa Black RQ described previously, would be a suitable quencher. In the embodiments described here, the quencher is a functional moiety which is initially attached to the probe, but other embodiments are possible in which the quencher is a separate molecule free in solution.

Hybridization Probes for ECL Detection

[0395] FIGS. **129** and **130** show the hybridization-responsive ECL probes **237**. These are often referred to as molecular beacons and are stem-and-loop probes, generated from a single strand of nucleic acid, that luminesce upon hybridization to complementary nucleic acids. FIG. **129** shows a single ECL probe **237** prior to hybridization with a target nucleic acid sequence **238**. The probe has a loop **240**, stem **242**, a luminophore **864** at the 5' end, and a quencher **248** at the 3' end. The loop **240** consists of a sequence complementary to the target nucleic acid sequence **238**. Complementary sequences on either side of the probe sequence anneal together to form the stem **242**.

[0396] In the absence of a complementary target sequence, the probe remains closed as shown in FIG. **129**. The stem **242** keeps the luminophore-quencher pair in close proximity to each other, such that significant resonant energy transfer can

occur between them, substantially eliminating the ability of the luminophore to emit light after electrochemical excitation.

[0397] FIG. **130** shows the ECL probe **237** in an open or hybridized configuration. Upon hybridization to a complementary target nucleic acid sequence **238**, the stem-and-loop structure is disrupted, the luminophore **864** and quencher **248** are spatially separated, thus restoring the ability of the luminophore **864** to emit light. The ECL emission **862** is optically detected as an indication that the probe has hybridized.

[0398] The probes hybridize with very high specificity with complementary targets, since the stem helix of the probe is designed to be more stable than a probe-target helix with a single nucleotide that is not complementary. Since double-stranded DNA is relatively rigid, it is sterically impossible for the probe-target helix and the stem helix to coexist.

Primer-Linked ECL Probes

[0399] Primer-linked stem-and-loop probes and primer-linked linear probes, otherwise known as scorpion probes, are an alternative to molecular beacons and can be used for real-time and quantitative nucleic acid amplification in the LOC device. Real-time amplification is performed directly in the hybridization chambers of the LOC device. The benefit of using primer-linked probes is that the probe element is physically linked to the primer, thus only requiring a single hybridization event to occur during the nucleic acid amplification rather than separate hybridizations of the primers and probes being required. This ensures that the reaction is effectively instantaneous and results in stronger signals, shorter reaction times and better discrimination than when using separate primers and probes. The probes (along with polymerase and the amplification mix) would be deposited into the hybridization chambers **180** during fabrication and there would be no need for an amplification section on the LOC device. Alternatively, the amplification section is left unused or used for other reactions.

Primer-Linked Linear ECL Probes

[0400] FIGS. **131** and **132** show a primer-linked linear ECL probe **693** during the initial round of nucleic acid amplification and in its hybridized configuration during subsequent rounds of nucleic acid amplification, respectively. Referring to FIG. **131**, the primer-linked linear ECL probe **693** has a double-stranded stem segment **242**. One of the strands incorporates the primer linked probe sequence **696** which is homologous to a region on the target nucleic acid **696** and is labelled on its 5' end with luminophore **864**, and linked on its 3' end to an oligonucleotide primer **700** via an amplification blocker **694**. The other strand of the stem **242** is labelled at its 3 end with a quencher molecule **248**. After the initial round of nucleic acid amplification has completed, the probe can loop around and hybridize to the extended strand with the, now, complementary sequence **698**. During the initial round of nucleic acid amplification, the oligonucleotide primer **700** anneals to the target DNA **238** (see FIG. **131**) and is then extended, forming a DNA strand containing both the probe sequence and the amplification product. The amplification blocker **694** prevents the polymerase from reading through and copying the probe region **696**. Upon subsequent denaturation, the extended oligonucleotide primer **700**/template hybrid is dissociated and so is the double stranded stem **242** of the primer-linked linear probe, thus releasing the quencher **248**. Once the temperature decreases for the annealing and extension steps, the primer linked probe sequence **696** of the primer-linked linear ECL probe curls around and hybridizes to the amplified complementary sequence **698** on the extended strand and light emission is detected indicating the presence of the target DNA. Non-extended primer-linked linear ECL probes retain their double-stranded stem and light emission remains quenched. This detection method is particularly well suited for fast detection systems as it relies on a single-molecule process.

Primer-Linked Stem-and-Loop ECL Probes

[0401] FIGS. **133**A to **133**F show the operation of a primer-linked stem-and-loop ECL probe **705**. Referring to FIG. **133**A, the primer-linked stem-and-loop ECL probe **705** has a stem **242** of complementary double-stranded DNA and a loop **240** which incorporates the probe sequence. One of the stem strands **708** is labelled at its 5' end with luminophore **864**. The other strand **710** is labelled with a 3'-end quencher **248** and carries both the amplification blocker **694** and oligonucleotide primer **700**. During the initial denaturation phase (see FIG. **133**B), the strands of the target nucleic acid **238** separate, as does the stem **242** of the primer-linked stem-and-loop ECL probe **705**. When the temperature cools for the annealing phase (see FIG. **133**C), the oligonucleotide primer **700** on the primer-linked stem-and-loop ECL probe **705** hybridizes to the target nucleic acid sequence **238**. During extension (see FIG. **133**D), the complement **706** to the target nucleic acid sequence **238** is synthesized forming a DNA strand containing both the probe sequence **705** and the amplified product. The amplification blocker **694** prevents the polymerase from reading through and copying the probe region **705**. When the probe next anneals, following denaturation (see FIG. **133**E), the probe sequence of the loop segment **240** of the primer-linked stem-and-loop probe (see FIG. **133**F) anneals to the complementary sequence **706** on the extended strand. This configuration leaves the luminophore **864** relatively remote from the quencher **248**, resulting in a significant increase in light emission.

ECL Control Probes

[0402] The hybridization chamber array **110** includes some hybridization chambers **180** with positive and negative ECL control probes used for assay quality control. FIGS. **134** and **135** schematically illustrate negative control ECL probes **786** without a luminophore, and FIGS. **136** and **137** are sketches of positive control ECL probes **787** without a quencher. The positive and negative control ECL probes have a stem-and-loop structure like the ECL probes described above. However, an ECL signal **862** (see FIG. **130**) will always be emitted from positive control ECL probes **787** and no ECL signal **862** is ever emitted from negative control ECL probes **786**, regardless of whether the probes hybridize into an open configuration or remain closed.

[0403] Referring to FIGS. **134** and **135**, the negative control ECL probe **786** has no luminophore (and may or may not have a quencher **248**). Hence, whether the target nucleic acid sequence **238** hybridizes with the probe as shown in FIG. **135**, or the probe remains in its stem **242** and loop **240** configuration as shown in FIG. **134**, the ECL signal is negligible. Alternatively, the negative control ECL probe could be designed so that it always remains quenched. For example, by having an artificial probe (loop) sequence **240** that will not

hybridize to any nucleic acid sequence within the sample under investigation, the stem **242** of the probe molecule will re-hybridize to itself and the luminophore and quencher will remain in close proximity and no appreciable ECL signal will be detected. This negative control would account for any low level emission that may occur if the quenching is not complete.

[0404] Conversely, the positive control ECL probe **787** is constructed without a quencher as illustrated in FIGS. **136** and **137**. Nothing quenches the ECL emission **862** from the luminophore **864** regardless of whether the positive control probe **787** hybridizes with the target nucleic acid sequence **238**.

[0405] FIGS. **123** and **124** show another possibility for constructing a positive control chamber. In this case, the calibration chambers **382** which are sealed from the amplicon (or any flow containing target molecules) can be filled with the ECL luminophore solution such that a positive signal is always detected at the electrode

[0406] Similarly, the control chambers can be negative control chambers because the lack of inlets prevents any targets from reaching the probes such that an ECL signal is never detected.

[0407] FIG. **52** shows a possible distribution of the positive and negative control probes (**378** and **380** respectively) throughout the hybridization chamber array **110**. For ECL, positive and negative control ECL probes **786** and **787** would replace control fluorescent probes **378** and **380**, respectively. The control probes are placed in hybridization chambers **180** along a line extending diagonally across the hybridization chamber array **110**. However, the arrangement of the control probes within the array is arbitrary (as is the configuration of the hybridization chamber array **110**).

Calibration Chambers for ECL Detection

[0408] The non-uniformity of the electrical characteristic of the photodiode **184**, response to any ambient light present at the sensor array, and light originating at other locations in the array, introduce background noise and offset into the output signal. This background is removed from each output signal by calibration chambers **382** in the hybridization chamber array **110** which either do not contain any probes, contain probes that have no ECL luminophore, or contain probes with a luminophore and quencher configured such that quenching is always expected to occur. The number and arrangement of the calibration chambers **382** throughout the hybridization chamber array is arbitrary. However, the calibration is more accurate if photodiodes **184** are calibrated by a calibration chamber **382** that is relatively proximate. Referring to FIG. **139**, the hybridization chamber array **110** has one calibration chamber **382** for every eight hybridization chambers **180**. That is, a calibration chamber **382** is positioned in the middle of every three by three square of hybridization chambers **180**. In this configuration, the hybridization chambers **180** are calibrated by a calibration chamber **382** that is immediately adjacent.

[0409] FIG. **93** shows a differential imager circuit **788** used to substract the signal from the photodiode **184** corresponding to the calibration chamber **382** as a result of the applied electrical pulse, from the ECL signal from the surrounding hybridization chambers **180**. The differential imager circuit **788** samples the signal from the pixel **790** and a "dummy" pixel **792**. Signals arising from ambient light in the region of the chamber array are also subtracted. The signals from the pixel **790** are small (i.e. close to dark signal), and without a reference to a dark level it is hard to differentiate between the background and a very small signal.

[0410] During use, the "read_row" **794** and "read_row_d" **795** are activated and M4 **797** MD4 **801** transistors are turned on. Switches **807** and **809** are closed such that the outputs from the pixel **790** and "dummy" pixel **792** are stored on pixel capacitor **803** and dummy pixel capacitor **805** respectively. After the pixel signals have been stored, switches **807** and **809** are deactivated. Then the "read_col" switch **811** and dummy "read_col" switch **813** are closed, and the switched capacitor amplifier **815** at the output amplifies the differential signal **817**.

ECL Levels and Signals Efficiency

[0411] The normal metric of efficiency in ECL is the number of photons obtained per "Faradaic" electron, i.e. per electron which participates in the electrochemistry. The ECL efficiency is denoted ϕ_{ECL}:

$$\phi_{ECL} = \frac{\int_0^\tau I d\tau}{\left(\frac{N_A}{F}\right)\int_0^\tau i d\tau} \tag{5}$$

where I is the intensity in photons per second, i is the current in amperes, F is Faraday's constant, and N_A is Avogadro's constant.

Efficiency of Coreactant ECL

[0412] Annihilation ECL in deoxygenated, aprotic solutions (e.g. nitrogen-flushed acetonitrile solutions) is simple enough to allow efficiency measurements, and the consensus value of ϕ_{ECL} is around 5%. Coreactant systems, however, have been generally declared to be beyond meaningful direct measurements of efficiency. Instead, emission intensity is related by scaling to easily-prepared standard solutions such as $Ru(bpy)_3^{2+}$, measured in the same format. The literature (see for example J. K. Leland and M. J. Powell, J. Electrochem. Soc., 137, 3127 (1990), and R. Pyati and M. M. Richter, Annu. Rep. Prog. Chem. C, 103, 12-78 (2007)) indicates that (without enhancers such as surfactants), the efficiency of $Ru(bpy)_3^{2+}$ ECL with TPrA coreactants peaks at levels comparable to the 5% seen for annihilation ECL in acetonitrile (e.g. 2% efficiency; see I. Rubinstein & A. J. Bard, J. Am. Chem. Soc., 103 512-516 (1981)).

ECL Potentials

[0413] The voltage at the working electrode for the $Ru(bpy)_3^{2+}$/TPrA system is approximately +1.1 V (generally measured in the literature with respect to a reference Ag/AgCl electrode). Voltages this high shorten electrode lifetimes but this is not an issue for single-use devices such as the LOC device used in the present diagnostic system.

[0414] The ideal voltage between the anode and cathode depends on the combination of solution components and electrode materials. Selecting the correct voltage can require compromising between the highest signal levels, reagent and electrode stability, and the activation of undesired side reactions such as electrolysis of the water in the chamber. In tests on buffered aqueous $Ru(bpy)_3^{2+}$/coreactant solution and platinum electrodes, the ECL emission is maximized at 2.1-

2.2 V (depending on the coreactant choice). Emission intensities drop to <75% of the peak values for voltages below 1.9 V and above 2.6 V, and to <50% of the peak values for voltages below 1.7 V and above 2.8 V. A preferred anode-cathode voltage difference for ECL operation in such systems is therefore 1.7-2.8 V, with the range 1.9-2.6 V being particularly preferred. This allows maximization of the emission intensity as a function of voltage, while avoiding voltages at which significant gas evolution at the electrodes is observed.

ECL Emission Wavelenght

[0415] The wavelength of the emitted light **862** from ECL has an intensity peak at around 620 nm (measured in air or vacuum), and the emission spans a relatively broad wavelength range. Significant emission occurs at wavelengths from around 550 nm to 700 nm. Furthermore, the peak emission wavelength can vary by ~10% due to changes in the chemical environment around the active species. The LOC device embodiments described here, which incorporate no wavelength-specific filters, have two advantages for capturing signals with such a broad and variable spectrum. The first advantage is sensitivity: any wavelength filter reduces light transmission, even within its pass band, so efficiency is improved by not including a filter. The second advantage is flexibility: adjustment of filter pass bands is not required after minor reagent changes, and the signals are less dependent on minor differences in non-target components of the input sample.

Solution Volume Participating in ECL

[0416] ECL relies on the availability of luminophore (and coreactant) in solution. However, as illustrated in FIG. **97**, the excited species **868** are generated only in the solution **872** near the electrodes **860** and **870**. The parameter boundary layer depth in the models presented here, is the depth of the layer of solution **872** around the electrode **860** in which the excited species **868** are generated.

[0417] This is a simplification, since solution dynamics can drive the available concentration upward or downward:

[0418] Increased availability: diffusion and electrophoretic effects will allow exchange with more of the solution.

[0419] Decreased availability: reagents can adsorb onto the electrodes and may become unavailable to the ECL process.

[0420] For a boundary layer depth value of 0.5 μm, the following observations are made:

[0421] ECL is observed in experiments where conjugation to magnetic beads with diameters up to 4.5 μm is used to attract the luminophore **864** to the anode **860**.

[0422] $Ru(bpy)_3^{2+}$/TPrA ECL emission **862** as a function of electrode spacing, for interdigitated electrode arrays, was found to be maximised at a 0.8 μm electrode spacing. The requirement for a coreactant **866** in aqueous solutions **872** can be lifted when electrode spacings are ~2 μm. This indicates that the excited species **868** diffuse multiple microns, which implies diffusive exchange on a similar scale for the species in the ground state.

Steady State and Pulsed Operation

[0423] During pulsed activation of the electrodes **860** and **870**, the intensity of the ECL emission **862** (see FIG. **130**) is generally higher than the intensity of the emission **862** from steady-state activation of the electrodes. Accordingly, the activation signal to the electrodes **860** and **870** is pulse-width modulated (PWM) by the CMOS circuitry **86** (see FIG. **102**).

Reagent Recycling and Species Lifetime

[0424] The Ru complex is not consumed in the $Ru(bpy)_3^{2+}$/TPrA ECL system, so the intensity of emission **862** does not reduce with successive reaction cycles. The lifetime of the rate-limiting step is approximately 0.2 milliseconds giving a total reaction recycling time of approximately 1 millisecond.

Electrophoretic Effects and Other Constraints

[0425] Given the complexity of the solutions in the hybridization chamber, a large number of phenomena take place when the ECL voltage is turned on. Electrophoresis of macromolecules, ohmic conduction, and capacitive effects from small ion migration occur simultaneously.

[0426] Electrophoresis of the oligonucleotides (probes and amplicon) can complicate the detection of probe-target hybrids, as DNA is highly negatively charged and attracted to the anode **860**. The time scale for this motion is typically short (in the order of milliseconds). Electrophoretic effects are strong even though the voltages are moderate (~1 V), because the separation between the anode **860** and cathode **870** is small.

[0427] Electrophoresis enhances the ECL emission **862** in some embodiments of the LOC device and degrades the emission in others. This is addressed by increasing or decreasing the electrode spacing to get the associated increases or decreases in electrophoretic effect. Interdigitation of the anode **860** and the cathode **870** above the photodiode **184** represents the extreme case of minimizing this separation. Such an arrangement produces ECL, even in the absence of a coreactant **866** at carbon electrodes **860** and **870**.

Ohmic Heating (DC Current)

[0428] The current required to maintain an ECL voltage of ~2.2 V, is determined as follows with reference to the ECL cell **874** schematically illustrated in FIG. **98**.

[0429] The DC current through the chamber is determined by two resistances: the interface resistance R_i between the electrodes **860** and **870** and the bulk of the solution, and the solution resistance R_s which is derived from the bulk solution resistivity and conduction path geometry. For solutions with ionic strengths relevant to the conditions in LOC devices, the chamber resistance is dominated by interfacial resistances at the electrodes **860** and **870**, and R_s can be neglected.

[0430] The effect of the interfacial resistance is estimated by scaling measurements of macroscopic current flow through similar solutions for the electrode geometries in the LOC devices.

[0431] Macroscopic measurements of current density through a similar solution, at platinum electrodes, were taken. Consistent with the worst-case (high current) approach being taken, overall ionic strength and ECL reactant concentrations in the test solution were higher than those used in the LOC devices. The anode area was smaller than the cathode area, and was surrounded by a cathode with comparable area in a ring geometry. For an anode consisting of a circle 2 mm in diameter, the current measured was 1.1 mA, giving a current density of 350 A/m^2.

[0432] In the heating model, the electrode area is for the square ring geometry schematically illustrated in FIG. **98**.

The anode is a ring with width 1 μm and thickness 1 μm. The surface area is 196 square microns, and therefore the calculated current I=69 nA.

[0433] The heating (power=V^2/R) was modelled for the worst case in which all the heat goes into raising the temperature of the water in the chamber. This leads to heating of chamber contents at 5.8° C./s, at a voltage difference of 2.2 V, if no allowance for heat removal by the bulk of the LOC device is made.

[0434] Heating of the chambers by ~20° C. can cause denaturation of most hybridization probes. For highly specific probes intended for mutation detection, it is preferable to further restrict heating to 4° C. or less. With this level of temperature stability, single base mismatch-sensitive hybridization, using appropriately designed sequences, becomes feasible. This allows the detection of mutations and allelic differences at the level of single nucleotide polymorphisms. Hence the DC current is applied to the electrodes **860** and **870** for 0.69 s, to limit the heating to 4° C.

[0435] A current of ~69 nA passing through the chamber is far more than can be accommodated as Faradaic current by the ECL species at micromolar concentrations. Therefore, low-duty-cycle pulsing of the electrodes **860** and **870** to further reduce heating (to 1° C. or less) while maintaining sufficient ECL emission **862**, does not introduce complications associated with reagent depletion. In other embodiments, the current is reduced to 0.1 nA which removes the need for pulsed activation of the electrodes. Even at currents as low as 0.1 nA, the ECL emission **862** is luminophore-limited.

Chamber and Electrode Geometry

Maximizing Optical Coupling Between ECL Luminescence and Photosensor

[0436] The immediate chemical precursors of ECL luminescence are generated within nanometres of the working electrode. Referring again to FIG. **97**, light emission (the excited species **868**) generally occurs within microns or less of that location. Hence the volume immediately adjacent to the working electrode (anode **860**) is visible to the corresponding photodiode **184** of the photosensor **44**. Accordingly, the electrodes **860** and **870** are directly adjacent the active surface area **185** of the corresponding photodiode **184** in the photosensor **44**. Furthermore, the anode **860** is shaped to increase the length of its lateral periphery 'seen' by the photodiode **184**. This aims to maximize the volume of excited species **868** that can be detected by the underlying photodiode **184**.

[0437] FIG. **96** schematically illustrates three embodiments of the anode **860**. A comb structure anode **878** has the advantage that the parallel fingers **880** can be interdigitated with the fingers of a cathode **870**. The interdigitated configuration is shown in FIG. **103**, and in a partial view of a LOC layout in FIGS. **120** and **124**. The interdigitated configuration provides a uniform dielectric gap **876** (see FIG. **97**) that is relatively narrow (1 to 2 microns) and the interdigitated comb structure is relatively simple for the lithographic fabrication process. As discussed above, a relatively narrow dielectric gap **876** between the electrodes **860** and **870** obviates the need for a coreactant in some solutions **872**, as the excited species **868** will diffuse between anode and cathode. The removal of the requirement for a coreactant removes the potential chemical impact of the coreactant on the various assay chemistries and provides a wider range of possible assay options.

[0438] Referring again to FIG. **96**, some embodiments of the anode **860** have a serpentine configuration **882**. To achieve high periphery length while maintaining tolerance against fabrication errors, it is convenient to form wide, rectangular meanders **884**.

[0439] The anode may have a more complex configuration **886** if necessary or desirable. For example, it may have a crenulated section **888**, a branched structure **890**, or a combination of the two. Partial views of LOC designs incorporating a branched structure **890** are shown in FIGS. **138** and **139**. The more complicated configurations such as **886** provide a long length of lateral periphery, and are best suited to solution chemistries where a coreactant is employed since patterning a closely-spaced opposing cathode is more difficult.

Electrode Thickness

[0440] Generally, ECL cells involve a planar working electrode which is viewed externally. Also, traditional microfabrication techniques for metal layers tend to lead to planar structures with metal thicknesses of approximately 1 micron. As has been indicated earlier, and shown schematically in FIGS. **96**, **99** and **100**, increasing the length of lateral periphery enhances the coupling between the ECL emission and the photodiode **184**.

[0441] A second strategy to further increase the efficiency of collection of emitted light **862** (see FIG. **130**) by the photodiode **184** is to increase the thickness of the anode **860**. This is shown schematically in FIG. **97**. The part of the participating volume **892** adjacent to the walls of the working electrode is the region most efficiently coupled to the photodiode **184**. Therefore, for a given width of working electrode **860**, the overall collection efficiency of the emitted light **862** can be improved by increasing the thickness of the electrodes. Further, since high current carrying capacity is not required, the width of the working electrode **860** is reduced as far as is practical. The thickness of the electrodes **860** and **870** can not increase without restrictions. Noting that the feature and separation sizes of the electrodes are likely to be of the order of 1 micron, and that liquid filling makes gaps which are wider than they are deep unfavourable, the optimum practical thickness for the electrodes is 0.25 micron to 2 microns.

Electrode Spacing

[0442] The spacing between the electrodes **860** and **870** is important for the quality of signals in LOC devices, particularly in embodiments where the electrodes are interdigitated. In embodiments where the anode **860** is a branched structure such as shown in FIG. **96** and FIG. **100**, the spacing between adjacent elements can also be important. ECL emission efficiency, and the collection efficiency of the emitted light, should both be maximised.

[0443] Generation of ECL emission tends to favour electrode spacings on the order of one micron or less. Small spacings are particularly attractive when performing ECL in the absence of a coreactant. The fact that the spacing can be comparable to the wavelength of the emitted light **862** is of limited importance. Therefore, in many embodiments where the emitted light **862** (see FIG. **130**) is measured at a location which does not require that the light have passed between the electrodes **860** and **870**, making the electrode spacing as small as practical is often the goal. In embodiments where the emitted light **862** must pass between the electrodes **860** and

870, however, it becomes necessary to move beyond considering just the ECL emission process, and consider the wave properties of light.

[0444] The wavelength of the emitted light **862** from ECL of $Ru(bpy)_3^{2+}$ is around 620 nm, and therefore 460 nm (0.46 microns) in water. In embodiments where the photodiode **184** and the ECL excited species **868** are on different sides of the electrode structure, and the electrode structure is metallic, the emitted light **862** must pass through a gap between elements of the metallic structures. If this gap is comparable to the wavelength of the light, diffraction generally reduces the intensity of propagating light which reaches the photodiode **184**. In cases where the emitted light **862** is incident on the gap at large angles, however, evanescent mode coupling can be harnessed to improve the strength of collected signals. Two measures are taken in the LOC devices to enhance the efficiency of coupling between the photodiode **184** and the emitted light **862**.

[0445] First, the separation between metallic elements is not reduced below approximately the wavelength of the emitted light in water, i.e. approximately 0.4 microns. When combined with other observations regarding small separations between interdigitated electrodes, this indicates an optimal range for the electrode spacing of 0.4 to 2 microns.

[0446] Second, the distance from the gap between elements to the photodiode **184** is minimised. In the LOC device embodiments described here, this indicates that the total thickness of layers between the electrodes **860** and **870** and the photodiode **184** be one micron or less. In embodiments where multiple layers are present between the electrodes and the photodiode, arranging their thicknesses to be quarter-wave or three-quarter wave layers has the further benefit of suppressing reflection of the emitted light **862**.

Electrode Models

[0447] FIG. **97** is a schematic partial cross-section of the electrodes **860** and **870** in the hybridization chamber. The volume around the lateral periphery of the anode **860** occupied by the excited species **868**, is sometimes referred to as the participating volume **892**. The occluded region **894** above the anode **860** is ignored because its optical coupling to the photodiode **184** is negligible.

[0448] A technique for determining whether a particular electrode configuration provides a foundation for the level of ECL emission **862** for the underlying photodiode **184** is set out below with reference to FIGS. **98**, **99** and **100**.

[0449] FIG. **98** is a ring geometry in which the anode **860** is around the edge of photodiode **184**. In FIG. **99**, the anode **860** is positioned within the periphery of the photodiode **184**. FIG. **100** shows a more complex configuration in which the anode **860** has a series of parallel fingers **880** to increase the length of its lateral edges.

[0450] For all of the above configurations, the model calculations are as follows. For a participating volume **892** of solution V_{ECL}, the total effective number of emitters N_{em} is:

$$N_{em}=N_{lum}\cdot\tau_p/\tau_{ECL}=V_{ECL}C_LN_A\cdot\tau_p/\tau_{ECL} \quad (6)$$

where the participating number of luminophores $M_{lum}=V_{ECL}C_L N_A$, τ_{ECL} is the lifetime of the ECL process, C_L is the luminophore concentration, τ_p is the pulse duration, and N_A is Avogadro' s number.

[0451] The number of isotropically emitted photons N_{phot} is:

$$N_{phot}=\phi_{EC}N_{em} \quad (7)$$

where ϕ_{ECL} is the ECL efficiency, defined as the average number of photons emitted by the ECL reaction of a single luminophore.

[0452] The signal count of electrons, S, from the photodiode is then

$$S=N_{phot}\cdot\phi_0\phi_q, \quad (8)$$

where ϕ_0 is the optical coupling efficiency (the number of photons absorbed by the photodiode **184**) and ϕ_q is the photodiode quantum efficiency. The signal is therefore:

$$S = V_{ECL}C_LN_A\frac{\tau_p}{\tau_{ECL}}\phi_{ECL}\phi_o\phi_q \quad (9)$$

[0453] For FIGS. **98** and **99** electrode configurations, ϕ_0 is:

ϕ_0=(25% photons which are directed towards the photodiode 184)×(10% of photons which are not reflected)

i.e., ϕ_0=2.5% for configurations shown in FIGS. **98** and **99**

[0454] For the electrode configuration of FIG. **100**, 50% of photons are emitted in a direction pointing towards the photodiode **184**, but the absorption efficiency as a function of angle is unchanged, so

ϕ_0=(50% photons which are directed towards the photodiode)×(10% of photons which are not reflected)

i.e., ϕ_0=5% for the configuration of FIG. **100**.

[0455] The participating volume **892** depends on the electrode configuration, and details are presented in the corresponding sections.

[0456] The input parameters for the calculations are listed in the following:

TABLE 5

Input Parameters

Parameter	Value	Comment
Luminophore concentration C_L	2.89 μM	Probe concentration calculated previously
ECL recycling period (lifetime) τ_{ECL}	1 ms	Combined lifetimes of reaction steps for luminophore.
Boundary layer depth D	0.5 μm	Effective volume (including diffusion and electrophoresis) of solution participating in ECL
Duration of current application τ_p	0.69 s	Chosen to limit ohmic heating to 4° C. (as described previously)
Chamber X dimension	28 μm	
Chamber Y dimension	28 μm	
Chamber height Z	8 μm	
Photodiode X dimension	16 μm	
Photodiode Y dimension	16 μm	
Electrode thickness (i.e., exposed edge height)	1 μm	
Electrode layer minimum width and gap	1 μm	Process critical dimension
Electrode interfacial current density	350 A/m^2	For ohmic heating
Solution volume resistivity	0.5 Ω · m	For ohmic heating
Voltage difference applied (working – counter electrode)	2.2 V	

Ring Geometry Around Periphery of Photodiode

[0457] Referring to FIG. **98**, the anode **860** is a ring around the edge of the photodiode **184**. In this configuration, the participating volume **892** is:

V_{ECL}=4×[(layer beside the electrode wall)+(quarter-cylinder above the electrode wall)]

[0458] Calculation results:

[0459] Photons generated from a 0.5 μm boundary layer: 3.1×10^5

[0460] Electron counts in photodiode: 2.3×10^3

[0461] This signal is readily detectable by the underlying photodiode **184** of the LOC device photosensor **44**.

Additional Fingers to Increase Edge Length

[0462] Referring to FIG. **100**, parallel fingers **880** are added across the anode **860**. Only horizontal edges shown in figure contribute to the participating volume **892**, to avoid double-counting the perpendicular edges. The participating volume **892** is then:

V_{ECL}=(8×2)×[(layer beside the electrode wall)+(quarter-cylinder above the electrode wall)]

[0463] Calculation results for FIG. **100** configuration:

[0464] Photons generated from a 0.5 μm boundary layer: 1.1×10^6

[0465] Electron counts in photodiode **184**: 8.0×10^3

[0466] This signal is easily detectable in the photodiode **184**.

Complete Overlay

[0467] This configuration shown in FIG. **101** and FIG. **102** is included as a limiting case of maximum surface area coupling. In practice, 90% or better coupling between the electrode surface area and the active surface area **185** of the photodiode **184** achieves a nearly optimal result, and even coupling of 50% of the photodiode active surface area **185** to the electrode surface area provides most of the benefit of the complete overlay configuration. Complete overlay can be achieved in two embodiments: first, as indicated schematically in FIG. **101**, by employing a transparent anode **860**, in a plane parallel with that of the photodiode **184** and with an area matched to that of the photodiode, and arranging the anode in immediate proximity to the photodiode **184**, such that emitted light **862** passes through the anode and onto the photodiode. In a second embodiment shown schematically in FIG. **102**, the anode **860** is again parallel to and registered with the photodiode area, but the solution **872** fills a void between the anode **860** and the photodiode **184**. For signal modelling of a complete overlay configuration, the anode is assumed to be a complete layer above the photodiode **184**, with half of the photons directed toward the photodiode **184** (absorption efficiency still 10%).

[0468] Photons generated from a 0.5 μm boundary layer: 7.7×10^5

[0469] Electron counts in photodiode: 1.2×10^4

[0470] It is possible to improve the signal and assay beyond the above models by using surfactants and probe immobilization at the anode.

Maximum Spacing Between ECL Probes and Photodiode

[0471] The on-chip detection of hybridization avoids the needs for detection via confocal microscopy (see Background of the Invention). This departure from traditional detection techniques is a significant factor in the time and cost savings associated with this system. Traditional detection requires imaging optics which necessarily uses lenses or curved mirrors. By adopting non-imaging optics, the diagnostic system avoids the need for a complex and bulky optical train. Positioning the photodiode very close to the probes has the advantage of extremely high collection efficiency: when the thickness of the material between the probes and the photodiode is on the order of 1 micron, the angle of collection of emission light is up to 174°. This angle is calculated by considering light emitted from a probe at the centroid of the face of the hybridization chamber closest to the photodiode, which has a planar active surface parallel to that chamber face. The cone of emission angles within which light is able to be absorbed by the photodiode is defined as having the emitting probe at its vertex and the corner of the sensor on the perimeter of its planar face. For a 16 micron×16 micron sensor, the vertex angle of this cone is 170°; in the limiting case where the photodiode is expanded so that its area matches that of the 28 micron×26.5 micron hybridization chamber, the vertex angle is 174°. A separation between the chamber face and the photodiode active surface of 1 micron or less is readily achievable.

[0472] Employing a non-imaging optics scheme does require the photodiode **184** to be very close to the hybridization chamber in order to collect sufficient photons of fluorescence emission. The maximum spacing between the photodiode and probes is determined as follows.

[0473] Utilizing a ruthenium chelate luminophore and the electrode configuration of FIG. **100**, we calculated 27,000 photons being absorbed by our 16 micron×16 micron sensor from the respective hybridization chamber, to generate 8000 electrons assuming a sensor quantum efficiency of 30%. In performing this calculation we assumed that the light-collecting region of our hybridization chamber has a base area which is the same as our sensor area, one quarter of the total number of the hybridization photons is angled so as to reach the sensor, and a conservative 10% estimate for the proportion of photons which do not scatter away from the sensor-dielectric interface. That is, the light gathering efficiency of the optical system is ϕ_0=0.025.

[0474] More accurately we can write ϕ_0=[(base area of the light-collecting region of the hybridization chamber)/(photodetector area)][Ω/4π][10% absorbed], where Ω=solid angle subtended by the photodetector at a representative point on the base of the hybridization chamber. For a right square pyramid geometry:

$\Omega=4\arcsin(a^2/(4d_0^2+a^2))$, where d_0=distance between the chamber and the photodiode, a the photodiode dimension.

[0475] Each hybridization chamber releases 1.1×10^6 photons. The selected photodetector has a detection threshold of 17 photons, and for values of d_0 greater than ten times the sensor size (i.e., essentially normal incidence) the proportion of photons not reflected at the sensor surface can be increased from 10% to 90%. Therefore, the minimum optical efficiency required is:

$\phi_0=17/(1.1\times10^6\times0.9)=1.72\times10^{-5}$

[0476] The base area of the light-emitting region of the hybridization chamber **180** is 29 micron×19.75 micron.

[0477] Solving for d_0, we will get the maximum limiting distance between the bottom of our hybridization chamber

and our photodetector to be d_0=1600 microns. In this limit, the collection cone angle as defined above is only 0.8°. It should be noted this analysis ignores the negligible effect of refraction.

LOC Variants

[0478] The LOC device **301** described and illustrated above in full is just one of many possible LOC device designs. Variations of the LOC device that use different combinations of the various functional sections described above will now be described and/or shown as schematic flow-charts, from sample inlet to detection, to illustrate some of the combinations possible. The flow-charts have been divided, where appropriate, into sample input and preparation stage **288**, extraction stage **290**, incubation stage **291**, amplification stage **292**, pre-hybridization stage **293** and detection stage **294**. For all the LOC variants that are briefly described or shown only in schematic form, the accompanying full layouts are not shown for reasons of clarity and succinctness. Also in the interests of clarity, smaller functional units such as liquid sensors and temperature sensors are not shown but it will be appreciated that these have been incorporated into the appropriate locations in each of the following LOC device designs.

LOC Device with ECL Detection

[0479] FIGS. **111** to **127** show a LOC variant **729** with electrochemiluminescence (ECL) detection. This LOC device prepares **288**, extracts **290**, incubates **291**, amplifies **292** and detects **294** both human and pathogen nucleic acids, as well as human and pathogen protein detection. ECL is used in the hybridization chamber arrays and proteomic assay chamber arrays for target detection.

[0480] As best shown in FIG. **117**, a biological sample (for example, whole blood) is added to the sample inlet **68**. The sample flows through the cap channel **94** to the anticoagulant surface tension valve **118**. The cap **46** is fabricated with an interface layer **594** positioned between the cap channel layer **80** and the MST channel layer **100** of the CMOS+MST device **48** (see FIG. **112**). The interface layer **594** allows a more complex fluidic interconnection between the reagent reservoirs and the MST layer **87** without increasing the size of the silicon substrate **84**.

[0481] FIG. **113** shows the MST layer **87** visible on the top surface of the CMOS+MST device **48**. FIG. **114** shows the cap channel layer **80** on the underside of the cap **46**. FIG. **115** superimposes the reservoirs, the cap channels **94** and the interface channels to illustrate the more sophisticated plumbing achieved with a cap **46** incorporating an interface layer **594**.

[0482] As best shown in FIG. **117**, the interface layer **594** requires the anticoagulant surface tension valve **118** to have two interface channels **596** and **598**. A reservoir-side interface channel **596** connects the reservoir outlet with the downtakes **92** and a sample-side interface channel **598** connects the uptakes **96** with the cap channel **94**.

[0483] Anticoagulant from the reservoir **54** flows through the MST channels **90** via the reservoir-side interface channel **596** to pin a meniscus at the uptakes **96**. The sample flow along the cap channel **94** dips into the sample-side interface channel **598** to remove the meniscus so that the anticoagulant combines with the blood sample as it continues onto the leukocyte dialysis section **328**.

[0484] The leukocyte dialysis section **328** incorporates a bypass channel **600** for filling the flow channel structures without trapped air bubbles (see FIGS. **117** and **126**). The blood sample flows through cap channel **94** to the upstream end of the large constituents interface channel **730**. The large constituents interface channel **730** is in fluid communication with the dialysis MST channels **204** via apertures in the form of 7.5 micron diameter holes **165** (see FIG. **126**).

[0485] Referring to FIG. **126**, each of the dialysis MST channels **204** lead from the 7.5 micron diameter holes **165** to respective dialysis uptakes **168**. The dialysis uptake holes **168** are open to the small constituents interface channel **732**. However the uptakes are configured to pin a meniscus rather than allow capillary driven flow to continue. The uptake belonging to the bypass channel **600** has a capillary initiation feature **202** configured to initiate capillary driven flow into the small constituents interface channel **732**. This ensures the flow begins at the upstream end of the small constituents interface channel **732** and sequentially unpins the menisci at the dialysis uptakes **168** as the flow progresses downstream.

[0486] FIG. **121** shows the downstream end of the leukocyte dialysis section **328**. The large constituents interface channel **730** feeds into the large constituents cap channel **736** and the small constituents interface channel **732** feeds the small constituents cap channel **734**. As best shown in FIG. **115**, the large constituents cap channel **736** feeds the leukocytes (and any other large constituents) into the chemical lysis section **130.1** via the lysis surface tension valve **128.1** where lysis reagent from reservoir **56.1** is added. The chemical lysis section **130.1** has a 3 micron filter downtake **738** at the outlet (see FIG. **117**). The filter downtake ensures that no large constituents reach the lysis chamber exit boiling-initiated valve **206**. After sufficient time, the boiling-initiated valve **206** opens the chemical lysis section **130.1** outlet and the sample flow is split into two streams. As best shown in FIG. **117**, one stream flows to the surface tension valve **132.1** for the first restriction enzyme, ligase and linker reservoir **58.1** and the other stream is drawn along a lysed leukocyte bypass channel **742** directly to the proteomic assay chamber array **124.1** in the hybridization and detection section **294**. Here the sample fills the proteomic assay chamber array **124.1** (see FIG. **119**) containing probes for hybridization with target human proteins. Probe-target hybrids are detected with a photosensor **44** (see FIG. **111**). The other stream flows into the leukocyte incubation section **114.1** together with restriction enzymes, ligase and linker primers from reservoir **58.1**.

[0487] Referring to FIG. **118**, after restriction enzyme digestion and linker ligation, the incubator outlet valve **207** (also a boiling-initiated valve) opens and flow continues into the leukocyte DNA amplification section **112.1**. The amplification mix and polymerase in reservoirs **60.1** and **62.1** are added via surface tension valves **138.1** and **140.1** respectively. Referring to FIG. **119**, after thermal cycling, the boiling-initiated valve **108** opens for the amplicon to enter the hybridization chamber array **110.1** containing probes for human DNA targets. Probe-target hybrids are detected with the photosensor **44**.

[0488] The erythrocytes and pathogens from the leukocyte dialysis section **328** are fed to the pathogen dialysis section **70** via the cap channel **734** (see FIGS. **117** and **127**). This operates in the same manner as the leukocyte dialysis section **328** with the exception that the filter downtakes have 3 micron holes **164** instead of the 7.5 micron holes **165** used for leukocyte dialysis. The erythrocytes remain in the large constituents interface channel **730** while the pathogens diffuse to the small constituents interface channel **732**.

[0489] FIG. **122** shows the downstream end of the pathogen dialysis section **70**. The erythrocytes flow into the large constituents cap channel **736** and the pathogens fill the small constituents cap channel **734**. It will be appreciated that 'large constituents' and 'small constituents' are used in a relative sense as the large constituents output of the pathogen dialysis section is part of the small constituents output of the leukocyte dialysis section. The constituents in the large constituents cap **736** or interface channels are simply larger than the constituents in the small constituents cap **734** or interface channels within that particular dialysis section. As best shown in FIGS. **115** and **116**, the erythrocytes in the large constituents cap channel **736** are directed to the surface tension valve **128.3** for the lysis reagent reservoir **56.3**. The lysis reagent combines with the erythrocytes as the sample fluid fills the chemical lysis section **130.3**. Boiling-initiated valve **206** at the outlet of the third chemical lysis section **130.3** retains the pathogens until lysis is complete. When the boiling-initiated valve **206** opens, the erythrocyte DNA flows directly into the proteomic assay chamber array **124.3** for protein analysis and detection by the photosensor **44** (see FIG. **119**).

[0490] The pathogens in the small constituents cap channel **734** are directed to the surface tension valve **128.2** of the second lysis reagent reservoir **56.2**. The lysis reagent combines with the pathogens as the sample fluid fills the second chemical lysis section **130.2**. After sufficient time, the boiling-initiated valve **206** opens the chemical lysis section **130.2** outlet and the sample flow is split into two streams. As best shown in FIGS. **116** and **118**, one stream flows to the surface tension valve **132.2** for the second restriction enzyme, ligase and linker reservoir **58.2** and the other stream is drawn along a bypass channel **744** directly to the hybridization and detection section **294**. Here the sample fills the proteomic assay chamber array **124.2** (see FIG. **119**) containing probes for hybridization with target pathogen proteins or other biomolecules. Probe-target hybrids are detected with the photosensor **44** (see FIG. **111**).

[0491] The other stream flows into the pathogen incubation section **114.2** together with restriction enzymes, ligase and linker primers from reservoir **58.2**. After restriction digestion and linker ligation, the incubator exit valve **207** (also a boiling-initiated valve) opens and flow continues into the pathogenic DNA amplification section **112.2** (see FIG. **118**). As the chamber fills, the amplification mix and polymerase in reservoirs **60.2** and **62.2** are added via surface tension valves **138.2** and **140.2** respectively. After thermal cycling, the boiling-initiated valve **108** opens for the amplicon to flow into the second hybridization chamber array **110.2** containing probes for pathogenic DNA targets. Probe-target hybrids are detected with the photosensor **44** (see FIG. **119**).

[0492] Referring to FIG. **120**, the hybridization chamber arrays **110.1** and **110.2** and proteomic assay chamber arrays **124.1** to **124.3** have heater elements **182** made from strips of titanium nitride. There are end-point liquid sensors **178** that detect when the flow has reached the end of the hybridization chamber array or proteomic assay chamber array and the heaters **182** are then activated after a time delay. The flow rate sensor **740** (see FIG. **125**) is included in the pathogen incubation section **114.2** to determine the time delay.

[0493] FIGS. **123** and **124** show the calibration chambers **382**. They are used to calibrate the photodiodes **184** to adjust for system noise and background levels. The photodiode's response and electrical noise characteristics can vary with location and due to thermal variations. The output signal from calibration chambers **382**, which do not contain any probes, closely approximates the noise and background in the output signal from all the chambers. Subtracting the calibration signal from the output signals generated by the other hybridization chambers substantially removes the noise and leaves the signal generated by the electrochemiluminescence (if any). Also, positive and negative control ECL probes **786** and **787** can be placed in some of the hybridization chambers **180** for assay quality control.

[0494] Referring to FIG. **116**, a humidifier **196**, composed of the water reservoir **188** and evaporators **190**, is located in the top left of the device. The position of the humidity sensor **232** is adjacent to the hybridization chamber array **110** where humidity measurement is most important to slow evaporation from the solution containing the exposed probes.

[0495] By combining the leukocyte and pathogen output dialysis sections, three output streams are produced (leukocytes, erythrocytes, and pathogens and other biomolecules) which are processed separately to enable higher sensitivity and parallel analysis. The output from each stream is lysed and separately directed to the proteomic assay chamber arrays for protein detection. The lysed leukocytes and pathogens are also separately directed to the incubation **114** and amplification **112** sections for amplification, followed by hybridization for nucleic acid detection.

LOC Device with Thermal Insulation Trench

[0496] As best depicted in FIG. **128**, a trench **896** is etched into the back of the silicon substrate **84**. The purpose of the trench is to thermally insulate the amplification section **112** from the hybridization chamber array **110**. The hybridization array contains detection probes that can degrade at high temperatures. The trench, when filled with air, has a thermal conductivity of the order of 6000 times less than that of the silicon substrate, thereby significantly reducing the heat flux into adjacent parts of the LOC device.

[0497] This provides two main advantages: an increase in the heating efficiency in the amplification section **112**; and a reduction in the undesirable temperature rise of the adjacent hybridization section **110**. Improved heating efficiency means less power is required to heat the amplification section **112** and the temperature reaches its desired end-point temperature faster and with better spatial uniformity within the amplification section. A reduction in the temperature rise in the hybridization section **110** allows for a wider range of probe chemistries and superior signal quality.

[0498] The trench can be placed around any region on the LOC device to thermally insulate the components in that region. The width and depth of the trench **896** are variable to suit the specific application.

CONCLUSION

[0499] The devices, systems and methods described here facilitate molecular diagnostic tests at low cost with high speed and at the point-of-care.

[0500] The system and its components described above are purely illustrative and the skilled worker in this field will readily recognize many variations and modifications which do not depart from the spirit and scope of the broad inventive concept.

1. A test module for lysing cells in a fluid, the test module comprising:

an outer casing with receptacle for receiving a fluid containing cells;

a lysis reagent reservoir containing a lysis reagent and having an outlet valve; and, a lysis section in fluid communication with the receptacle for holding the fluid during lysis of the cells; wherein,

the outlet valve is upstream of the lysis section and configured to open as the fluid flows into the lysis section thereby adding the lysis reagent to the fluid.

2. The test module according to claim **1** wherein the outlet valve is a surface tension valve with an aperture configured to pin a meniscus that retains the lysis reagent therein until contact with the fluid removes the meniscus and the lysis reagent is added to the fluid flow into the lysis section.

3. The test module according to claim **2** wherein the lysis section is configured as a lysis microchannel to draw the fluid from the receptacle by capillary action, the lysis section having an active valve at a downstream end of the lysis microchannel for retaining the fluid during lysis of the cells.

4. The test module according to claim **3** wherein the active valve is a boiling-initiated valve with a meniscus anchor for retaining the fluid in the lysis section, the boiling-initiated valve also having a valve heater for boiling the liquid such that the meniscus unpins from the meniscus anchor and capillary driven flow out of the lysis section resumes.

5. The test module according to claim **4** wherein the microchannel has a cross sectional area transverse to the flow of between 8 square microns and 20,000 square microns.

6. The test module according to claim **5** further comprising a supporting substrate wherein the lysis section and the lysis reagent reservoir are supported on the supporting substrate and configured as a lab-on-a-chip (LOC) device.

7. The test module according to claim **6** further comprising CMOS circuitry between the supporting substrate and the lysis section, the CMOS circuitry being configured for operative control of the valve heater at the downstream end of the microchannel.

8. The test module according to claim **7** further comprising a polymerase chain reaction (PCR) section with at least one heater for thermally cycling the fluid to amplify nucleic acid sequences released from the cells.

9. The test module according to claim **8** further comprising at least one sensor wherein the CMOS circuitry is configured to use the sensor for feedback control of the at least one PCR heater.

10. The test module according to claim **8** further comprising a plurality of heaters and at least one temperature sensor and at least one liquid sensor such that the CMOS circuitry controls initial activation of the heaters in response to the at least one liquid sensor and heater power in response to the at least one temperature sensor.

11. The test module according to claim **9** wherein each of the plurality of heaters is independently operable.

12. The test module according to claim **11** wherein the PCR section is configured as a PCR microchannel with the same cross section as the lysis microchannel, the PCR section also having an active valve at a downstream end of the PCR microchannel for retaining the fluid during amplification of the nucleic acid sequences.

13. The test module according to claim **12** further comprising a PCR mix reservoir and a polymerase reservoir wherein the PCR mix reservoir contains dNTPs, primers and buffer solution and the polymerase reservoir contains polymerase enzymes.

14. The test module according to claim **13** further comprising a cap which defines the lysis reagent reservoir, the PCR mix reservoir and the polymerase reservoir, wherein the lysis section and the PCR section are between the cap and the supporting substrate.

15. The test module according to claim **1** further comprising a dialysis section wherein the cells in the fluid are of different sizes, the dialysis section being configured for separating cells larger than a predetermined threshold into a portion of the sample which is processed separately from the remainder of the sample containing only cells smaller than the predetermined threshold.

16. The test module according to claim **15** wherein the nucleic acid sequences are from the cells larger than the predetermined threshold.

17. The test module according to claim **16** further comprising an anticoagulant reservoir wherein the fluid is a whole blood sample such that anticoagulant is added to the whole blood upstream of the dialysis section and the dialysis section is configured to concentrate the leukocytes into a portion of the whole blood sample.

18. The test module according to claim **1** further comprising a hybridization section downstream of the PCR section, the hybridization section having an array of probes for hybridization with predetermined target nucleic acid sequences in the amplicon from the PCR section; and, a photosensor for detecting hybridization of probes within the array of probes.

19. The test module according to claim **18** wherein the hybridization section has electrodes positioned for receiving an electrical pulse, and the probes are electrochemiluminescent (ECL) probes for hybridization with the target nucleic acid sequences to form probe-target hybrids, the probe-target hybrids being configured to emit a photon of light when excited by current between the electrodes.

20. The test module according to claim **19** wherein the photosensor is an array of photodiodes positioned in registration with the ECL probes respectively.

* * * * *